IDA

INSTITUTE FOR DEFENSE ANALYSES

Report on the Advanced Technology Demonstration (ATD) of the Vehicular-Mounted Mine Detection (VMMD) Systems at Aberdeen, Maryland, and Socorro, New Mexico

Frank Rotondo
Tom Altshuler
Erik Rosen
Cynthia Dion-Schwarz
Elizabeth Ayers

19990727 032

PREFACE

This document presents an analysis of the results of an advanced technology demonstration of five vehicular-mounted mine detection systems developed for the detection of antitank land mines. Three of the systems, built by EG&G, Inc.; GDE Systems, Inc., and Geo-Centers, Inc., were developed for the U.S. Army Night Vision and Electronic Sensors Directorate. Two systems, built by Coleman Research Corporation and Computing Devices Canada, participated in this demonstration through funds from the Project Manager, Mines, Countermine, and Demolition. (Computing Devices Canada built its system for the Canadian Forces through the Defence Research Establishment Suffield.) The advanced technology demonstration took place at the Aberdeen Test Center, Aberdeen, Maryland, on June 8–19, 1998, and the Energetic Materials Research and Testing Center, Socorro, New Mexico, on July 13–24, 1998.

This document was prepared for the Director of Defense Research and Engineering, Office of the Under Secretary of Defense (Acquisition and Technology), under a task titled, "Technical Support to Communication and Electronics Command Night Vision and Electronic Systems Directorate Mine Detection Program."

CONTENTS

TABLES

FIGURES

EXECUTIVE SUMMARY

BACKGROUND

This report summarizes the results of an Advanced Technology Demonstration (ATD) of five vehicular-mounted mine detection (VMMD) systems developed for detection of antitank landmines. Three of the systems, built by EG&G, Inc.; GDE Systems, Inc., and Geo-Centers, Inc., were developed for the U.S. Army Night Vision and Electronic Sensors Directorate. Two systems, built by Coleman Research Corporation and Computing Devices Canada, participated in this demonstration through funds from the Project Manager, Mines, Countermine, and Demolition. (Computing Devices Canada built its system for the Canadian Forces through the Defence Research Establishment Suffield.) The demonstration took place at two locations: the Aberdeen Test Center, Aberdeen, Maryland, on June 8–19, 1998, and the Energetic Materials Research and Testing Center, Socorro, New Mexico, on July 13–24, 1998.

The purpose of the VMMD program is to develop and demonstrate technology needed to produce a remotely operated vehicle that will detect and mark antitank landmines during military mine clearance operations. The system will ultimately consist of a mine overpass vehicle upon which is mounted a sensor system to detect mines and a communication system that provides for data transfer between the detection vehicle and the remote operator.

DEMONSTRATION DESCRIPTION

All five contractors' sensor suites included ground-penetrating radar (GPR) and electromagnetic induction (EMI) sensors. Four of the five contractors (Computing Devices Canada, EG&G, GDE, and GeoCenters) also used infrared (IR) sensors. (Coleman's sensor suite did include IR, but it was not used in this ATD.) In general, contractors used automatic target recognition (ATR) algorithms to analyze their sensor data; however, Computing Devices Canada and Geo-Centers used a man-in-the-loop to evaluate IR images in real time. Four of the five contractors (Coleman , EG&G, GDE, and GeoCenters) mounted their systems on high-mobility multipurpose wheeled vehicles (HMMWVs); Computing Devices Canada used a remote-controlled detection vehicle.

The antitank mine threats that these systems will ultimately encounter include metal-cased mines and mines with low-metal content (these mines have plastic cases but do have a small amount of metal in their internal mechanisms). These mines may be laid on ground surface or underground, and they may be located on road beds or in off-road conditions. All these variables were incorporated in this demonstration.

The systems were tested on 3-m-wide test lanes. The Aberdeen test included 3,185 m² of on-road lanes and 1,140 m² of off-road lanes. The Socorro test included 3,090 m² of on-road lanes and 269 m² of off-road lanes.

There were about equal numbers of metal and low-metal mines, and combined these comprised about 95 percent of the mine types in this test (the remaining 5 percent being nonmetal mine surrogates). About 40 percent of the mines were emplaced on the surface; the balance were buried at depths ranging from 1.5 to 4 in. below the surface.

MEASURING PERFORMANCE

To score performance, contractor declarations were matched to mines on the basis of a separation distance, R_{halo}, between the edge of a mine and the location of a contractor's declaration. R_{halo} was taken to be 1 m, as directed in the Operational Requirements Document for this program. If more than one declaration was within R_{halo} of a mine, the contractor was credited with a single detection (the closest one to the mine), and the others were ignored. If a contractor's declaration did not fall within R_{halo} of any mine, it was considered a false alarm.

SYSTEM PERFORMANCE

Tables ES-1 and ES-2 provide a summary of the on-road and off-road performances, respectively, of each contractor in the demonstration. False-alarm rates (FAR, in units m⁻²) are listed, as are detection probabilities (P_d) for surface and subsurface mines at Aberdeen and Socorro. Also given are the exit criteria that should be met at this demonstration in order to justify proceeding to the next phase of this program.

CONCLUSIONS

As can be seen in Tables ES-1 and ES-2, the exit criteria were typically met by a majority of contractors at each test site, except the on-road FAR at Aberdeen (met by only one contractor), and the off-road, subsurface P_d at Socorro (again, met by one contractor).

Reduction of the *FAR* is one of the serious challenges for this program, as the ultimate requirements on *FAR* (described in the Operational Requirements Document) are substantially below those achieved in this demonstration.

Other conclusions, which are substantiated in this report, are listed here:

- The contractors' GPR sensors were, overall, the most effective sensors for the detection of AT mines. The GPRs also, generally, contributed the most false alarms of the three sensor types.

- Subsurface, low-metal mines in off-road conditions seemed to be the most difficult mines to detect in this ATD.

- Metal cased AT mines were detected with a high probability by the VMMD systems discussed herein. Both GPR and EMI sensors were effective at finding these mines at the depths tested in this ATD.

- Surface mines were also shown to be detectable with a high probability in this series of tests. Both GPR and IR systems were effective, regardless of the metal content of the mine.

- The along-track and cross-track position resolutions typically achieved in this series of tests suggest that the mine halo can be reduced from 1 m without eliminating real detections.

Table ES-1. Summary of On-Road Performance at Aberdeen and Socorro

Contractor	*FAR* (exit criterion $<0.042\ m^{-2}$)		Subsurface P_d (exit criterion > 0.85)		Surface P_d (exit criterion > 0.90)	
	Aberdeen	Socorro	Aberdeen	Socorro	Aberdeen	Socorro
Computing Devices Canada	0.054	0.032	0.93	0.89	1.0	1.0
Coleman Research Corp.	0.034	0.037	0.77	0.91	0.92	1.0
EG&G, Inc.	0.081	0.043	0.93	0.92	1.0	0.97
GDE Systems	0.068	0.037	0.91	0.90	0.97	1.0
GeoCenters, Inc.	0.056	0.032	0.99	0.91	1.0	1.0

Table ES-2. Summary of Off-Road Performance at Aberdeen and Socorro

Contractor	FAR (exit criterion <0.17 m^{-2})		Subsurface P_d (exit criterion > 0.80)		Surface P_d (exit criterion > 0.90)	
	Aberdeen	Socorro	Aberdeen	Socorro	Aberdeen	Socorro
Computing Devices Canada	0.050	0.048	0.99	0.63	1.0	1.0
Coleman Research Corp.	0.201	0.041	0.91	0.73	0.96	1.0
EG&G, Inc.	0.099	0.058	0.96	0.70	0.96	1.0
GDE Systems	0.085	0.065	0.91	0.80	0.94	1.0
GeoCenters, Inc.	0.066	0.035	0.90	0.70	1.0	1.0

I. INTRODUCTION

A. BACKGROUND OF THE ADVANCED TECHNOLOGY DEMONSTRATION

This report summarizes the results of an Advanced Technology Demonstration (ATD) of five Vehicular Mounted Mine Detection (VMMD) systems developed for the detection of antitank (AT) landmines. Three of the systems, built by EG&G, Inc.; GDE Systems, Inc., and Geo-Centers, Inc., were developed for the U.S. Army Night Vision and Electronic Sensors Directorate. Two systems, built by Coleman Research Corporation and Computing Devices Canada, participated in this demonstration through funds from the Project Manager, Mines, Countermine, and Demolition. (Computing Devices Canada built its system for the Canadian Forces through the Defence Research Establishment Suffield.) The ATD took place at the Aberdeen Test Center (ATC), Aberdeen, Maryland, on June 8–19, 1998, and the Energetic Materials Research and Testing Center, Socorro, New Mexico, on July 13–24, 1998.

B. MOTIVATION AND OBJECTIVES OF THE ATD

During combat, when timely maneuvers are critical, countermine engineers use plows, rollers, and explosives to breach minefields. These breaching devices, designed to rapidly cut well-defined paths through mined areas, are not appropriate for clearing large tracts of land or extended lengths of road for unrestricted use. Instead, wide-area clearance of mines must be performed in two stages, first by detecting the mines and then by removing the mines or destroying them in place. Currently, mines are detected visually, through physical contact (probing), or by using hand-held mine detection systems, specifically the AN/PSS-12 pulsed induction metal detector. These techniques are time consuming, hazardous, and can be unreliable. Consequently, the Army Science and Technology Working Group approved the development of a VMMD system that can rapidly, safely, and reliably detect mines. Such a system could also be used to detect the leading edge of a minefield, even if plows, rollers, or explosives would ultimately be used to breach the field.

The purpose of the program is to develop and demonstrate the technology needed to produce a remotely operated vehicle that will detect mines and mark their locations during military mine clearance operations. The system will ultimately consist of a mine overpass vehicle upon which is mounted a sensor system that detects mines, a marking system to designate detection locations, and a communication system that provides data transfer between the detection vehicle and the remote operator. The system will be called the Ground Standoff Mine Detection System (GSTAMIDS).

The mine threats that GSTAMIDS will encounter include metal-cased mines and mines with low-metal content (these mines have plastic cases but do have a small amount of metal in their internal mechanisms). These mines may be laid on ground surface or buried underground.

The final system requirements are published in the GSTAMIDS Operational Requirements Document (ORD, 1996). ATD criteria were written by the Army Science and Technology Working Group (ASTWG) and adopted by TECOM (1996). Separate criteria exist for the transition from the ATD to the Engineering Manufacturing Development (EMD) phase in the VMMD development.[1] The EMD criteria constitute the most relevant criteria for judging the performance of the contractors in this ATD, and are thus referred to as the ATD's *exit criteria* in the remainder of this report.

The ORD requirements, TECOM requirements, and EMD criteria (exit criteria) are summarized in Table I-1. Further details regarding the VMMD requirements can be found in the references.

C. VMMD TECHNOLOGY

VMMD systems should aim to speed up the forward progress of troops (as compared with current mine detection methods). Important characteristics of such a system include accuracy of location, high probability of mine detection, and a low probability of false alarms. The sensor suites from each of the contractors use a combination of relatively mature technologies and advanced automatic target recognition (ATR) algorithms to achieve these goals. Technologies used by all of the five contractors include ground-penetrating radar (GPR), an infrared (IR) and/or optical system, and a pulsed electromagnetic induction (EMI) metal-detection system. One contractor's sensor suite contains a thermal neutron analysis (TNA) sensor, used to confirm the presence of

---

[1] *Ground Standoff Minefield Detection System Milestone I: Program Initiation Milestone Decision Review*, Office of the Program Manager for Mines, Countermine, and Demolitions, July 1997.

explosives. All contractors collect and analyze the data from each of their sensors. Data processing is done in real time so that the operators can be notified about mine encounters as soon as they occur.

Table I-1. Summary of Exit Criteria of the VMMD System

Operation Characteristic	GSTAMIDS ORD		TECOM Criteria		ATD Exit Criteria	
	Off-Road Minimum (Goal)	On-Road Minimum (Goal)	Off-Road Minimum (Goal)	On-Road Minimum (Goal)	Off-Road Minimum	On-Road Minimum
Detection Speed (km/h)	7.2 (12)[a]	15 (25)[a]	2 (3)	3.6 (5)	2	3.6
Minimum Standoff Distance (m)	1 (5)[b]	1 (5)[b]	1	1	Not specified	Not specified
Detector Swath (m)	2.5	2.5	3.0	3.0	3.0	3.0
Detection Probability (P_d) (%) Surface AT mines Buried AT mines	90 (100) 80 (95)	90 (100) 90 (100)	92 (98) 90 (95)	95 (99) 92 (95)	90 80	90 85
Maximum False Alarm Rate *(FAR)* (per squared meter)[c]	0.010 (0.007)	0.005 (0.002)	0.083 (0.05)	0.020 (0.013)	0.17	0.042
Marking accuracy/halo size (m)	1.0 (0.5)	1.0 (0.5)	1.0 (0.5)	1.0 (0.5)	1.0	1.0

[a] These are alert rates: the GSTAMIDS ORD states that the vehicles may slow down to an unspecified speed for landmine verification.

[b] Verification distance.

[c] The GSTAMIDS ORD and ATD exit criteria quote these numbers in units of number per meter of forward progress. All test lanes in this ATD were 3 m wide, so the equivalent *FAR* per squared meter shown here is simply the exit criteria divided by 3.

CRC, EG&G, GDE, and GeoC mounted their sensors on a high-mobility multipurpose wheeled vehicle (HMMWV) for this ATD; CDC's sensors were mounted on a remote-controlled detection vehicle (RDV). Features common to each system include the following:

- Three-meter wide detection coverage
- Integrated differential Global Positioning System (dGPS)
- Electronic marking of detections (geolocations)
- ATR Algorithms.

Tables I-2 through I-5 summarize the characteristics of the different sensors.

Individual contractors used their sensor suites in different ways. In general, CDC and EG&G used all three detection sensors (the GPR, EMI, and IR sensors) at both

Table I-2. GPR Characteristics

Contractor	Type	BW (GHz)	Pulse Width	Antenna	Coherent	Comments
EG&G	Impulse	0.5–5	300 psec	Bistatic Split Pair (Parabolic)	No	45% look ahead, vertical polarization
GeoCenters	Impulse	0.7–1.3	1 nsec	Transverse EM (Rhombus)	N/A	Patented energy-focused GPR
GDE	Swept Frequency	0.5–2.1	200 steps	Zigalog PCB	Yes	
Coleman	Swept Frequency	1–3	90 steps	Spiral	Yes	
CDC	All Specifications Proprietary					Mfr. IAI-ELTA

Table I-3. Optical Characteristics

Contractor	Band (μm)	Manufacturer*	NE ΔT
EG&G	3–5, 8–12, Visible	Mitsubishi, FLIR, Cohu	0.06 K, 0.08 K, N/A
GeoCenters	3–5	Amber/Raytheon	0.0025 K
GDE	8–12	Agema	<0.1 K
Coleman	3–5, 8–12	FLIR	0.003 K
CDC	8–12	Agema (THV-1000)	MRT <0.1 K

* Agema and FLIR Systems, Inc., merged recently, but at the time these systems were purchased, these two companies were separate.

Table I-4. Pulsed EMI Characteristics

Contractor	PW/Frequency	# Coils	Coil Size (m)	Manufacturer	Comment
EG&G	30 μsec	9	0.3 × 0.45	EG&G	Dual Orthogonal Illumination
GeoCenters	5 msec/75 Hz	6	0.5	Geonics	
GDE	---	6	0.5	Vallon	
Coleman	70 Hz	6	0.27	Schiebel	6 AN/PSS–12s
CDC	---	24	0.25	Schiebel	VAMIDS

Table I-5. Confirmation Sensor Characteristics

Contractor	Type	Responds to	Comment
CDC	Thermal Neutron Analysis	Nitrogen Content	SAIC Canada Minescans

Aberdeen and Socorro. CRC used only the GPR and EMI sensors during this ATD. GDE and GeoC used their GPR and EMI sensors at all times, but the IR sensors were used

selectively. GeoC used the IR sensor almost exclusively for surface mine detection; GDE always used the IR sensor during the Socorro test, but not always at Aberdeen. CDC, the only contractor to have a confirmation sensor (TNA), used the TNA sensor selectively. See Appendix A for details of each contractor's use of its sensor suites.

Although each contractor used ATR algorithms to analyze GPR and EMI sensor data, not all contractors used ATR to evaluate IR data. In particular, CDC had no ATR algorithm and used a man-in-the-loop to evaluate the IR images in real time. GeoC did have an ATR, but primarily used a man-in-the-loop to evaluate IR images during this ATD. EG&G and GDE both used ATR exclusively for IR data analysis.

Each contractor's GPR sensor had an above-ground distance of about 0.3 to 0.5 m (and in some cases, greater than 0.5 m). CRC, EG&G, GDE, and GeoC had their EMI sensors at a relatively large above-ground distance (>0.5 m) and did not raise or lower them during operation. CDC's EMI sensor had a variable above-ground distance which could be as little as a few centimeters, because this sensor was used to detect low-metal as well as metal-cased mines. As a result, CDC's metal detector had to be raised when surface landmines were encountered. All contractors' IR systems were mounted atop their vehicles and had a large standoff distance (>2 m). CDC's confirmation (TNA) system normally rode high above the ground but was lowered to within centimeters of the ground for ~2–3 minutes during target confirmation.

All contractors incorporated electronic- and physical-marking systems. The physical-marking systems varied:

- CDC's marks were made with a water-based gel;

- CRC's were made by depositing 2.5-in. diameter disks from 10 equally spaced dispensers across the vehicle;

- EG&G's marks were made with chalk deposited by 32 elements spaced at 4-in. intervals across the front bumper of the vehicle;

- GDE sprayed 4-in. by 4-in. paint marks using several solenoids located across the vehicle; and

- GeoC sprayed a water-based paint from a series of nozzles spaced at 6-in. intervals across the vehicle.

D. ORGANIZATION OF THIS REPORT

This report is structured as follows.

- Chapter II contains a description of the ATD, including details on the test lanes at Socorro and Aberdeen, and the mine types and disposition used at each site.

- Chapter III defines the measures of performance, notably detection probability (P_d), false-alarm rate (FAR), probability of false alarm (P_{fa}), and position resolution of the sensors.

- Chapter IV compares the performance of the contractors at each test site, as well as combined data from both sites, on- and off-road, for detecting surface and subsurface mines. It also compares position accuracy and average vehicle speed during the tests.

- Chapter V gives the details of each contractor at both test sites for individual sensors, sensor pairs, and the complete system. The section provides details of the contractors' effectiveness at detecting metal, low-metal, and nonmetal mines. It also evaluates position resolution, as well as the contractors' performance during special (additional) runs.

- Chapter VI contains conclusions.

- Appendix A contains an in-depth description of the contractors' systems.

- Appendix B contains a lane-by-lane catalog of the mines detected and missed during each run.

- Appendix C contains comprehensive summaries of the contractors' performance for surface and subsurface mines in on-road and off-road consitions, as well as for special runs. Results are categorized by sensor type as well as by metal content of the mines.

II. TEST DESCRIPTION

A. ATC TEST LANES

VMMD technologies were tested in two road environments, each including one or more calibration and test lanes:

A. *On-road.* Mines were buried in three calibration lanes and three test lanes consisting of dirt with gravel scattered throughout. The test lanes were 3.0 m wide and varied in length from about 315 m to 380 m. The lanes were oriented in approximately the east-west direction. The total area covered by the on-road lanes was 3,184.6 m².

B. *Off-road.* Mines were buried in two calibration lanes and two test lanes consisting of natural dirt covered by grass. The length of each test lane was 190 m and the width of each lane was 3 m. The number of mines emplaced in each test lane was 29. The off-road lanes were aligned parallel to one another in approximately the east-west direction and separated by about 10 m. The total area covered by the off-road test lanes was 1,140.3 m².

To avoid ambiguity in detection determination, the mine density was chosen to ensure that the areas encompassing the mines did not overlap.[2] The mines are classified by their metal content: "metal" refers to mines with metal cases, "low metal" refers to mines with nonmetallic cases that contain some metal parts (generally in the fuzing or firing mechanism), and "nonmetal" refers to surrogate mines with no metal content. These will be denoted by M, LM, and NM, respectively, in this report. In all mines, the detonators were made safe, usually by removing part of the firing pin or striker mechanism; in some cases the booster charge was removed. To ensure accurate metal content in the low-metallic mines, any metal removed was replaced with an equivalent amount of metallic surrogate. Mines were emplaced both on the surface and at several depths below the surface ranging from 1 to 4 in. Depth was measured from the ground's surface to the upper-most part of the mines. To ensure accurate ground truth for comparison to demonstrator declarations of potential target locations, the positions of the

---

[2] For circular mines, the area encompassing a mine is defined as the area inside a circle of radius r_m + halo, centered about the mine. r_m is the radius of the mine, and *halo* refers to the radius added to the outside edge of a mine for determining matches to sensor declarations (see Figure III-1).

mines were surveyed after the mines were placed in the holes but before the holes were filled. It should be noted that there is some evidence that the metallic clutter at the Aberdeen site is worse than at the Socorro site (Socorro is discussed later in this chapter). The evidence comes from data collected by the AN/PSS–12 of each site. The AN/PSS–12 contains a sensitivity knob which operators periodically adjust, so a direct comparison of the sites is difficult. However, many more metallic alarms were collected at Aberdeen than at Socorro.

1. Mines Emplaced in On-Road Test Lanes at Aberdeen

The VMMD technologies were tested on three on-road lanes at Aberdeen. On-road calibration lanes were made available to the demonstrators before testing. Each of the on-road calibration lanes contained a mix of mines that closely matched the characteristics (type, burial depth) of the mines that would be encountered in the test lane. Because the test lanes were located within 10 to 40 m of each other, there was system interference between contractors when testing on adjacent lanes. This interference problem was overcome by requiring contractors to test one after the other.

Table II-1 lists the number, metal content, and diameter of the type of AT mines emplaced in each on-road test lane at Aberdeen. Also given are the totals by lane and mine type, as well as the length and mine density of each lane. Note that all the mines are approximately the same size, as indicated by their diameter. The diameter difference between the smallest mine (the TMA4 with diameter of 0.280 m) and the largest mine (the M15 with diameter of 0.337 m) is only 0.057 m.

The difference between the M15 and M15I mines is related to the explosive content of the mine. The M15I is a metal-cased mine containing a surrogate to the explosive that is normally found in an M15 mine. It is thus inert, denoted by the "I" in its name. The same explosive content differences are found in the M19 and M19I mines, and the TM62M and TM62MI mines. The only nonmetal mine is the EM12, which is a surrogate in the sense that it is designed to look like a mine and be detected as a mine. There is little variation between the total number of mines, lane length, and mine density for each of the three on-road test lanes. If the inert mines are grouped with their non-inert counterparts, then the M19 (and M19I) appears the most at 24 over the three lanes, while the EM12 and TM46 appear the fewest number of times, at 6.

Table II-1. Mines Emplaced in On-Road Lanes at Aberdeen

Name	Metal Content	Diameter (m)	Lane 11	Lane 12	Lane 15	Totals
EM12[a]	NM	0.3048	2	2	2	6
M15	M	0.3370	4	3	5	12
M15I	M	0.3370	3	4	2	9
M19[b]	LM	0.3320	4	5	3	12
M19I[b]	LM	0.3320	4	3	5	12
TM46	M	0.3050	2	2	2	6
TM62M	M	0.3200	2	2	0	4
TM62MI	M	0.3200	6	6	6	18
TM62P	LM	0.3200	5	5	5	15
TMA4	LM	0.2800	5	5	5	15
Total			37	37	35	109
Lane Length (m)			315.1	380.0	366.1	1061.2
Mines per meter of road			0.117	0.097	0.096	0.103

[a] These are plastic surrogates.

[b] The M19 and M19I are square mines of width 0.3320 m.

Table II-2 shows the distribution of mines for on-road test lanes by their metal content and their emplaced depth. Due to rounding, percentages do not always add up to 100 percent. For each of the three on-road test lanes, the number of metal and low-metal mines are nearly the same, and comprise approximately 95 percent of the total mines. Only two nonmetal mines were used in each of the on-road test lanes. The depth distribution of mines in each on-road test lane was nearly the same. Approximately 40 percent of the mines were located on the surface. The remaining 60 percent of the mines were buried, most at the 1.5-in. and 2-in. depths. Only about 15 percent of the mines were buried more deeply than 2 in.

Table II-3 shows, for a given burial depth, the percentage of metal, low-metal, and nonmetal mines on the combined on-road test lanes. We observe three notable trends. First, only one type of metal mine was buried at 4 in., the TM62M (and TM62MI). Second, only the low-metal TM62P mine was buried at 3 in. Third, the only nonmetal mine in the baseline, the EM12, appeared on the surface or at a burial depth of 2 in.

Table II-2. Mine Types and Depths for On-Road Lanes at Aberdeen

	Lane 11	Lane 12	Lane 15	Totals
Total Number Emplaced	37	37	35	109
Metal Content				
M	17 (46%)	17 (46%)	15 (43%)	49 (45%)
LM	18 (49%)	18 (49%)	18 (51%)	54 (50%)
NM	2 (5%)	2 (5%)	2 (6%)	6 (6%)
Depth				
Surface	14 (38%)	14 (38%)	15 (43%)	43 (39%)
1.5 in.	7 (19%)	7 (19%)	7 (20%)	21 (19%)
2 in.	10 (27%)	10 (27%)	8 (23%)	28 (26%)
3 in.	3 (8%)	3 (8%)	3 (9%)	9 (8%)
4 in.	3 (8%)	3 (8%)	2 (6%)	8 (7%)

Table II-3. Mine Depths and Metal Content for On-Road Lanes at Aberdeen

	Metal	Low Metal	Nonmetal	Totals
Total Number Emplaced	49	54	6	109
Depth				
Surface	18 (37%)	22 (43%)	3 (50%)	43 (39%)
1.5 in.	12 (25%)	9 (17%)	0 (0%)	21 (19%)
2 in.	11 (22%)	14 (26%)	3 (50%)	28 (26%)
3 in.	0 (0%)	9 (17%)	0 (0%)	9 (8%)
4 in.	8 (16%)	0 (0%)	0 (0%)	8 (7%)

2. Mines Emplaced in Off-Road Test Lanes at Aberdeen

Table II-4 lists the AT mines emplaced in the two off-road test lanes at Aberdeen. The only nonmetal mine, the EM12, was not emplaced in either off-road test lane. The M15 (and M15I) appears the most at 15 times, while the TM46 appears the least at 2 times. The total number of mines emplaced in the off-road test lanes was only 58, compared to 109 for the on-road test lanes. There was one less lane than for the on-road test lanes, and each lane was about half the length of the average length of the on-road test lanes. The resultant mine density for both off-road test lanes was 0.153 m^{-1}, or approximately 50 percent greater than the on-road test lane mine densities.

Table II-5 shows the distribution of mines for the off-road test lanes by metal content and emplaced depth. About half the mines were metallic while the other half were low metal. No nonmetal mines were used on the off-road lanes at Aberdeen. Again, approximately 40 percent of the mines were located on the surface. One mine in lane 2 was emplaced at a depth of 1 in. This was the only occurrence of a mine emplaced at this depth at Aberdeen for both on-road and off-road test lanes. Only 17 percent of the mines were buried at depths greater than 2 in. As with the on-road test lanes, about 40 percent

of the mines were emplaced at depths of 1.5 in. and 2 in., but more mines were buried 1.5 in. deep than 2 in. deep. For the on-road test lanes, more mines were buried at 2 in. than at 1.5 in. (see Table II-3).

Table II-4. Mines Emplaced in Off-Road Lanes at Aberdeen

Name	Metal Content	Diameter (m)	Lane 2	Lane 4	Totals
EM12[a]	NM	0.3048	0	0	0
M15	M	0.3370	6	5	11
M15I	M	0.3370	2	2	4
M19[b]	LM	0.3320	4	3	7
M19I[b]	LM	0.3320	1	3	4
TM46	M	0.3050	1	1	2
TM62M	M	0.3200	4	2	6
TM62MI	M	0.3200	3	5	8
TM62P	LM	0.3200	4	4	8
TMA4	LM	0.2800	4	4	8
Total			29	29	58
Lane Length (m)			190.0	190.1	380.1
Mines per meter of road			0.153	0.153	0.153

[a] These are plastic surrogates.

[b] The M19 and M19I are square mines of width 0.3320 m.

Table II-5. Mine Types and Depths for Off-Road Lanes at Aberdeen

	Lane 2	Lane 4	Totals
Total Number Emplaced	29	29	58
Metal Content			
M	16 (55%)	15 (52%)	31 (53%)
LM	13 (45%)	14 (48%)	27 (47%)
NM	0 (0%)	0 (0%)	0 (0%)
Depth			
Surface	12 (41%)	12 (41%)	24 (41%)
1 in.	1 (3%)	0 (0%)	1 (2%)
1.5 in.	7 (24%)	8 (28%)	15 (26%)
2 in.	4 (14%)	4 (14%)	8 (14%)
3 in.	2 (7%)	2 (7%)	4 (7%)
4 in.	3 (10%)	3 (10%)	6 (10%)

Table II-6 shows the mine distribution for the off-road test lanes at Aberdeen by depth and metal content. No nonmetal mines were emplaced in the off-road test lanes at

Aberdeen. As with the on-road test lanes, the metal TM62M (and TM62MI) mine was the only mine found at a depth of 4 in., and the low-metal TM62P mine was the only mine buried at 3 in. (depths were chosen to be consistent with doctrine for each mine model).

Table II-6. Mine Depths and Metal Content for Off-Road Lanes at Aberdeen

	Metal	Low Metal	Totals
Total Number Emplaced	31	27	58
Depth			
Surface	12 (39%)	12 (44%)	24 (41%)
1 in.	1 (3%)	0 (0%)	1 (2%)
1.5 in.	8 (26%)	7 (26%)	15 (26%)
2 in.	4 (13%)	4 (15%)	8 (14%)
3 in.	0 (0%)	4 (15%)	4 (7%)
4 in.	6 (19%)	0 (0%)	6 (10%)

B. SOCORRO TEST LANES

VMMD technologies were tested in two road environments each including one or more calibration and test lanes:

- *On-road.* Mines were buried in seven calibration and seven test lanes consisting of dirt with rocks scattered throughout. The on-road test lanes were prepared by removing, replacing, and compacting the soil in the road-bed. The test lanes were approximately 80 to 190 m long and 3 m wide. Lane orientation varied over the site. The total area covered by the on-road lanes was 3,090 m^2.

- *Off-road.* Mines were buried in one calibration lane and one test lane consisting of an unprepared dirt road. The test lane was 89.6 m long and 3 m wide. The number of mines emplaced in the off-road test lane was 24. The total area covered by the off-road test lane was 268.8 m^2.

Unlike Aberdeen, the calibration and test lanes were located in four geographically distinct areas. The four areas were separated by no less than 50 m. Test lane 1 was located in area A. Test lanes 4 and 6 were located in area B. Test lane 8 was located in area C, and test lanes 11, 12, 13, and 16 were located in area D. The soil characteristics of area A were noticeably different from the other three areas.

Mine density was chosen to ensure that the areas encompassing the mines plus halo did not overlap. The same ten mine types used at Aberdeen were emplaced at Socorro. Mines were emplaced both on the surface and at several depths below the surface ranging from 1 inch deep to depths not exceeding 4 in. Depth was measured from the surface to the top of the mines. To ensure accurate ground truth for comparison to

demonstrator declarations of potential target locations, the positions of the mines were surveyed after the mines were placed in the holes but before the holes were filled.

1. Mines Emplaced in On-Road Test Lanes at Socorro

The VMMD technologies were tested on seven on-road lanes at Socorro. Seven on-road calibration lanes were made available to the demonstrators before testing. Each of the on-road calibration lanes contained a mix of mines whose type and burial depths closely matched the characteristics of the mines that would be encountered in the test lane. The seven on-road test lanes were approximately 80 to 190 m long and 3.0 m wide, resulting in an approximate total test area of 3,090 m^2, which is nearly the same as at Aberdeen, where the area was 3,185 m^2. In a given area, the test lanes ran parallel to one another and were separated by at least 10 m. Because the Socorro site was divided into four areas, contractors could take turns in a given area and avoid system interference problems.

Table II-7 lists the number, type, metal content, and diameter of the AT mines emplaced in each on-road test lane at Socorro. Also given are the totals by lane and mine type, as well as the length and mine density of each lane.

Table II-7. Mines Emplaced in On-Road Lanes at Socorro

Name	Metal Content	Diameter (m)	Lane 1	Lane 4	Lane 6	Lane 8	Lane 11	Lane 12	Lane 13	Totals
EM12[a]	NM	0.3048	1	1	1	1	1	1	1	7
M15	M	0.3370	1	2	1	3	2	1	2	12
M15I	M	0.3370	0	0	1	1	2	1	1	6
M19[b]	LM	0.3320	2	3	1	2	2	1	1	12
M19I[b]	LM	0.3320	1	1	2	3	2	2	3	14
TM46	M	0.3050	1	1	1	1	1	1	1	7
TM62M	M	0.3200	3	3	4	5	0	3	2	20
TM62MI	M	0.3200	2	2	0	1	5	1	3	14
TM62P	LM	0.3200	2	2	2	3	2	2	2	15
TMA4	LM	0.2800	1	2	2	4	2	2	2	15
Total			14	17	15	24	19	15	18	122
Lane Length (m)			80.0	170.1	160.0	190.0	160.0	110.0	160.0	1030.1
Mines per meter of road			0.175	0.100	0.094	0.126	0.119	0.136	0.113	0.118

[a] These are plastic surrogates.

[b] The M19 and M19I are square mines of width 0.3320 m.

The total number of mines, lane length, and mine density for each of the seven on-road test lanes at Socorro varied greatly. The TM62M (and TM62MI) appeared the

most, at 34 times. The nonmetal EM12 and the metal TM46 were used sparingly; only one of each was buried in each of the seven test lanes. The total number of mines buried in a given lane ranged from 14 in lane 1 to 24 in lane 8. The length of the lanes varied from 80 m for lane 1 to 190 m for lane 8. Finally, the mine density varied by a factor of 2: from 0.094 m^{-1} in lane 6 to 0.175 m^{-1} in lane 1. The total number of mines emplaced in the on-road test lanes was 122, compared to 109 at Aberdeen.

Table II-8 shows the distribution of mines for on-road test lanes by metal content and emplaced depth. For each of the seven on-road test lanes, the number of metal and low-metal mines was nearly the same, and comprised approximately 95 percent of the total mines. Only one nonmetal mine was used in each of the on-road test lanes. In terms of emplaced depth, there was little variation in the distribution of mines in each on-road test lane. Approximately 40 percent of the mines were located on the surface. The remaining 60 percent of the mines were buried, most at the 1.5-in. and 2-in. depths. Only about 15 percent of the mines were buried more deeply than 2 in.

Table II-8. Mine Types and Depths for On-Road Lanes at Socorro

	Lane 1	Lane 4	Lane 6	Lane 8	Lane 11	Lane 12	Lane 13	Totals
Total Number Emplaced	14	17	15	24	19	15	18	122
Metal Content								
M	7 (50%)	8 (47%)	7 (47%)	11 (46%)	10 (53%)	7 (47%)	9 (50%)	59 (48%)
LM	6 (43%)	8 (47%)	7 (47%)	12 (50%)	8 (42%)	7 (47%)	8 (44%)	56 (46%)
NM	1 (7%)	1 (6%)	1 (7%)	1 (4%)	1 (5%)	1 (7%)	1 (6%)	7 (6%)
Depth								
Surface	5 (36%)	8 (47%)	6 (40%)	8 (33%)	8 (42%)	5 (33%)	8 (44%)	48 (39%)
1.5 in.	3 (21%)	3 (18%)	4 (27%)	6 (25%)	5 (26%)	4 (27%)	4 (22%)	29 (24%)
2 in.	4 (29%)	4 (24%)	3 (20%)	6 (25%)	4 (21%)	4 (27%)	4 (22%)	29 (24%)
3 in.	1 (7%)	1 (6%)	1 (7%)	2 (8%)	1 (5%)	1 (7%)	1 (6%)	8 (7%)
4 in.	1 (7%)	1 (6%)	1 (7%)	2 (8%)	1 (5%)	1 (7%)	1 (6%)	8 (7%)

Table II-9 shows the number of mines by burial depth for the metal, low-metal, and nonmetal mines for the on-road test lanes at Socorro. The same trends observed at Aberdeen were present at Socorro. Namely, the metal TM62M (and TM62MI) mine was the only mine found at a depth of 4 in., and the low-metal TM62P mine was the only mine buried at 3 in. In addition, the nonmetal EM12 mine was only emplaced at a depth of 2 in.; at Aberdeen, this mine was found on the surface.

Table II-9. Mine Depths and Metal Content for On-Road Lanes at Socorro

	Metal	Low Metal	Non-metal	Totals
Total Number Emplaced	59	56	7	122
Depth				
Surface	24 (41%)	24 (43%)	0 (0%)	48 (39%)
1.5 in.	14 (24%)	15 (27%)	0 (0%)	29 (24%)
2 in.	13 (22%)	9 (16%)	7 (100%)	29 (24%)
3 in.	0 (0%)	8 (14%)	0 (0%)	8 (7%)
4 in.	8 (14%)	0 (0%)	0 (0%)	8 (7%)

2. Mines Emplaced in Off-Road Test Lanes at Socorro

The AT mines emplaced in the one off-road test lane at Socorro are listed in Table II-10. The only nonmetal mine, the EM12, was not emplaced in lane 16. In addition, none of the inert mines were emplaced in lane 16. The TM62M appears the most at 9 times, while the TM46 appears the least at 1 time. The total number of mines emplaced in the off-road test lanes was only 24, compared to 122 for the on-road test lanes, and it is also less than half the total number of mines emplaced in the off-road test lanes at Aberdeen. The mine density for the off-road test lane was 0.268 m^{-1}, or approximately twice that of the average mine density for the on-road test lanes. This is an important point which will be discussed in relation to the performance measure of false-alarm rate in Chapter 3.

Table II-10. Mines Emplaced in Off-Road Lanes at Socorro

Name	Metal Content	Diameter (m)	Lane 16
EM12[a]	NM	0.3048	0
M15	M	0.3370	4
M15I	M	0.3370	0
M19[b]	LM	0.3320	4
M19I	LM	0.3320	0
TM46	M	0.3050	1
TM62M	M	0.3200	9
TM62MI	M	0.3200	0
TM62P	LM	0.3200	3
TMA4	LM	0.2800	3
Total			24
Lane Length (m)			89.6
Mines per meter of road			0.268

[a] These are plastic surrogates.

[b] The M19 and M19I are square mines of width 0.3320 m.

II-9

The distribution of mines for the off-road test lane by metal content and emplaced depth is shown in Table II-11. More than half of the mines are metallic, while the remainder are low metal. No nonmetal mines were used on the off-road lane at Socorro. This is consistent with the test lanes at Aberdeen. Approximately 40 percent of the mines were located on the surface. The remaining 62 percent of the mines were buried at depths of 1.5, 2, 3, and 4 in. As with the on-road test lanes, about 40 percent of the mines were emplaced at depths of 1.5 and 2 in., and 25 percent of the mines were emplaced more deeply than 2 in., with 2 buried at 3 in. and 4 buried at 4 in.

Table II-12 shows the mine distribution for the off-road test lanes at Socorro by burial depth and metal content. As with the on-road test lanes, the metal TM62M (and TM62MI) mine was the only mine found at a depth of 4 in., and the low-metal TM62P mine was the only mine buried at 3 in.

Table II-11. Mine Types and Depths for Off-Road Lane at Socorro

	Lane 16
Total Number Emplaced	24
Metal Content	
M	14 (58%)
LM	10 (42%)
NM	0 (0%)
Depth	
Surface	9 (38%)
1.5 in.	6 (25%)
2 in.	3 (13%)
3 in.	2 (8%)
4 in.	4 (17%)

Table II-12. Mine Depths and Metal Content for Off-Road Lane at Socorro

	Metal	Low Metal	Totals
Total Number Emplaced	14	10	24
Depth			
Surface	6 (43%)	3 (30%)	9 (38%)
1.5 in.	3 (21%)	3 (30%)	6 (25%)
2 in.	1 (7%)	2 (20%)	3 (13%)
3 in.	0 (0%)	2 (20%)	2 (8%)
4 in.	4 (29%)	0 (0%)	4 (17%)

Note that only metal mines were emplaced at a depth of 4 in. and only low-metal mines were emplaced at a depth of 3 in. Because the distribution of metal, low-metal, and nonmetal mines is not uniform for two of the five burial depths at both sites, no performance measures will be analyzed as a function of depth.

C. ATD SCHEDULE

Table II-13 shows the order in which the test lanes were completed by each contractor. The nomenclature is L-# where L is a one- or two-digit number indicating the lane number, and # is either a 1 or 2 corresponding to the first and second passes of the lane. For both sites, all five contractors were able to complete the required tests. Each on-road and off-road test lane was traversed two times, where the direction of travel of was reversed between successive runs on the same lane. Note that GeoC completed the test requirements first at both sites.

D. ADDITIONAL RUNS

In addition to the scored runs conducted during daylight hours, four additional runs were made. They included night runs, physical marking runs, tele-operated runs, and morning runs. These tests were included in the overall ATD as a measure of system performance under special circumstances. Table II-14 shows which contractors performed the four additional tests at each of the sites. Note that all five contractors conducted night tests at both sites and that four out of the five contractors conducted physical marking tests. At Aberdeen, the only other additional run was the tele-operated run conducted by GeoC. At Socorro, EG&G and GeoC conducted tele-operated tests, and CRC and GDE conducted morning tests. Note that CDC's vehicle was always tele-operated, hence separate tele-operated runs were not necessary. Each of the additional tests typically involved two or three passes of a given lane. Table II-15 gives a complete list of the lanes that were used for each of the additional runs, where N denotes night run, PM denotes a physical-marking run, EM denotes an electronic-marking run performed in conjunction with a physical-marking run, T denotes tele-operated run, and M denotes morning run. All the additional runs were made on the on-road lanes

Table II-13. ATD Completion Schedule (Lane No.– Pass)

Aberdeen						
	Jun. 9	**Jun. 10**	**Jun. 11**	**Jun. 15**	**Jun. 16**	**Jun. 17**
CDC	2-1, 2-2	15-1, 15-2	11-1, 11-2	12-1	12-2, 4-1	4-2
CRC	12-1, 12-2	4-1, 4-2, 11-1			11-2, 2-1, 2-2, 15-1, 15-2	
EG&G	11-1, 11-2		12-1	15-1	15-2, 12-2, 4-1	2-1, 4-2, 2-2
GDE	15-1, 11-1	15-2, 12-1	12-2, 11-2, 2-1	2-2	4-1	4-2
GeoC	11-1, 12-1, 12-2, 11-2, 15-1, 15-2	2-1, 2-2	4-1, 4-2			

Socorro						
	Jul. 14	**Jul. 15**	**Jul. 16**	**Jul. 17**	**Jul. 20**	**Jul. 21**	**Jul. 22**
CDC	13-1, 11-1	11-2, 13-2	1-1, 1-2, 4-1, 4-2	8-1, 8-2	12-1, 12-2, 16-1	6-1, 6-2, 16-2	
CRC		8-1, 8-2, 1-1, 1-2	6-1, 6-2, 4-1, 4-2, 11-1, 11-2, 12-1, 12-2	13-1	13-2, 16-1, 16-2		
EG&G			8-1, 8-2, 11-1, 13-1, 11-2, 13-2	4-1, 4-2	6-1, 6-2	12-1, 12-2, 16-1, 16-2	1-1, 1-2
GDE		8-1, 8-2, 6-1, 6-2	13-1, 13-2, 1-1	11-1	4-1, 4-2, 1-2	12-1, 12-2	11-2, 16-1, 16-2
GeoC	1-1, 1-2	11-1,13-1, 12-1,12-2, 13-2, 11-2	8-1, 8-2, 4-1, 4-2, 6-1, 6-2	16-1, 16-2			

Table II-14. Additional Runs for Contractors at Aberdeen and Socorro

Contractor	Aberdeen				Socorro			
	Night	Physical Marking	Tele-Operated	Morning	Night	Physical Marking	Tele-Operated	Morning
CDC	✓				✓		*	
CRC	✓	✓			✓	✓		✓
EG&G	✓	✓			✓	✓	✓	
GDE	✓	✓			✓	✓		✓
GeoC	✓	✓	✓		✓	✓	✓	

* CDC's system is tele-operated, hence separate tele-operated runs were not necessary.

Night runs were made several hours after sunset; morning runs were made before 10:00 a.m. Tele-operated runs involved the remote operation of the contractor vehicle. For physical marking runs, the vehicle sprayed marks onto the surface of the lanes to designate an alarm. The marks were surveyed and an alarm file was created after the vehicle completed a lane. Usually, the contractor provided electronic alarms in addition to the physical alarms, allowing the direct comparison of the two methods of alarm marking.

The results of the additional runs appear in Appendix B. Tables B-6 through B-8 summarize the additional runs conducted at Aberdeen, and Tables B-17 through B-24 summarize the additional runs conducted at Socorro. In Chapter V of this report (Individual Contractor Performance), we will discuss these additional tests. The reason for not including additional runs in Chapter IV (Performance Comparisons) is related to the poor statistical significance of the performance measures of the additional runs. There are three reasons why these performance measures are not statistically significant. First, there were only a very small number of mine encounters for a given test condition, the result of a given contractor making only two or three passes on a lane. Second, not all contractors performed each test (except the night test). Third, for all the additional tests, the contractors did not make passes on the same lanes. For instance (see Table II-15), at Socorro, GeoC conducted three night runs on lanes 11, 12, and 13, while EG&G conducted night runs on lanes 4 and 6. This lack of comparable encounters allows us only to make observations relating to the specifics of each of the additional runs.

Table II-15. ATD Additional Runs Schedule (Lane No.– Run Type, Pass)

Aberdeen								
	Jun. 9	**Jun. 10**	**Jun. 11**	**Jun. 15**	**Jun. 16**	**Jun. 17**	**Jun. 18**	**Jun. 19**
CDC		15-N1, 15-N2						
CRC						15-N1, 15-N2	11-PM1	
EG&G		12-N1, 11-N2					15-EM1, 15-PM1	
GDE						11-N1, 11-N2	15-PM1	
GeoCenters		11-N1, 11-N2				11-T1, 11-T2		12-EM1, 12-PM1

Socorro							
	Jul. 14	**Jul. 15**	**Jul. 16**	**Jul. 17**	**Jul. 20**	**Jul. 21**	**Jul. 22**
CDC					11-N1, 13-N2, 13-N3		
CRC					8-EM1, 8-PM1, 8-EM2, 8-PM2, 4-N1, 4-N2, 6-N3		4-M1, 4-M2, 6-M3
EG&G	6-N1, 4-N2, 4-N3						4-EM1, 4-PM1, 4-EM2, 4-PM2, 4-EM3, 4-PM3, 6-T1, 6-T2, 6-T3
GDE					8-N1, 8-N2	8-EM1, 8-PM1, 8-EM2, 8-PM2	4-M1, 4M2
GeoCenters	11-N1, 12-N2, 13-N3				8-EM1, 8-PM1, 8-EM2, 8-PM2, 8-T1, 8-T2		

Key: N = night run
PM = physical marking run
EM = electronic marking run

T = tele-operated run
M = morning run

III. MEASURES OF PERFORMANCE

A. DETERMINING A DETECTION

Contractor declarations of potential mine locations are either matched to an emplaced mine and considered a "detection," or not matched to a mine and called a "false alarm." Declarations are matched to emplaced mines if the declaration is within a critical distance, R_{halo}, of the edge of the mine. The value for R_{halo} is taken to be 1 m, as is directed in the GSTAMIDS ORD. This distance criterion can produce more than one candidate declaration which matches a particular emplaced mine. For this case, the demonstrator is credited with a single detection of the mine, attributed to the nearest declaration, while the other declarations within R_{halo} are considered redundant and are not counted as either detections or false alarms. If the declaration is within R_{halo}, but outside the mine lane, it is still scored as a valid detection. If a declaration is not within R_{halo} of any emplaced mine, and is located within the mine lane, then that declaration is considered a false alarm. These possible outcomes are illustrated in Figure III-1.
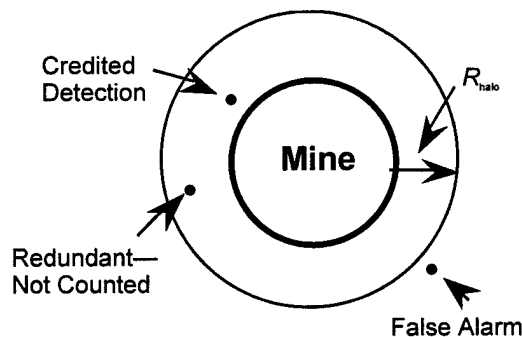
Figure III-1. Mine and Halo

B. DETECTION PROBABILITY AND FALSE-ALARM RATE

The probability of detection is simply the fraction of the emplaced mines that are detected by a contractor:

$$P_d = \frac{\text{number of mines detected}}{\text{number of mines emplaced}} \qquad (1)$$

We calculated P_d for each road condition (on- and off-road), mine depth (surface and subsurface), metal content of the mine (metal, low metal, and nonmetal), and sensor type.

The false-alarm rate, *FAR*, is defined as the number of false alarms in the test site divided by the total area of the site, A_{site}.[3] The *FAR* is separately calculated for each road condition and sensor type combination. Note that some false alarms can be credited to a single sensor, while others could be credited to more than one sensor. If more than one sensor produced a single false alarm, we use that alarm in each of the sensor's *FAR*. Thus, the *FAR* for a contractor's total system will not be the sum of the *FAR*s from each of the individual sensors.

C. CORRECTION TO THE FALSE-ALARM RATE

The false-alarm rate as defined by TECOM can be misleading when the density of mines within the mine lane is large, because only the fraction of the mine lane that is not included within R_{halo} of each of the mines can provide an opportunity for a false alarm. Dividing the number of false alarms by the entire mine lane area, A_{site}, makes *FAR* into a quantity that is dependent on the mine density in the test lane, as well as on the choice of R_{halo}. Therefore, if the density of the mines within the mine lane is large (which is the case for all mine lanes and especially true in the off-road lane used at Socorro), then the *FAR* underestimates the true density of false alarms and misrepresents the performance of the sensors. This is clearly not a satisfactory definition of the false-alarm rate.

A better measure of the false-alarm rate should only be dependent on the sensor and on the bare (unmined) soil characteristics of the region being surveyed. To construct this more robust metric for the false-alarm rate, the number of false alarms should be divided by the area of the lane that is *not* within R_{halo} of a mine (in other words, use the same area from which the false alarms are drawn). This formulation should be used because within the halo radius of a mine there is no "operational" opportunity for a false alarm. We define this area to be A_{site_fa}, where $A_{site\_fa} = (A_{site} - \Sigma_{mines} A_{dec})$. A_{dec} is the average area covered by a mine plus its halo:

$$A_{dec} = \pi\left(\overline{R_{mine}} + R_{halo}\right)^2 \quad . \tag{2}$$

---

3   See Section 2.2.4 of *Detailed Test Plan for the Engineering Development Test (Advanced Technology Demonstration) of the Ground Standoff Minefield Detection System*, TECOM Project No. 8-ES-025-GMD-001.

The difference between this "true" false-alarm rate and the *FAR* defined by TECOM depends on the density of mines in the test lanes. For example, the *FAR* on some on-road lanes at Socorro will be as much as 30 percent larger using the true measure. In an extreme case, 41 percent of Socorro's off-road lane (lane 16) was covered by mines plus their halos, thereby making the true *FAR* 1.6 times larger than the *FAR* from TECOM's definition.

In spite of this deficiency, we use TECOM's *FAR* definition in the remainder of this report.

D. PROBABILITY OF FALSE ALARM

The probability of a false alarm, P_{fa}, is defined as the probability that there will be a false alarm within the area of the average mine plus its halo. We use this measure of P_{fa} as a surrogate for the true P_{fa}, which is the number of false alarms divided by the number of opportunities for false alarms. Since it is difficult, if not impossible, to determine the actual number of opportunities within a mine lane, this areal-based surrogate metric is necessary. The areal-based definition used herein also provides an excellent intuitive measure: since all of the mines are very similar in size, P_{fa} gives the probability that a mine in this test was detected purely by an "accident" caused by the overlap of a false alarm with a mine's halo.

As in previous tests evaluated by IDA (Andrews et al., 1996 and 1998), we use the quantities A_{site_fa} and A_{dec}, as defined above, to compute the P_{fa}. Only the *unique* area of the mine lane covered by the characteristic false-alarm area associated with each false alarm is used to determine P_{fa} (see Figure III-2). Thus, no double counting, and no counting of area within R_{halo} of the emplaced mines results. This ensures a P_{fa} that is bound by zero and one.
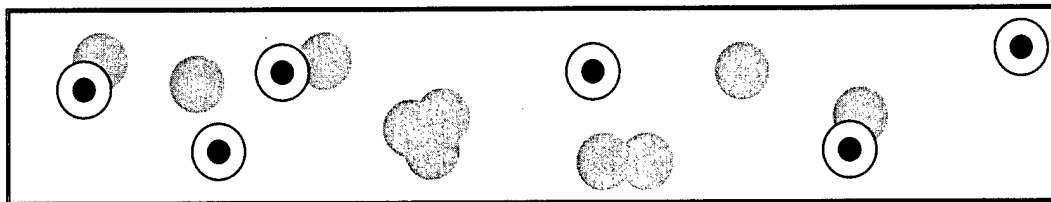
Figure III-2. Example of a P_{fa} Calculation in a Mine Lane. The mines are marked by the black circles. The *halo* area is defined by the circle surrounding the mines. The gray circles represent the false alarms. Only the area shown in gray is counted in the determination of P_{fa}.

Thus, P_{fa}, is then calculated as the sum of the unique area of declaration (A_{dec}) for each false alarm divided by the total area of the site where there is an opportunity for a false alarm:

$$P_{fa} = \left(\frac{\sum\limits_{unique} A_{dec}}{A_{site\_fa}} \right) . \qquad (3)$$

The quantity $\sum\limits_{unique} A_{dec}$ is the sum of A_{dec} for all false alarms, but, as shown in Figure III-2, does not double count overlaps of area. Again, since the mines used in this test are all AT mines of similar size, P_{fa} effectively gives the probability that any of the mines in the test would be detected by a random false alarm.

E. STATISTICAL UNCERTAINTY

P_d and *FAR* are statistical measures. The confidence to which they are determined will depend on the size of the populations measured. Error bars are calculated for probability of detection using a binomial distribution and determining the 90-percent confidence interval (Bevington, 1969). The binomial distribution is employed to estimate lower and upper bounds for the detection rates from the demonstration (Simonson, 1998). To determine the confidence interval, binomial probabilities are calculated for the likelihood of detecting X mines out of N opportunities for each population of interest (see Figure III-3). The lower and upper bounds are determined iteratively such that the binomial distribution for each bound contains the measured P_d within its 90-percent confidence interval. If the confidence intervals of the performance metrics for different systems overlap, there is no statistically significant difference between the two measurements at the indicated confidence level. If the confidence intervals of the metric are separated, then one system has performed "better" than the other, in terms of that metric.

Uncertainties are calculated only for the probability of detection. A substantial effort was made to include a sufficient number of encounters to provide statistical confidence in the determination of P_d. But when the mines are divided into categories such as metal content, depth, filler, etc., the uncertainty for these subsets increases substantially.
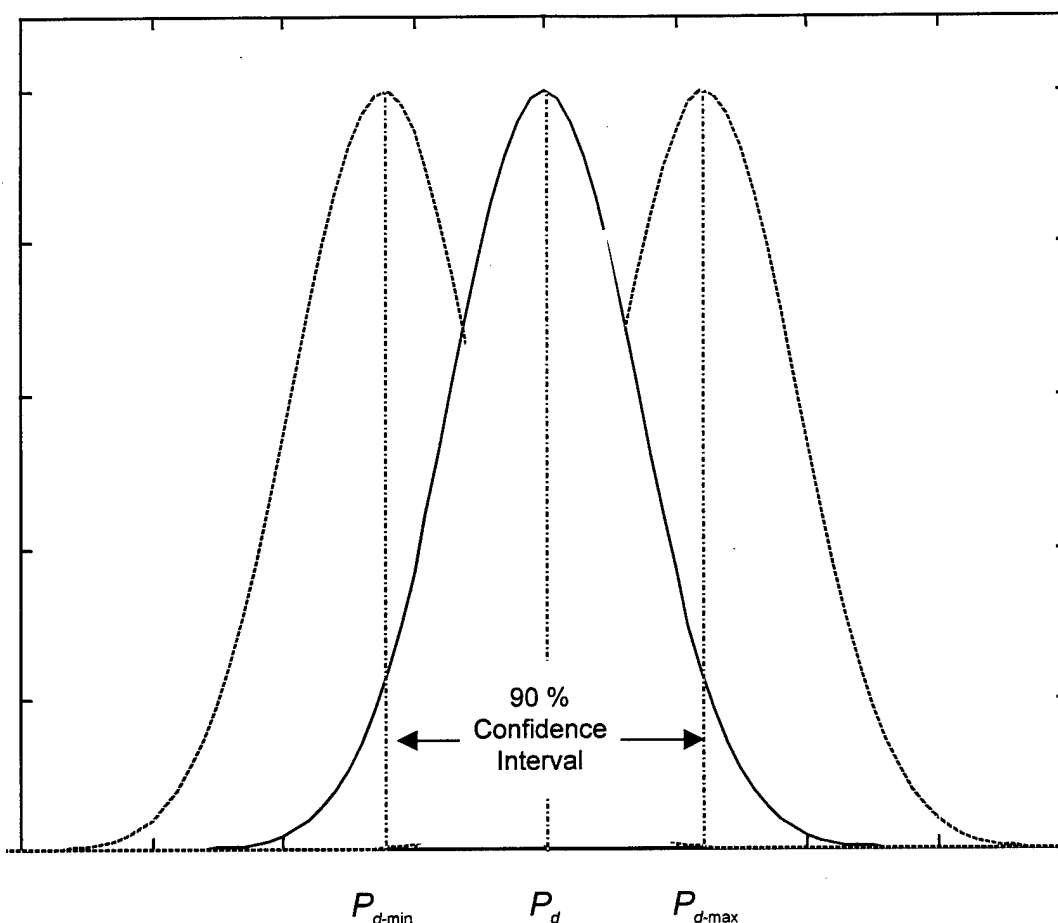
**Figure III-3. Binomial Distribution Model for Upper Bound of the
Confidence Interval for Probability of Detection**

The figure shows three overlapping bell curves with vertical dashed lines at their peaks labeled along the x-axis as $P_{d\text{-min}}$, P_d, and $P_{d\text{-max}}$. A horizontal double-arrow between the outer two curves is labeled "90 % Confidence Interval".

F. ROC CURVES AND THE d PERFORMANCE METRIC

It is possible to represent sensor capability by means of a receiver operating characteristic (ROC) curve. The ROC curve describes the relationship between P_d and P_{fa} as a sensor's threshold for declaring a detection is changed. The average ratio of a target's signal to the clutter signal, called the d metric in this report, can be derived from P_d and P_{fa} and is another measure of a sensor's capability.

Figures III-4 and III-5 illustrate these principles. Figure III-4 shows the signal-strength distribution of clutter and noise (on the left), as well as the signal-strength distribution of target, clutter, and noise (on the right). For the purpose of this discussion, we assume that the signal contribution from clutter and noise is the same when surveying mined or unmined ground, hence the difference between the distributions in Figure III-4 is a simple offset that is due to the target's signal strength. In this example, the

III-5

distributions are Gaussian, and the offset is chosen to be 3σ. The value for d is thus 3, and is the average value of the target-to-clutter value.
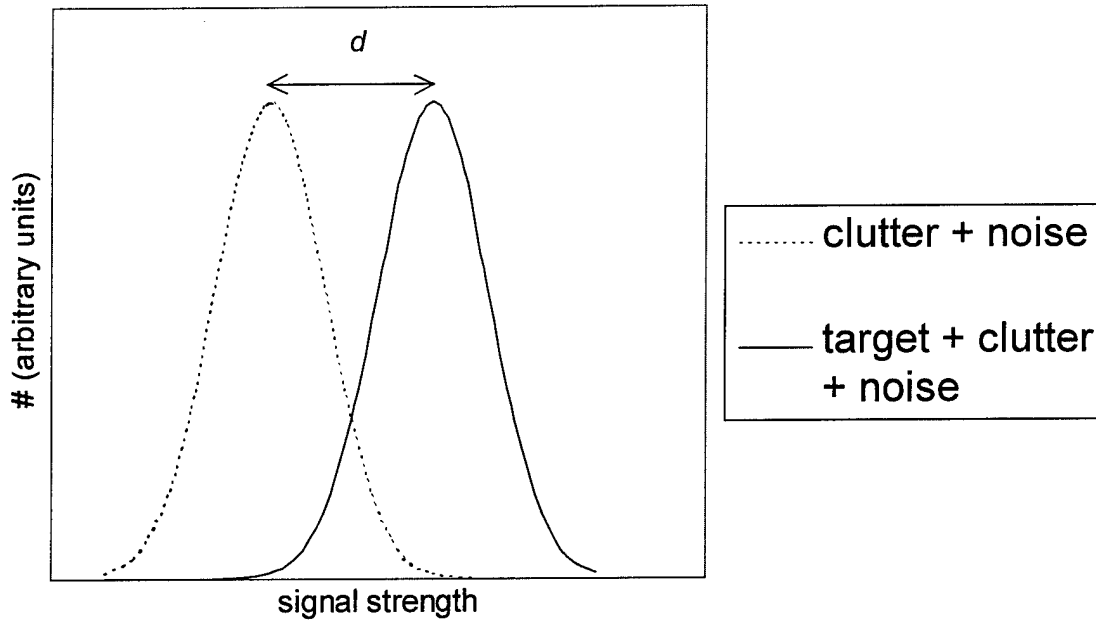
Figure III-4. Separation of the Signal Strength of Clutter + Noise and Target + Clutter + Noise. In this example, the separation of the distributions is 3σ, where σ is the standard deviation of each of the distributions. This separation is given by the quantity d. See text for details.

Consider a threshold that is set on Figure III-4 such that all signals below the threshold are not considered mines, and all signals above the threshold are considered mines. Both the probability for correctly choosing mines (accepting signals from the solid curve), as well as the probability for choosing false alarms (accepting signals from the dashed curve) change as the threshold level changes. These probabilities are the P_d and P_{fa}, respectively. Even though the P_d and P_{fa} values change with the choice of threshold, the fundamental ability of the sensor to separate targets from false alarms does not change, since the curves in Figure III-4 are always separated by $d = 3$.

Figure III-5 shows P_d vs. P_{fa} for $d = 1$, 2, and 3. Since each of these curves represents a single value of d (or a single value for the average target-to-clutter separation), they represent *isoperformance curves* for the sensors. If the detection and false alarm probabilities are known, d can be computed:

$$d = \sqrt{2}\left(\text{erfinv}(1 - 2P_{fa}) - \text{erfinv}(1 - 2P_d)\right) , \tag{4}$$

where erfinv(x) is the inverse error function of x.
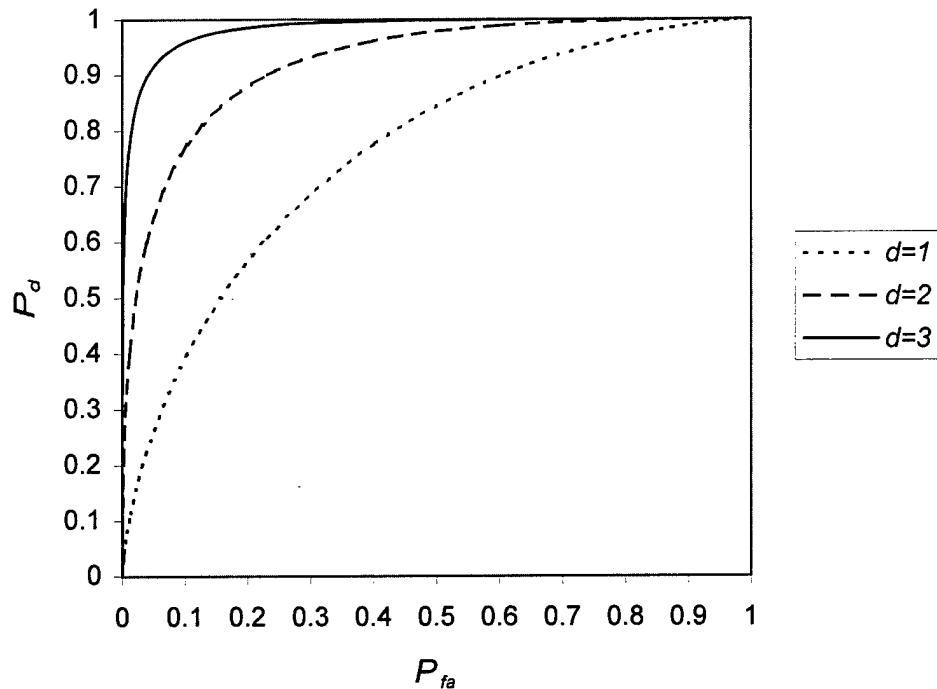
Figure III-5. P_d vs. P_{fa} for Different Values of d. Each curve represents points made by varying the threshold on a sensor, while keeping the performance of the sensor constant. See text for details.

The advantage of using the ROC curves to assess performance—which is no more than plotting a contractor's performance on P_d vs. P_{fa} plots and computing the values for the d metric—permits us to separate a contractor's choice of threshold from its ability to distinguish mines from clutter. This can sometimes be more telling than simply looking at P_d and *FAR*. When computing the error on the value of d, we take the errors on P_d, place them in Eq. 4 above, and obtain the error bounds on d. We do not include errors in P_{fa}, which are small but still contribute to the overall uncertainty in the d metric.

G. POSITION RESOLUTION

For each contractor, we compile the distribution of *miss distances* for all detections (both credited and redundant) in the along-track and cross-track dimensions. The miss distance is defined as the difference between the declaration position and the center of a mine. From these distributions we compute the position resolution, or root mean square (RMS), as well as the offset, or bias, of the sensor systems in detecting AT landmines. The RMS is a measure of the intrinsic position resolution of the sensor system. The bias of the sensor system is a measure of the systematic offset in the estimated position of the mines.

III-7

We assume that the miss-distance distributions will exhibit two characteristic shapes: first, a flat shape caused by randomly distributed "lucky" false alarm overlaps; and second, a Gaussian shape that results from the detector system actually sensing mines. This shape assumption is in fact an excellent match to the actual distributions, as will be shown in the contractor performance section of this report.

To extract the RMS resolution and bias of the contractors' sensors, it is not accurate to simply compute the mean and standard deviation of the miss-distance distribution, because random false alarms contribute a constant (flat) background to these distributions. This false-alarm background contributes to the RMS, and, ideally, we want only to measure the RMS and bias of the sensor detecting a mine.

We can separate the false alarms from the detections by fitting the along- and cross-track distributions to the following function:

$$ f = c + a \cdot e^{-\frac{(x-m)^2}{2w^2}} \quad . \tag{4} $$

The constant term c represents the flat false-alarm contribution to the detections; the Gaussian parameters a, m, and w model the response of the sensor system to the mines, with w and m representing the RMS and bias, respectively. The miss-distance data used in the fit was binned in 10-cm bins, with the error in each bin taken to be the square root of the number of entries in the bin. If there are no entries in a bin, we took the error to be 1. The fits are performed by finding the function parameters of f which minimize the χ^2 of the fit, where $\chi^2 = \sum_i (x_{fit} - x_i)^2 \sigma_i^2$, where i is the index of a given bin.

In summary, the RMS gives the resolution (or spread) of the sensors' position estimate, while the bias gives the average offset in the sensor's position estimate. We provide the RMS resolution and bias for each of the contractors for different road conditions, mine dispositions, and sensor types.

H. DETECTION SPEED

We calculated the average detection speed of the five contractors at Aberdeen and Socorro for both on-road and off-road conditions (see Chapter IV). Speeds were computed for the scored daytime runs by comparing the first and last lines of each electronic alarm file. Each line contained a time-stamp and associated vehicle-position. Detection speed was found simply by dividing the distance traveled by the time required to travel the distance. This was done for each pass of a given road-type and averages were then

taken. One contractor, EG&G, did not include time-stamps in their electronic alarm files, and so we could not compute the detection speed of its system.

IV. PERFORMANCE COMPARISON

Using data collected at the Aberdeen site, the Socorro site, and the combined data from both test sites, we compare the contractors' performance. Our analysis separates detection of subsurface and surface mines and on-road and off-road performance, as in the exit criteria.

A. ON-ROAD, SUBSURFACE MINES

1. Aberdeen Results

Figure IV-1 shows P_d vs. *FAR* for the five contractors, as well as the exit criteria for this test. CDC, GeoC, EG&G, and GDE achieved a P_d greater than the exit criterion of 85 percent. CRC, on the other hand, exhibited a detection rate somewhat below the exit criteria (over 7 percentage points), and its 90-percent confidence interval also failed to meet the detection probability criterion. CRC was the only contractor to achieve the *FAR* criterion of 0.042/m². P_d and *FAR* results are summarized in Table IV-1.

It is difficult to judge the best performance from Figure IV-1 because the tradeoff between P_d and *FAR* is not obvious. IDA has adopted a model-based approach using the receiver operating characteristic (ROC) curve and a Gaussian formalism to model the sensor performance. The goal of this approach is to establish a performance metric by modeling the dependence of P_d on *FAR*. The ROC model generates unique curves of constant performance. The location of any point on a single curve is dependent on the sensor threshold. If one assumes that the mine detection tests provide sensor performance at a single threshold, relative performance of different sensors can be interpreted using the ROC model. The difficulty with this assumption is that for an operational field test, the user tends to adjust the gain during the testing process, for instance during the calibration process, thereby changing the apparent threshold. Still, averaged over the set of mines and potential false alarms encountered in the field, an "average" threshold exists and the ROC model can be employed to evaluate performance. To determine relative performance, the single point representing P_d vs. P_{fa} for each sensor is plotted. P_{fa} is used instead of *FAR* to provide a consistent link to the statistical performance models employed.
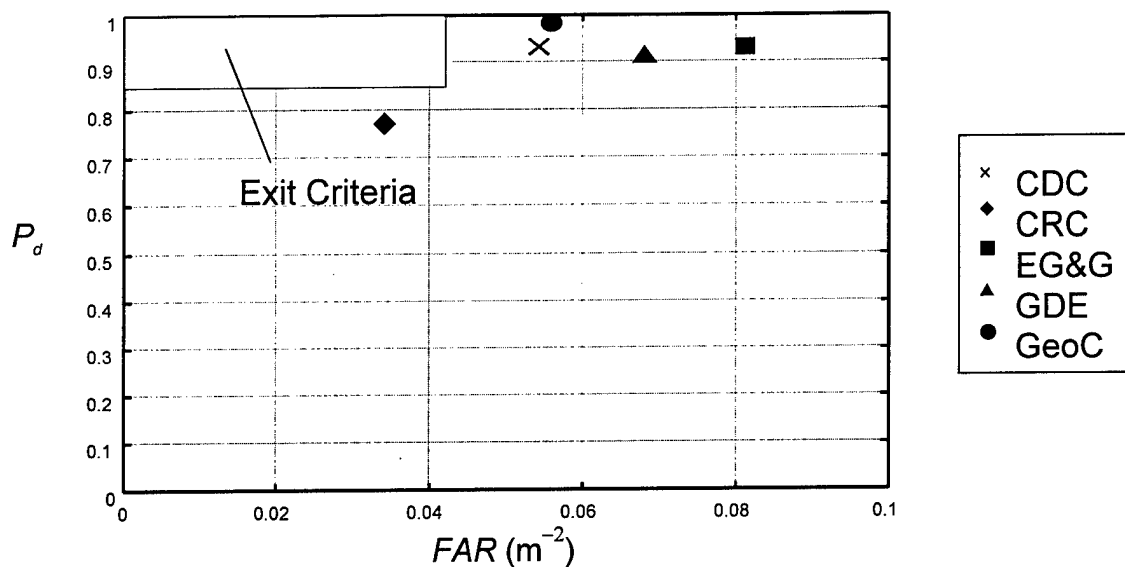
Figure IV-1. P_d vs. FAR for On-Road, Subsurface Mines at Aberdeen

Table IV-1. On-Road Subsurface Performance, All Sensors

Contractor	Aberdeen			Socorro		
	FAR (m^{-2})	P_d [Confidence]†	#det./ #enc.	FAR (m^{-2})	P_d [Confidence]†	#det/ #enc.
CDC	0.054	0.932 [0.884-0.965]	123/132	0.032	0.892 [0.840-0.932]	132/148
CRC	0.034	0.773 [0.704-0.832]	102/132	0.037	0.905 [0.855-0.942]	134/148
EG&G	0.081	0.932 [0.884-0.965]	123/132	0.043	0.919 [0.872-0.953]	136/148
GDE	0.068	0.909 [0.856-0.947]	119/132	0.037	0.899 [0.848-0.937]	133/148
GeoC	0.056	0.985 [0.953-0.998]	130/132	0.032	0.912 [0.863-0.948]	135/148

$\dagger$ This is a 90-percent confidence interval using the Binomial approach discussed in Chapter III.

The relative performance of different sensors is then determined by assuming a Gaussian model for the distribution function of the response of the sensor to noise/clutter and mines. This approach results in a single relative performance measure, the "d" metric (Van Trees, 1968) for each sensor. Although there are limits to this methodology

(Altshuler et al., 1997, and Andrews et al., 1998), the approach does provide a metric that is consistent within a single test. Thus, we do not advocate comparisons based on the d metric from different tests even within this ATD. ROC curves and the d metric are discussed in detail in Chapter III.

Figure IV-2a shows the ROC approach (P_d versus P_{fa}). The isoperformance curves (curves of constant d) on this plot are shown as solid lines, and represent a contractor's ability to separate detections from false alarms. Based on these curves, it seems that GeoC showed the best performance for on-road, subsurface mines, with the other four contractors at a comparable level. Figure IV-2b presents the d metric for each contractor, with a 90-percent confidence interval. It is apparent from this figure that all the contractors except GeoC perform in a statistically similar manner because their confidence intervals overlap.
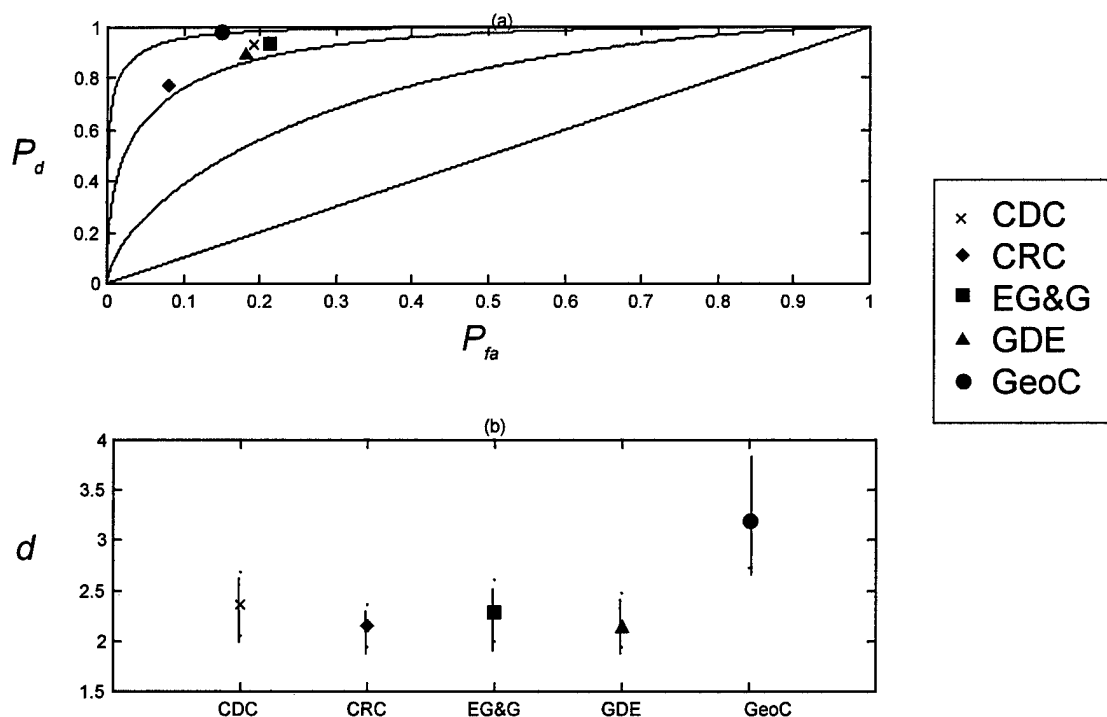
Figure IV-2. (a) P_d vs. P_{fa}, and (b) the d Metric, for On-Road, Subsurface Mines at Aberdeen

FAR and P_{fa} are related to one another as described in Chapter III. Recall that FAR is computed by counting all false alarms and dividing by the area of the lane. P_{fa} gives the probability that an alarm will exist within the equivalent area of the average mine plus its halo (A_{dec}). Thus, if false alarms tend to be clumped together in space, P_{fa} will not grow as quickly as FAR. Hence, a small FAR-to-P_{fa} ratio indicates that the false alarms are not very correlated in space, while a large ratio indicates that there is a clumping of false

alarms in space. Table IV-2 shows the FAR-to-P_{fa} ratio at Aberdeen and Socorro. Note that CDC has the lowest FAR-to-P_{fa} ratio at Aberdeen (0.280). This low ratio may be due to data fusion of the individual sensors that is more extensive than that done by the other contractors.

Table IV-2. Ratio of FAR to P_{fa} for On-Road Lanes

Site	CDC	CRC	EG&G	GDE	GeoC
Aberdeen	0.280	0.420	0.383	0.382	0.375
Socorro	0.264	0.308	0.326	0.336	0.260

Figure IV-3 shows P_d versus FAR for the five contractors, for the three different mine metal contents. GeoC, CDC, and EG&G show a slight decrease in P_d for low-metal and nonmetal mines. CRC and GDE exhibit a much sharper drop in the ability to sense these plastic-cased (dielectric) mines.
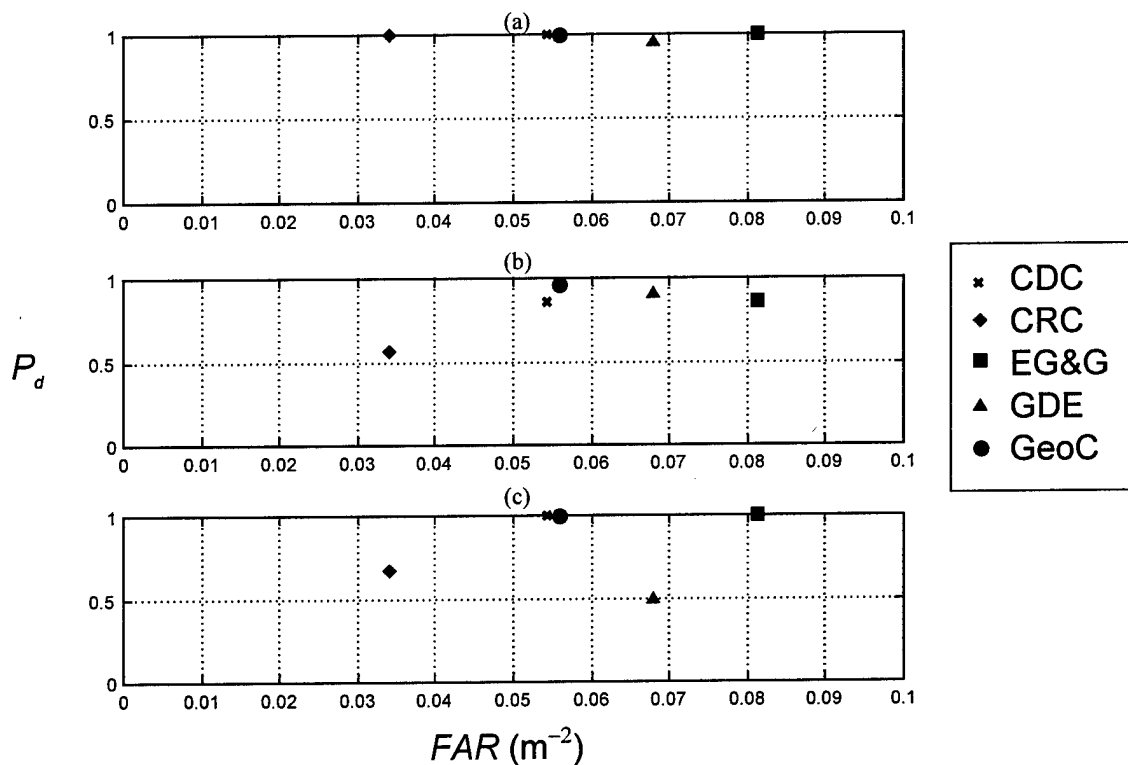
Figure IV-3. P_d vs. FAR for (a) Metal, (b) Low-Metal, and (c) Nonmetal Mines, On-Road, Subsurface at Aberdeen

Figure IV-4 and Table IV-3 show interesting trends in sensor performance.[1] First, note that for all five contractors the GPR was the single sensor with the highest P_d. In some cases, the GPR did so well that the marginal increase in P_d from the IR and EMI sensors was hardly significant, such as with CDC, GDE, and GeoC. (Details of the marginal benefits of the three detectors will be provided in the discussion on individual contractor performance in Chapter V.) For example, if CDC had run with only its GPR, its P_d would essentially be the same while its *FAR* would have dropped by over 20 percent. CRC and EG&G, on the other hand, depended more on their entire sensor package to achieve their results. CRC relied heavily on its EMI detector in the case of metal mines, with very little increase in *FAR* from the EMI sensor, as will be seen in Chapter V. (Note that CRC did not use its IR sensor in any ATD tests.) As will also be seen in Chapter V, EG&G's GPR and EMI did well on metal mines, while in the case of low- and nonmetal mines their IR detector proved critical (and resulted in a noticeable increase in *FAR*). It should be noted that only CDC and EG&G used their IR sensor to attempt to detect subsurface mines. GeoC limited their IR detection to surface mines only, and suffered no IR false alarms at Aberdeen.
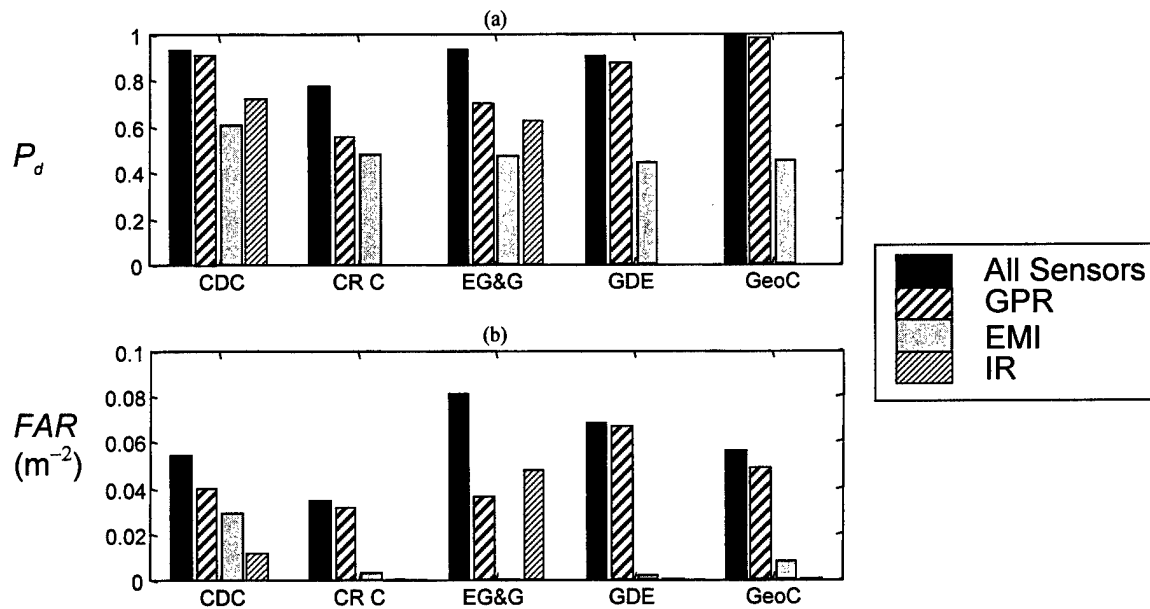
Figure IV-4. (a) P_d and (b) *FAR* as Functions of Sensor Type for On-Road, Subsurface Mines at Aberdeen

---

[1] Recall that the *FAR* of all sensors should not be equal to the *FAR* of the individual sensors. Refer to the definition of *FAR* in Chapter III for details.

Table IV-3. Detection Rate [90-Percent Confidence Intervals] for Each Sensor for Subsurface Mines at Aberdeen

Site	Sensor	CDC	CRC	EG&G	GDE	GeoC
Aberdeen	GPR	0.909 [0.856/0.947]	0.553 [0.477-0.627]	0.697 [0.624/0.763]	0.871 [0.812/0.917]	0.977 [0.942/0.994]
	EMI	0.606 [0.530/0.678]	0.477 [0.402/0.553]	0.470 [0.395/0.546]	0.439 [0.365/0.515]	0.447 [0.373/0.523]
	IR	0.720 [0.648/0.784]	N/A	0.621 [0.546/0.692]	N/A	N/A
Socorro	GPR	0.811 [0.750/0.863]	0.818 [0.757/0.869]	0.905 [0.855/0.942]	0.885 [0.832/0.926]	0.912 [0.863/0.948]
	EMI	0.588 [0.517/0.657]	0.473 [0.402/0.544]	0.466 [0.396/0.537]	0.480 [0.409/0.551]	0.473 [0.402/0.544]
	IR	0.696 [0.627/0.759]	N/A	0.243 [0.185/308]	0	0.176 [0.126/0.236]

As with the full system performance, it is desirable to use a single performance metric to compare the subsystems of each of the VMMD systems. Care must be taken with this type of comparison when complex data fusion is used. But for most of these systems, a simple logical OR (or location-correlated logical OR[2]) is used to combine results from the three sensors. Therefore, we can compare the detection performance of each of the subsystems for the different VMMD systems using the d metric for each sensor. Figure IV-5a–c shows P_d versus P_{fa} for the GPR, EMI, and IR sensors, respectively. Table IV-4 presents the d metric for each of the contractor's subsystems. At Aberdeen, GeoC exhibits the highest d metric for a GPR. This performance exceeds the 90-percent confidence interval of all other contractors' GPRs. The same can be stated for the EG&G EMI system, which exhibited perfect detection of metal mines with no false alarms. Only CDC and EG&G used their IR for subsurface detection at Aberdeen. Using the d metric and the 90-percent confidence interval, it is possible to conclude that the CDC IR outperformed the EG&G IR.

2. Socorro Results

All of the contractors achieved the exit criterion for P_d at Socorro (see Figure IV-6). As shown in Table IV-1, the contractors are tightly bunched in P_d, with system performance between 89 and 92 percent. The overall range of *FAR* is much tighter than at

---

2 A location-correlated logical OR uses a distance criterion between alarms from two different sensors to determine if the sensor responses result from a single target. If the distance between the alarms from different sensors is less than a given distance, the two alarms are combined, and a single declaration is made.

Aberdeen: 0.032–0.043 m^{-2} at Socorro versus 0.034–0.081 m^{-2} at Aberdeen. All of the contractors except EG&G achieved the *FAR* exit criterion. EG&G narrowly missed this criterion.
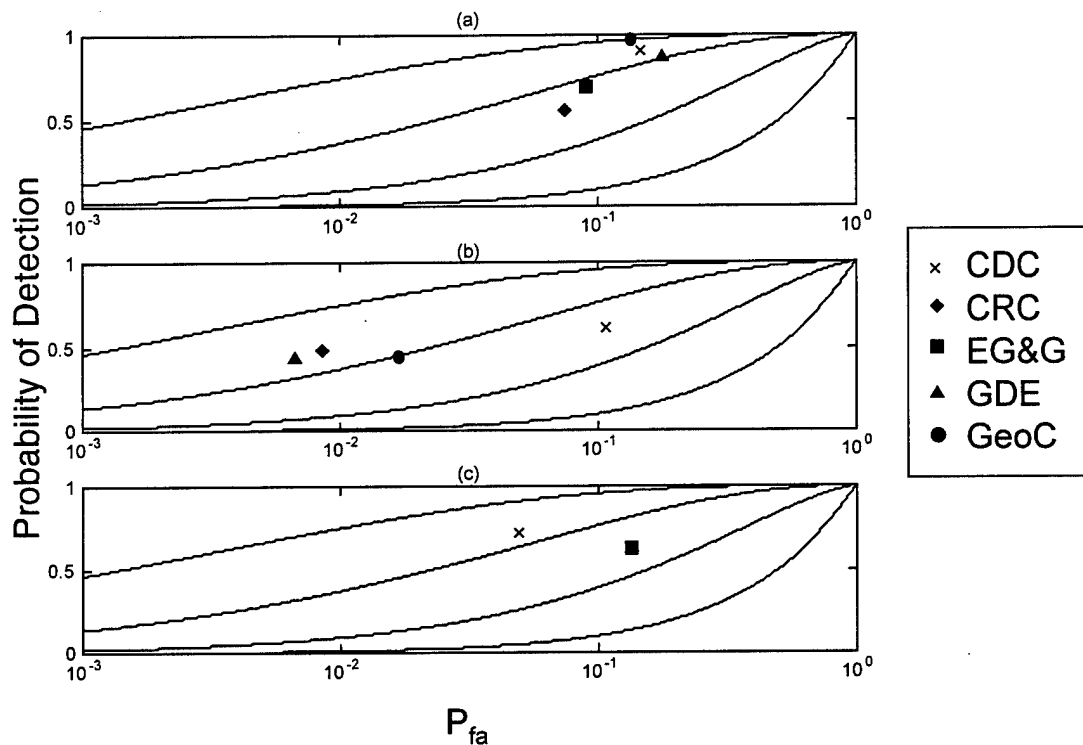
Figure IV-5. P_d **vs.** *FAR* **for (a) GPR Sensor, (b) EMI Sensor, and (c) IR Sensors for On-Road, Subsurface Mines at Aberdeen. Note that** P_{fa} **is shown on a log scale; therefore, contractors with no false alarms for a particular sensor are off scale.**

At Socorro the *FAR*-to-P_{fa} ratios for both CDC and GeoC are similar and smaller than those of the other three contractors (see Table IV-2). Here, it appears that CDC and GeoC have less overlap of the detection areas surrounding their false alarms. (Note that both CDC and GeoC have the lowest overall false alarm rate.) The consequence of this is that CRC, EG&G, and GDE have an opportunity to reduce their *FAR* if a more sophisticated algorithm is used to correlate closely spaced declarations.

The similarity in the contractors' performance can be seen in Figure IV-7a, which is designed to spread out disparate performances among different isoperformance curves (these curves are again shown as black lines on the plot), and also in Figure IV-7b, which shows the *d* metric and the 90-percent confidence interval around that metric. It is apparent that all five contractors' *d* metric confidence intervals overlap. Thus, at Socorro

there is no statistically significant difference between the contractors in detecting on-road subsurface mines.

Table IV-4. *d* Metric with Confidence Intervals for Each Sensor

Site	Sensor	CDC	CRC	EG&G	GDE	GeoC
Aberdeen	GPR	2.38 [2.11/2.67]	1.58 [1.39/1.77]	1.41 [1.22/1.61]	2.06 [1.71/2.31]	3.11 [2.68-3.64]
	EMI	1.51 [1.31/1.70]	2.33 [2.13/2.52]	†	2.32 [2.13/2.51]	1.99 [1.80/2.18]
	IR	2.24 [2.04/2.44]	N/A	1.41 [1.22-1.61]	N/A	N/A
Socorro	GPR	2.22 [2.01/2.43]	2.08 [1.87/2.29]	2.53 [2.28-2.79]	2.51 [2.27-2.75]	2.52 [2.26/2.80]
	EMI	2.48 [2.30/2.66]	†	2.79 [2.62/2.97]	2.46 [2.28/2.64]	3.28 [3.10/3.46]
	IR	2.77 [2.58/2.96]	N/A	1.28 [1.08/1.48]	††	2.16 [1.94/2.37]

† Subsystem produced zero false alarms.

†† Subsystem had no detections, but at least one false alarm.
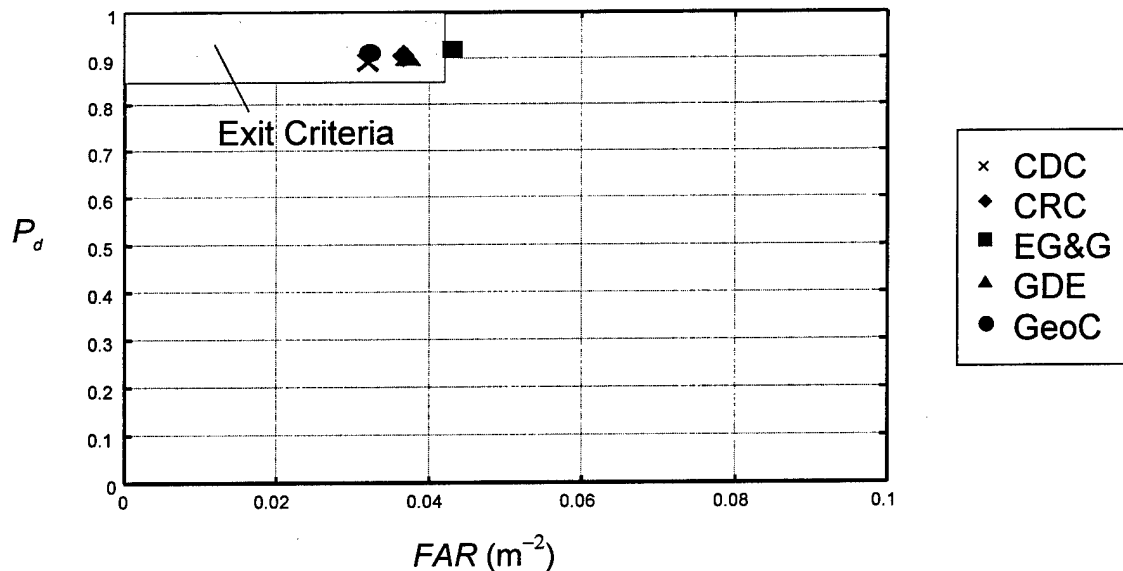
Figure IV-6. P_d vs. *FAR* for On-Road, Subsurface Mines at Socorro

As at Aberdeen, the overall detection performance of the contractors is lower for low- and nonmetal mines than for metallic mines. Figure IV-8 shows the P_d versus the *FAR* for the different types of mines.
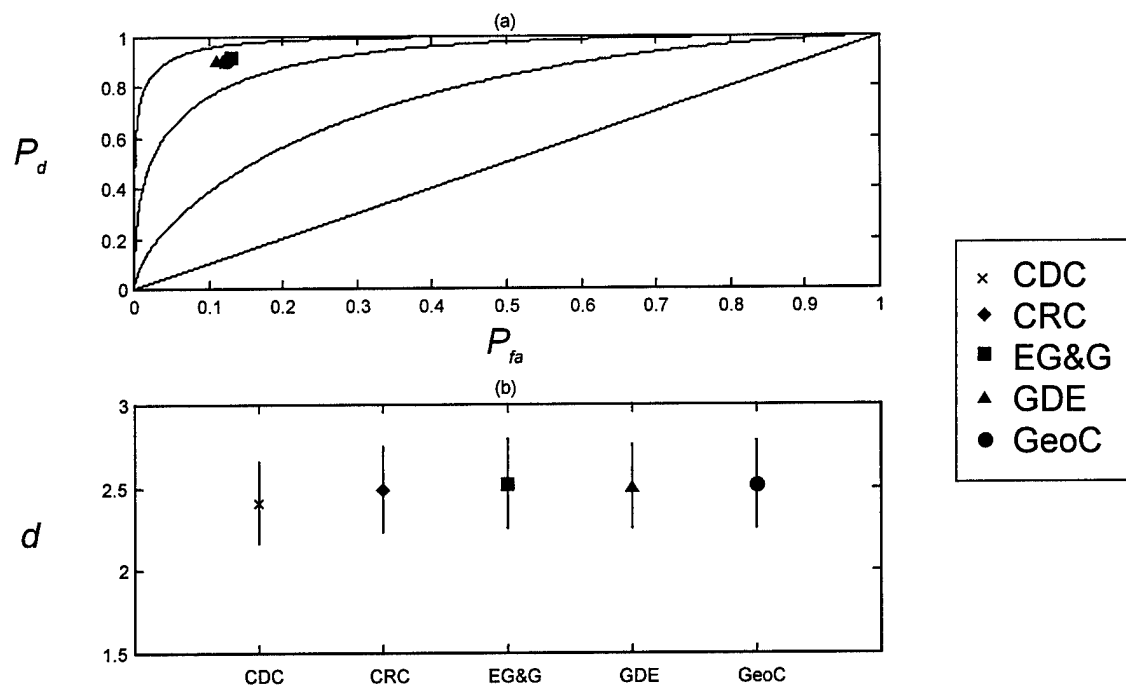
Figure IV-7. (a) P_d vs. P_{fa}, and (b) the d Metric, for On-Road, Subsurface Mines at Socorro
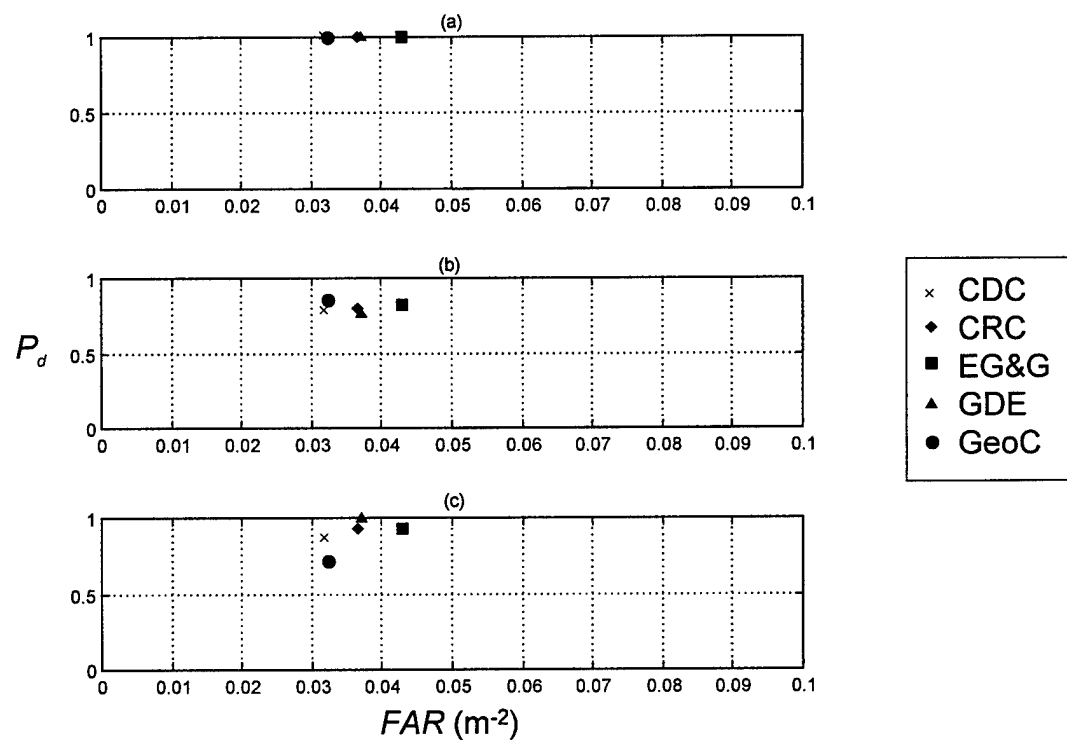
Figure IV-8. P_d vs. FAR for (a) Metal, (b) Low-Metal, and (c) Nonmetal Mines, On-Road, Subsurface at Socorro

The most effective detector for on-road, subsurface mines at Socorro was the GPR. In all cases, this dominates the detections as well as the false-alarm rate (see Figure IV-9). In the case of EG&G, GDE, and GeoC, the EMI and IR detectors add very little improvement in detection over the GPR alone. In fact, had EG&G and GDE not used EMI or IR, their false-alarm rates would have improved about 15 percent and 10 percent, respectively. CDC and CRC could not have achieved their near-90 percent P_d without other detectors, though in the case of CDC the "cost" of these detectors is about a 25-percent increase in the *FAR* (all of CRC's *FAR* is due to the GPR, however).
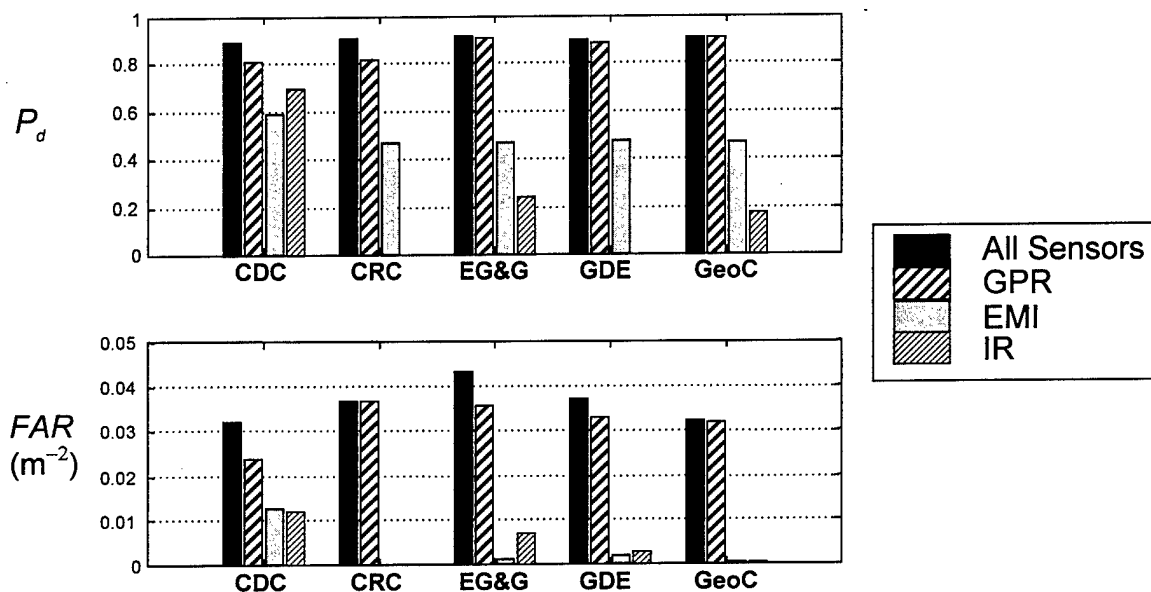
Figure IV-9. (a) P_d and (b) *FAR* as Functions of Sensor Type for On-Road, Subsurface Mines at Socorro

By using the ROC curve formalism or the d metric (Figure IV-10 and Table IV-4) we can compare the performance of the subsystems at Socorro. CRC's and CDC's GPR confidence intervals for the d metric in Table IV-4 overlapped, but seemed to outperform EG&G, GDE, and GeoC. CRC's EMI system had zero false alarms and the best overall subsurface performance at Socorro. GeoC exhibited EMI performance that is better (considering the 90-percent confidence interval) than CDC, EG&G, or GDE. Finally, as seen at Aberdeen, the CDC IR outperformed those of EG&G and GeoC when detecting subsurface mines.
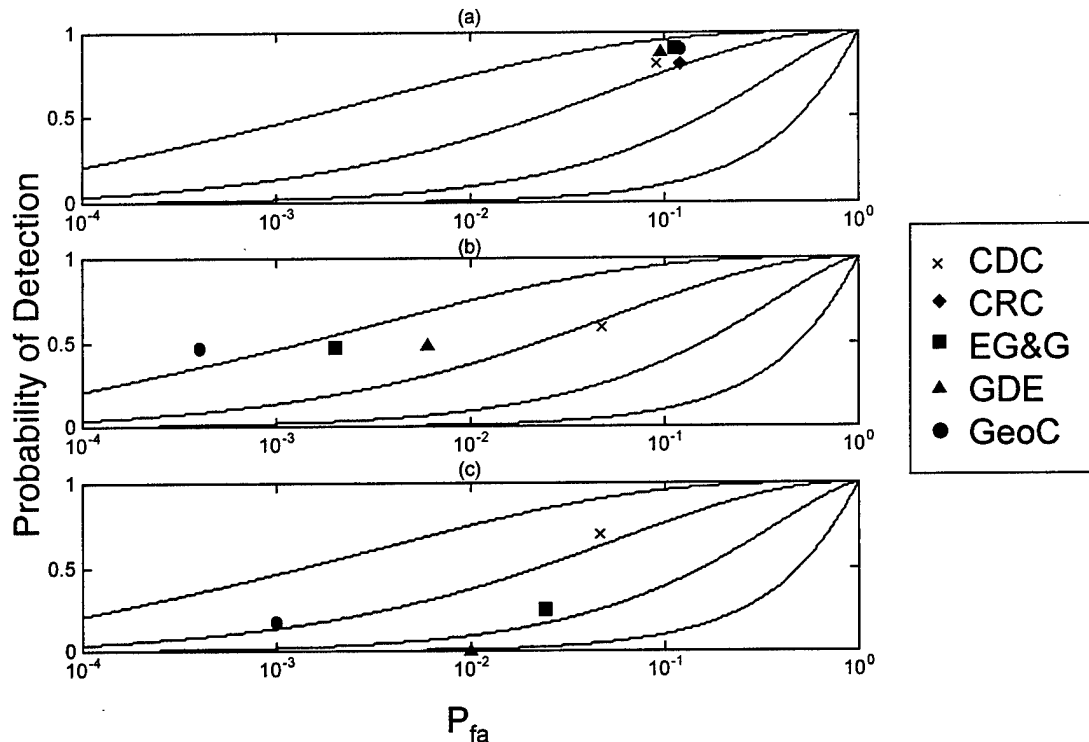
Figure IV-10. P_d vs. P_{fa} for (a) GPR Sensor, (b) EMI Sensor, and (c) IR Sensors for On-Road, Subsurface Mines at Socorro. Note that P_{fa} is on a log scale; therefore, contractors with no false alarms for a particular sensor are off scale.

B. ON-ROAD, SURFACE MINES

1. Aberdeen Results

Figure IV-11 shows that all of the contractors exceeded the 0.90 detection probability exit criterion. Only CRC also met the *FAR* criterion as well. (See Table IV-5 for details.) Interpreting the tradeoff between P_d and *FAR* as shown in Fig. IV-11 is difficult, so we turn to Fig. IV-12 to view the performances against isoperformance curves. This figure shows that all of the contractors performed nearly along the same isoperformance curve.

Although CRC and GDE did not achieve 100-percent detection rate, calculation of the *d* metric shows that the 90-percent confidence intervals of all contractors overlap.

As shown in Figure IV-13, four of the five contractors did not show any decrease in detection probability as the metal content of the surface mines decreased. CRC detected all surface metal mines but had a lower probability of detecting low- and non-metal surface mines.
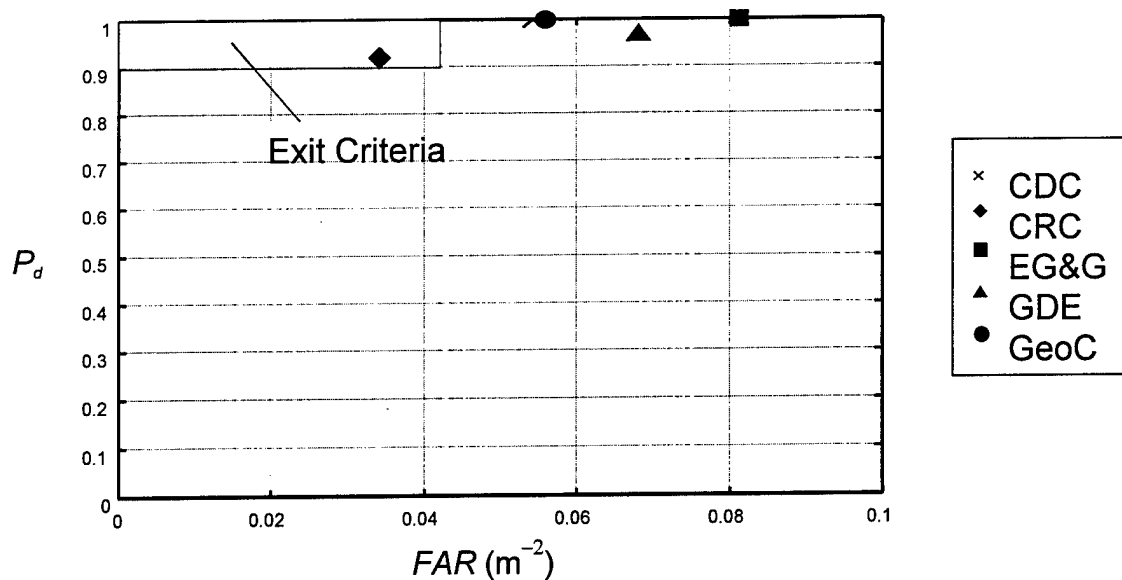
IV-11

Figure IV-11. P_d vs. *FAR* for On-Road, Surface Mines at Aberdeen
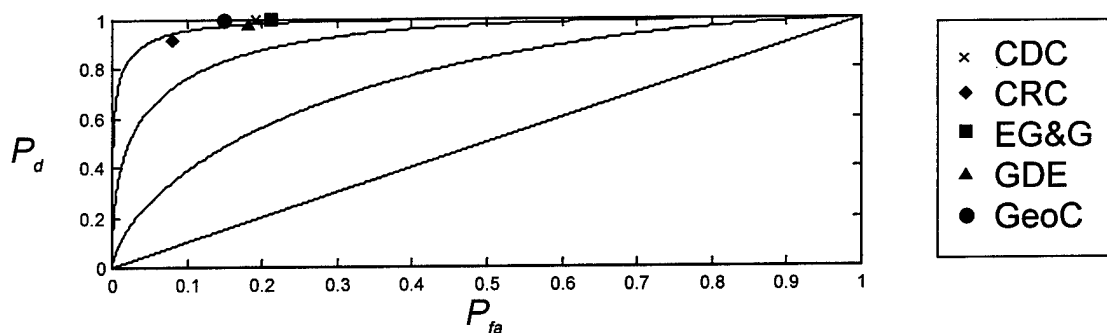
Figure IV-12. P_d vs. P_{fa}, for On-Road, Surface Mines at Aberdeen

For surface mines, the GPR sensor is no longer the best performer for all the contractors. Figure IV-14 shows that both CDC's and GeoC's IR sensor gave the best detection performance in their systems. (Note that both these contractors had a man-in-the-loop in the processing of their data.) EG&G's IR sensor detected almost 80 percent of surface mines.
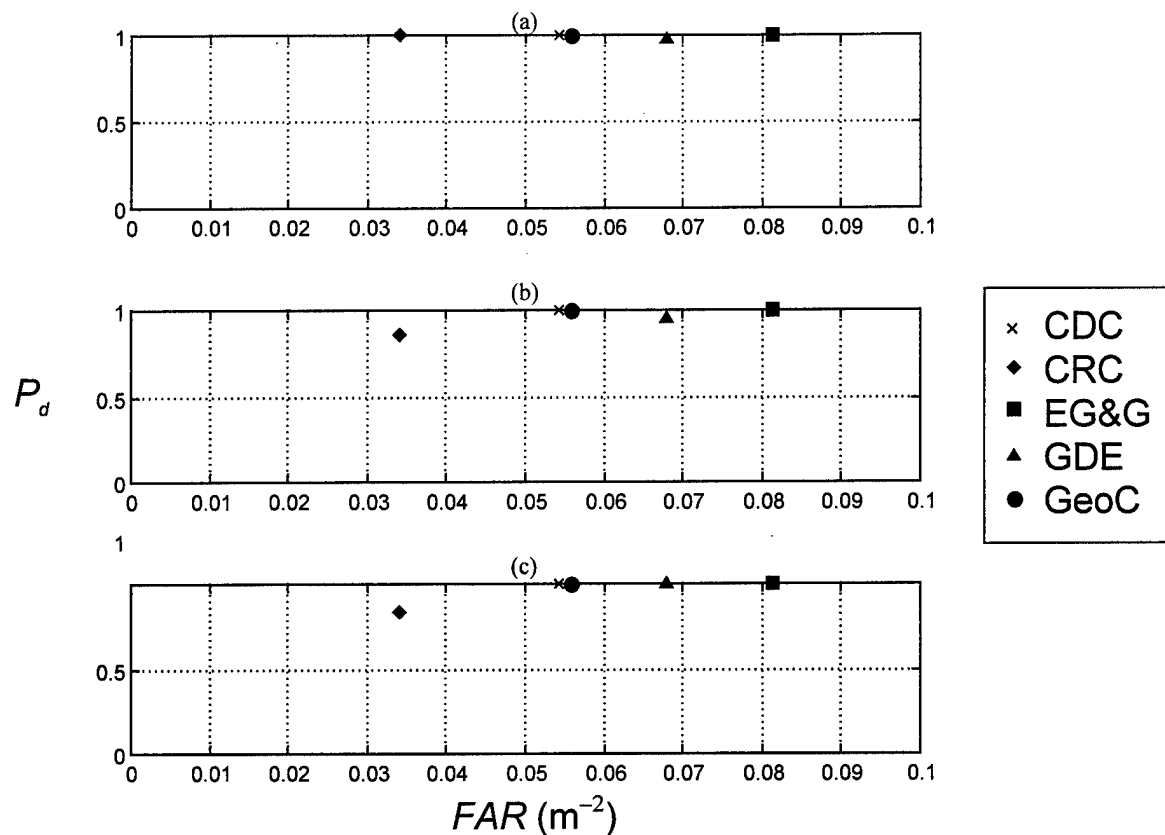
Figure IV-13. P_d vs. *FAR* for (a) Metal, (b) Low-Metal, and (c) Nonmetal Mines, On-Road, Surface at Aberdeen

Table IV-5. On-Road Surface Performance

Contractor	Aberdeen			Socorro		
	FAR (m^{-2})	P_d [Confidence]	#det./ #enc.	FAR (m^{-2})	P_d [Confidence]	#det/ #enc.
CDC	0.054	1.0 [0.966/1.00]	86/86	0.032	1.0 [0.969/1.00]	96/96
CRC	0.034	0.919 [0.852/0.962]	79/86	0.037	1.0 [0.966/1.00]	96/96
EG&G	0.081	1.0 [0.966/1.00]	86/86	0.043	0.969 [0.921/0.992]	93/96
GDE	0.068	0.965 [0.912/0.991]	83/86	0.037	1.0 [0.966/1.00]	96/96
GeoC	0.056	1.0 [0.966/1.00]	86/86	0.032	1.0 [0.966/1.00]	96/96

IV-13
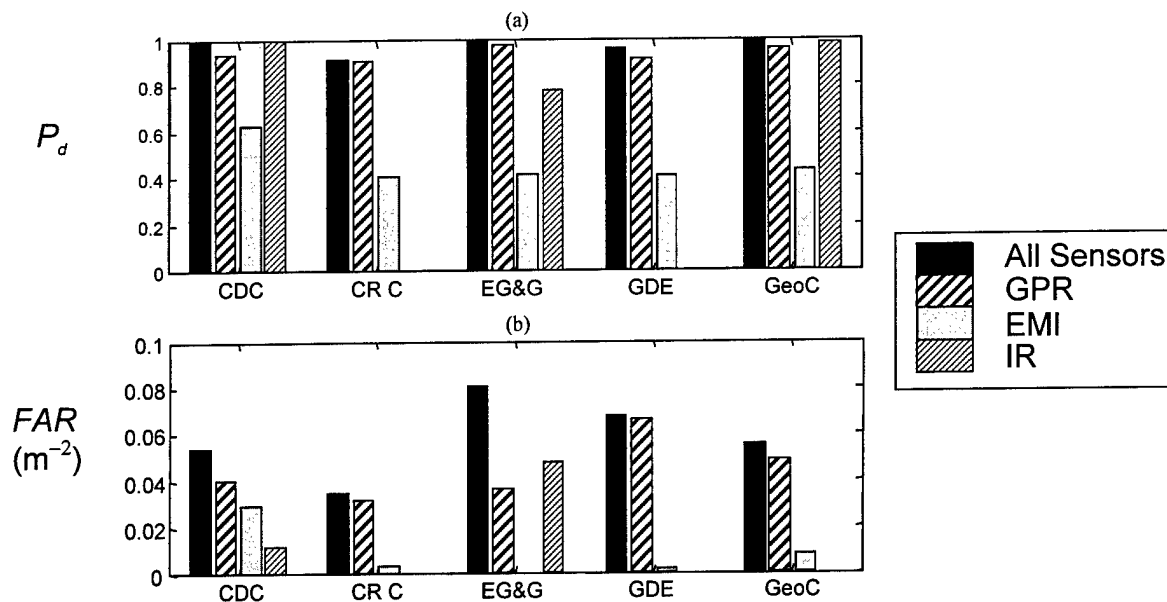
Figure IV-14. (a) P_d and (b) FAR as Functions of Sensor Type for On-Road, Surface Mines at Aberdeen

2. Socorro Results

As shown in Figure IV-15, CDC, CRC, GDE, and GeoC met both the P_d and FAR exit criteria (they all, incidentally, achieved a P_d of 100 percent). EG&G met the P_d exit criterion but missed the FAR criterion by less than 3 percent.
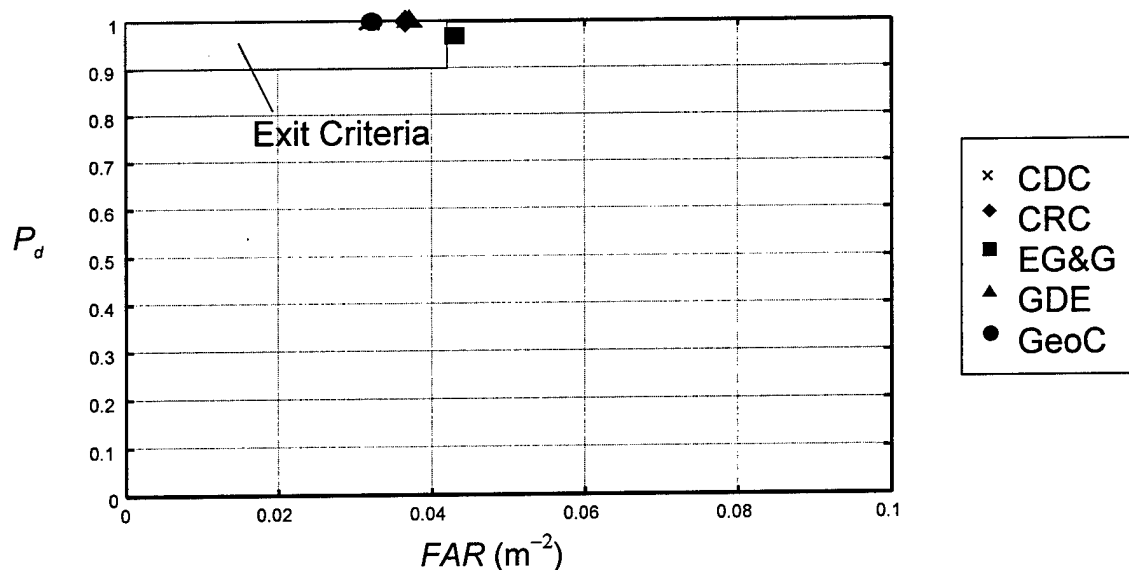
Figure IV-15. P_d vs. FAR for On-Road, Surface Mines at Socorro

As shown in Fig. IV-16, the IR sensor is CDC's strongest, as it was for detecting surface mines at Aberdeen. For GeoC the IR was not as robust as the GPR (which is reverse of the performance on surface mines at Aberdeen), although the IR is clearly more effective on surface mines than subsurface mines at the Socorro site (see Figure IV-9).
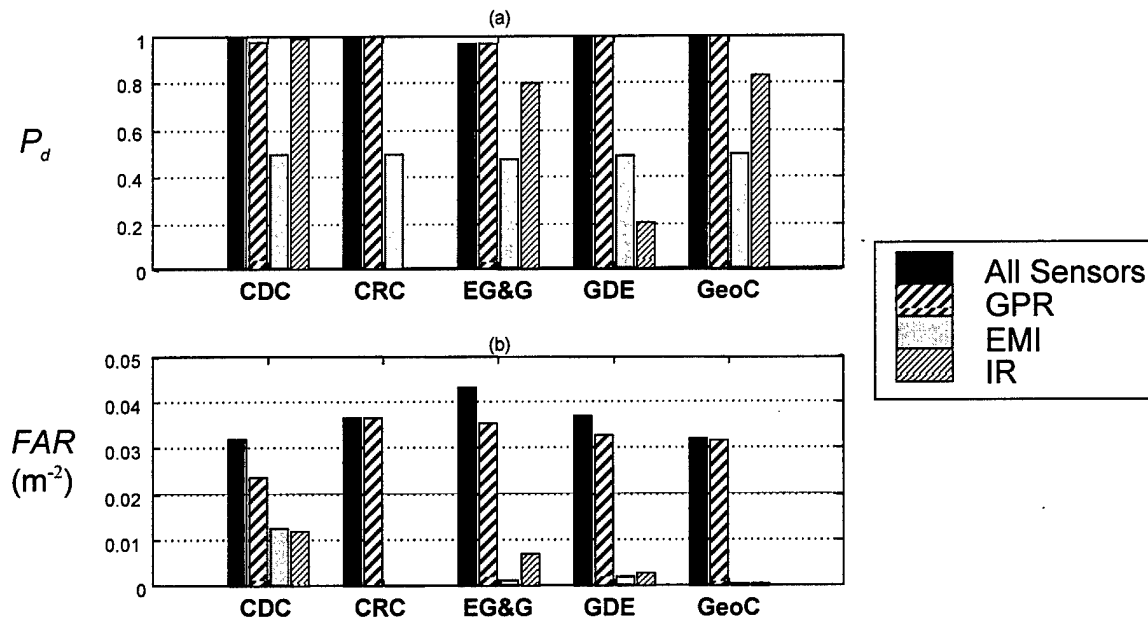
Figure IV-16. (a) P_d and (b) FAR as Functions of Sensor Type for On-Road, Surface Mines at Socorro

C. OFF-ROAD, SUBSURFACE MINES

At Aberdeen the contractors surveyed two off-road lanes twice, covering a total area of 2,280.8 m^2. Within the mine lanes there were 68 subsurface mines encountered. At Socorro, the contractors surveyed seven lanes twice, covering a total area of 537.5 m^2, with 30 subsurface mines encountered. On this site the total area of the mine and halo was 202.6 m^2, or approximately 38 percent of the test lane. Thus, in only 62 percent of the mine lane at Socorro was there an opportunity for a false alarm. At Aberdeen, the total mine area was 442.2 m^2, which constitutes only 19 percent of the test site.

1. Aberdeen Results

The off road exit criteria were more lenient: P_d must be greater than 80 percent for subsurface mines, while FAR must be less than 0.17 m^{-2}. All of the contractors except CRC met both the P_d and FAR criteria (see Figure IV-17). CDC appeared to be the best performer in these off-road, subsurface conditions at Aberdeen (see Table IV-6 for

details). If the *d* metric is used (see Figure IV-18) it is apparent that the CDC system performed well, but the *d* metric confidence interval overlaps that of EG&G and overlaps just slightly that of GeoC. It is worth noting that the errors associated with the *d* metric are large because the number of mines encountered is small (only 68).
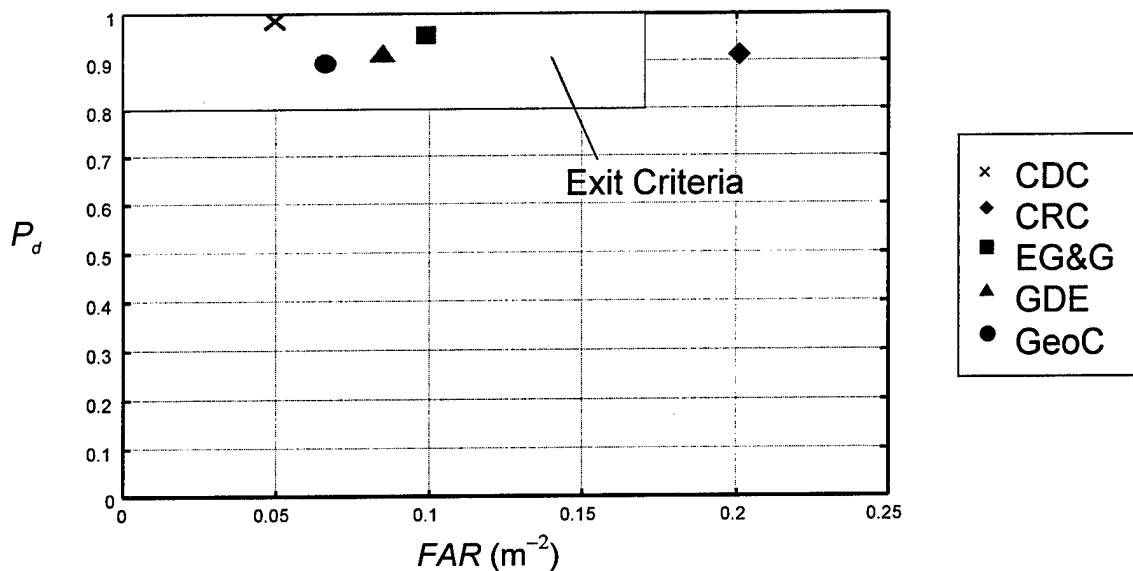
Figure IV-17. P_d vs. FAR for Off-Road, Subsurface Mines at Aberdeen

Figure IV-19 shows that the detection performance of the contractors on subsurface mines diminishes for low-metal mines, which is consistent with the results from all portions of this ATD. For the off-road, subsurface test in Aberdeen, this effect is least pronounced with CDC.

Figure IV-20 shows that the GPR sensor once again was the best performer, in terms of P_d, for detecting subsurface mines in all of the contractors' systems (also see Table IV-7). The other sensors did add to the detection probability of the contractors, except for the GeoC system, where the EMI and IR added no marginal benefit in detection (but also did not contribute to the false alarms). In all cases, the GPR contributed the bulk of the false alarms. CDC and GeoC exhibited the largest GPR P_d (see Table IV-7). As demonstrated throughout this ATD, CDC had superior IR performance. In addition, for this test, both EG&G and GeoC showed robust EMI performance. Table IV-8 summarizes the *d* metric for the off-road, subsurface condition.

IV-16

Table IV-6. Off-Road Subsurface Performance

Contractor	Aberdeen			Socorro		
	FAR (m^{-2})	*P$_d$* [Confidence]	#det./ #enc.	*FAR* (m^{-2})	*P$_d$* [Confidence]	#det/ #enc.
CDC	0.050	0.985 [0.931/0.999]	67/68	0.048	0.633 [0.466/0.779]	19/30
CRC	0.201	0.912 [0.833/0.962]	62/68	0.041	0.733 [0.569/0.860]	22/30
EG&G	0.099	0.956 [0.890/0.988]	65/68	0.058	0.700 [0.534/0.834]	21/30
GDE	0.085	0.912 [0.833/0.962]	62/68	0.065	0.800 [0.642/0.910]	24/30
GeoC	0.066	0.897 [0.815/0.951]	61/68	0.035	0.700 [0.534/0.834]	21/30
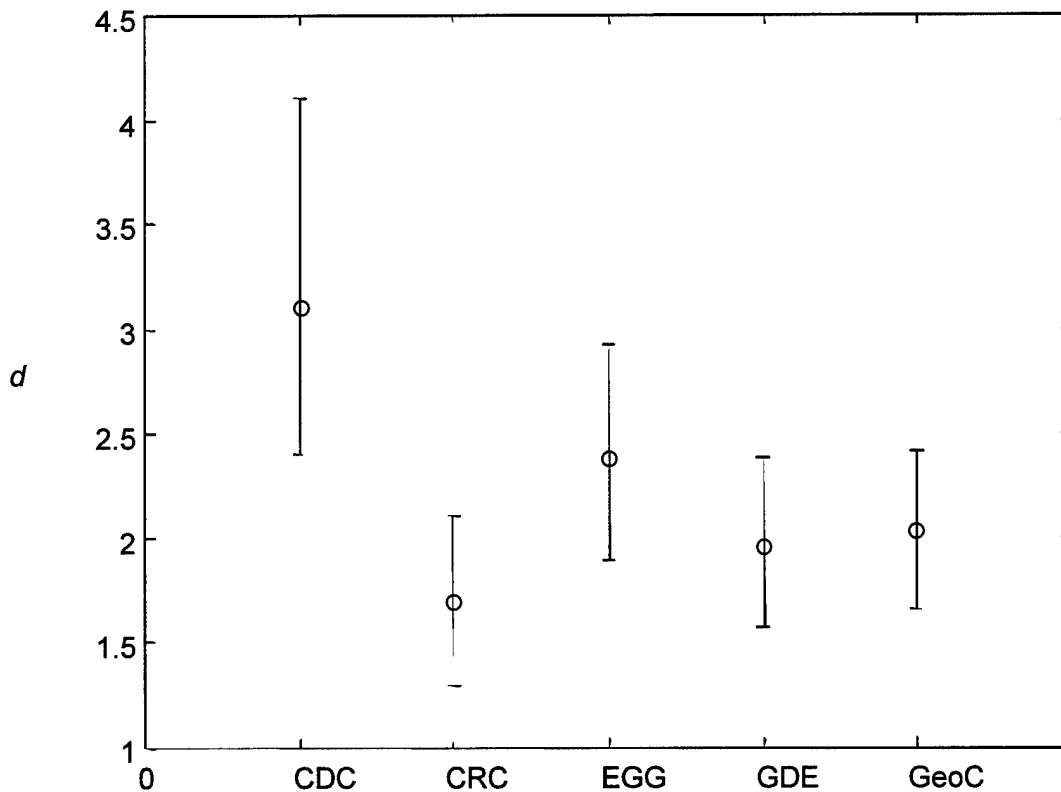
Figure IV-18. The *d* Metric for Off-Road, Subsurface Mines at Aberdeen

IV-17

Table IV-7. Detection Rate and 90-Percent Confidence Intervals
for Each Sensor, Off-Road, Subsurface

Site	Sensor	CDC	CRC	EG&G	GDE	GeoC
Aberdeen	GPR	0.926 [0.851/0.971]	0.779 [0.680/0.859]	0.794 [0.696/0.871]	0.618 [0.511/0.717]	0.897 [0.815/0.951]
	EMI	0.647 [0.540/0.744]	0.588 [0.481/0.690]	0.559 [0.452/0.662]	0.632 [0.525/0.730]	0.441 [0.338/0.548]
	IR	0.838 [0.746/0.907]	N/A	0.456 [0.352/0.563]	0.412 [0.310/0.519]	N/A
Socorro	GPR	0.467 [0.308/0.631]	0.300 [0.166/0.466]	0.600 [0.433/0.751]	0.800 [0.642/0.910]	0.700 [0.534/0.834]
	EMI	0.567 [0.401/0.722]	0.533 [0.369/0.692]	0.533 [0.369/0.692]	0.533 [0.369/0.692]	0.533 [0.369/0.692]
	IR	0.267 [0.140/0.431]	N/A	0.100 [0.027/0.239]	N/A	N/A

Table IV-8. *d* metric with Confidence Intervals for Each Sensor, Off-Road, Subsurface

Site	Sensor	CDC	CRC	EG&G	GDE	GeoC
Aberdeen	GPR	2.48 [2.07/2.93]	1.67 [1.37/1.98]	1.66 [1.35/1.97]	1.15 [0.87/1.42]	2.04 [1.67/2.43]
	EMI	1.76 [1.49/2.04]	1.80 [1.53/2.07]	2.38 [2.11/2.65]	1.84 [1.56/2.11]	2.54 [2.27/2.81]
	IR	2.83 [2.51/3.17]	N/A	1.44 [1.17/1.71]	1.44 [1.17/1.71]	N/A
Socorro	GPR	1.32 [0.90/1.74]	1.63 [1.18/2.06]	1.36 [0.93/1.78]	1.71 [1.223/2.21]	1.65 [1.21/2.09]
	EMI	2.24 [1.82/2.66]			2.49 [2.08/2.91]	
	IR	0.54 [0.08/0.99]	N/A	0.23 [-0.41/0.80]	N/A	N/A

1. Socorro Results

At Socorro, only GDE met both the off-road P_d and *FAR* exit criteria for subsurface mines (see Figure IV-21). The remaining four contractors were within the *FAR* criterion but missed on P_d. It is difficult to determine a best performance in these conditions—even when viewing the P_d vs. P_{fa} plot (not shown here), no single contractor emerges as a standout. It is interesting to note that the range of contractors' *FAR* in the off-road lane at Socorro was much wider than the on-road lanes (as expected), while it was smaller than in the off-road lane at Aberdeen.
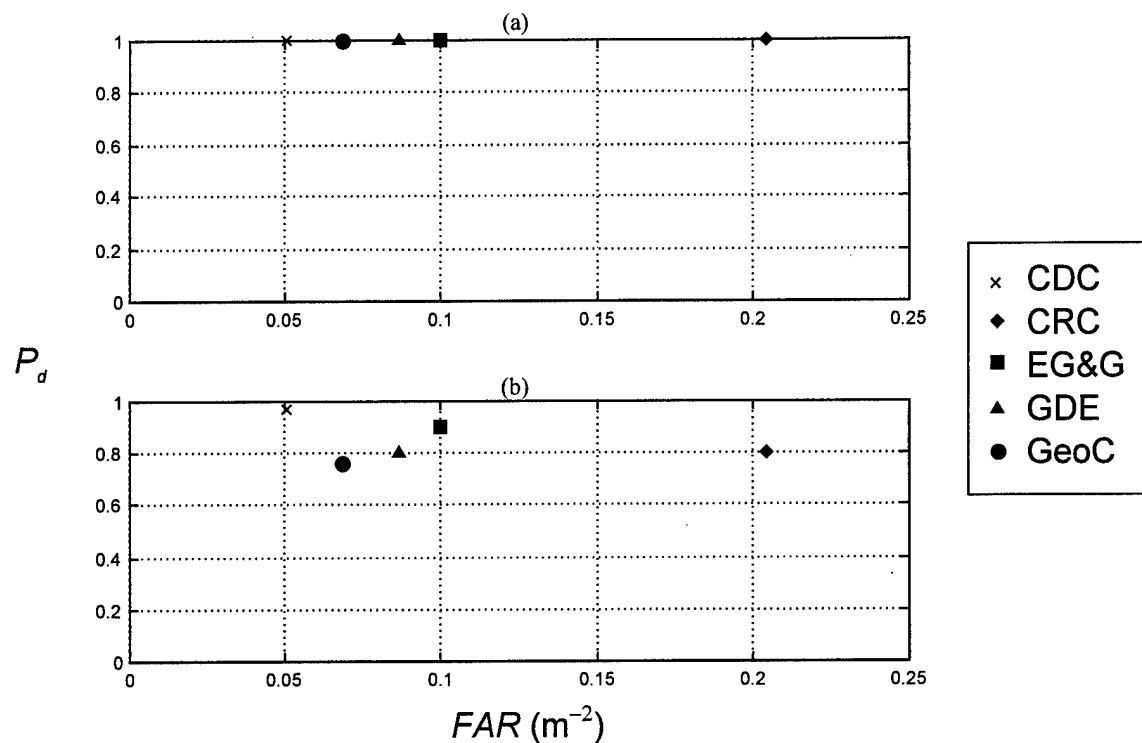
Figure IV-19. P_d for (a) Metal Mines and (b) Low-Metal Mines, Off-Road, Subsurface at Aberdeen
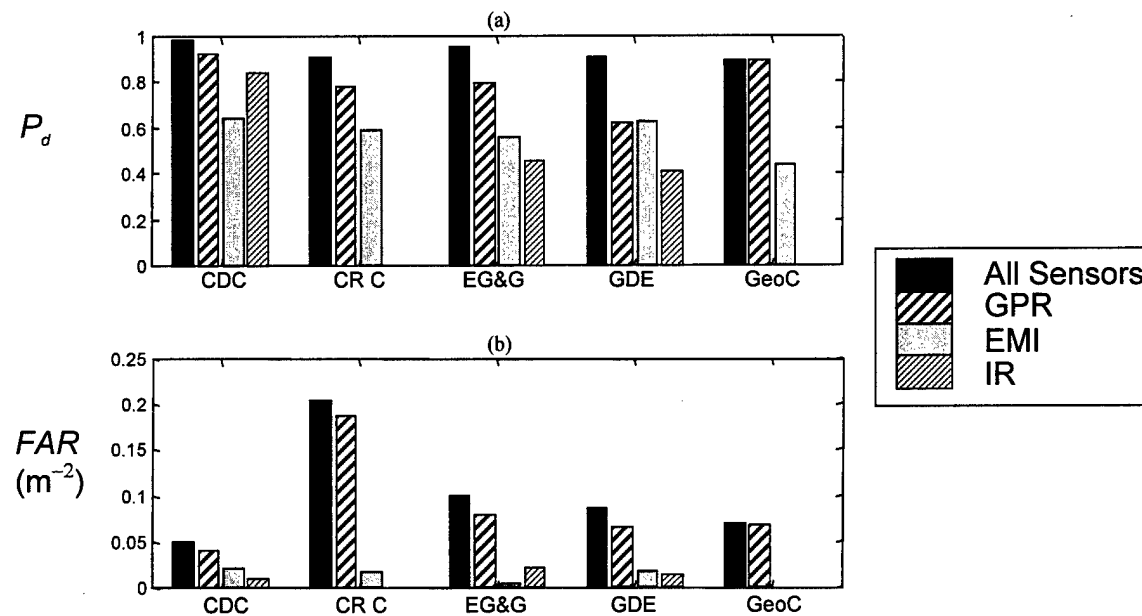
Figure IV-20. (a) P_d and *FAR* as Functions of Sensor Type for Off-Road, Subsurface Mines at Aberdeen

IV-19
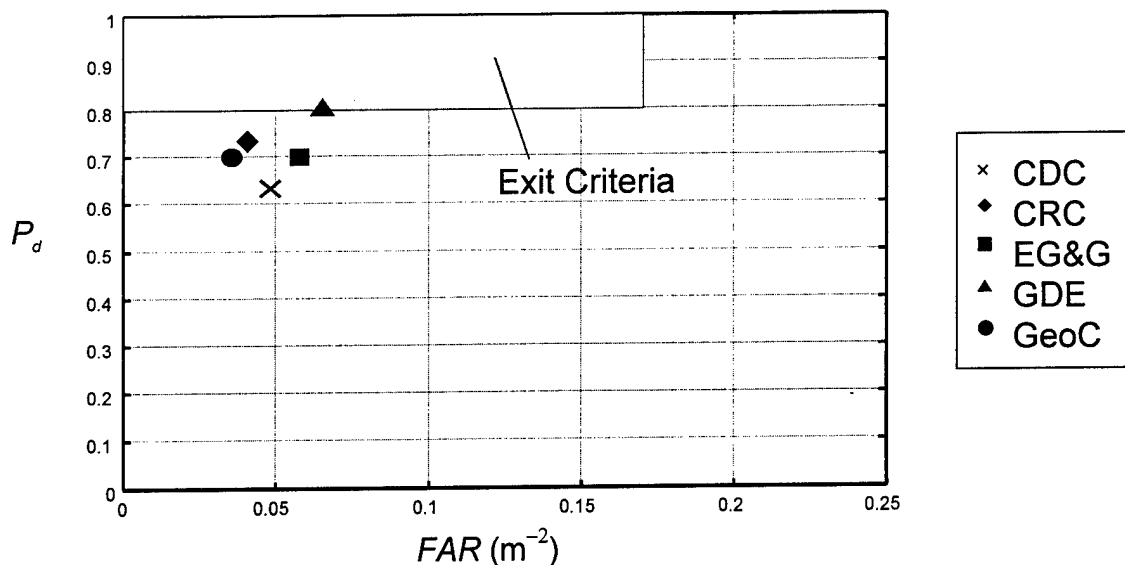
Figure IV-21. P_d **vs.** *FAR* **for Off-Road, Subsurface Mines at Socorro**

Figure IV-22 unequivocally shows the problem in these off-road conditions: all of the contractors had difficulties detecting low-metal mines, while the metal mines posed no problem at all. Detecting low-metal, subsurface mines at Socorro became more difficult off road: a typical P_d on road was 80 percent, while off road it fell to about 40 percent. Also note the higher P_d (about 80 percent or more) for low-metal, subsurface mines at the off-road Aberdeen lanes. It seems that the off-road conditions at Socorro posed a difficult challenge for low-metal, subsurface mine detection.

Figure IV-23 shows that CDC's and CRC's highest detection probability was achieved with their EMI detectors, which is different from their performances in other conditions of this ATD. This may be due to the challenging environment of Socorro's soil for GPR sensors.

D. OFF-ROAD, SURFACE MINES

1. Aberdeen Results

CDC, GeoC, GDE, and EG&G met the off-road P_d and *FAR* exit criteria for surface mines (see Fig. IV-24). CDC achieved excellent performance in this category, as they had the same P_d as GeoC but had a *FAR* that was about two-thirds as large. CRC met the P_d criterion but missed the *FAR* exit criterion.
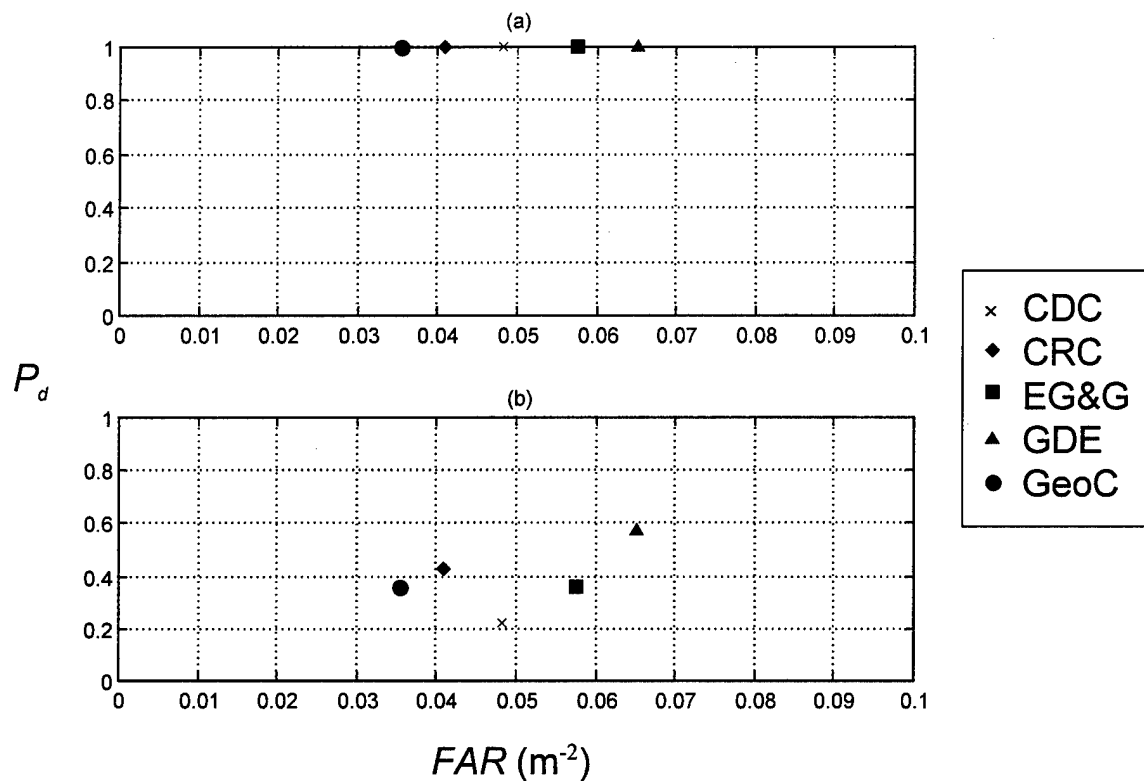
Figure IV-22. P_d for (a) Metal Mines and (b) Low-Metal Mines, Off-Road, Subsurface at Socorro
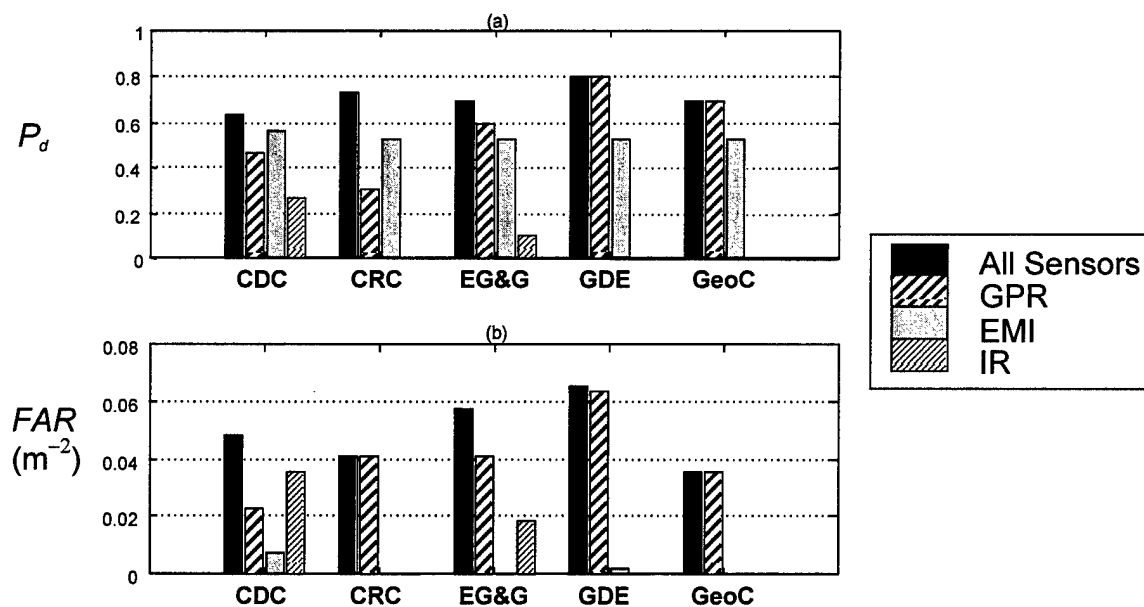
Figure IV-23. (a) P_d and (b) *FAR* as Functions of Sensor Type for Off-Road, Subsurface Mines at Socorro
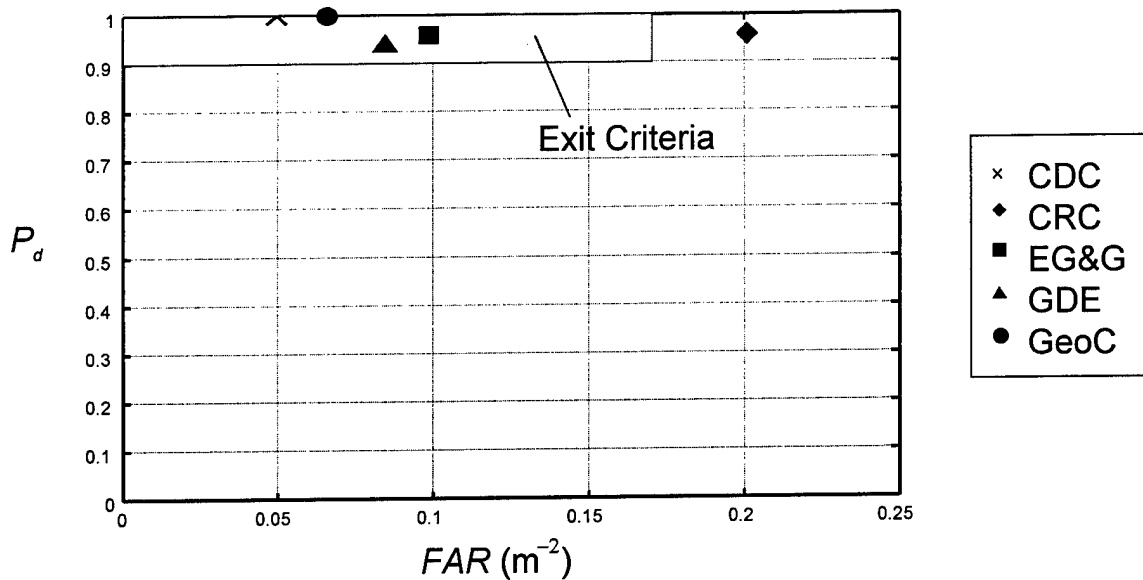
Figure IV-24. P_d vs. FAR for Off-Road, Surface Mines at Aberdeen

Figure IV-25 shows that for all contractors, P_d decreased when detecting low-metal mines. Note that this degradation was not evident in the on-road condition at Aberdeen (cf. with Fig. IV-13), implying that the off-road condition is more challenging for the detection of surface mines.

Again, the IR sensors performed well at detecting surface mines. Figure IV-26 shows that the IR sensor was comparable to the GPR for CDC, EG&G, and GeoC. The IR sensor had a lower contribution to false alarms than the GPR for the four contractors that used both sensors.

2. Socorro Results

As shown in Figure IV-27, all contractors met the exit criteria for off-road, surface mines at Socorro. All contractors achieved a detection probability of 1; the GeoC FAR (0.035 m^{-2}) was the lowest of the five contractors.
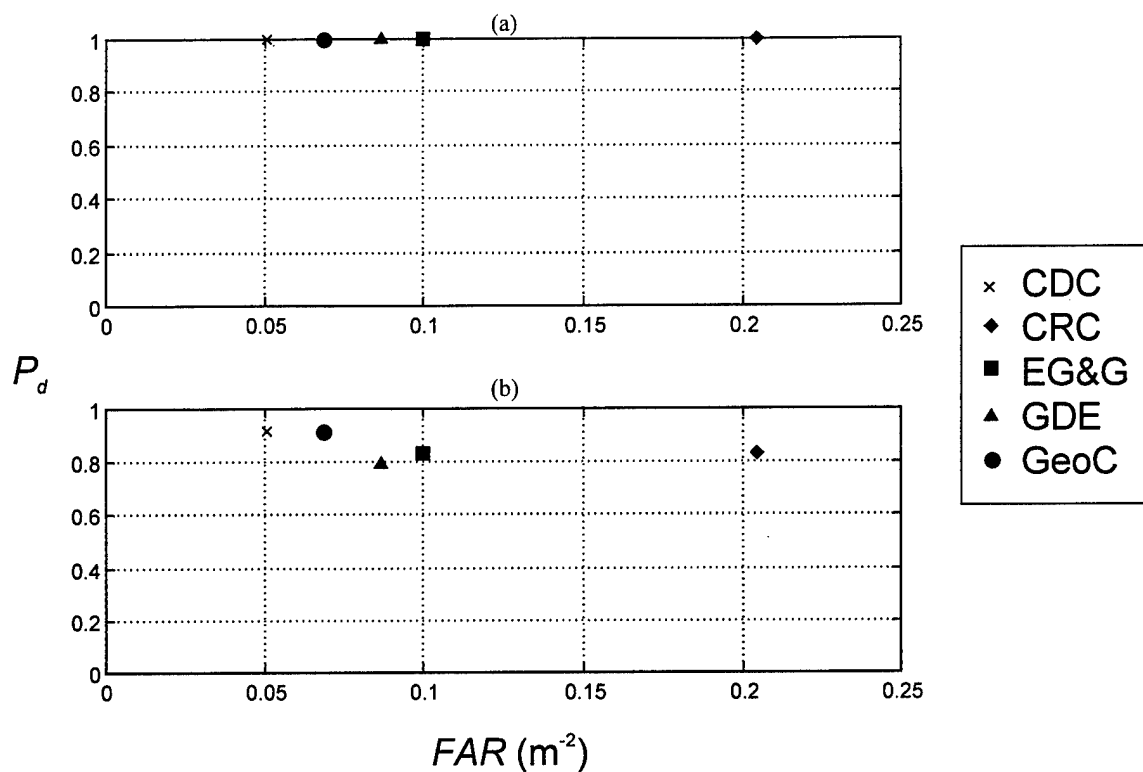
Figure IV-25. P_d for (a) Metal Mines and (b) Low-Metal Mines, Off-Road, Surface at Aberdeen
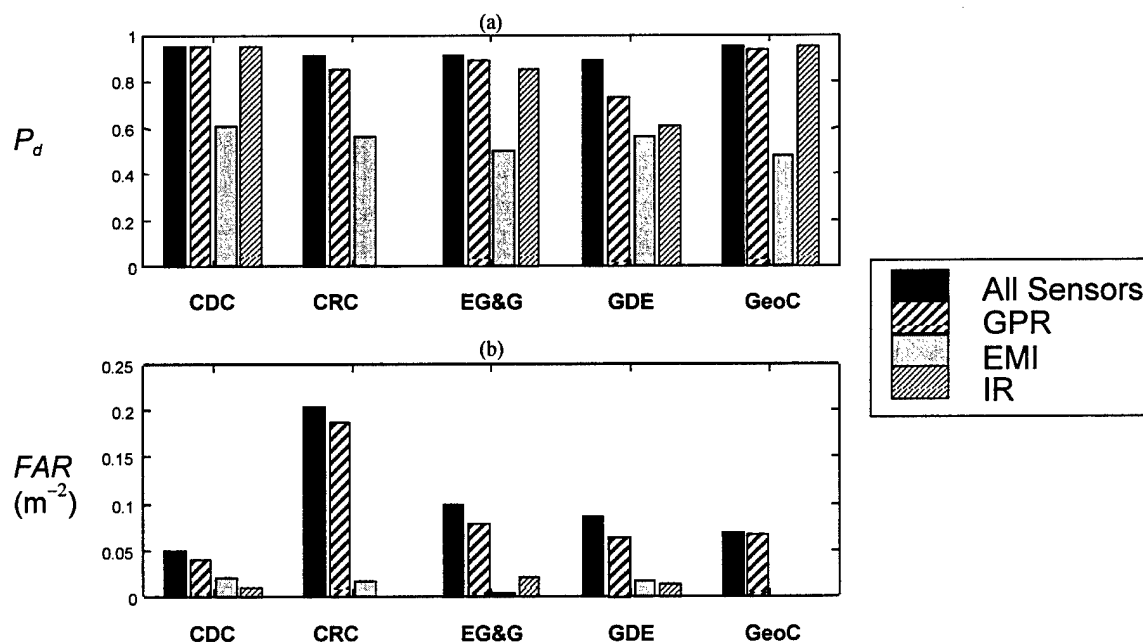
Figure IV-26. (a) P_d and (b) *FAR* as Functions of Sensor Type for Off-Road, Surface Mines at Aberdeen
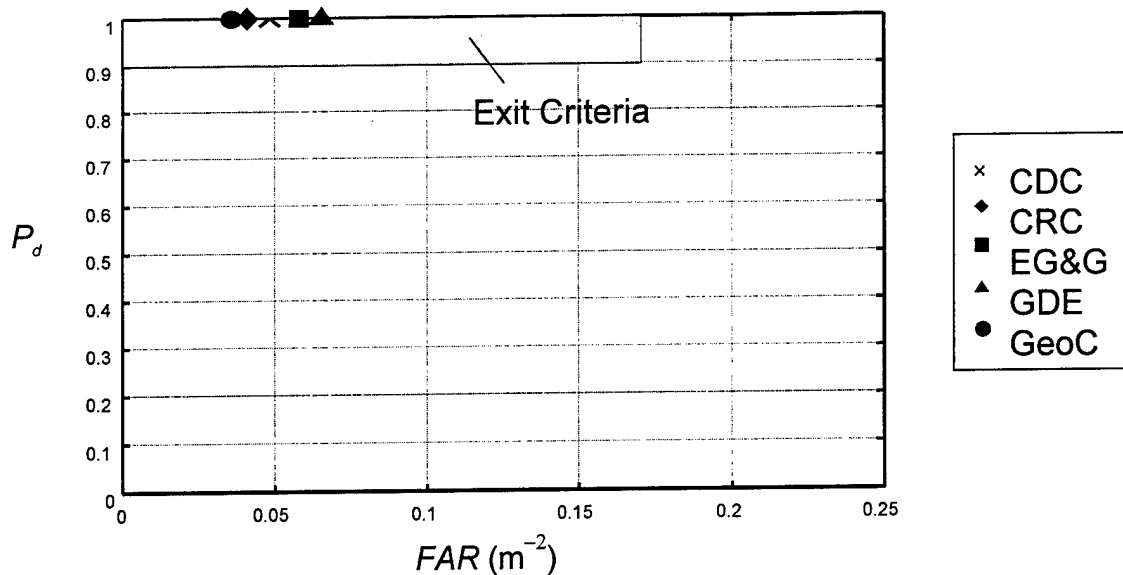
Figure IV-27. P_d **vs.** *FAR* **for Off-Road, Surface Mines at Socorro**

E. POSITION RESOLUTION

In this section, we compare the position resolutions (standard deviations, or RMS, of the miss distance distributions) achieved by the contractors. For information regarding the method we use to measure the RMS resolutions, see the discussion in Chapter III. For more detailed analyses of the contractors' position resolutions, including a breakdown of resolution for the different sensor types, see the individual contractor performance summaries in Chapter V.

Figure IV-28 shows the along-track and cross-track resolutions at Aberdeen in both the on-road and off-road lanes. Contractors typically recorded along- and cross-track resolutions between 10 and 30 cm; however, GDE recorded almost a 50-cm cross-track resolution in the off-road lanes at Aberdeen, and CRC posted just over a 30-cm cross-track resolution in the off-road lane at Aberdeen. Note that there is a trend for the contractors to slightly lose resolution (obtain larger RMS) as they go off road. This trend, however, is not universal: EG&G and GeoC did exhibit better along-track resolutions off road. No single contractor stands out as having the best overall resolution at Aberdeen.

Figure IV-29 is a summary of the contractors' position resolutions at the Socorro test site. All the resolutions were between about 10 and 30 cm, with some contractors consistently achieving about 10-cm to 15-cm resolutions. No trend is evident between the on-road and off-road conditions.

IV-24

Aberdeen, along-track resolution

Aberdeen, cross-track resolution
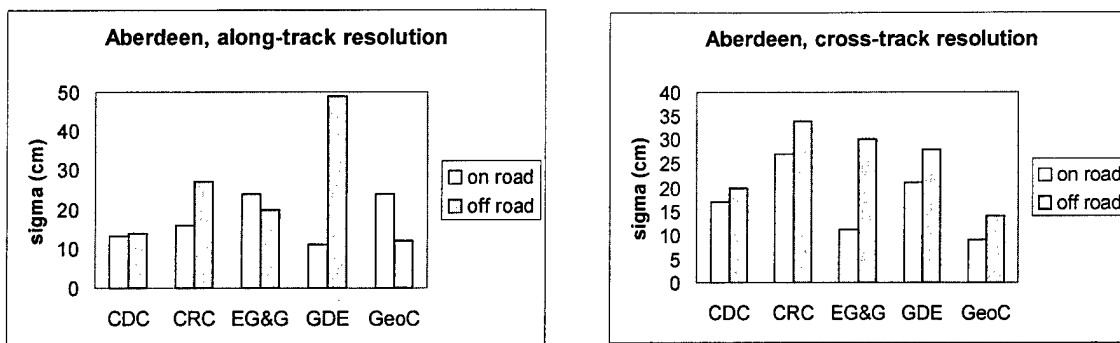
Figure IV-28. Along-Track and Cross-Track Position Resolution (RMS)
for On-Road and Off-Road Lanes at Aberdeen

Socorro, along-track resolution

Socorro, cross-track resolution
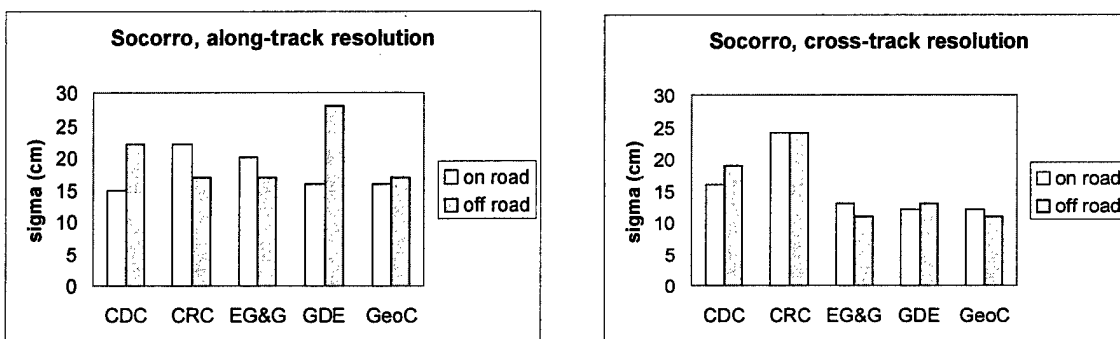
Figure IV-29. Along-Track and Cross-Track Position Resolution (RMS) for On-Road
and Off-Road Lanes at Aberdeen and Off-Road Lanes at Socorro

A sensor will only lose about 0.3 percent of its detection probability if its along-track or cross-track declarations are required to be within a distance that extends three times the RMS position resolution from the center of a mine (assuming there is no bias). Thus, if a sensor has a 20-cm resolution, the requirement that a declaration be placed within 60 cm from the center of a mine (or, equivalently in this ATD, reducing the halo size to 45 cm) would have almost no effect on P_d. Since a 20-cm resolution is reasonably representative of the contractors' average performance, we can state that the current grading criterion—a 1-m halo from the edge of a mine (which corresponds to about a 1.15-m requirement from the center of an AT mine)—is too large. If a smaller halo were chosen, most of the contractors in this ATD would have had about the same P_d performance. Using a smaller halo may increase the FAR as defined in this report, but the false alarm probability P_{fa}, which properly accounts for the areal opportunity for false alarms, would not increase.

F. COMBINED ABERDEEN AND SOCORRO RESULTS

In this section we study the contractors' performance using the combined results of the Aberdeen and Socorro tests.

1. On-road, Subsurface Mines

As shown in Figure IV-30, none of the contractors strictly met the EMD exit criteria for on-road, subsurface mines using the combined data from Aberdeen and Socorro. CRC was statistically consistent within the criteria: it met the *FAR* criterion and was within statistical error of the P_d criterion (CRC had the lowest P_d of the five contrac-. tors). CDC and GeoC both met the P_d criterion and were within about 5 percent of the *FAR* criterion. GDE and EG&G met the P_d criterion, but were further away from the *FAR* criterion.
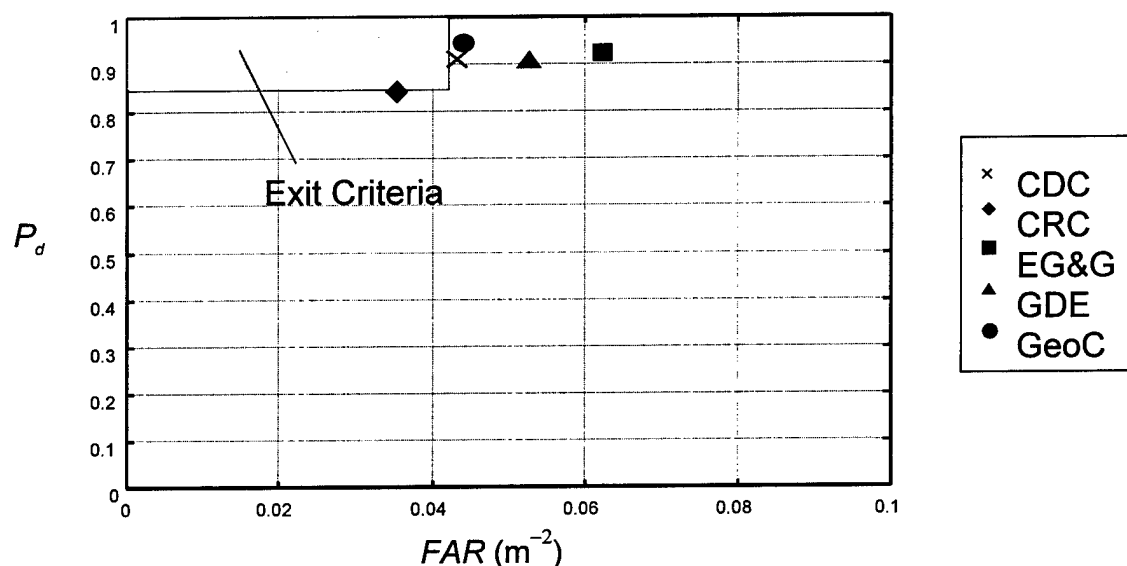
Figure IV-30. P_d vs. *FAR* for On-Road, Subsurface Mines at Aberdeen and Socorro (Combined)

2. On-road, Surface Mines

Figure IV-31 shows the P_d vs. *FAR* results for on-road, surface mines for the combined tests of Aberdeen and Socorro. CRC, while posting the lowest P_d of the five contractors, was the only contractor that met P_d and *FAR* exit criteria outright. CDC and GeoC, both of which achieved 100-percent P_d, missed the *FAR* criterion by less than 5 percent. GDE and EG&G, both of which achieved a P_d of over 98 percent, missed the *FAR* criterion by wider margins.
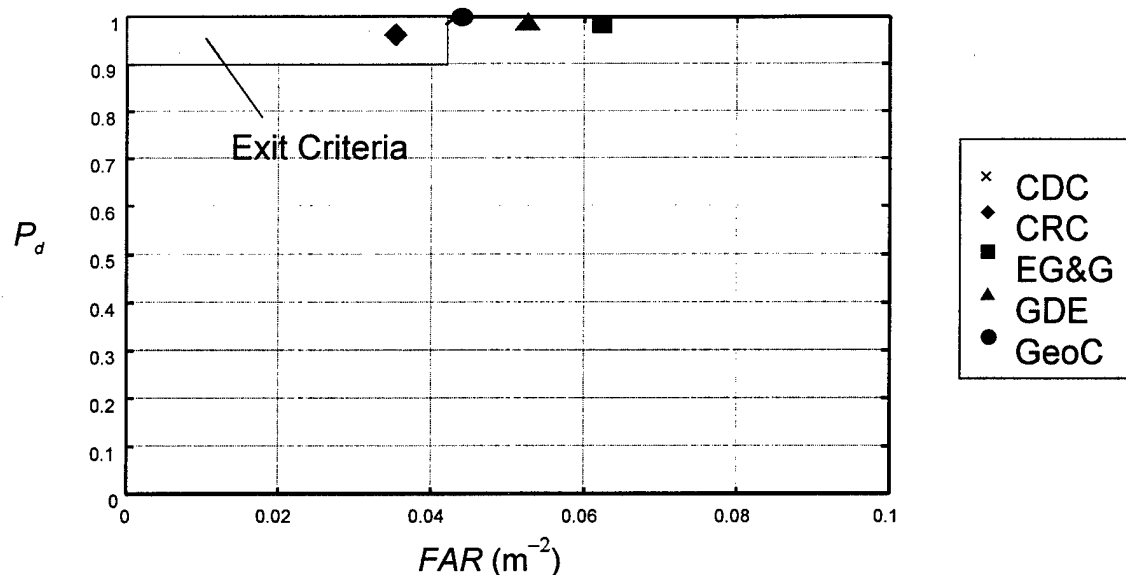
Figure IV-31. P_d vs. FAR for On-Road, Surface Mines at Aberdeen and Socorro (Combined)

3. Off-road, Subsurface Mines

Figure IV-32 shows the P_d vs. *FAR* results for off-road, subsurface mines for the combined tests of Aberdeen and Socorro. Note that CDC, EG&G, GDE, and GeoC all met the P_d and *FAR* exit criteria. One contractor, CRC, missed these exit criteria— although its P_d passed the criterion, the *FAR* missed the criterion by less than 1 percent.

4. Off-road, Surface Mines

Figure IV-33 shows the P_d vs. *FAR* results for off-road, surface mines for the combined tests of Aberdeen and Socorro. CDC, GeoC, EG&G, and GDE met both the P_d and *FAR* criteria. CRC met the P_d criterion but missed the *FAR* criterion by 1 percent. CDC and GeoC achieved P_d of 100 percent with only about one-third of the false alarms allowed by the exit criterion. GDE and EG&G were about in the middle of the P_d and *FAR* ranges allowed by the exit criteria.
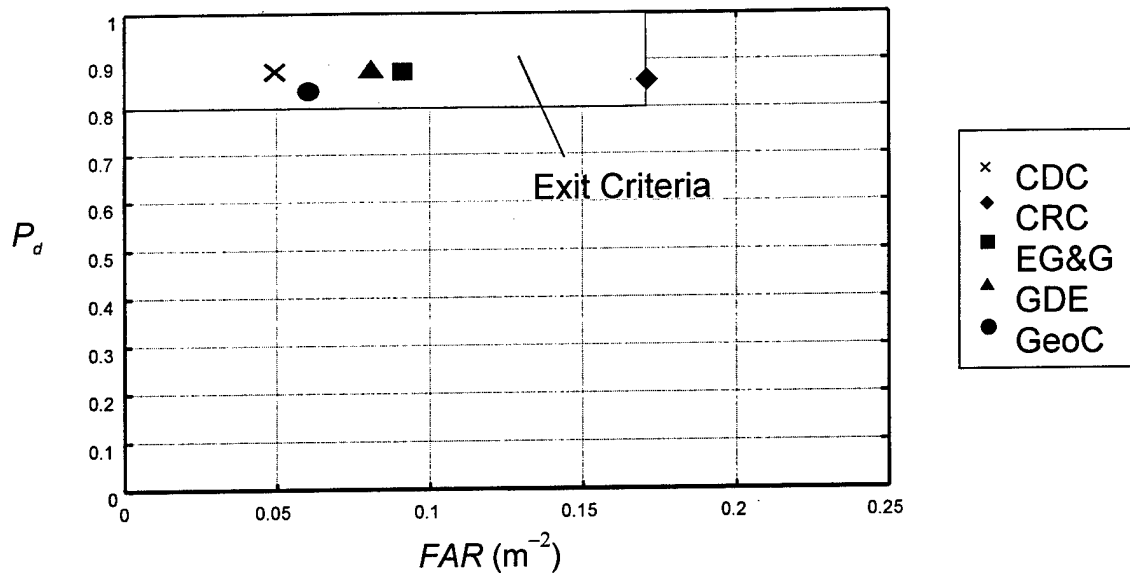
Figure IV-32. P_d **vs.** *FAR* **for Off-Road, Subsurface Mines at Aberdeen and Socorro (Combined)**
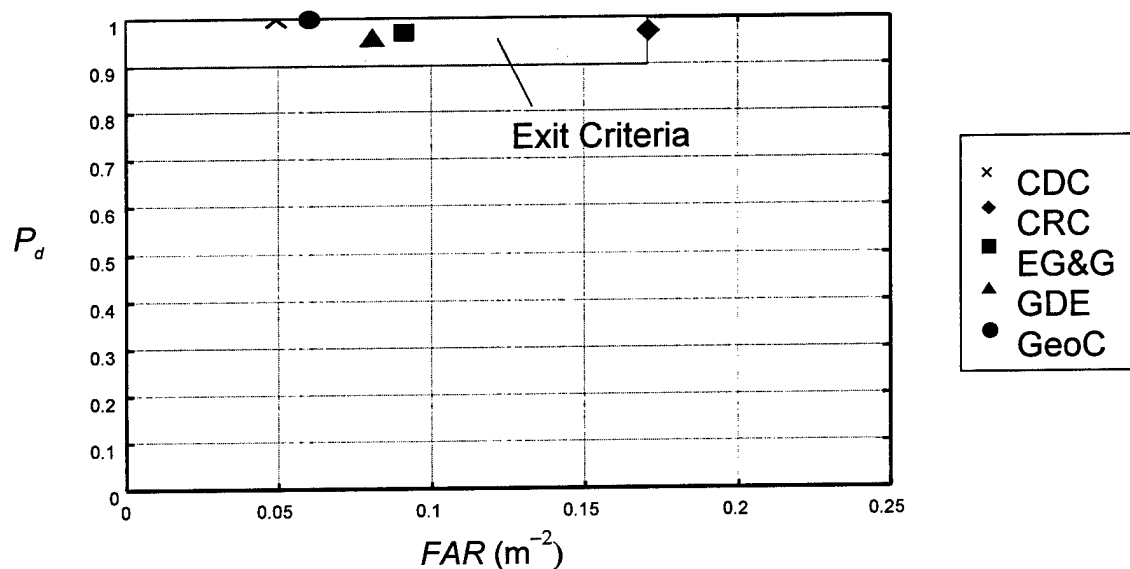
Figure IV-33. P_d **vs.** *FAR* **for Off-Road, Surface Mines at Aberdeen and Socorro (Combined)**

G. VEHICLE SPEED

Table IV-9 shows the average vehicle speeds (also called *detection speeds* in this report) of the five contractors at Aberdeen and Socorro for both on-road and off-road lanes. EG&G did not include time-stamps in its electronic alarm files, and so we could not compute the detection speed of their system.

IV-28

Table IV-9. System Detection Speed at Aberdeen and Socorro

	Aberdeen		Socorro	
Contractor	On-Road Speed (km/hr)	Off-Road Speed (km/hr)	On-Road Speed (km/hr)	Off-Road Speed (km/hr)
CDC	0.616	0.689	0.507	0.309
CRC	1.472	1.190	1.097	0.887
EG&G	N/A	N/A	N/A	N/A
GDE	1.699	1.278	1.233	1.229
GeoC	1.114	0.859	1.183	1.057

None of the contractors met the detection speed exit criteria of 3.6 km/hr for on-road and 2.0 km/hr for off-road. For each contractor at both sites, off-road speeds were less than on-road speeds. GDE was the fastest at both sites, both on and off road. CDC was the slowest, with speeds less than one-half those of the other contractors. This was probably a result of their TNA verification system, which required the vehicle to stop periodically for approximately 2–3 minutes.

V. INDIVIDUAL CONTRACTOR PERFORMANCE

In this section we examine in detail the systems employed by each contractor. We are especially concerned with which sensors are dominant on each system, and how the other sensors on board provide marginal improvements to the entire system. In addition, we look at how the sensors perform against mines of varying metal content, as well as the position resolution of the sensors. Finally, we report the results of special runs completed by each of the contractors.

A. CDC PERFORMANCE

1. Individual Sensor and Sensor Pair Performance

As shown in Table V-1, CDC's system found 100 percent of the on-road and off-road surface mines emplaced at Aberdeen and Socorro. Subsurface mines were detected by its system at about a 90-percent level or above, except for the off-road lane at Socorro, where the P_d was about 63 percent.

CDC's GPR made the bulk of the subsurface detections, except for the off-road lane at Socorro, where the EMI sensor made most of the detections. CDC's IR sensor was the most effective for detecting surface mines, although the GPR was as good, both off-road at Aberdeen and on-road at Socorro.

CDC's GPR was usually responsible for the bulk of its false alarms, except for the off-road lane at Socorro, where the IR contributed the largest number to the system total.

Even though CDC's GPR typically achieved the best detection probability of any single sensor in its system, there were improvements in the system performance due to the other sensors. In fact, no single pair of sensors stood out as being responsible for the total system performance. For example, in most cases the GPR and IR alone performed as well as the entire system (within errors); however, in the off-road, subsurface condition at Socorro, the EMI in conjunction with the GPR was needed to achieve the results CDC posted.

Table V-1. CDC's False-Alarm Rates and Detection Probabilities Listed for Individual Sensors, Sensor Pairs, and the Total System. Results from the Aberdeen and Socorro Sites are listed separately. False alarm rates are quoted in the units m^{-2}, and detection probabilities are given in percent. G, M, and I refer to the GPR, EMI, and IR sensors, respectively.

CDC

Aberdeen	G	M	I	GM	MI	GI	TOTAL
on-road FAR	0.039	0.029	0.012	0.053	0.036	0.045	0.054
on-road, subsurface Pd	90.9	60.6	72	93.2	87.1	92.4	93.2
on-road, surface Pd	94.2	62.8	100	96.5	100	100	100
off road FAR	0.04	0.021	0.008	0.049	0.027	0.041	0.05
off-road, subsurface Pd	92.7	64.7	83.8	94.1	88.2	98.5	98.5
off-road, surface Pd	100	60.4	100	100	100	100	100
Socorro	G	M	I	GM	MI	GI	TOTAL
on-road FAR	0.024	0.013	0.012	0.032	0.022	0.027	0.032
on-road, subsurface Pd	81.1	58.8	69.6	88.5	85.8	86.5	89.2
on-road, surface Pd	97.9	50	99	97.9	100	100	100
off road FAR	0.022	0.007	0.035	0.028	0.037	0.048	0.048
off-road, subsurface Pd	46.7	56.7	26.7	63.3	56.7	50	63.3
off-road, surface Pd	88.9	66.7	100	88.9	100	100	100

2. Detection Probability Versus Metal Content of Mine

Table V-2 summarizes CDC's detection probability versus metal content, for on and off road, surface and subsurface conditions. The detection probability is given for all sensors, as well as for individual sensor types.

Table V-2. CDC's Detection Probability vs. Metal Content at Aberdeen and Socorro

CDC/Aberdeen		On Road				Off Road			
		ALL	GPR	EMI	IR	ALL	GPR	EMI	IR
Surface	M	1	0.94	1	1	1	1	1	1
	LM	1	0.93	0.39	1	1	1	0.21	1
	NM	1	1	0.17	1	na	na	na	na
Subsurface	M	1	0.98	0.98	0.73	1	0.97	1	0.95
	LM	0.86	0.83	0.28	0.69	0.97	0.87	0.2	0.7
	NM	1	1	0.17	1	na	na	na	na

CDC/Socorro		On Road				Off Road			
		ALL	GPR	EMI	IR	ALL	GPR	EMI	IR
Surface	M	1	1	1	0.98	1	1	1	1
	LM	1	0.96	0	1	1	0.67	0	1
	NM	na	na	na	na	na	0	na	na
Subsurface	M	1	0.9	1	0.74	1	0.69	1	0.44
	LM	0.78	0.72	0.22	0.63	0.21	0.21	0.07	0.07
	NM	0.86	0.79	0.21	0.79	na	na	na	na

All metal-cased mines were found by CDC, regardless of the depth of the mine and the test location. Their EMI sensor was, on average, the best sensor for finding the metal mines. The GPR performed well at detecting metal mines, except in the off-road,

subsurface condition at Socorro. The IR sensor was very reliable at detecting surface metal mines, but showed a degradation of performance for subsurface metal mines.

Low-metal, surface mines were detected with a higher probability than low-metal, subsurface mines. The GPR sensor was the best sensor for the detection of low-metal mines, averaged over all conditions, although the IR sensor performed about as well as the GPR for the surface condition.

3. Position Resolution

a. On-Road Tests

Figure V-1 shows CDC's miss-distance distributions in the on-road tests at Aberdeen. The mean (bias) of the along-track distribution is –4 cm (meaning that the mine locations were offset by an average of 4 cm from the center of the mine); however, this bias is not especially significant because it is well within the radius of the mine. The RMS resolution along-track is 13 cm. Cross-track, the mean is 0 cm (that is, unbiased) and the standard deviation (RMS) is 17 cm. These distributions were typical for CDC at both Aberdeen and Socorro.

Table V-3 summarizes the bias and RMS, broken down by surface and subsurface mines, as well as by sensor, for the on-road tests at Aberdeen and Socorro. The data show there are no significant trends; that is, no sensor performed significantly differently from the overall performance of all sensors, nor was there a dependence on mine location (surface or subsurface). In addition, CDC's performance did not differ significantly at Aberdeen or Socorro.
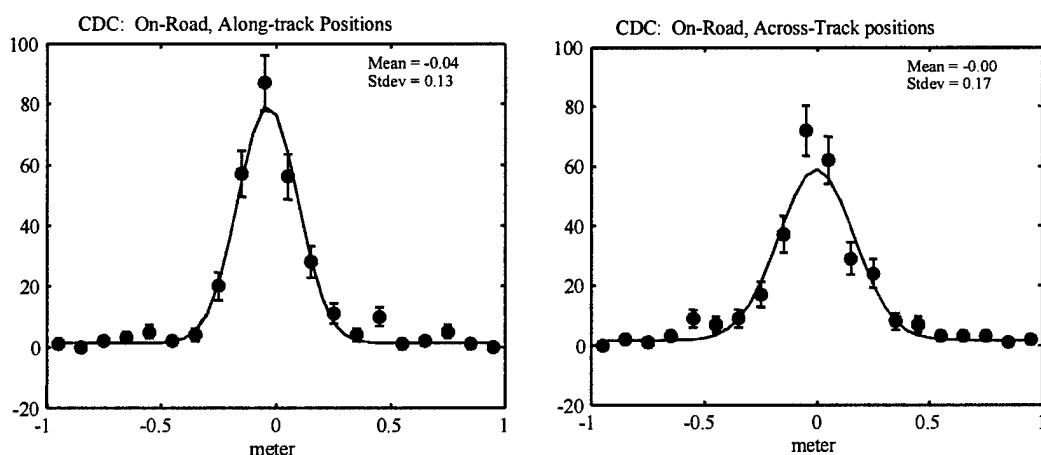
Figure V-1. CDC's Miss-Distance Distributions for Surface and Subsurface Mines in On-Road Tests at Aberdeen. Data points include the GPR, EMI, and IR sensors. The solid curve is the best fit of a constant plus a Gaussian.

Table V-3. CDC Bias and Resolution Performance on Road at Aberdeen and Socorro

	Aberdeen Position Resolution				Socorro Position Resolution			
Type	Along-track		Cross-track		Along-track		Cross-track	
	Mean (bias) (m)	Standard Deviation (RMS) (m)	Mean (bias) (m)	Standard Deviation (RMS) (m)	Mean (bias) (m)	Standard Deviation (RMS) (m)	Mean (bias) (m)	Standard Deviation (RMS) (m)
All sensors, subsurface + surface	−0.04	0.13	0.00	0.17	−0.03	0.15	−0.04	0.16
All sensors, subsurface	−0.03	0.14	−0.02	0.12	0.01	0.13	−0.02	0.15
GPR	−0.01	0.15	−0.02	0.13	0.02	0.13	−0.03	0.15
EMI	−0.03	0.14	−0.02	0.11	0.05	0.11	−0.04	0.15
IR	−0.05	0.12	−0.02	0.11	0.00	0.15	−0.01	0.15
All sensors, surface	−0.04	0.11	0.02	0.20	−0.06	0.13	−0.07	0.15
GPR	−0.03	0.11	0.02	0.19	−0.06	0.13	−0.06	0.14
EMI	−0.09	0.10	0.04	0.18	−0.09	0.15	−0.07	0.12
IR	−0.04	0.11	0.02	0.18	−0.06	0.13	−0.07	0.13

b. Off-Road Tests

Figure V-2 shows the combined results for the measured mine locations in the off-road tests at Aberdeen for CDC. Along-track, the mean (bias) of the distribution is −12 cm, which appears to be slightly biased. That is, in this off-road case, the measured mine location is typically several centimeters behind the actual location of the center of the mine, with respect to the vehicle's direction of travel. The intrinsic resolution along-track is, however, consistent with the on-road test, at 14 cm. The cross-track measurements again appear to have no bias, and, at 20 cm, the standard deviation is consistent with the on-road tests.

This slight bias in the along-track off-road test appears to be primarily due to the performance of the EMI sensor (see Table V-4). Also shown in the table are the resolutions for the off-road tests at Socorro. There were poor statistics at this test, although it is apparent in the table that the bias caused by the EMI detector (as in the off-road Aberdeen test) was not present. The larger intrinsic resolution at Socorro is not particularly statistically significant here because too few data points were collected.

V-4
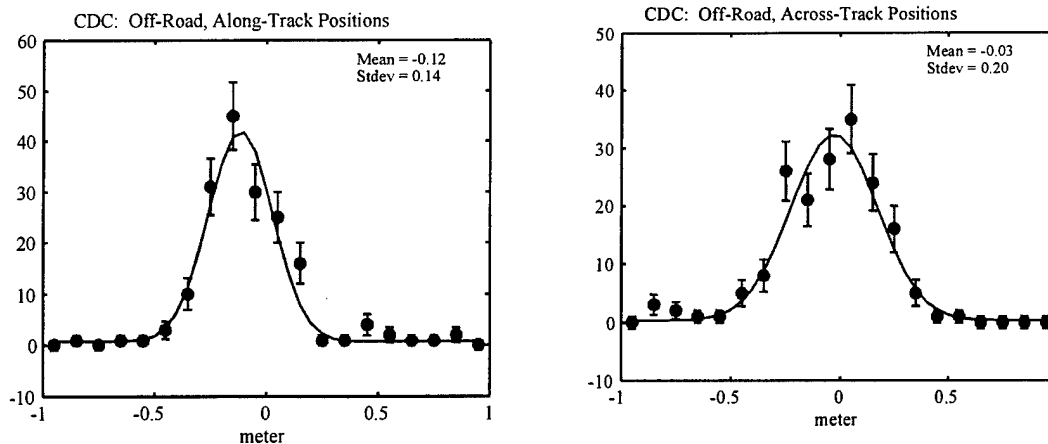
Figure V-2. Results of the Surface and Subsurface Measured Mine Locations for the CDC Off-Road Tests at Aberdeen. Data from the GPR, EMI, and IR sensors are included in this plot.

4. P_d and R_{halo}

The bias and RMS resolution performance of the sensors affect how well, as a function of R_{halo}, CDC's system detects the mines. Figure V-3 shows a plot of P_d versus R_{halo} for the tests at Aberdeen and Socorro. These figures summarize the overall implication of CDC's relatively small sensor bias and intrinsic sensor resolution (as tabulated in section 2).

As shown in the plots, the detection probability for CDC's sensors reached its maximum for an R_{halo} of much less than 1 m. If this ATD had required R_{halo} to be as small as approximately 40 cm, then CDC's P_d performance would have been nearly the same. Even an R_{halo} of as small as 25 cm would have resulted in very little degradation of performance, and CDC would likely have still met most of the P_d exit criteria.

Table V-4. CDC Bias and Resolution Performance off Road at Aberdeen and Socorro

	Aberdeen Position Resolution				Socorro Position Resolution			
Type	Along-track		Cross-track		Along-track		Cross-track	
	Mean (bias) (m)	Standard Deviation (RMS) (m)	Mean (bias) (m)	Standard Deviation (RMS) (m)	Mean (bias) (m)	Standard Deviation (RMS) (m)	Mean (bias) (m)	Standard Deviation (RMS) (m)
All sensors, subsurface + surface	−0.12	0.14	−0.03	0.20	−0.08	0.22	−0.06	0.19
All sensors, subsurface	−0.14	0.14	−0.01	0.21	−0.01	0.21	−0.02	0.16
GPR	−0.13	0.14	−0.02	0.19	0.06	0.19	−0.08	0.15
EMI	−0.19	0.09	0.03	0.19	0.00	0.22	0.01	0.15
IR	−0.10	0.15	−0.02	0.21	−0.07	0.20	0.02	0.16
All sensors, surface	−0.07	0.14	−0.05	0.19	Not well fit	Not well fit	Not well fit	Not well fit
GPR	−0.02	0.11	−0.05	0.15	Not well fit	Not well fit	−0.12	0.19
EMI	−0.15	0.10	−0.02	0.19	Not well fit	Not well fit	−0.09	0.24
IR	−0.07	0.14	−0.06	0.21	Not well fit	Not well fit	Not well fit	Not well fit

CDC

a) On-road at Aberdeen   b) On-road at Socorro

— Subsurface
---- Surface

c) Off-road at Aberdeen   d) Off-road at Socorro
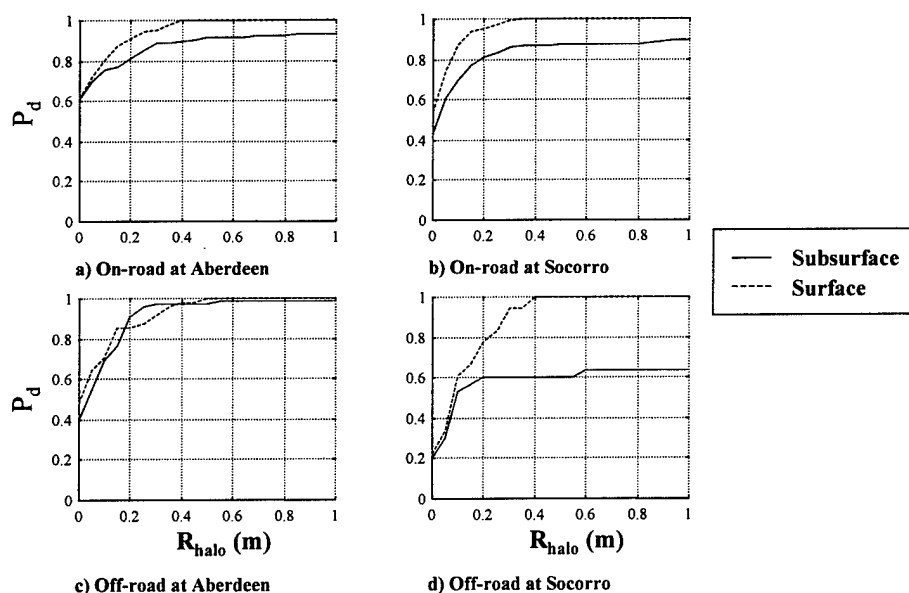
Figure V-3. P_d vs. R_{halo} for CDC's Sensor Suite at Aberdeen and Socorro

5. Additional Runs

a. Aberdeen Results

The only additional runs by CDC at Aberdeen were the two night runs conducted on lane 15.[1] Table V-5 shows the cumulative P_d and FAR for the scored on-road, day runs and the night runs on lane 15. The P_d and FAR are shown for all sensors (Total) and for the IR sensor only. The reason for presenting the results for the night runs in this way is because we expect the IR will be the only sensor that behaves differently at night. In Table V-5, we notice that the P_d for subsurface mines for the night runs is less than during the day, while IR surface detections are unaffected at night. The total and IR FARs for the night runs are nearly the same as the FARs for the day runs.

Table V-5. Comparison of CDC On-Road Day and Night Runs at Aberdeen

	On-Road Day		Night	
	Surface	Subsurface	Surface	Subsurface
Total P_d	1.0	0.932	1.0	0.975
IR P_d	1.0	0.720	1.0	0.600
Total FAR	0.054 m^{-2}		0.055 m^{-2}	
IR FAR	0.012 m^{-2}		0.012 m^{-2}	

b. Socorro Results

The only additional runs by CDC at Socorro were the one night run conducted on lane 11 and the two night runs conducted on lane 13.[2] The cumulative P_ds and FARs for the scored on-road day runs and the night runs on lanes 11 and 15 are shown in Table V-6. The results are different from Aberdeen. The IR P_d for subsurface mines is larger at night than during the day, while surface detections are not different in the day and night. In fact, the IR sensor detected all the subsurface mines detected during the night runs. It

---

[1] The results of these runs are summarized in Table B-8 in Appendix B and can be compared to the results CDC obtained on its scored daytime runs on lane 15 as shown in Table B-5.

[2] The results of these runs are summarized in Tables B-22 and B-24 in Appendix B and can be compared to the results CDC obtained on its scored daytime runs on lanes 11 and 13 as shown in Tables B-13 and B-15, respectively.

should be noted that the total and IR *FAR* at night was about twice the *FAR* of the day runs.

Table V-6. Comparison of CDC On-Road Day and Night Runs at Socorro

	On-Road Day		Night	
	Surface	Subsurface	Surface	Subsurface
Total P_d	1.0	0.892	1.0	0.903
IR P_d	0.990	0.696	1.0	0.903
Total *FAR*	0.032 m^{-2}		0.058 m^{-2}	
IR *FAR*	0.012 m^{-2}		0.026 m^{-2}	

B. CRC PERFORMANCE

1. Individual Sensor and Sensor Pair Performance

As shown in Table V-7, CRC's GPR detected more surface mines than its EMI sensor, regardless of condition. It also detected most of the subsurface mines, except on the off-road lane at Socorro, where its EMI sensor detected the bulk of the mines. CRC did not utilize its IR detector in these tests.

The GPR dominated the false-alarm rate in all cases. The EMI sensor had no false alarms at Socorro, either on- or off-road, and at its worst contributed 0.018 m^{-2} to the false-alarm rate off road at Aberdeen (which represented less than 10 percent of the GPR's *FAR*).

It was the combination of sensors that enabled the CRC system to achieve the results that they posted; neither the GPR nor the EMI sensor would have performed as well on its own under most conditions.

2. Detection Probability Versus Metal Content of Mine

Table V-8 summarizes CRC's detection probability versus metal content, for on and off road, surface and subsurface conditions. The detection probability is given for all sensors, as well as for individual sensor types.

Table V-7. CRC's False-Alarm Rates and Detection Probabilities Listed for Individual Sensors, Sensor Pairs, and the Total System. Results from the Aberdeen and Socorro sites are listed separately. False-alarm rates are quoted in the units m^{-2}, and detection probabilities are given in percent. G, M, and I refer to the GPR, EMI, and IR sensors, respectively.

Aberdeen	G	M	I	GM	MI	GI	TOTAL
on-road FAR	0.031	0.003	na	0.034	na	na	0.034
on-road, subsurface Pd	55.3	47.7	na	77.3	na	na	77.3
on-road, surface Pd	90.7	40.7	na	91.9	na	na	91.9
off road FAR	0.183	0.018	na	0.201	na	na	0.201
off-road, subsurface Pd	77.9	58.8	na	91.2	na	na	91.2
off-road, surface Pd	89.6	56.3	na	95.8	na	na	95.8
Socorro	G	M	I	GM	MI	GI	TOTAL
on-road FAR	0.037	0	na	0.037	na	na	0.037
on-road, subsurface Pd	81.8	47.3	na	90.5	na	na	90.5
on-road, surface Pd	100	50	na	100	na	na	100
off road FAR	0.041	0	na	0.041	na	na	0.041
off-road, subsurface Pd	30	53.3	na	73.3	na	na	73.3
off-road, surface Pd	100	66.7	na	100	na	na	100

Table V-8. CRC's Detection Probability vs. Metal Content at Aberdeen and Socorro

CRC/Aberdeen		On Road				Off Road			
		ALL	GPR	EMI	IR	ALL	GPR	EMI	IR
Surface	M	1	0.97	0.97	na	1	0.92	1	na
	LM	0.86	0.86	0	na	0.92	0.88	0.13	na
	NM	0.83	0.83	0	na	na	na	na	na
Subsurface	M	1	0.53	1	na	1	0.79	1	na
	LM	0.56	0.56	0.02	na	0.8	0.77	0.07	na
	NM	0.67	0.67	0	na	na	na	na	na

CRC/Socorro		On Road				Off Road			
		ALL	GPR	EMI	IR	ALL	GPR	EMI	IR
Surface	M	1	1	1	na	1	1	1	na
	LM	1	1	0	na	1	1	0	na
	NM	na	na	na	na	na	na	na	na
Subsurface	M	1	0.81	1	na	1	0.19	1	na
	LM	0.8	0.8	0	na	0.43	0.43	0	na
	NM	0.93	0.93	0	na	na	na	na	na

All metal-cased mines were found by CRC, regardless of the depth of the mine and the test location. CRC's EMI sensor was the best sensor for finding the metal mines. At both sites, surface metal mines were detected by its GPR with a higher probability than were subsurface metal mines.

Surface, low-metal mines were detected with a higher probability than subsurface, low-metal mines. The GPR sensor was CRC's only reliable sensor for detecting low-metal mines.

3. Position Resolution

a. On-Road Tests

Figure V-4 shows CRC's miss-distance distributions in the on-road tests at Aberdeen. Along-track, the mean (bias) of the distribution is –18 cm. This bias indicates that the CRC system systematically measures the location of the center of the mine behind its actual position (and outside the mine radius). This bias appears in measurements of both the surface and subsurface mine locations, and appears to be primarily caused by a systematic offset in the GPR's measurement of mine location. The Standard Deviation (RMS) along-track is 16 cm, about as large as the mean radius of the land mines used in this test. Cross-track, the mean is 14 cm and the standard deviation is 27 cm. Both of these distributions have very nearly the expected Gaussian distribution, except for a second peak around 50 cm in the along-track distribution.
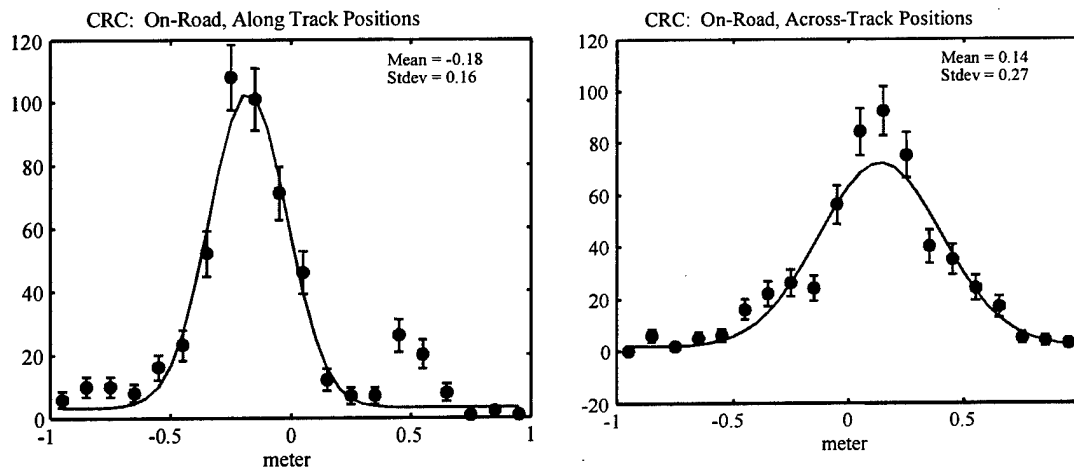
Figure V-4. Miss-Distance Distributions of the Measured Surface and Subsurface Mine Locations for the CRC On-Road Tests at Aberdeen. Data points include the GPR and EMI sensors. The solid curve is the best fit of a constant plus a Gaussian.

CRC's metal detector causes this second peak. The data from the metal detector exhibit two distinct normal distributions, on either side of the mean (see Figure V-5). Although the cross-track distribution of the metal detector measurements also exhibits these double-distributions, it does not show up in the overall along-track distributions as an artifact, or second peak (see Figure V-5). Instead, the overall distribution is widened significantly, so that the overall cross-track intrinsic resolution is 27 cm. The metal

detector's measurements are well within the 1-m halo, however, although the RMS of this sensor is large.
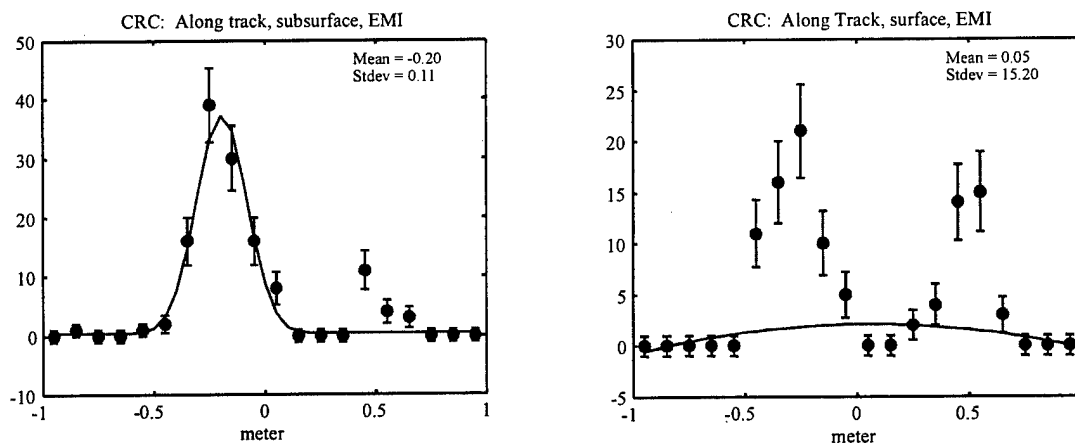
Figure V-5. Miss-Distance Distribution for CRC's EMI Sensor, On-Road at Aberdeen. Note the double peaks.

Table V-9 summarizes the measured biases and RMS in the on-road tests, broken down by surface and subsurface mines, as well as by sensor. Also shown are the measurements from the on-road tests at Socorro. Note that for subsurface mines, the GPR measurement is significantly offset and has a large RMS. Nevertheless, there is no significant overall dependence of the measurements on mine location (surface or subsurface). The performances in the on-road tests at both Aberdeen and Socorro did not differ from one another.

b. Off-Road Tests

Figure V-6 shows CRC's miss-distance distributions in the off-road tests at Aberdeen. Along-track, the mean (bias) of the distribution is −14 cm. This bias appears to be primarily due to the performance of the metal detector. Again, the along-track distribution exhibits a second peak around 40 cm, due to the metal detector's measurements. The offset in the main peak (at −14 cm) is due in this case to an offset in the metal detector's measurement.

The cross-track distribution (as shown in Figure V-6) is also biased by about 17 cm. This bias appears to be due to a bias in the GPR measurement of 15 cm subsurface and 21 cm surface (see Table V-10).

Also shown in the table are the measurements from the off-road tests at Socorro. These results do not differ significantly from the Aberdeen measurements, although the statistics are poor.

Table V-9. CRC Bias and Resolution Performance at Aberdeen and Socorro: On-Road Performance

Type	Aberdeen Position Resolution				Socorro Position Resolution			
	Along-track		Cross-track		Along-track		Cross-track	
	Mean (bias) (m)	Standard Deviation (RMS) (m)	Mean (bias) (m)	Standard Deviation (RMS) (m)	Mean (bias) (m)	Standard Deviation (RMS) (m)	Mean (bias) (m)	Standard Deviation (RMS) (m)
All sensors, subsurface + surface	−0.18	0.16	0.14	0.27	−0.16	0.22	0.11	0.24
All sensors, subsurface	−0.21	0.14	0.15	0.32	−0.24	0.21	0.10	0.29
GPR	−0.42	0.32	0.23	0.20	−0.26	0.29	0.12	0.15
EMI	−0.20	0.11	0.08	0.38	0.00	Not well fit	0.08	Not well fit
IR	N/A	N/A	N/A	N/A	N/A	N/A	N/A	N/A
All sensors, surface	−0.15	0.15	0.13	0.17	−0.14	0.20	0.10	0.18
GPR	−0.11	0.13	0.12	0.13	−0.13	0.18	0.09	0.14
EMI	0.05	See Note	0.05	See Note	0.07	Not well fit	0.14	Not well fit
IR	N/A	N/A	N/A	N/A	N/A	N/A	N/A	N/A

Note: These distributions of the On-Road surface metal detector measurements were non-Gaussian and thus not well fit. The mean can be computed, but a meaningful standard deviation cannot.

CRC: Off-Road, Along-Track Positions

Mean = -0.14
Stdev = 0.27

CRC: Off-Road, Across-Track Positions

Mean = 0.17
Stdev = 0.34
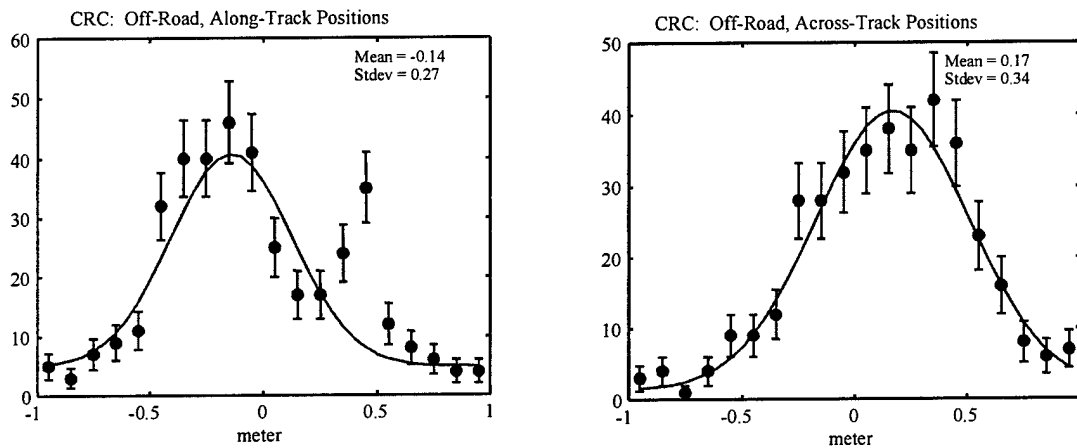
Figure V-6. Results of the Measured Surface and Subsurface Mine Locations for the CRC Off-Road Tests at Aberdeen. Data from the GPR and EMI sensors are included in these plots.

Table V-10. CRC Bias and Resolution Performance at Aberdeen and Socorro: Off-Road Performance

Type	Aberdeen Position Resolution				Socorro Position Resolution			
	Along-track		Cross-track		Along-track		Cross-track	
	Mean (bias) (m)	Standard Deviation (RMS) (m)	Mean (bias) (m)	Standard Deviation (RMS) (m)	Mean (bias) (m)	Standard Deviation (RMS) (m)	Mean (bias) (m)	Standard Deviation (RMS) (m)
All sensors, subsurface + surface	−0.14	0.27	0.17	0.34	−0.21	0.17	0.12	0.24
All sensors, subsurface	−0.21	0.20	0.11	0.35	−0.22	0.12	0.06	0.56
GPR	−0.04	0.30	0.15	0.30	Not well fit	Not well fit	Not well fit	Not well fit
EMI	−0.27	0.13	0.08	0.46	−0.23	0.12	0.07	0.74
IR	N/A	N/A	N/A	N/A	N/A	N/A	N/A	N/A
All sensors, surface	−0.14	0.28	0.21	0.30	−0.18	0.20	0.13	0.15
GPR	−0.05	0.10	0.21	0.18	−0.15	0.20	0.12	0.11
EMI	0.00	See Note	0.11	0.53	Not well fit	Not well fit	Not well fit	Not well fit
IR	N/A	N/A	N/A	N/A	N/A	N/A	N/A	N/A

Note: These distributions of the On-Road surface metal detector measurements were non-Gaussian and thus not well fit. The mean can be computed, but a meaningful standard deviation cannot.

4. P_d and R_{halo}

The bias and RMS resolution performance of the sensors affect how well, as a function of R_{halo}, CRC's system detects the mines. Figure V-7 shows a plot of P_d versus R_{halo} for the tests at Aberdeen and Socorro. These figures summarize the overall implication of CRC's bias and intrinsic sensor resolution (as tabulated in section 2).

As shown in the plots, the detection probability for CRC's sensors was maximized for a R_{halo} of approximately 60 cm. If this ATD had required R_{halo} to be significantly smaller (for instance, 25 cm), then CRC's P_d performance would have been significantly degraded, except for the on-road performance at Socorro. This is because the combination of CRC's sensor bias systematically misplaces the center of the mine, and intrinsic RMS resolution widens the probable area of mine location.

V-13
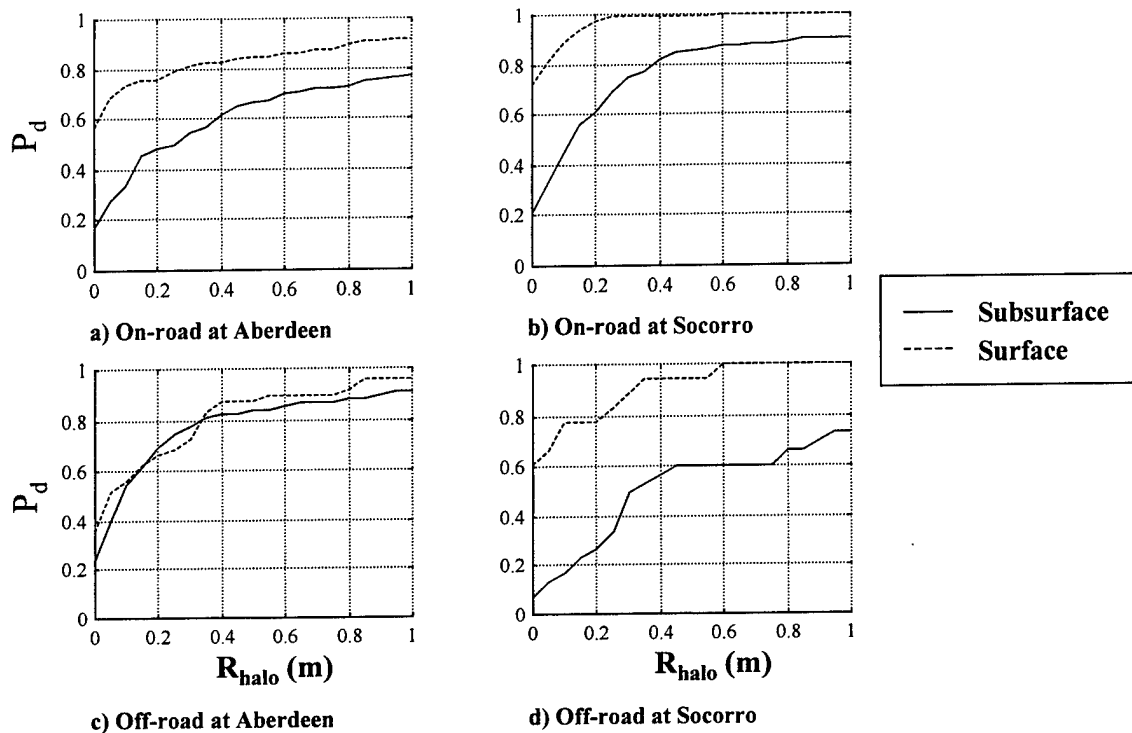
**Figure V-7. P_d vs. R_{halo} for CRC's Sensor Suite at Aberdeen and Socorro**

5. Additional Runs

a. Aberdeen Results

Additional runs by CRC at Aberdeen include two night runs on lane 15 and one physical-marking run on lane 11.[3] Table V-11 shows the cumulative P_ds and FARs for the scored on-road day runs and the night runs on lane 15. Notice that CRC did not use its IR during either the day or night runs. The P_ds for surface and subsurface mines are actually higher for the night runs, and the FAR at night is lower than the FAR for the day runs. Recall that the night runs were only conducted on two passes of one lane (lane 15), so the error bars are rather large. Examination of Tables B-3 through B-5 in Appendix B shows that CRC had its best P_ds on lane 15 (both over 90 percent), whereas on lane 12 both P_ds

---

3   The results of these runs are summarized in Tables B-6 and B-8 in Appendix B and can be compared to the results CRC obtained on its scored daytime runs on lanes 11 and 15 as shown in Tables B-3 and B-5.

were approximately 70 percent, and on lane 11 one was 92 percent and the other 84 percent. CRC began the week testing on lane 12, then moved to lane 11, and finally finished its on-road tests on lane 15 on June 16 (see Table II-13). The following night, CRC conducted its night runs on lane 15 (see Table V-II-15). It is possible that CRC's above average performance on lane 15 at night is related to its gradual performance improvement over the course of the week.

Table V-11. Comparison of CRC On-Road Day and Night Runs at Aberdeen

	On-Road Day		Night	
	Surface	Subsurface	Surface	Subsurface
Total P_d	0.919	0.773	1.0	0.900
IR P_d	N/A	N/A	N/A	N/A
Total FAR	0.034 m^{-2}		0.022 m^{-2}	
IR FAR	N/A		N/A	

Table V-12 shows the cumulative P_ds and FARs for the scored on-road day runs, and the P_d and FAR obtained for one pass on lane 11 using CRC's physical marking system (where alarm positions are determined by surveying the marks deposited on the ground). The P_ds for surface and subsurface mines are nearly the same for both sets of runs, while the FAR for the physical-marking run is one-half of the FAR for the on-road, day runs. This surprising result indicates a difference in the treatment of physical declarations that actually improves the system's FAR performance compared to electronic-marking runs.

Table V-12. Comparison of CRC On-Road Day (Electronic-Marking)
and Physical-Marking Runs at Aberdeen

	On-Road Day (EM)		Physical Marking (PM)	
	Surface	Subsurface	Surface	Subsurface
Total P_d	0.919	0.773	0.929	0.783
Total FAR	0.034 m^{-2}		0.017 m^{-2}	

We examine the position resolution of the physical-marking runs and compare these to the position resolutions for the electronic-marking, on-road day runs. Table V-13 summarizes the results. We notice that the position resolution (RMS) is much poorer for the physical-marking system. The RMS in both the along-track and cross-track directions for the physical-marking system as used on lane 11 is greater than for the on-road, day RMS from electronic marking. In addition, the mean for the on-road day runs was –0.18 m, while for the physical-marking run, it was +0.15 m. Recall that the errors for the physical-marking run are large due to the small number of mines encountered.

Table V-13. Comparison of CRC Position Resolution for On-Road Day (Electronic-Marking) and Physical-Marking Runs at Aberdeen

	On-Road Day (EM)		Physical Marking (PM)	
	Mean (m)	RMS (m)	Mean (m)	RMS (m)
Along Track	–0.18	0.16	0.15	0.47
Cross Track	0.14	0.27	0.06	0.41

b. Socorro Results

Additional runs by CRC at Socorro include two night runs on lane 4, one night run on lane 6, two physical-marking runs on lane 8, two morning runs on lane 4, and one morning run on lane 6.[4] The cumulative P_ds and FARs for the on-road day runs, and the night runs on lane 4 and 6 are shown in Table V-14. The P_d for subsurface mines is slightly higher at night than for day, and that the FAR is slightly lower for the night runs. Again, CRC did not use its IR for either the day or night runs.

---

[4] The results of these runs are summarized in Table B-18 through B-20 in Appendix B and can be compared to the results CRC obtained on its scored daytime runs on lanes 4, 6, and 8 as shown in Tables B-10 through B-12, respectively.

Table V-14. Comparison of CRC On-Road Day and Night Runs at Socorro

	On-Road Day		Night	
	Surface	Subsurface	Surface	Subsurface
Total P_d	1.0	0.905	1.0	0.963
IR P_d	N/A	N/A	N/A	N/A
Total *FAR*	0.037 m^{-2}		0.025 m^{-2}	
IR *FAR*	N/A		N/A	

For the two physical-marking runs conducted by CRC on lane 8 at Socorro, both electronic and physical-marking files were produced. That is, for a given pass of a lane, the contractor produced the usual electronic alarm file as well as physically marked the ground with alarms, the positions of which could subsequently be surveyed. Correlating in the results of these two types of alarm files gives some indication of how the contractor's physical marking system works. One might expect there to be a one-to-one correspondence between the number of alarms in corresponding EM and PM files. There are circumstances, however, that might negate this one-to-one correspondence, such as a clogged dispenser. In addition, for a given down-track position, the number of cross-track physical marking alarms may be limited by the finite number of dispensers on the contractor's vehicle. Position resolution issues may also become important when comparing the electronic alarms with the physical alarms.

Table 15 shows cumulative P_ds and *FAR*s for CRC's on-road day runs and the physical-marking runs on lane 8 at Socorro. The P_d is 1.0 for surface mines for both the on-road day runs and the physical-marking runs. For subsurface mines, the P_d is slightly higher for the physical-marking runs, although the error bars are large. The *FAR* for physical-marking runs is two-thirds that of electronic-marking runs.

In Table 16, the position resolution for the physical-marking runs is compared to the position resolution of the on-road day runs. We notice that the location accuracy in the along-track direction as measured by the standard deviation is greater for the physical-marking runs, but the cross-track location accuracy is nearly the same for both sets of tests. The means are similar in both the along-track and cross-track directions.

V-17

Table V-15. Comparison of CRC On-Road Day and Physical-Marking Runs at Socorro

	On-Road Day		Physical Marking (PM)	
	Surface	Subsurface	Surface	Subsurface
Total P_d	1.0	0.905	1.0	1.0
Total *FAR*	0.037 m^{-2}		0.023 m^{-2}	

Table V-16. Comparison of CRC Position Resolution for On-Road Day and Physical-Marking Runs at Socorro

	On-Road Day		Physical Marking (PM)	
	Mean (m)	Std (m)	Mean (m)	Std (m)
Along Track	–0.16	0.22	–0.09	0.35
Cross Track	0.11	0.24	0.15	0.23

Note the differences between the two methods of producing alarms (electronic and physical) for the two runs on lane 8. Table 17 shows P_ds, *FAR*s, and number of alarms for CRC's two physical-marking runs on lane 8 at Socorro. For the first pass of lane 8 (EM-1 and PM-1), the P_ds and *FAR*s are identical, but the number of physical marks (PM) is slightly less than the number of electronic marks (EM). For the second pass of lane 8, the PM and EM P_ds are both 1.0, but the PM *FAR* is about half the rate for the corresponding electronic marking (EM) system. Note that the number of physical marks is much less than the number of electronic marks (79 compared to 176). This result again indicates a difference in the treatment of physical declarations that actually improves the system's *FAR* performance compared to electronic-marking runs.

Table V-17. Comparison of CRC Lane 8 Physical-Marking Runs (EM and PM) at Socorro

	EM-1	PM-1	EM-2	PM-2
P_d	1.0	1.0	1.0	1.0
FAR (m^{-2})	0.018	0.018	0.056	0.028
# Alarms	85	77	176	79

CRC was one of two contractors that conducted morning runs at Socorro. These runs consisted of two passes of lane 4 followed by one pass of lane 6. The intention was to conduct the tests around sunrise. In reality, the tests were not begun until 8:47 A.M. and did not conclude until 9:41 A.M., and CRC began one of its day tests at 10:43 A.M. Thus, the differences in the conditions of the morning tests and the day tests were not as significant as intended. The Table V-18 shows the P_ds and FARs for the on-road day runs and the morning runs on lane 4 and lane 6. For each set of tests, all the surface mines were detected. The P_d for the subsurface mines was slightly higher for the morning runs, and the FARs for the two test conditions were nearly the same.

Table V-18. Comparison of CRC On-Road Day and Morning Runs at Socorro

	On-Road Day		Morning	
	Surface	Subsurface	Surface	Subsurface
Total P_d	1.0	0.905	1.0	0.963
Total FAR	0.037 m^{-2}		0.035 m^{-2}	

C. EG&G PERFORMANCE

1. Individual Sensor and Sensor Pair Performance

As illustrated in Table V-19, EG&G's GPR was its most effective single sensor: it had the highest P_d for all conditions at both Aberdeen and Socorro. It was especially effective in surface detections, as the other sensors contributed insignificantly to the total detection probability. The EMI and IR detectors, however, did contribute to the subsurface mine detection probability, especially at Aberdeen.

The false-alarm rate for the EG&G system was usually dominated by its GPR sensor. The only condition where this was not the case was in the on-road condition at Aberdeen, where its IR sensor registered a false-alarm rate that was 30 percent higher than the GPR. The EMI sensor registered a very low false-alarm rate.

No single pair of sensors was responsible for the detection performance of the entire system. Although the GPR was the workhorse, at times the EMI sensor and the IR sensor contributed in important ways to the overall detection performance.

Table V-19. EG&G's False-Alarm Rates and Detection Probabilities Listed for Individual Sensors, Sensor Pairs, and the Total System. Results from the Aberdeen and Socorro sites are listed separately. False-alarm rates are quoted in the units m^{-2}, and detection probabilities are given in percent. G, M, and I refer to GPR, EMI, and IR, respectively.

EG&G

Aberdeen	G	M	I	GM	MI	GI	TOTAL
on-road FAR	0.036	0	0.047	0.036	0.047	0.081	0.081
on-road, subsurface Pd	69.7	47	62.1	72.7	85.6	92.4	93.2
on-road, surface Pd	97.7	41.9	77.9	97.7	88.4	100	100
off road FAR	0.078	0.004	0.02	0.081	0.023	0.095	0.099
off-road, subsurface Pd	79.4	55.9	45.6	89.7	77.9	86.8	95.6
off-road, surface Pd	93.8	50	89.6	93.8	91.7	95.8	95.8
Socorro	G	M	I	GM	MI	GI	TOTAL
on-road FAR	0.036	0.001	0.007	0.037	0.008	0.042	0.043
on-road, subsurface Pd	90.5	46.6	24.3	90.5	60.1	91.9	91.9
on-road, surface Pd	96.9	47.9	80.2	96.9	86.5	96.9	96.9
off road FAR	0.041	0	0.019	0.041	0.019	0.058	0.058
off-road, subsurface Pd	60	53.3	10	70	53.3	63.3	70
off-road, surface Pd	100	66.7	88.9	100	100	100	100

2. Detection Probability Versus Metal Content of Mine

Table V-20 summarizes EG&G's detection probability versus metal content, for on- and off-road, surface and subsurface conditions. The detection probability is given for all sensors, as well as for individual sensor types.

At both sites, metal-cased mines were detected by EG&G with a very high probability, regardless of the depth. EG&G's EMI sensor was, on average, the best sensor for finding the metal mines. The GPR performed well at detecting metal mines, except for off-road, subsurface mines. The IR sensor showed a degradation of performance for subsurface metal mines compared to surface metal mines.

Low-metal mines were detected with a higher probability when they were on the surface. Neither the GPR nor the IR sensors stood out as the dominant sensor for selecting low-metal mines, but rather a combination of the sensors achieved their performance with this mine type.

Table V-20. EG&G's Detection Probability vs. Metal Content at Aberdeen and Socorro

EG&G/Aberdeen		On Road				Off Road			
		ALL	GPR	EMI	IR	ALL	GPR	EMI	IR
Surface	M	1	1	1	0.75	1	1	1	0.96
	LM	1	0.98	0	0.77	0.92	0.88	0	0.83
	NM	1	0.83	0	1	na	na	na	na
Subsurface	M	1	0.94	1	0.5	1	0.82	1	0.42
	LM	0.86	0.48	0	0.7	0.9	0.77	0	0.5
	NM	1	0.5	0	1	na	na	na	na

EG&G/Socorro		On Road				Off Road			
		ALL	GPR	EMI	IR	ALL	GPR	EMI	IR
Surface	M	0.96	0.96	0.96	0.83	1	1	1	0.83
	LM	0.98	0.98	0	0.77	1	1	0	1
	NM	na	na	na	na	na	na	na	na
Subsurface	M	1	1	0.97	0.23	1	0.81	1	0.19
	LM	0.83	0.8	0.02	0.23	0.36	0.36	0	0
	NM	0.93	0.93	0	0.36	na	na	na	na

3. Position Resolution

a. On-Road Tests

Figure V-8 shows EG&G's miss-distance distributions in the on-road tests at Aberdeen. Along-track, the mean (bias) of the distribution is 9 cm.

As shown in Table V-21, this skew in the along-track distribution appears to be caused by the measurements of the locations of the surface mines in the along-track direction. The along-track distribution shows that these measurements were slightly biased (in the positive direction), which in turn shows up as a slight skew in the overall (surface and subsurface) distribution. These measurements are summarized in Table V-21. Measurements from the on-road tests at Socorro are also listed; they are similar to the Aberdeen results.

From Table V-21 it appears that all three sensors were likewise offset, so the cause of the bias is not clear. The RMS along track is 24 cm, which is slightly larger than the mean radius of the land mines used in this test. Cross-track, the mean is 7 cm (nearly unbiased) and the standard deviation is 11 cm, less than the mean radius of land mines used in this test. As can be seen by the data, the performance of individual sensors does not differ significantly from the overall performance.

EG&G: On-Road, Along-Track Positions

Mean = 0.09
Stdev = 0.24

EG&G: On-Road, Across-Track Positions

Mean = 0.07
Stdev = 0.11
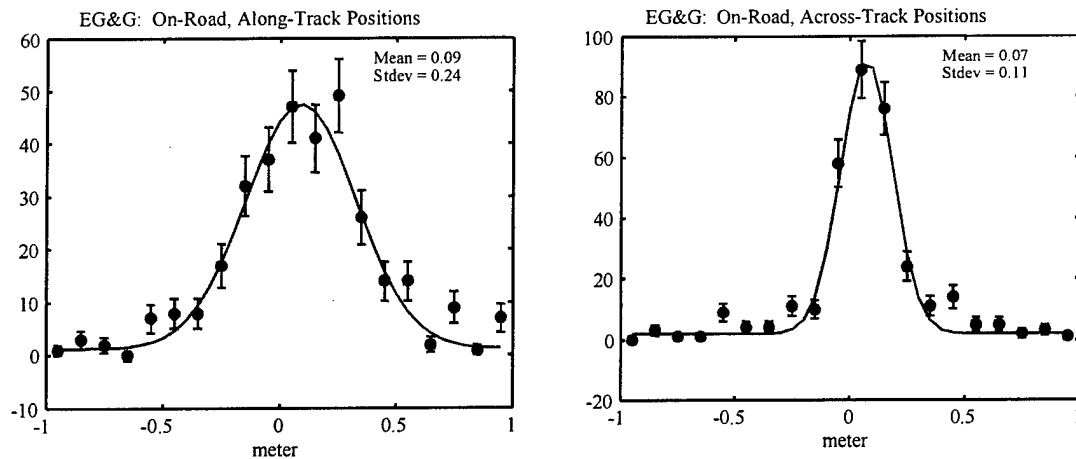
Figure V-8. Results of the Measured Surface and Subsurface Mine Locations for the EG&G On-Road Tests at Aberdeen. Data from the GPR, EMI, and Optical sensors are included in these plots.

Table V-21. EG&G Bias and Resolution Performance at Aberdeen and Socorro: On-Road Performance

Type	Aberdeen Position Resolution				Socorro Position Resolution			
	Along-track		Cross-track		Along-track		Cross-track	
	Mean (bias) (m)	Standard Deviation (RMS) (m)	Mean (bias) (m)	Standard Deviation (RMS) (m)	Mean (bias) (m)	Standard Deviation (RMS) (m)	Mean (bias) (m)	Standard Deviation (RMS) (m)
All sensors, subsurface + surface	0.09	0.24	0.07	0.11	0.14	0.20	0.09	0.13
All sensors, subsurface	0.07	0.20	0.10	0.11	0.18	0.19	0.09	0.12
GPR	0.06	0.21	0.09	0.11	0.16	0.20	0.10	0.13
EMI	0.08	0.16	0.11	0.10	0.24	0.14	0.08	0.09
IR	−0.01	0.15	0.06	0.09	0.06	0.11	0.07	0.10
All sensors, surface	0.12	0.26	0.05	0.11	0.08	0.18	0.06	0.11
GPR	0.14	0.25	0.05	0.10	0.07	0.17	0.05	0.10
EMI	0.16	0.17	0.06	0.09	0.11	0.14	0.07	0.09
IR	0.25	0.13	0.04	0.10	0.07	0.10	0.07	0.08

V-22

b. Off Road

Figure V-9 shows EG&G's miss-distance distribution in the off-road tests at Aberdeen. Along track, the mean (bias) of the distribution is 9 cm, while the RMS along-track is 20 cm, consistent with the on-road test. The cross-track measurements again appear to probably have no bias, but at 30 com, the RMS is inconsistent with the on-road tests. This larger intrinsic resolution is likely caused by a larger resolution than previously found in the GPR and EMI sensors. Table V-22 details the results from these distributions for both the Aberdeen and Socorro off-road tests.
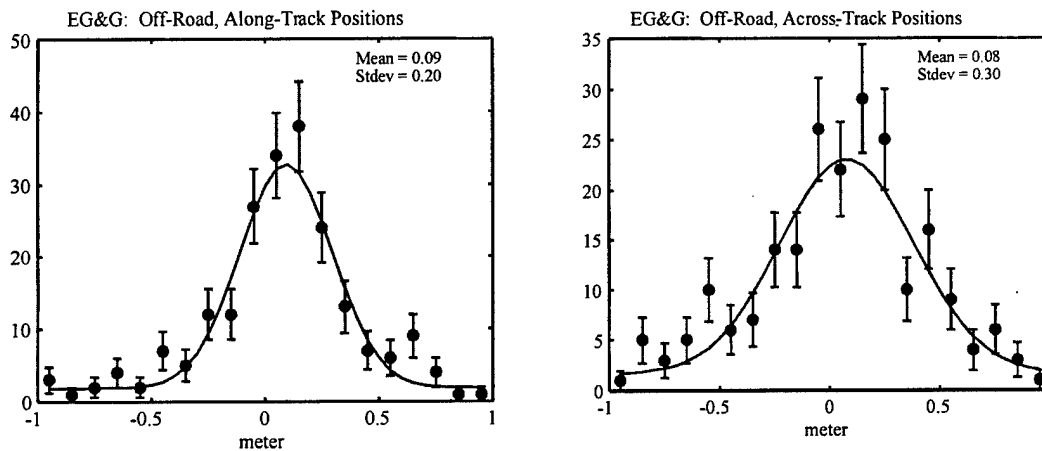
Figure V-9. Results of the Measured Surface and Subsurface Mine Locations for the EG&G Off-Road Tests at Aberdeen. Data from the GPR, EMI, and optical sensors are included in these plots.

4. P_d and R_{halo}

The bias and RMS resolution performance of the sensors affect how well, as a function of R_{halo}, EG&G's system detects the mines. Figure V-10 shows a plot of P_d versus R_{halo} for the tests at Aberdeen and Socorro. These figures summarize the overall implication of EG&G's relatively small bias and intrinsic sensor resolution (as tabulated in section 2).

As shown in the plots, the detection probability for EG&G's sensors reached a maximum when R_{halo} was approximately 30 cm. If this ATD had required R_{halo} to be as small as 25 cm, then EG&G's P_d performance would have been approximately unchanged.

V-23

Table V-22. EG&G Bias and Resolution Performance at Aberdeen and Socorro:
Off-Road Performance

Type	Aberdeen Position Resolution				Socorro Position Resolution			
	Along-track		Cross-track		Along-track		Cross-track	
	Mean (bias) (m)	Standard Deviation (RMS) (m)	Mean (bias) (m)	Standard Deviation (RMS) (m)	Mean (bias) (m)	Standard Deviation (RMS) (m)	Mean (bias) (m)	Standard Deviation (RMS) (m)
All sensors, subsurface + surface	0.09	0.20	0.08	0.30	0.15	0.17	0.07	0.11
All sensors, subsurface	0.09	0.16	0.07	0.27	0.23	0.15	0.10	0.10
GPR	0.07	0.22	0.01	0.29	0.21	0.15	0.09	0.11
EMI	0.10	0.12	0.07	0.23	Poor stats	Poor stats	Poor stats	Poor stats
IR	0.09	0.12	0.23[a]	0.33	Poor stats	Poor stats	Poor stats	Poor stats
All sensors, surface	0.08[b]	0.23	0.15[b]	0.20	0.06	0.20	0.07	0.11
GPR	0.14[b]	0.20	0.00[b]	0.02	0.05	0.18	0.07	0.13
EMI	0.06[b]	0.17	0.13[b]	0.15	0.13	0.15	Poor stats	Poor stats
IR	0.05[b]	0.12	0.14[b]	0.21	Poor stats	Poor stats	0.08	0.09

[a] This distribution is not normally distributed. Although the bias appears to be real, it is probably not as severe as 23 cm.

[b] These distributions had poor statistics; thus, the error on the mean is quite large. This means that it cannot be determined if the offsets in surface mine locations is due to a real bias in the sensors.

5. Additional Runs

a. Aberdeen Results

Additional runs by EG&G at Aberdeen include one night run on lane 12, one night run on lane 11, and one physical-marking run (resulting in two alarm files—one electronic-marking file and one physical-marking file) on lane 15.[5] Table 23 shows the cumulative P_ds and FARs for the on-road day runs, and the night runs on lane 11 and lane 12. The total P_d is lower on the night run for subsurface mines. Notice also that the IR P_d drops significantly for both surface and subsurface mines at night. For subsurface mines at night, the IR P_d is nearly zero. The FARs for both sets of tests were very high, with

---

[5] The results of these runs are summarized in Tables B-6 through B-8 in Appendix B and can be compared to the results EG&G obtained on the on-road day runs on lanes 11, 12, and 15 as shown in Tables B-3 through B-5.

about half the false alarms attributed to the IR for the on-road day runs, and only about 10 percent of the false alarms due to the IR for the night runs.

EG&G

a) On-road at Aberdeen

b) On-road at Socorro

—— Subsurface

---- Surface

c) Off-road at Aberdeen

d) Off-road at Socorro
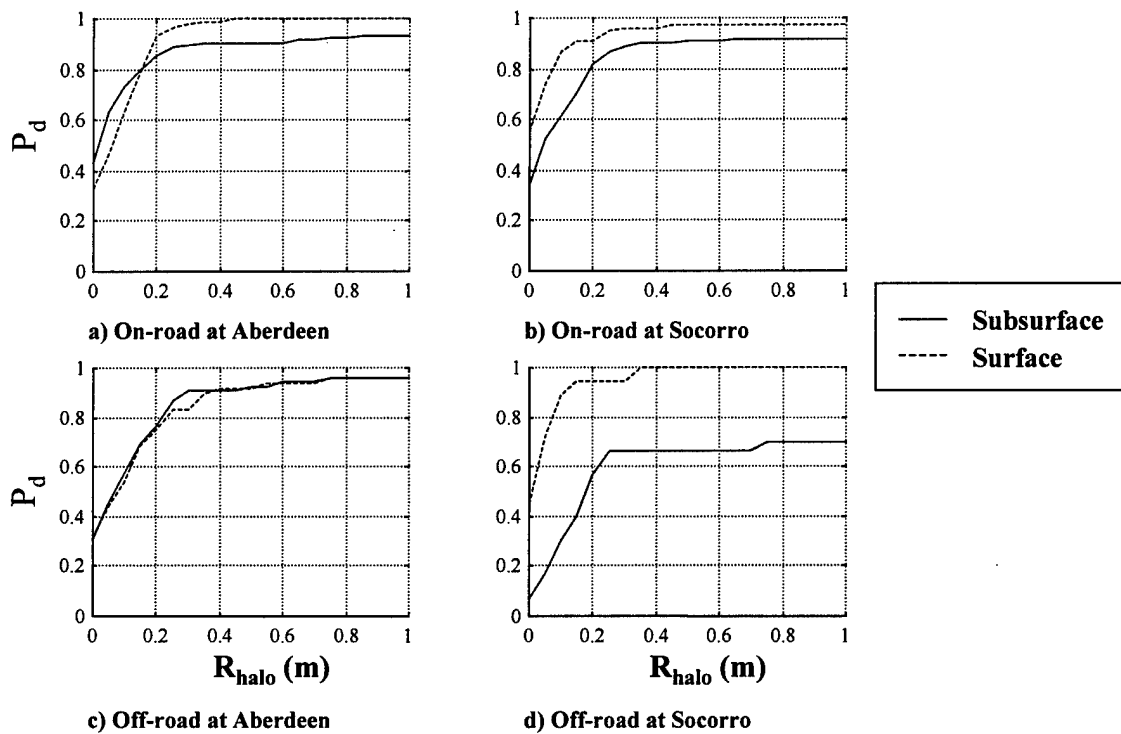
Figure V-10. P_d vs. R_{halo} for EG&G's Sensor Suite at Aberdeen and Socorro

Table V-23. Comparison of EG&G On-Road Day and Night Runs at Aberdeen

	On-Road Day		Night	
	Surface	Subsurface	Surface	Subsurface
Total P_d	1.0	0.932	1.0	0.739
IR P_d	0.779	0.621	0.393	0.022
Total FAR	0.081 m^{-2}		0.143 m^{-2}	
IR FAR	0.047 m^{-2}		0.014 m^{-2}	

For the physical-marking run conducted by EG&G on lane 15 at Aberdeen, both electronic- and physical-marking files were produced.[6] Table V-24 compares the performance measures of the on-road day runs with the physical-marking run on lane 15. For both surface and subsurface mines, the P_ds for the physical-marking run are significantly lower than the P_ds for the day runs. Table V-B-8 in Appendix B shows that EG&G missed surface metal mines for the PM run. The *FAR* for the physical-marking run is much lower than comparable day runs with electronic marking.

Table V-24. Comparison of EG&G On-Road Day and Physical-Marking Runs at Aberdeen

	On-Road Day (EM)		Physical Marking (PM)	
	Surface	Subsurface	Surface	Subsurface
Total P_d	1.0	0.932	0.667	0.700
Total *FAR*	0.081 m^{-2}		0.027 m^{-2}	

Table V-25 shows the position resolution for the on-road day runs and the physical-marking run. Note that the RMS values in the along-track and cross-track directions are smaller for the physical-marking run, but not significantly. The along- and cross-track biases are similar in physical-marking and electronic-marking runs.

Table V-25. Comparison of EG&G Position Resolution for On-Road Day and Physical-Marking Runs at Aberdeen

	On-Road Day		Physical Marking (PM)	
	Mean (m)	RMS (m)	Mean (m)	RMS (m)
Along Track	0.09	0.24	0.08	0.18
Cross Track	0.07	0.11	0.0	0.08

Table V-26 compares the P_ds and *FAR*s for the EM and PM systems for the physical-marking run on lane 15. Two of the undetected mines for the PM system were surface, metal mines (see Table B-8 in Appendix B). Since these mines were detected by the EM system, the probable cause of the poor PM P_d is a malfunction of the physical-

---

6   The results of these runs are shown in Table B-8.

marking system. Note also in Table V-26 that the number of alarms for the PM system is about 30 percent less than the number of alarms for the EM system.

Table V-26. Comparison of EG&G Lane 15 Electronic-Marking and Physical-Marking Runs (EM and PM) at Aberdeen

	EM-1	PM-1
P_d	0.857	0.686
FAR (m^{-2})	0.042	0.028
# Alarms	91	61

b. Socorro Results

Additional runs by EG&G at Socorro include one night run on lane 6, two night runs on lane 4, three tele-operated runs on lane 6, and three physical-marking runs (resulting in six alarm files—three electronic and three physical) on lane 4.[7] The cumulative P_ds and FARs for the on-road day runs, and the night runs on lanes 4 and 6 are shown in Table V-27. For surface mines, we note that the total P_ds are nearly the same for day and night runs, and that the IR performed better at night. For subsurface mines, the IR was used sparingly both during the day and during the night. The total FAR for the night runs was lower than for the day runs, with the IR contributing a negligible number of false alarms under both test conditions.

Table V-27. Comparison of EG&G On-Road Day and Night Runs at Socorro

	On-Road Day		Night	
	Surface	Subsurface	Surface	Subsurface
Total P_d	0.969	0.919	1.0	0.889
IR P_d	0.802	0.243	1.0	0.185
Total FAR	0.043 m^{-2}		0.028 m^{-2}	
IR FAR	0.007 m^{-2}		0.009 m^{-2}	

---

[7] The results of these runs are summarized in Tables B-17 through B-19 in Appendix B and can be compared to the results EG&G obtained on its scored daytime runs on lanes 4 and 6 shown in Tables B-10 and B-11, respectively.

Table V-28 shows the cumulative P_ds and *FAR*s for the on-road day runs and the tele-operated runs conducted on lane 6. The P_d for both surface and subsurface mines is slightly higher for the tele-operated runs, and the *FAR* for the tele-operated runs is approximately 50 percent greater than the *FAR* for the day runs. Recall that the error bars for the tele-operated runs are large due to the limited number of mine encounters. Still, it is clear that the tele-operated system performed capably.

Table V-28. Comparison of EG&G On-Road Day and Tele-operated Runs at Socorro

	On-Road Day		Tele-operated	
	Surface	Subsurface	Surface	Subsurface
Total P_d	0.969	0.919	1.0	0.963
Total *FAR*	0.043 m^{-2}		0.063 m^{-2}	

For the three physical-marking runs conducted by EG&G on lane 4 at Socorro, both electronic and physical marking files were produced. The results of these runs are shown in Table V-B-17. Table V-29 compares the performance measures of the on-road day runs and the physical-marking runs on lane 4. For the physical-marking runs, all surface and subsurface mines were detected, but the PM *FAR* was three times the *FAR* for the day runs.

Table V-29. Comparison of EG&G On-Road Day and Physical-Marking Runs at Socorro

	On-Road Day		Physical Marking (PM)	
	Surface	Subsurface	Surface	Subsurface
Total P_d	0.969	0.919	1.0	1.0
Total *FAR*	0.043 m^{-2}		0.122 m^{-2}	

In Table V-30, the position resolution of the physical-marking system is compared to the position resolution of the electronic marking system. The location accuracy of the PM system, as given by the standard deviation of along-track and cross-track offsets, is about 50 percent greater than the EM system in the along-track direction and slightly less than the EM system in the cross-track direction. For both along- and cross-track directions, the mean is 9 cm less for the PM system than for the EM system.

**Table V-30. Comparison of EG&G Position Resolution for On-Road Day
and Physical-Marking Runs at Socorro**

	On-Road Day		Physical Marking (PM)	
	Mean (m)	RMS (m)	Mean (m)	RMS (m)
Along Track	0.14	0.20	0.04	0.31
Cross Track	0.09	0.13	0.0	0.09

Table V-31 summarizes the results of the physical-marking system with the electronic-marking system for the three passes of lane 4. We first note that the P_ds are all 1.0 for both systems on all three passes. For the first two passes, the number of alarms is less for the PM system than the EM system, resulting in lower FARs for the PM system. For the third pass, the number of alarms and FARs is the same for the EM and PM systems.

Table V-31. Comparison of EG&G Lane 4 Physical-Marking Runs (EM and PM) at Socorro

	EM-1	PM-1	EM-2	PM-2	EM-3	PM-3
P_d	1.0	1.0	1.0	1.0	1.0	1.0
FAR (m^{-2})	0.092	0.084	0.106	0.094	0.186	0.186
# Alarms	85	79	91	80	131	131

D. GDE PERFORMANCE

1. Individual Sensor and Sensor Pair Performance

As shown in Table V-32, GDE's GPR sensor was the greatest contributor to detections. At Socorro, there was no real marginal benefit from either the EMI sensor or the IR sensor. At Aberdeen, however, both the metal and IR sensors contributed to the system's total detections.

The GPR sensor also contributed bulk of the false alarms. In fact, the only case where there was any significant contribution to the false alarms from the EMI and IR sensors was in the off-road lane at Aberdeen, where the GPR still contributed about 70 percent of the total false alarms.

V-29

The GPR-EMI sensor pair matched the total system performance in all conditions except for the off-road lane at Aberdeen. There, the three sensors were each important contributors to the total detections. In the on- and off-road lanes at Aberdeen, the EMI sensor contributed significantly to the total detection probability.

Table V-32. GDE's False-Alarm Rates and Detection Probabilities Listed for Individual Sensors, Sensor Pairs, and the Total System. Results from the Aberdeen and Socorro sites are listed separately. False-alarm rates are quoted in the units m^{-2}, and detection probabilities are given in percent. G, M, and I refer to GPR, EMI, and IR, respectively.

Aberdeen	G	M	I	GM	MI	GI	TOTAL
on-road FAR	0.067	0.002	0	0.068	0.002	0.067	0.068
on-road, subsurface Pd	87.1	43.9	0	90.9	43.9	87.1	90.9
on-road, surface Pd	91.9	40.7	0	96.5	40.7	91.9	96.5
off road FAR	0.063	0.018	0.012	0.079	0.029	0.07	0.085
off-road, subsurface Pd	61.8	63.2	41.2	82.4	76.5	83.8	91.2
off-road, surface Pd	77.1	56.3	62.5	91.7	83.3	85.4	93.8
Socorro	G	M	I	GM	MI	GI	TOTAL
on-road FAR	0.033	0.002	0.003	0.035	0.004	0.036	0.037
on-road, subsurface Pd	88.5	48	0	89.9	48	88.5	89.9
on-road, surface Pd	100	49	20.8	100	59.4	100	100
off road FAR	0.063	0.002	0	0.065	0.002	0.063	0.065
off-road, subsurface Pd	80	53.3	0	80	53.3	80	80
off-road, surface Pd	100	66.7	22.2	100	72.2	100	100

2. Detection Probability Versus Metal Content of Mine

Table V-33 summarizes GDE's detection probability versus a metal content, for on- and off-road, surface and subsurface conditions. The detection probability is given for all sensors, as well as for individual sensor types.

Metal-cased mines were detected by GDE with a very high probability, regardless of the depth of the mine and the test site. Its EMI sensor was, on average, the best sensor for finding the metal mines. Its GPR performed better at Socorro at detecting metal mines than it did at Aberdeen.

Low-metal mines were detected with a higher probability when they were placed on ground surface compared to below the surface. The GPR stood out as the dominant sensor for detecting low-metal mines. The IR sensor, even when it was operational, never exceeded a 58-percent detection probability for low-metal mines (this was in the surface, off-road condition at Aberdeen).

V-30

Table V-33. GDE's Detection Probability vs. Metal Content at Aberdeen and Socorro

GDE/Aberdeen		On Road				Off Road			
		ALL	GPR	EMI	IR	ALL	GPR	EMI	IR
Surface	M	0.97	0.86	0.97	0	1	0.71	1	0.67
	LM	0.95	0.95	0	0	0.88	0.83	0.13	0.58
	NM	1	1	0	0	na	na	na	na
Subsurface	M	0.95	0.87	0.94	0	1	0.66	1	0.45
	LM	0.91	0.91	0	0	0.8	0.57	0.17	0.37
	NM	0.5	0.5	0	0	na	na	na	na

GDE/Socorro		On Road				Off Road			
		ALL	GPR	EMI	IR	ALL	GPR	EMI	IR
Surface	M	1	1	0.98	0.21	1	1	1	0.25
	LM	1	1	0	0.21	1	1	0	0.17
	NM	na	na	na	na	na	na	na	na
Subsurface	M	1	0.97	1	0	1	1	1	0
	LM	0.77	0.77	0.02	0	0.57	0.57	0	0
	NM	1	1	0	0	na	na	na	na

3. Position Resolution

a. On-Road Tests

Figure V-11 shows the GDE's miss-distance distributions in the on-road tests at Aberdeen. Along track, the mean (bias) of the distribution is 9 cm, while the RMS is 11 cm (which is significantly less than the mean radius of the land mines used in this test). Cross track, the mean is –8 cm, and the standard deviation is 21 cm (slightly larger than the mean radius of land mines used in this test). Both of these distributions are clearly normally distributed, as expected. The slight bias in the along-track distribution appears to be caused by the GPR sensor (see Table V-34). There are no significant trends apparent in the table; that is, performance of individual sensors does not differ significantly from the overall performance, and there is no dependence on mine location (surface or subsurface). The data from the on-road tests at Socorro are similar to the results at Aberdeen.

V-31

GDE: On-Road, Along Track Positions — Mean = 0.09, Stdev = 0.11

GDE: On-Road, Across-Track Positions — Mean = -0.08, Stdev = 0.21
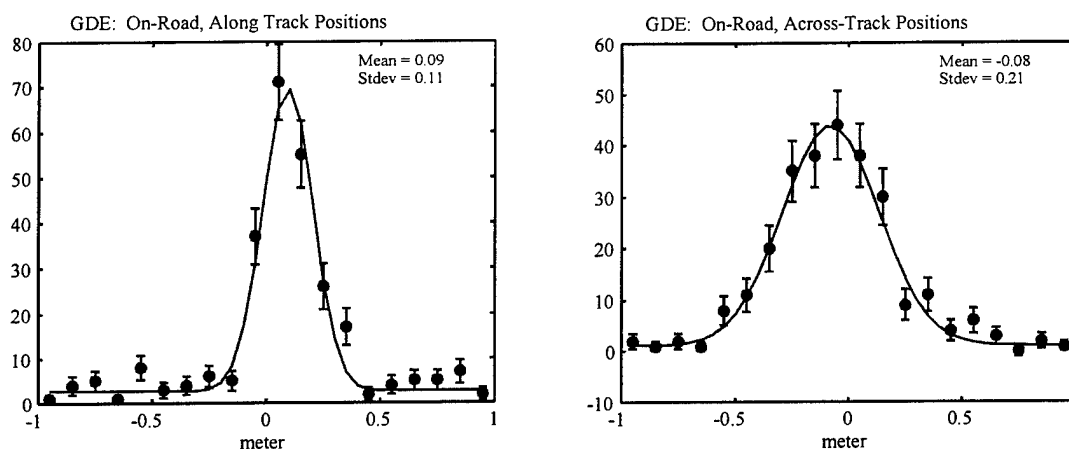
Figure V-11. GDE's Miss-Distance Distribution for Surface and Subsurface Mines in On-Road Tests at Aberdeen. Data points include the GPR and EMI sensors. The solid curve is a best fit of a constant plus a Gaussian.

Table V-34. GDE Bias and Resolution Performance at Aberdeen and Socorro: On-Road Performance

Type	Aberdeen Position Resolution				Socorro Position Resolution			
	Along-track		Cross-track		Along-track		Cross-track	
	Mean (bias) (m)	Standard Deviation (RMS) (m)	Mean (bias) (m)	Standard Deviation (RMS) (m)	Mean (bias) (m)	Standard Deviation (RMS) (m)	Mean (bias) (m)	Standard Deviation (RMS) (m)
All sensors, subsurface + surface	0.09	0.11	−0.08	0.21	0.11	0.16	−0.14	0.12
All sensors, subsurface	0.09	0.12	−0.06	0.22	0.09	0.17	−0.14	0.11
GPR	0.10	0.12	−0.06	0.21	0.09	0.17	−0.15	0.11
EMI	0.06	0.09	−0.12	0.20	−0.01	0.09	−0.16	0.11
IR	N/A	N/A	N/A	N/A	N/A	N/A	N/A	N/A
All sensors, surface	0.09	0.10	−0.10	0.20	0.13	0.14	−0.15	0.13
GPR	0.10	0.10	−0.10	0.20	0.13	0.14	−0.15	0.13
EMI	0.06	0.08	−0.12	0.20	0.02	0.09	−0.19	0.14
IR	N/A	N/A	N/A	N/A	Not well fit	Not well fit	−0.11	0.18

b. Off Road

Figure V-12 shows GDE's miss-distance distribution in the off-road tests at Aberdeen for GDE. Along track, the mean (bias) of the distribution is −4 cm, while the RMS is 49 cm (which is significantly larger than the mean radius of land mines used).

However, this RMS is much smaller than the mine halo, so it would likely not affect the overall P_d. This larger measured RMS appears to be caused by degradation in the resolutions of all three sensors (see Table V-35). However, at 28 cm, the cross-track measurements of the intrinsic resolution are consistent with the on-road tests. And once again, there is probably no bias in the cross-track position measurements.
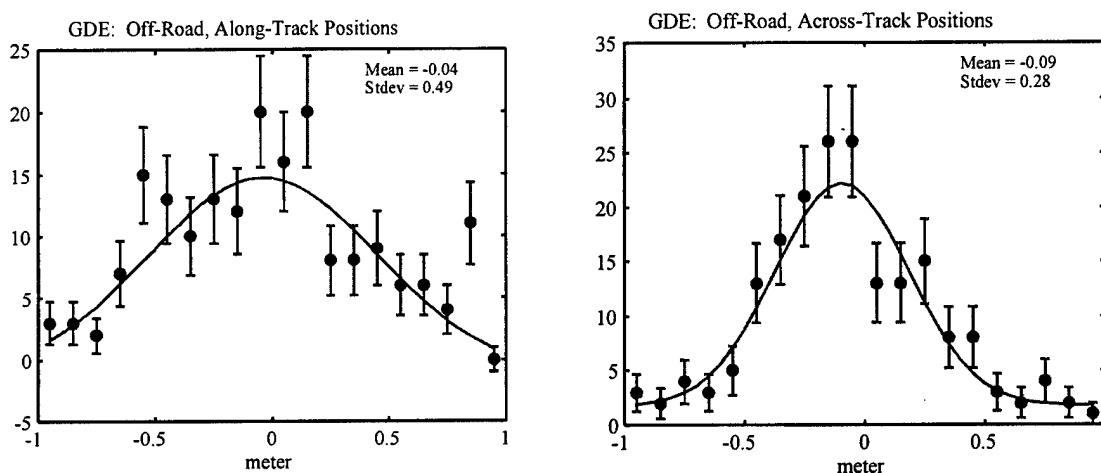
Figure V-12. GDE's Miss-Distance Distribution for Surface and Subsurface Mines in Off-Road Tests at Aberdeen. Data points include GPR, EMI, and IR sensors. The solid curve is a best fit of a constant plus a Gaussian.

Table V-35 also includes the results from the off-road tests at Socorro. Although there were poor statistics at Socorro, the data in this Table V-show that the sensor performance off-road did not differ from the performance at Aberdeen.

4. P_d and R_{halo}

The bias and RMS resolution performance of the sensors affect how well, as a function of R_{halo}, GDE's system detects the mines. Figure V-13 shows a plot of P_d versus R_{halo} for the tests at Aberdeen and Socorro. These figures summarize the overall implication of GDE's bias and intrinsic sensor resolution (as tabulated in section 2).

As can be seen from the plots, the detection probability for GDE's sensors was maximized for a R_{halo} of approximately 50 cm. If this ATD had required R_{halo} to be as small as 25 cm, then GDE's P_d performance would have been somewhat degraded, particularly at Aberdeen.

Table V-35. GDE Bias and Resolution Performance at Aberdeen and Socorro:
Off-Road Performance

Type	Aberdeen Position Resolution				Socorro Position Resolution			
	Along-track		Cross-track		Along-track		Cross-track	
	Mean (bias) (m)	Standard Deviation (RMS) (m)	Mean (bias) (m)	Standard Deviation (RMS) (m)	Mean (bias) (m)	Standard Deviation (RMS) (m)	Mean (bias) (m)	Standard Deviation (RMS) (m)
All sensors, subsurface + surface	−0.04	0.49	−0.09	0.28	0.23	0.28	−0.12	0.13
All sensors, subsurface	−0.13	0.32	−0.07	0.32	0.12	0.14	−0.12	0.16
GPR	−0.07	0.37	−0.10	0.28	0.12	0.14	−0.11	0.16
EMI	−0.09	0.22	−0.09	0.28	0.01	0.10	−0.23	0.09
IR	−0.49	0.14	0.00	0.53	N/A	N/A	N/A	N/A
All sensors, surface	−0.10	0.35	−0.15	0.22	Not well fit	Not well fit	−0.10	0.08
GPR	−0.05	0.27	−0.19	0.20	Not well fit	Not well fit	−0.10	0.08
EMI	0.04	0.09	−0.16	0.13	Not well fit	Not well fit	−0.11	0.02
IR	Not well fit	Not well fit	−0.08	0.24	Poor stats	Poor stats	Poor stats	Poor stats

5. Additional Runs

a. Aberdeen Results

Additional runs by GDE at Aberdeen include two night runs on lane 11 and one physical-marking run (resulting in one PM alarm file) on lane 15.[8] Table V-36 shows the cumulative P_ds and FARs for the on-road day runs, and the night runs on lane 11. The night runs resulted in P_ds of 1.0 for both surface and subsurface mines and the false-alarm rate was considerably less than for the day runs. GDE did not use its IR sensor for the day runs. At night, GDE's IR sensor detected only 25 percent of the surface mines and none of the subsurface mines.

---

[8] The results of these runs are summarized in Tables B-6 and B-8 in Appendix B and can be compared to the results GDE obtained on its on-road day runs on lanes 11 and 15 as shown in Tables B-3 and B-5, respectively.
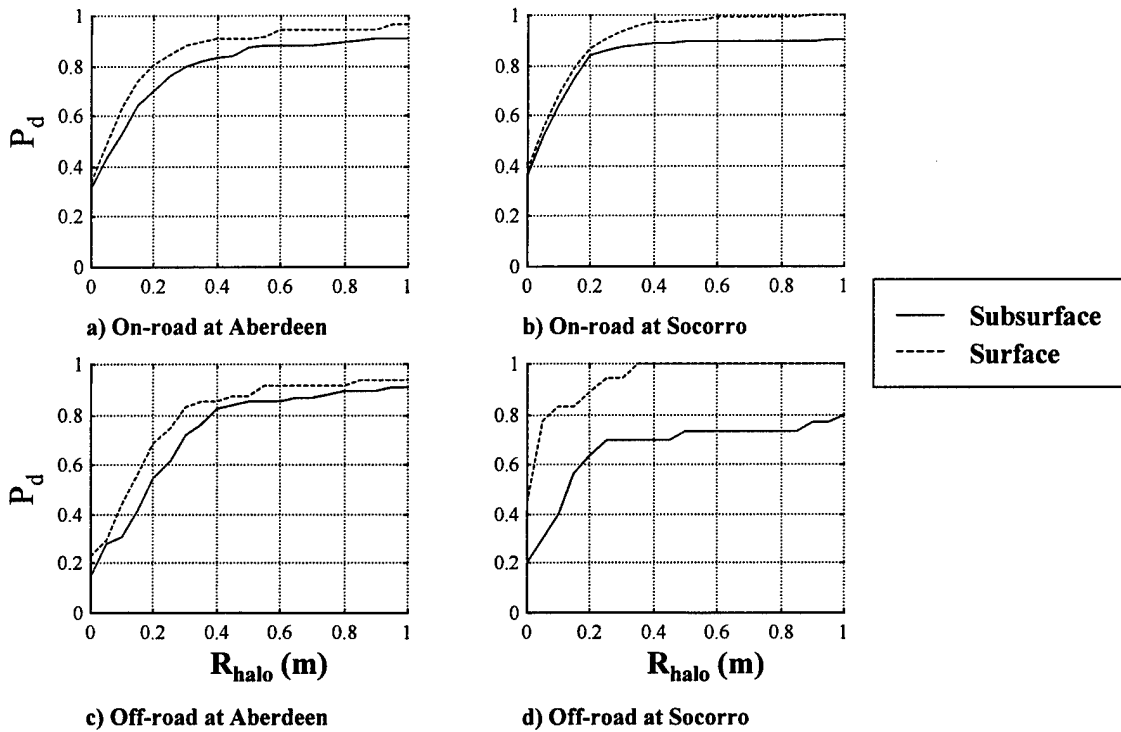
Figure V-13. P_d vs. R_{halo} for GDE's Sensor Suite at Aberdeen and Socorro

Table V-36. Comparison of GDE On-Road Day and Night Runs at Aberdeen

	On-Road Day		Night	
	Surface	Subsurface	Surface	Subsurface
Total P_d	0.965	0.909	1.0	1.0
IR P_d	N/A	N/A	0.250	0.0
Total FAR	0.068 m^{-2}		0.015 m^{-2}	
IR FAR	N/A		0.000 m^{-2}	

For the physical-marking run conducted by GDE on lane 15 at Aberdeen, only a PM file was produced.[9] Table V-37 compares the performance measures of the on-road

---

[9] The results of these runs are shown in Table B-8.

day runs with the physical-marking run on lane 15. Notice that the P_d is higher and the *FAR* lower for the PM run than the on-road day runs. Furthermore, referring to Table V-B-5 in Appendix B, we see that for the on-road day runs on lane 15, GDE had a very high *FAR* of 0.101 m^{-2} on its first run and a *FAR* of 0.047 m^{-2} on its second run. The *FAR* of GDE's second on-road day run on lane 15 is nearly the same as the *FAR* for GDE's PM run on this lane.

Table V-37. Comparison of GDE On-Road Day and Physical-Marking Runs at Aberdeen

	On-Road Day (EM)		Physical Marking (PM)	
	Surface	Subsurface	Surface	Subsurface
Total P_d	0.965	0.909	1.0	1.0
Total *FAR*	0.068 m^{-2}		0.042 m^{-2}	

Table V-38 compares the position resolution for GDE's PM run on lane 15 with the position resolution of the on-road day runs where an electronic-marking system was used. For the along-track direction, the RMS is about three times larger for the PM system, while the mean differs by 13 cm. In the cross-track direction, the PM location errors are half the magnitude of the EM location errors.

Table V-38. Comparison of GDE Position Resolution for On-Road Day and Physical-Marking Runs at Aberdeen

	On-Road Day (EM)		Physical Marking (PM)	
	Mean (m)	RMS (m)	Mean (m)	RMS (m)
Along Track	0.09	0.11	−0.04	0.29
Cross Track	−0.08	0.21	−0.03	0.10

b. Socorro Results

Additional runs by GDE at Socorro include two night runs on lane 8, two morning runs on lane 4, and two physical-marking runs (resulting in four alarm files—two

electronic-marking and two physical-marking) on lane 8.[10] The cumulative P_ds and FARs for the on-road day runs, and the night runs on lane 8 are shown in Table V-39. The total P_ds are the same for surface mines and nearly the same for subsurface mines. The total FAR for the night runs is about half the rate for the day runs. Note that GDE only detected surface mines with its IR, and that the IR P_d is greater at night than at day. False-alarm rates for the IR are negligible.

Table V-39. Comparison of GDE On-Road Day and Night Runs at Socorro

	On-Road Day		Night	
	Surface	Subsurface	Surface	Subsurface
Total P_d	1.0	0.899	1.0	0.906
IR P_d	0.208	0.0	0.5	0.0
Total FAR	0.037 m^{-2}		0.016 m^{-2}	
IR FAR	0.003 m^{-2}		0.000 m^{-2}	

GDE conducted its morning tests on lane 4 between 5:00 A.M. and 6:30 A.M. Table V-40 shows the cumulative P_ds and FARs for the on-road day runs, and the morning runs on lane 4. All the surface mines were detected for both sets of tests, and the P_d for subsurface mines was greater for the morning runs. The FAR for the morning runs was extremely low. Examination of Table V-B-10 in Appendix B shows that in general GDE performed well on lane 4. In fact for the day runs on lane 4, there was only one false alarm per pass, compared to three and five false alarms for the two morning runs.

For the two physical-marking runs conducted by GDE on lane 8 at Socorro, both electronic- and physical-marking files were produced. The results of these runs are shown in Table V-B-20. Table V-41 compares the performance measures of the on-road day runs with the physical-marking runs on lane 8. The P_ds and FARs are very similar.

---

[10] The results of these runs are summarized in Tables B-18, B-20, and B-21 in Appendix B and can be compared to the results GDE obtained on its on-road day runs on lanes 4 and 8 as shown in Tables B-10 and B-12, respectively.

Table V-40. Comparison of GDE On-Road Day and Morning Runs at Socorro

	On-Road Day		Morning	
	Surface	Subsurface	Surface	Subsurface
Total P_d	1.0	0.899	1.0	1.0
Total FAR	0.037 m^{-2}		0.008 m^{-2}	

Table V-41. Comparison of GDE On-Road Day and Physical-Marking Runs at Socorro

	On-Road Day (EM)		Physical Marking (PM)	
	Surface	Subsurface	Surface	Subsurface
Total P_d	1.0	0.899	1.0	0.938
Total FAR	0.037 m^{-2}		0.028 m^{-2}	

Table V-42 shows comparisons of position resolution for the physical-marking runs and the on-road day runs. For the along-track direction, the mean and standard deviation are greater for the physical-marking system. The physical-marking system has a smaller mean and standard deviation in the cross-track direction compared to the electronic-marking system used in the on-road day tests, but the differences are smaller than the along-track differences.

Table V-42. Comparison of GDE Position Resolution for On-Road Day and Physical-Marking Runs at Socorro

	On-Road Day (EM)		Physical Marking (PM)	
	Mean (m)	RMS (m)	Mean (m)	RMS (m)
Along Track	0.11	0.16	0.24	0.26
Cross Track	−0.14	0.12	−0.06	0.10

Table V-43 shows the P_ds, FARs, and number of alarms for the two physical-marking runs. The results of the electronic-marking system and the physical-marking system for the same pass of the lane are shown side by side. For each EM/PM

comparison, the P_ds are identical, the FARs are identical for the second pass and nearly identical for the first pass, and the number of alarms differ by only one. The magnitude of the difference between the number of physical marks and the number of electronic marks was smallest for GDE compared to the other contractors.

Table V-43. Comparison of GDE Lane 8 Physical-Marking Runs (EM and PM) at Socorro

	EM-1	PM-1	EM-2	PM-2
P_d	0.958	0.958	0.958	0.958
FAR (m^{-2})	0.016	0.018	0.039	0.039
# Alarms	50	51	70	69

E. GEOCENTERS (GeoC) PERFORMANCE

1. Individual Sensor and Sensor Pair Performance

As shown in Table V-44, the GeoC system found 100 percent of the surface mines during the ATD. GeoC's subsurface detection was at or better than the 90-percent level, except for the off-road lane at Socorro, where P_d was 70 percent.

The GPR was clearly the overall best sensor for detection. At Socorro, there was no marginal benefit from the EMI and IR sensors, while at Aberdeen, the EMI and IR sensors contributed in only a small way to the overall P_d. Note, however, that almost all of the false alarms were contributed by the GPR—at their worst the combined EMI and IR sensors tallied a false-alarm rate that was just over 14 percent of the GPR's (this occurred on-road at Aberdeen). Hence, the EMI and IR sensors only contributed positively to the system as a whole.

2. Detection Probability Versus Metal Content of Mine

Table V-45 summarizes GeoC's detection probability versus metal content, for on and off road, surface and subsurface. The detection probability is given for all sensors, as well as for individual sensor types.

Table V-44. GeoC's False-Alarm Rates and Detection Probabilities Listed for Individual Sensors, Sensor Pairs, and the Total System. Results from the Aberdeen and Socorro sites are listed separately. False-alarm rates are quoted in the units m^{-2}, and detection probabilities are given in percent. G, M, and I refer to GPR, EMI, and IR, respectively.

GeoC

Aberdeen	G	M	I	GM	MI	GI	TOTAL
on-road FAR	0.048	0.008	0	0.056	0.008	0.048	0.056
on-road, subsurface Pd	97.7	44.7	0	98.5	44.7	97.7	98.5
on-road, surface Pd	96.5	43	98.8	100	98.8	100	100
off road FAR	0.065	0.0008	0	0.066	0.0008	0.065	0.066
off-road, subsurface Pd	89.7	44.1	0	89.7	44.1	89.7	89.7
off-road, surface Pd	97.9	47.9	100	97.9	100	100	100
Socorro	**G**	**M**	**I**	**GM**	**MI**	**GI**	**TOTAL**
on-road FAR	0.032	0.0002	0.0003	0.032	0.0005	0.032	0.032
on-road, subsurface Pd	91.2	47.3	17.6	91.2	59.5	91.2	91.2
on-road, surface Pd	100	50	83.3	100	91.7	100	100
off road FAR	0.035	0	0	0.035	0	0.035	0.035
off-road, subsurface Pd	70	53.3	0	70	53.3	70	70
off-road, surface Pd	100	66.7	94.4	100	94.4	100	100

Table V-45. GeoC's Detection Probability vs. Metal Content at Aberdeen and Socorro

GeoC/Aberdeen		On Road				Off Road			
		ALL	GPR	EMI	IR	ALL	GPR	EMI	IR
Surface	M	1	0.92	0.97	1	1	1	0.96	1
	LM	1	1	0.05	0.98	1	0.96	0	1
	NM	1	1	0	1	na	na	na	na
Subsurface	M	1	1	0.94	0	1	1	0.79	0
	LM	0.97	0.95	0.02	0	0.77	0.77	0	0
	NM	1	1	0	0	na	na	na	na

GeoC/Socorro		On Road				Off Road			
		ALL	GPR	EMI	IR	ALL	GPR	EMI	IR
Surface	M	1	1	1	0.83	1	1	1	1
	LM	1	1	0	0.83	1	1	0	0.83
	NM	na	na	na	na	na	na	na	na
Subsurface	M	1	1	1	0.11	1	1	1	0
	LM	0.86	0.86	0	0.27	0.36	0.36	0	0
	NM	0.71	0.71	0	0.07	na	na	na	na

All metal-cased mines were found by GeoC. Both its EMI and GPR sensors were very effective at finding the metal mines. Their IR sensor performed well on metal-cased mines that were located on the surface, except at Socorro.

Surface, low-metal mines were detected with a higher probability than subsurface, low-metal mines. The GPR sensor was the best sensor for the detection of low-metal mines, averaged over all conditions. The IR sensor performed about as well as the GPR

for the surface condition at Aberdeen, but did not perform as well in the surface condition at Socorro or for subsurface conditions at either site.

3.   Position Resolution

a.   On Road

Figure V-14 shows GeoC's miss-distance distribution in the on-road tests at Aberdeen. Along track, the mean (bias) of the distribution is –16 cm. This bias appears to be real, albeit overstated because the data are not well fit by a Gaussian distribution. This bias appears to be caused by the measured locations of the surface mines, regardless of the sensor. The RMS along track is 24 cm, which is slightly more than the mean radius of the land mines used in this test. Cross track, the mean is 4 cm and the RMS is 9 cm, significantly less than the mean radius of land mines. Table V-46 summarizes the means and RMSs, broken down by surface and subsurface mines, as well as by sensor. There are no significant trends in the sensor performance, although there is a dependence on mine location (surface or subsurface).

The results from the on-road tests at Socorro, also shown in the table, were different from the Aberdeen results in an important respect: the measurements of the mine locations were unbiased, and the RMS was smaller.
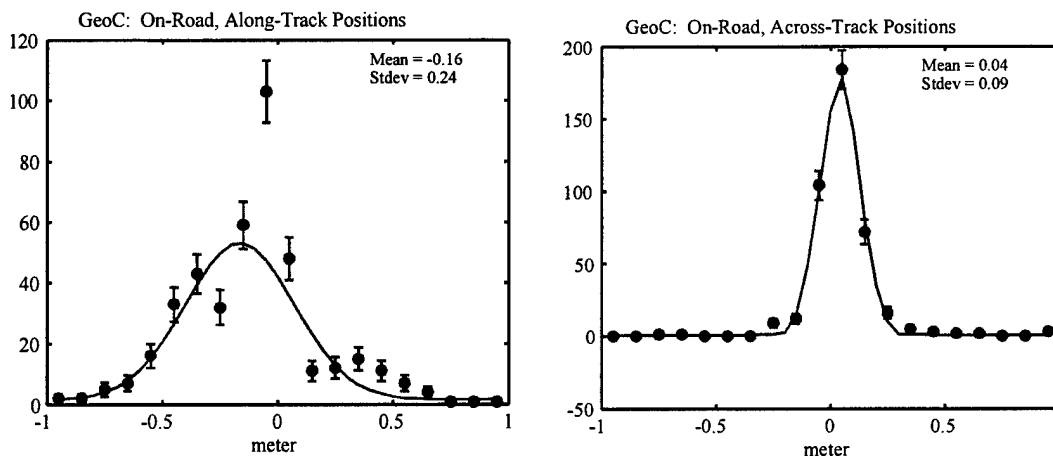
Figure V-14. GeoC's Miss-Distance Distribution for Surface and Subsurface Mines in On-Road Tests at Aberdeen. Data points include the GPR, EMI, and IR sensors. The solid curve is the best fit of a constant plus a Gaussian.

Table V-46. GeoC Bias and Resolution Performance at Aberdeen and Socorro: On-Road Performance

Type	Aberdeen Position Resolution				Socorro Position Resolution			
	Along-track		Cross-track		Along-track		Cross-track	
	Mean (bias) (m)	Standard Deviation (RMS) (m)	Mean (bias) (m)	Standard Deviation (RMS) (m)	Mean (bias) (m)	Standard Deviation (RMS) (m)	Mean (bias) (m)	Standard Deviation (RMS) (m)
All sensors, subsurface + surface	–0.16	0.24	0.04	0.09	–0.07	0.16	0.03	0.12
All sensors, subsurface	–0.08	0.11	0.04	0.09	–0.05	0.15	0.02	0.13
GPR	–0.10	0.10	0.04	0.08	–0.03	0.13	0.01	0.11
EMI	–0.05	0.09	0.04	0.09	–0.07	0.16	0.03	0.14
IR	N/A	N/A	N/A	N/A	Not well fit	Not well fit	0.01	0.20
All sensors, surface	–0.20	0.24	0.05	0.08	–0.09	0.16	0.03	0.11
GPR	–0.11	0.23	0.03	0.07	–0.04	0.14	0.02	0.09
EMI	–0.21	0.21	0.05	0.07	–0.09	0.15	0.03	0.11
IR	–0.32	0.18	0.04	0.10	Not well fit	Not well fit	0.04	0.13

b. Off Road

Figure V-15 shows GeoC's miss-distance distribution for surface and subsurface mines in off-road tests at Aberdeen. Along track, the mean (bias) of the distribution is –12 cm, which is similar to the on-road test. At 14 cm, the intrinsic resolution along track is, however, better than in the on-road test. The cross-track measurements again appear to have no bias, and at 14 cm, the RMS is consistent with the on-road tests. The bias in the along-track, off-road test appears to be primarily due to the performance of all sensors. Other results for the sensors are tabulated in Table V-46, including the measurements from the off-road tests at Socorro. Note that these Socorro results do not show statistically significant differences from the off-road performance at Aberdeen.

GeoC: Off-Road, Along-Track Positions   GeoC: Off-Road, Across-Track Positions
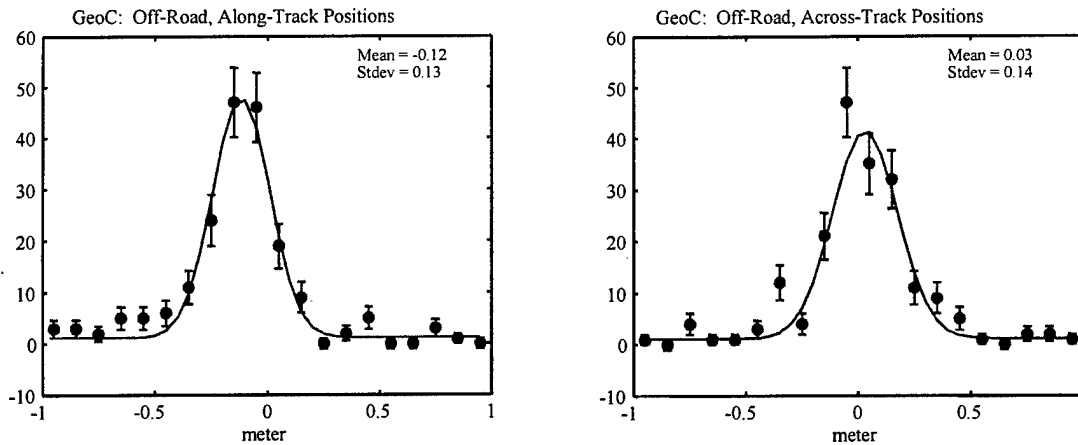
Figure V-15. Results of the Measured Surface and Subsurface Mine Locations for the GeoC Off-Road Tests at Aberdeen. Data from the GPR, EMI, and IR sensors are included in these plots.

Table V-47. GeoC Bias and Resolution Performance at Aberdeen: Off-Road Performance

Type	Aberdeen Position Resolution				Socorro Position Resolution			
	Along-track		Cross-track		Along-track		Cross-track	
	Mean (bias) (m)	Standard Deviation (RMS) (m)	Mean (bias) (m)	Standard Deviation (RMS) (m)	Mean (bias) (m)	Standard Deviation (RMS) (m)	Mean (bias) (m)	Standard Deviation (RMS) (m)
All sensors, subsurface + surface	−0.12	0.13	0.03	0.14	−0.08	0.17	0.02	0.11
All sensors, subsurface	−0.10	0.12	0.04	0.14	−0.05	0.14	0.03	0.13
GPR	−0.13	0.11	0.01	0.12	−0.05	0.15	-0.03	0.12
EMI	−0.05	0.08	0.04	0.15	−0.05	0.15	0.03	0.14
IR	N/A	N/A	N/A	N/A	N/A	N/A	N/A	N/A
All sensors, surface	−0.14	0.14	0.02	0.14	−0.12	0.21	0.01	0.09
GPR	−0.12	0.14	-0.01	0.12	−0.01	0.22	-0.02	0.10
EMI	−0.09	0.09	0.02	0.15	−0.07	0.15	0.06	0.06
IR	−0.14	0.11	0.05	0.14	Not well fit	Not well fit	0.03	0.07

4. P_d and R_{halo}

The bias and RMS resolution performance of the sensors affect how well, as a function of R_{halo}, GeoC's system detects the mines. Figure V-16 shows a plot of P_d versus R_{halo} for the tests at Aberdeen and Socorro. These figures summarize the overall

implication of GeoC's relatively small bias and intrinsic sensor resolution (as tabulated in section 2).

GeoC

a) On-road at Aberdeen

b) On-road at Socorro

c) Off-road at Aberdeen

d) Off-road at Socorro
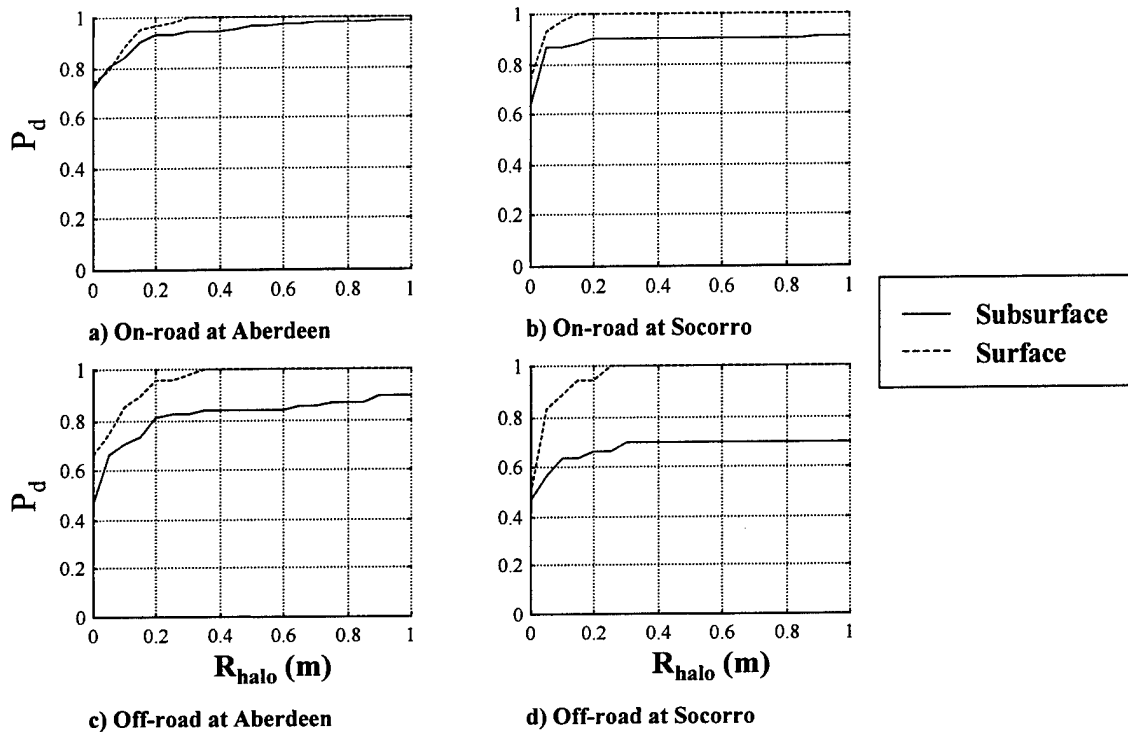
Figure V-16. P_d vs. R_{halo} for GeoC's Sensor Suite at Aberdeen and Socorro

As can be seen from the plots, the detection probability for GeoC's sensors was maximized for a R_{halo} of approximately 30 cm. If this ATD had required R_{halo} to be as small as 25 cm, then GeoC's P_d performance would have likely been unchanged. Even if R_{halo} were as small as 15 cm, GeoC would have likely still met the P_d exit criteria for this ATD.

5. Additional Runs

a. Aberdeen Results

Additional runs by GeoC at Aberdeen include two night runs on lane 11, two tele-operated runs on lane 11, and one physical-marking run (resulting in two files—one EM

alarm file and one PM alarm file) on lane 12.[11] Table V-48 shows the cumulative P_ds and *FAR*s for the on-road day runs and the night runs. GeoC detected all the surface mines for each set of tests, and the IR sensor detected all but one of the surface mines during the day runs. For both day and night runs, the IR did not detect any of the subsurface mines. The false-alarm rates for the night runs were almost 50 percent less than for the day runs. No IR false alarms occurred during the day or night.

Table V-48. Comparison of GeoC On-Road Day and Night Runs at Aberdeen

	On-Road Day		Night	
	Surface	Subsurface	Surface	Subsurface
Total P_d	1.0	0.985	1.0	1.0
IR P_d	0.988	0.0	1.0	0.0
Total *FAR*	0.056 m^{-2}		0.033 m^{-2}	
IR *FAR*	0.000 m^{-2}		0.000 m^{-2}	

For the tele-operated runs, GeoC made two passes of lane 11. Table V-49 shows the cumulative results of those passes and the on-road day runs. The P_ds are 1.0 for the surface mines, and the subsurface P_ds differ by only 1 to 2 percent from the surface P_ds. The false-alarm rate for the tele-operated runs is less than for the on-road day runs.

Table V-49. Comparison of GeoC On-Road Day and Tele-operated Runs at Aberdeen

	On-Road Day		Tele-operated	
	Surface	Subsurface	Surface	Subsurface
Total P_d	1.0	0.985	1.0	1.0
Total *FAR*	0.056		0.015 m^{-2}	

---

[11]   The results of these runs are summarized in Tables B-6 and B-7 in Appendix B and can be compared to the results GeoC obtained on its on-road day runs on lanes 11 and 12 as shown in Tables B-3 and B-4, respectively.

For the physical-marking run conducted by GeoC on lane 12 at Aberdeen, both electronic and physical-marking files were produced.[12] Table V-50 compares the performance measures of the on-road day runs with the physical-marking run on lane 12. The subsurface P_d for the physical-marking run is slightly lower than for the day runs, and the FAR is also lower.

Table V-50. Comparison of GeoC On-Road Day and Physical-Marking Runs at Aberdeen

	On-Road Day (EM)		Physical Marking (PM)	
	Surface	Subsurface	Surface	Subsurface
Total P_d	1.0	0.985	1.0	0.913
Total FAR	0.056 m^{-2}		0.038 m^{-2}	

Table V-51 shows that the along-track position resolution was better for the physical-marking run than for the on-road, day runs. The cross-track resolutions differ only slightly.

Table V-51. Comparison of GeoC Position Resolution for On-Road Day and Physical-Marking Runs at Aberdeen

	On-Road Day (EM)		Physical Marking (PM)	
	Mean (m)	RMS (m)	Mean (m)	RMS (m)
Along Track	−0.16	0.24	−0.02	0.10
Cross Track	0.04	0.09	0.0	0.09

Similar performance was found for the physical-marking system when directly compared to the electronic-marking system for the same pass of lane 12 at Aberdeen (see Table V-52). The P_ds are the same, the PM FAR is slightly less than the EM FAR, and the number of alarms is about 10 percent less for the physical-marking system.

---

[12] The results of this run are shown in Table B-7.

Table V-52. Comparison of GeoC Lane 12 Electronic-Marking and Physical-Marking Runs (EM and PM) at Aberdeen

	EM-1	PM-1
P_d	0.946	0.946
FAR (m^{-2})	0.042	0.038
# Alarms	112	102

b. Socorro Results

Additional runs by GeoC at Socorro include one night run on lanes 11, 12, and 13, two tele-operated runs on lane 8, and two physical-marking runs (resulting in four files—two EM alarm files and two PM alarm files) on lane 8.[13] Table V-53 shows the cumulative P_ds and FARs for the on-road day runs, and the night runs on lanes 11, 12, and 13. During the day, all surface mines were detected, with the IR sensor detecting 83 percent. Over 90 percent of the subsurface mines were detected for the day runs, but less than 20 percent of these were detected by the IR sensor. This result differs from the results at Aberdeen where the IR P_d was zero for subsurface mines. At night, the total P_d was 1.0 for surface mines, and the IR sensor detected all of them. For subsurface mines at night, the total P_d dropped off only slightly, but the IR sensor did not detect any mines. The total FAR for the night runs was nearly the same as the day FAR, and the IR FAR was zero for both test conditions.

---

[13] The results of these runs are summarized in Tables B-20 through B-24 in Appendix B and can be compared to the results GeoC obtained on its on-road day runs on lanes 8, 11, 12, and 13 as shown in Tables B-12 through B-15, respectively.

Table V-53. Comparison of GeoC On-Road Day and Night Runs at Socorro

	On-Road Day		Night	
	Surface	Subsurface	Surface	Subsurface
Total P_d	1.0	0.912	1.0	0.839
IR P_d	0.833	0.176	1.0	0.0
Total FAR	0.032 m^{-2}		0.029 m^{-2}	
IR FAR	0.000 m^{-2}		0.000 m^{-2}	

GeoC tele-operated performance at Socorro (see Table V-54) closely matches the performance trends observed at Aberdeen. The surface P_ds are the same, and the subsurface P_ds differ slightly. Again, the FAR for the tele-operated runs is less than for the day runs.

Table V-54. Comparison of GeoC On-Road Day and Tele-operated Runs at Socorro

	On-Road Day		Tele-operated	
	Surface	Subsurface	Surface	Subsurface
Total P_d	1.0	0.912	1.0	0.906
Total FAR	0.032 m^{-2}		0.019 m^{-2}	

For the physical-marking runs conducted by GeoC on lane 8 at Socorro, both electronic- and physical-marking files were produced. Table B-20 shows the results of this run. Table V-55 compares the performance measures of the on-road day runs with the physical-marking runs on lane 8. The subsurface P_d for the physical-marking run is slightly lower than for the day runs, and the FAR is also lower.

Table V-55. Comparison of GeoC On-Road Day and Physical-Marking Runs at Socorro

	On-Road Day		Physical Marking (PM)	
	Surface	Subsurface	Surface	Subsurface
Total P_d	1.0	0.912	1.0	0.844
Total *FAR*	0.032 m^{-2}		0.022 m^{-2}	

Table V-56 shows that the along-track position resolution as measured by the RMS was worse for the physical-marking run compared to the on-road day runs, although the mean was less. The cross-track resolutions differ only slightly.

Similar performance was found for the physical-marking system when directly compared to the electronic-marking system for the same pass of lane 8 at Socorro (see Table V-57). The P_ds are the same, the PM *FAR* is slightly less than the EM *FAR*, and the number of PM alarms is less than the number of EM alarms.

Table V-56. Comparison of GeoC Position Resolution for On-Road Day and Physical-Marking Runs at Socorro

	On-Road Day		Physical Marking (PM)	
	Mean (m)	RMS (m)	Mean (m)	RMS (m)
Along Track	-0.07	0.16	0.01	0.31
Cross Track	0.03	0.12	0.01	0.08

Table V-57. Comparison of GeoC Lane 8 Physical-Marking Runs (EM and PM) at Socorro

	EM-1	PM-1	EM-2	PM-2
P_d	0.875	0.833	1.0	0.958
FAR (m^{-2})	0.021	0.016	0.033	0.028
# Alarms	64	50	79	68

VI. CONCLUSIONS

The following general conclusions can be drawn from the VMMD ATD results:

1. The exit criteria were typically met by a majority of contractors at each test site, the exceptions being the on-road *FAR* at Aberdeen (met only by one contractor) and the off-road, subsurface P_d at Socorro (again, met by one contractor).

2. Reduction of the *FAR* is one of the serious challenges for this program, as the ultimate (ORD) requirements on *FAR* are substantially below those achieved in this ATD.

3. The contractors' GPR sensors were, overall, the most effective sensors for the detection of AT mines. The GPRs also, generally, contributed the most false alarms of the three sensor types.

4. Subsurface, low-metal mines in off-road conditions seemed to be the most difficult mines to detect in this ATD.

5. Metal-cased AT mines were detected with a high probability. Both GPR and EMI sensors were effective at finding these mines at the depths tested in this ATD.

6. Surface mines were detected with a high probability. Both GPR and IR systems were effective, regardless of the metal content of the mine.

7. The along-track and cross-track position resolutions typically achieved suggest that the mine halo can be reduced from 1 m without eliminating real detections.

REFERENCES

Altshuler et al. (1997), "Mine and UXO Detection: Measures of Performance and their Implication in Real-World Scenarios," *Proceedings of SPIE*, Vol. 3079, p. 284, April 1997.

Andrews, A. M., V. George, T. W. Altshuler, M. Mulqueen (1996), "Results of the Countermine Task Force Mine Detection Technology demonstration at Fort A.P. Hill, Virginia, March 18–22, 1996," IDA Paper P-3192, July 1996.

Andrews et al. (1998), "Performance in December 1996 Hand-Held Landmine Detection Tests at Aberdeen Proving Ground, Coleman Research Corp. (CRC), GDE Systems, Inc. (GDE), and AN/PSS–12," IDA Document D-2126, March 1998.

Bevington, P. R. (1969), "Data Reduction and Error Analysis for the Physical Sciences," McGraw-Hill.

"Detailed Test Plan for the Engineering Development Test (Advanced Technology Demonstration) of the Ground Minefield Detection System," TECOM Project No. 89-ES-025-GMD-001, Section 2.2.4, 1989.

Ground Standoff Minefield Detection System. Milestone I: Program Initiation Milestone Decision Review, Office of the Project Manager, Mines, Countermine, and Demolitions, July 1997.

Operational Requirements Document (ORD) for the Ground Standoff Minefield Detection System, 1996.

Simonson, K. H. (1998), "Statistical Considerations in Designing Tests of Mine Detection Systems: I—Measures Related to Probability of Detection," Sandia National Laboratories.

Van Trees, H L. (1968), "Detection, Estimation, and Modulation Theory," John Wiley and Sons.

GLOSSARY

AT	antitank
ATC	Aberdeen Test Center
ATD	Advanced Technology Demonstration
ATR	Automatic Target Recognition
CDC	Computing Devices Canada
CRC	Coleman Research Corp.
dGPS	differential Global Positioning System
EG&G	EG&G, Inc.
EMI	electromagnetic induction
FAR	false-alarm rate
GDE	GDE Systems, Inc.
GeoC	Geo-Centers, Inc.
GPR	Ground-Penetrating Radar
GSTAMIDS	Ground Standoff Mine Detection System
HMMWV	high-mobility multipurpose wheeled vehicle
NVESD	U.S. Army Night Vision and Electronic Sensors Directorate
ORD	Operational Requirements Document
P_d	probability of detection
TECOM	Test and Evaluation Command
TNA	Thermal Neutron Activation
VMMD	Vehicular-Mounted Mine Detection

APPENDIX A

DESCRIPTION OF CONTRACTOR SYSTEMS

APPENDIX A

DESCRIPTION OF CONTRACTOR SYSTEMS

A. COMPUTING DEVICES CANADA (CDC)

The CDC VMMD system has a 3-m wide detection system mounted on a Remote Detection Vehicle (RDV). This system was adapted from an existing Improved Landmine Detection System design developed for the Canadian Forces by Defence Research Establishment Suffield and CDC. The system includes a GPR sensor, an EMI minimum metal detector, a forward-looking IR detector and a thermal neutron activation (TNA) detector. The GPR, EMI, and IR detectors operate independently, and their data is combined in a central processor. Confirmation of detected land mines is provided by the TNA detector. Tele-operation and remote control are done in a command vehicle, which follows the RDV. A visible-light camera is mounted on top of the RDV to assist the control vehicle operator with the navigation of the RDV.

A telemetry link, including data processing and a radio link, enables communication between the RDV and the command vehicle.

The GPR subsystem is a 3-m wide antenna mounted 70 cm above the ground surface in front of the RDV. The specifications of this system are proprietary.

The EMI subsystem consists of 24 transmitter/receiver pairs of coils in three 1-m trays mounted on a sensor platform in front of the GPR system. It is used to detect all AT land mines with metal content. The 24 transmit/receive coils are connected with a controller that collects the data and interfaces with the central fusion system.

The IR system is a 9–14 μm IR camera mounted on a boom in front of the RDV. It is used to detect both buried and surface mines. The camera collects images as the RDV moves forward, and these images are processed for fusion in the integration processor.

The TNA system is a land mine confirmation sensor developed by SAIC Canada. The RDV tows the sensor on a trailer. It is used to confirm the presence of explosives in suspected land mines found by the other sensors. The sensor contains Californium

(CF-252), which acts as a high-energy neutron source. As the neutrons are slowed down (thermalized), they are captured by the nuclei in the soil and the target, and, in particular, by the nitrogen present in modern explosives. If nitrogen is present, then characteristic 10.8 MeV photons will be emitted from the nitrogen nucleus, which is detected by scintillating material in the sensor. By collecting all the high-energy photons emitted from the target and surrounding material and searching for the characteristic peak in energy around 10.8 MeV, the presence of nitrogen, and therefore explosives, is confirmed.

The data are processed and fused in a central integration processor. The data from one or more of the GPR, EMI, or IR sensors are processed to provide a confidence level for detection. A potential detection of a land mine in any one system is correlated with the navigation system. The position is computed using a combination of navigation, attitude of the sensor, and dGPS data. If the confidence level of a potential detection is significant, then the TNA confirmation sensor is positioned over the suspected land mine and the RDV stops. If the TNA confirms the presence of explosive, the system declares a detection, the data are recorded, and the position is marked (both physically and electronically).

B. COLEMAN RESEARCH CORPORATION (CRC)

The CRC system has a 3-m wide swath detection system mounted on a HMMWV. The system includes a frequency-stepped GPR subsystem, an EMI metal detector, and an IR sensor suite. CRC's IR sensor was not used in this ATD. Each of the sensors has its own electronics suite for the processing of data and automatic target detection. The data are combined in a central processing unit, which also controls the data storage and the electronic and the physical marking. In addition, a driving camera (visible light) is mounted on the HMMWV to remotely display the view to the vehicle's driver. The vehicle is not tele-operated.

The GPR subsystem comprises an array of 33 antennas (16 transmitting, 17 receiving). It is used to detect all types of AT land mines. It is mounted on a frame in front of the HMMWV covering a 3-m swath. The antennas are arranged with two receiving antennas around each transmitting antenna (with most receiving antennas servicing the two adjacent transmitting antennas). The transmitters step in 20 MHz frequency steps, from 900 MHz to 2.7 GHz. The measurement rate is 28 Hz.

Data are processed in a DSP board. The processing includes classification of targets and background, which scores the detections. If a mine is detected by the GPR, the data are passed forward to a spatial processor for location analysis and marking.

The EMI subsystem comprises six metal detectors. It is used to detect high-metal-content AT land mines. It is mounted on the frame in front of the GPR antenna array. The six metal detectors are spaced equally and cover a 3-m width swath. The subsystem pulses at a rate of 70 Hz.

Data are processed independently from the rest of the system. When the EMI subsystem detects a land mine, the data are passed forward to the spatial processor for location analysis and marking.

The IR subsystem, which was not used in this ATD, comprises two IR cameras: one cooled IR camera covering 3–5 μm, and one room-temperature IR camera covering 7–14 μm. The system is used to detect all types of AT land mines. It is mounted on a boom from the roof of the vehicle. Both cameras take data continually, at a frame rate of 30 Hz. The field of view covers a 3 by 5 m swath in front of the vehicle.

Data are processed in a PowerPC. The algorithms filter the images and search for features for subsequent classification. When the subsystem detects a land mine, the data are passed forward to the spatial processor for location analysis and marking.

Processing of the data is done independently by each sensor suite. Data are fused by a simple logical OR of the results. A spatial processor correlates the results from the sensors with a dGPS, records the data, and electronically and physically marks the mine locations.

C. EG&G

The EG&G VMMD system has a 3-m swath system of three sensors. The system includes a ground-penetrating radar (GPR) subsystem, a pulsed electromagnetic induction (EMI) metal detector, and an optical system that includes two infrared cameras and a visible-light camera. The system resides on a HMMWV: the GPR and EMI systems are on a sensor platform on the front of the vehicle and the optical system is mounted on the roof. Each of the three subsystems operates independently with its own automated target recognition algorithm; data are fused in an integration processor. The processor also tracks the vehicle and sensor position using a global positioning system (GPS) and serves as a controller for the electronic and physical marking of detectors. The vehicle may be remotely operated using the JPO UGV Standard Tele-operation System (STS).

The GPR system includes nine identical GPR modules mounted on the sensor platform, angled forward at 45 degrees. The system is used to detect all types of AT land mines. Each GPR module uses ultra-wide bandwidth (UVB) radar signals for the

detection of buried land mines. Each module contains separate transmitting and receiving impulse-radiating antennas that can transmit and receive impulses of about 300 ps (effective bandwidth of 250 MHz to 5 GHz). These unipolar 300 ps impulses have a 10 V amplitude, with a repetition rate of 5 MHz. The received signals are amplified and sampled. A single GPR controller unit provides all timing and control, including the triggering control for the transmission and sampling of signals. Operation of the GPR modules is interleaved so that cross talk is minimized.

As the VMMD moves forward GPR data are collected every 3 in., as measured by a tickwheel. A two-dimensional picture is built, based on along-track and depth measurements (energy returns which depend on depth). Background information is also collected and subtracted from the raw data. The real-time GPR processor collects single-channel energies and mark messages, as well as resolves cross-channel issues. The cross-track dimension of mine locations is found by interpolating among adjacent channels.

The pulsed-EMI system also includes nine identical transmitter/receiver modules across the width of the sensor platform. This system is used to detect AT land mines with a high metal content. This system is located in front of the GPR system, and each EMI module lies in a node of the radar system. Each EMI module transmits an ultra-wide bandwidth, pulsed magnetic field (30 μsec pulse width) through a coil and detects and analyzes the eddy current decays present in high-metal-content land mines. The magnetic field generator can create waveforms of specific shapes, strengths, and polarization, so that they can be localized to the area of interest. All transmitters on the nine modules are excited simultaneously so that they act as a single transmitter coil. Cross talk between modules and from transmitters is minimized in the receivers (mostly by correct geometric placement of the receivers).

EMI data are collected every 3 in. The receivers measure the eddy current response of metal mines, and the resulting signal is analyzed by a real-time processor for features such as amplitude responses and decay time. This measurement is scored against a library of signals, which contains features of metal AT mines as well as innocuous objects. The processor also interpolates the cross-track data among adjacent channels before declaring the mine.

The optical system includes three cameras mounted on the top of the vehicle. The system is used to detect all types of AT land mines, both buried and surface. The effective width of the viewing area is 4 m for each camera. Two of the cameras are infrared (3–5 and 8–12 μm bandwidth) and one is a color, visible light camera. The

infrared cameras are used to detect both buried and surface mines while the visible-light camera is used to detect surface mines. Data from each of the cameras is collected continually (subject to the frame rate). The infrared cameras are cooled to reduce noise. All three cameras are controlled with a central processor, which processes and analyzes the images. For the infrared system, the processed images are filtered, and features such as shape and size are extracted from mine-like objects for further characterization. The images from the visible camera are processed and analyzed for mine-like characteristics based on shape, size, and color. Any one of the three camera systems can declare a mine.

If any one subsystem detects a mine, then the central processor controls the electronic and physical marking of the mine. Data such as mine location [the differential GPS (dGPS) corrects for antenna tilts] are saved, as well as the raw sensor information.

D. GDE SYSTEMS

The GDE VMMD system has a 3-m swath of sensors. The system includes a GPR subsystem, a pulsed-EMI metal detector, and an IR camera. Each of the systems operates independently with its own automated target recognition algorithm; data are fused and land mines marked by an integration processor. The processor also tracks the vehicle using a dGPS, tracks the sensor position, and serves as a controller for the electronic and physical marking of mines. The vehicle may be remotely operated using the JPO UGV STS.

The GPR system comprises five independent GPR antenna arrays. It is used to detect all types of AT land mines. Each array includes two transmitter/receiver pairs. The array is a stepped-frequency, bistatic antenna operating between 0.5 and 3.0 GHz. As the vehicle moves forward, data are collected and stored. A real-time, digital signal processing (DSP) post-processor analyzes the data for anomalies and discriminates land mines from clutter.

The pulsed-EMI system includes six identical coil antennas across the width of the sensor platform. This system is used to detect high-metal-content AT land mines. The system is located in front of the GPR system in a non-metal housing. The EMI detects the eddy-current response to pulses. Each EMI detector is successively interrogated for anomalies by a central processor.

The IR system includes an 8–12 μm IR camera mounted on top of the vehicle. It is used to detect surface and near-surface land mines. The field of view is 3.1 by 1.5 m

ahead of the sensor platform. The camera is used as a forward-looking sensor to search for anomalies for discrimination.

The information from all three sensors is fused in the system's control using automatic integrated target recognition. As the vehicle moves forward and the sensors collect data, features such as size, shape, depth, metal content, burial depth, and electrical properties are extracted from the data. The fusion algorithm uses these features to build a three-dimension picture of targets, which allow the detection of land mines and discrimination from clutter. The targets are scored and the data are saved only for positive (land mine) detections. The position of land mines is physically marked, and electronically marked using a GPS system.

E. GEOCENTERS (GeoC)

The GeoC VMMD system has a 3.5-m swath detection system (maximum response within 3-m) mounted on a HMMWV. The system includes a GPR subsystem, a pulsed-EMI metal detector, and an IR sensor. Each of the systems operates independently with its own automated target recognition algorithm; data are combined in an integration processor. This processor also tracks the vehicle and sensor positions using a GPS and serves as a controller for electronic and physical marking. The vehicle is equipped with the JPO UGV STS.

The GPR subsystem is an energy-focusing radar that comprises an integrated array of radar transmitters and receivers, controlling electronics, communications hardware, and a rack-mounted PC. It is used to detect all types of AT land mines. It is located on a sensor platform in front of the HMMWV. The array comprises three ~1-m wide array modules, each containing five pulsed transmitters, five sampled receivers, and a custom digital signal-processing board. Each array module raster-scans the ground, focusing the combined energy spatially into the ground (into a voxel) from incremented sets of four transmitters. The sampling of the receivers is gated to correspond to the timed response from the specific volume in the ground. Each raster scan from the three antenna modules is 70 voxels (3 m) across by 64 voxels (~46 cm) deep. Successive raster-scans every 2 in. (driven by a tick wheel) are collected and added together to build up a three-dimensional picture of the ground. The pulsed, transmitted waveform has a bandwidth of 0.7–1.3 GHz, and the received signals are sampled up to 1 Msample/second (bandwidth of 3 GHz).

As the vehicle moves forward, raster-scan data are acquired. The background is calculated and subtracted, and the three-dimensional energy-return response is analyzed

using a fuzzy-logic, feature-extraction algorithm. The integration processor uses these feature scores to calculate a confidence level result in real time. Confidence levels, locations of potential mine targets, and the raw data are saved.

The pulsed-EMI system includes six transmitter/receiver coils located in front of the GPR system. It is used to detect high-metal-content AT land mines. The six coils are connected to six sets of electronic boards operating in a master/slave mode. This mode allows one coil system to operate as a master and the other five as a slave using the master's trigger, ensuring correct synchronization. Each coil operates at a 75-Hz repetition rate and 84 W peak-power output. The data are sampled every 2 in. A two-dimensional picture of land mines is built up from the six coils as the vehicle moves forward.

As data are acquired, the background (primarily induced by the metal signature of the vehicle) is subtracted and the energy return results compared with a pre-set threshold. The EMI computer cross-correlates data from adjacent channels and extracts features (such as shape and size) from the data. This allows the refinement of the location and confidence level for the marking of high-metal-content land mines. The confidence levels, locations and raw data are saved.

The IR subsystem is a 3–5 μm cooled infrared camera mounted on the roof of the vehicle. The system is used to detect all types of AT land mines. Data from the camera is collected continually. The camera is controlled from a central processing unit, although its pointing calibration is performed semi-automatically. The images are collected and subtracted from the background. A feature extraction algorithm calculates a confidence level for each target.

The integration processor combines the data from all three systems using the calculated confidence levels and feature values. A target confidence is calculated based on current data, statistics extracted from previous data, expert input, and algorithms that process features. If the integration processor declares a mine-like target, the location is calculated using the integrated GPS system, the tick-wheel, and information about the attitude of the detecting sensor. The results are electronically and physically marked.

APPENDIX B

TEST RESULTS

APPENDIX B
TEST RESULTS

Tables B-1 through B-24 summarize the text results lane by lane for both Aberdeen and Socorro. A check indicates the mine was detected by the contractor indicated in the column heading. For the scored daytime test runs, each contractor made two passes down the lanes. Column headings for daytime runs identify the contractor by a three-letter code, followed by a number representing the pas of the lane. Tables B-1 through B-5 summarize the scored daytime runs at Aberdeen. Tables B-9 through B-16 summarize the scored daytime runs at Socorro. Tables B-6 through B-8 and tables B-17 through B-24 summarize the additional runs at Aberdeen and Socorro. These additional runs include night (N), tele-operated (T), morning (M), and physical-marking (EM and PM) runs. For the physical-marking runs, contractors recorded two sets of alarms for each [ass of a lane. The first set of alarms (EM) was recorded electronically in the same manner as the scored test runs. The second set of alarms (PM) was generated by surveying the locations of physical markings (chalk or paint) that were deposited on the ground as the vehicle traversed the lane.]

The mine types are described in Chapter 2. "Alarms" are all sensor target declarations that occurred within the lane, "detections" are mines for which the sensor indicated an alarm within the 1-m halo, "false alarms" are all alarms not within 1-m of the edge of an emplaced mine, and "multiple hits" are redundant detections. The sum of detections, false alarms, and multiple hits is equal to the number of alarms. P_d is the number of detections divided by the number of mines emplaced in the lane. *FAR* is the number of false alarms divided by the lane area.

Table B-1. Lane 2 Results at Aberdeen

Mine ID	Mine Type	Depth (in.)	Contractor/Run Number										Totals
			CDC-1	CDC-2	CRC-1	CRC-2	EGG-1	EGG-2	GDE-1	GDE-2	GEO-1	GEO-2	
20101	TM62P	3	✓	✓	✓		✓	✓	✓	✓		✓	8/10
20102	M19	Surface	✓	✓	✓	✓	✓	✓	✓	✓	✓	✓	10/10
20105	TM62M	4	✓	✓	✓	✓	✓	✓	✓	✓	✓	✓	10/10
20106	TM62P	3	✓	✓	✓	✓	✓	✓		✓			7/10
20107	TM62P	Surface	✓	✓	✓	✓	✓	✓	✓		✓	✓	9/10
20108	M15I	1.5	✓	✓	✓	✓	✓	✓	✓	✓	✓	✓	10/10
20109	M15I	1.5	✓	✓	✓	✓	✓	✓	✓	✓	✓	✓	10/10
20110	M19I	1.5	✓	✓	✓	✓	✓	✓	✓	✓	✓	✓	10/10
20113	TM62M	Surface	✓	✓	✓	✓	✓	✓	✓	✓	✓	✓	10/10
20114	M19	1.5	✓	✓	✓	✓	✓	✓		✓	✓	✓	9/10
20117	TMA4	Surface	✓	✓	✓	✓	✓		✓	✓	✓	✓	9/10
20118	TM62M	4	✓	✓	✓	✓	✓	✓	✓	✓	✓	✓	10/10
20119	M19	1.5	✓	✓	✓	✓	✓			✓			6/10
20122	TM62M	Surface	✓	✓	✓	✓	✓	✓	✓	✓	✓	✓	10/10
20123	TMA4	2	✓		✓	✓	✓	✓	✓	✓			7/10
20124	M15	Surface	✓	✓	✓	✓	✓	✓	✓	✓	✓	✓	10/10
20125	TM62MI	2	✓	✓	✓	✓	✓	✓	✓	✓	✓	✓	10/10
20126	M15	1.5	✓	✓	✓	✓	✓	✓	✓	✓	✓	✓	10/10
20127	TMA4	Surface	✓	✓	✓	✓	✓	✓	✓	✓	✓	✓	10/10
20128	TM62MI	4	✓	✓	✓	✓	✓	✓	✓	✓	✓	✓	10/10
20129	M15	1.5	✓	✓	✓	✓	✓	✓	✓	✓	✓	✓	10/10
20130	M15	Surface	✓	✓	✓	✓	✓	✓	✓	✓	✓	✓	10/10
20131	TMA4	2	✓	✓	✓	✓	✓	✓	✓	✓	✓	✓	10/10
20132	M19	Surface	✓	✓	✓	✓	✓		✓	✓	✓	✓	9/10
20135	TM46	2	✓	✓	✓	✓	✓	✓	✓	✓	✓	✓	10/10
20136	M15	1	✓	✓	✓	✓	✓	✓	✓	✓	✓	✓	10/10
20137	M15	Surface	✓	✓	✓	✓	✓	✓	✓	✓	✓	✓	10/10
20138	TM62MI	Surface	✓	✓	✓	✓	✓	✓	✓	✓	✓	✓	10/10
20139	TM62P	Surface	✓	✓		✓	✓	✓	✓	✓	✓	✓	9/10

		CDC-1	CDC-2	CRC-1	CRC-2	EGG-1	EGG-2	GDE-1	GDE-2	GEO-1	GEO-2
Totals		29/29	28/29	28/29	28/29	29/29	26/29	26/29	28/29	25/29	26/29
Alarms		61	67	182	122	195	105	90	110	61	52
Detections		29	28	28	28	29	26	26	28	25	26
False Alarms		12	17	91	42	111	57	36	66	14	19
Multiple Hits		20	22	63	52	55	22	28	16	22	7
P_d		1.0	0.966	0.966	0.966	1.0	0.897	0.897	0.966	0.862	0.897
FAR (m^{-2})		0.021	0.030	0.160	0.074	0.195	0.100	0.063	0.116	0.025	0.033

Table B-2. Lane 4 Results at Aberdeen

Mine ID	Mine Type	Depth (in.)	CDC-1	CDC-2	CRC-1	CRC-2	EGG-1	EGG-2	GDE-1	GDE-2	GEO-1	GEO-2	Totals
4101	TM62P	Surface	✓	✓	✓	✓	✓	✓	✓	✓	✓	✓	10/10
4102	TM62M	4	✓	✓	✓	✓	✓	✓	✓	✓	✓	✓	10/10
4103	M19I	1.5	✓	✓	✓	✓	✓	✓	✓	✓	✓	✓	10/10
4106	M19I	1.5	✓	✓	✓	✓	✓	✓	✓	✓	✓	✓	10/10
4109	TMA4	Surface	✓	✓		✓	✓	✓		✓	✓	✓	8/10
4110	M15	1.5	✓	✓	✓	✓	✓	✓	✓	✓	✓	✓	10/10
4111	M19	Surface	✓	✓	✓	✓	✓	✓	✓	✓	✓	✓	10/10
4114	TM62M	Surface	✓	✓	✓	✓	✓	✓	✓	✓	✓	✓	10/10
4115	M15	Surface	✓	✓	✓	✓	✓	✓	✓	✓	✓	✓	10/10
4116	TM62P	3	✓	✓	✓	✓	✓	✓	✓		✓	✓	9/10
4117	M19I	1.5	✓	✓		✓	✓	✓	✓		✓	✓	8/10
4120	M15I	1.5	✓	✓	✓	✓	✓	✓	✓	✓	✓	✓	10/10
4121	TM62P	Surface	✓	✓	✓	✓	✓	✓	✓	✓	✓	✓	10/10
4122	TMA4	2	✓	✓			✓		✓	✓	✓	✓	7/10
4123	TM62MI	2	✓	✓	✓	✓	✓	✓	✓	✓	✓	✓	10/10
4124	TM62MI	4	✓	✓	✓	✓	✓	✓	✓	✓	✓	✓	10/10
4125	M15	Surface	✓	✓	✓	✓	✓	✓	✓	✓	✓	✓	10/10
4126	TM62MI	Surface	✓	✓	✓	✓	✓	✓	✓	✓	✓	✓	10/10
4127	TM46	2	✓	✓	✓	✓	✓	✓	✓	✓	✓	✓	10/10
4128	TMA4	Surface	✓	✓	✓		✓	✓	✓	✓	✓	✓	9/10
4129	TMA4	2	✓	✓		✓	✓	✓		✓	✓	✓	8/10
4130	M19	Surface	✓	✓	✓	✓	✓	✓	✓	✓	✓	✓	10/10
4133	M19	1.5	✓	✓	✓	✓	✓		✓	✓	✓	✓	9/10
4136	TM62MI	Surface	✓	✓	✓	✓	✓	✓	✓	✓	✓	✓	10/10
4137	M15	1.5	✓	✓	✓	✓	✓	✓	✓	✓	✓	✓	10/10
4138	M15I	1.5	✓	✓	✓	✓	✓	✓	✓	✓	✓	✓	10/10
4139	TM62P	3	✓	✓	✓	✓	✓	✓	✓		✓	✓	9/10
4140	M15	Surface	✓	✓	✓	✓	✓	✓	✓	✓	✓	✓	10/10
4141	TM62MI	4	✓	✓	✓	✓	✓	✓	✓	✓	✓	✓	10/10
Totals			29/29	29/29	25/29	27/29	29/29	27/29	27/29	26/29	29/29	29/29	
Alarms			67	95	283	262	61	84	99	86	104	127	
Detections			29	29	25	27	29	27	27	26	29	29	
False Alarms			33	51	188	138	20	37	45	46	49	68	
Multiple Hits			5	15	70	97	12	20	27	14	26	30	
P_d			1.0	1.0	0.862	0.931	1.0	0.931	0.931	0.897	1.0	1.0	
FAR (m^{-2})			0.058	0.089	0.330	0.242	0.035	0.065	0.079	0.081	0.086	0.119	

Table B-3. Lane 11 Results at Aberdeen

Mine ID	Mine Type	Depth (in.)	CDC-1	CDC-2	CRC-1	CRC-2	EGG-1	EGG-2	GDE-1	GDE-2	GEO-1	GEO-2	Totals
11101	TM62M	Surface	✓	✓	✓	✓	✓	✓	✓	✓	✓	✓	10/10
11102	TM62M	4	✓	✓	✓	✓	✓	✓	✓	✓	✓	✓	10/10
11103	TM62P	3	✓	✓	✓		✓	✓	✓	✓	✓	✓	9/10
11104	M15	1.5	✓	✓	✓	✓	✓	✓	✓	✓	✓	✓	10/10
11105	M15	Surface	✓	✓	✓	✓	✓	✓	✓	✓	✓	✓	10/10
11106	M19	1.5	✓	✓	✓	✓	✓		✓	✓	✓	✓	9/10
11109	TM62MI	2	✓	✓	✓	✓	✓	✓	✓	✓	✓	✓	10/10
11110	TM62P	Surface	✓	✓	✓	✓	✓	✓	✓	✓	✓	✓	10/10
11111	TM46	2	✓	✓	✓	✓	✓	✓	✓	✓	✓	✓	10/10
11112	M19	Surface	✓	✓	✓	✓	✓	✓	✓	✓	✓	✓	10/10
11115	M19I	2	✓	✓				✓	✓	✓	✓	✓	7/10
11118	TMA4	2	✓	✓		✓	✓	✓	✓	✓	✓	✓	9/10
11119	M19	1.5	✓	✓	✓	✓	✓	✓	✓	✓	✓	✓	10/10
11122	M15I	Surface	✓	✓	✓	✓	✓	✓	✓	✓	✓	✓	10/10
11123	M15I	1.5	✓	✓	✓	✓	✓	✓	✓	✓	✓	✓	10/10
11124	TMA4	Surface	✓	✓	✓	✓	✓	✓	✓	✓	✓	✓	10/10
11125	TM62P	3	✓	✓	✓	✓	✓	✓	✓	✓	✓	✓	10/10
11126	TM62MI	Surface	✓	✓	✓	✓	✓	✓	✓	✓	✓	✓	10/10
11127	M15I	1.5	✓	✓	✓	✓	✓	✓	✓	✓	✓	✓	10/10
11128	TM62MI	4	✓	✓	✓	✓	✓	✓	✓		✓	✓	9/10
11129	M15	1.5	✓	✓	✓	✓	✓	✓	✓		✓	✓	9/10
11130	M15	Surface	✓	✓	✓	✓	✓	✓	✓		✓	✓	9/10
11131	TM62MI	2	✓	✓	✓	✓	✓	✓	✓		✓	✓	9/10
11132	M19	1.5	✓	✓	✓	✓	✓	✓	✓	✓	✓	✓	10/10
11135	EM12	Surface	✓	✓	✓	✓	✓		✓	✓	✓	✓	9/10
11136	TM62MI	Surface	✓	✓	✓	✓	✓	✓	✓	✓	✓	✓	10/10
11137	M19I	2	✓	✓	✓	✓		✓	✓	✓	✓	✓	9/10
11140	TM46	2	✓	✓	✓	✓	✓	✓	✓	✓	✓	✓	10/10
11141	TM62P	Surface	✓	✓	✓	✓	✓	✓	✓	✓	✓	✓	10/10
11142	TMA4	2	✓	✓			✓		✓	✓	✓	✓	7/10
11143	M19I	Surface	✓	✓	✓	✓	✓	✓	✓	✓	✓	✓	10/10
11146	M19I	Surface	✓	✓	✓	✓	✓	✓	✓	✓	✓	✓	10/10
11149	TM62MI	4	✓	✓	✓	✓	✓	✓	✓	✓	✓	✓	10/10
11150	TMA4	Surface	✓	✓	✓	✓	✓	✓	✓	✓	✓	✓	10/10
11151	TM62P	3		✓		✓	✓	✓		✓	✓	✓	7/10
11152	TMA4	2		✓		✓	✓	✓		✓	✓	✓	7/10
11153	EM12	2	✓	✓		✓	✓	✓	✓	✓	✓	✓	9/10
Totals			34/37	37/37	31/37	34/37	35/37	34/37	35/37	33/37	37/37	37/37	
Alarms			100	91	136	134	76	99	94	83	116	103	
Detections			34	37	31	34	35	34	35	33	37	37	
False Alarms			47	36	44	26	24	47	49	42	49	36	
Multiple Hits			19	18	61	74	17	18	10	8	30	30	
P_d			0.919	1.0	0.838	0.919	0.946	0.919	0.946	0.892	1.0	1.0	
FAR (m^{-2})			0.051	0.039	0.047	0.028	0.026	0.051	0.053	0.045	0.053	0.039	

B-7

Table B-4. Lane 12 Results at Aberdeen

Mine ID	Mine Type	Depth (in.)	CDC-1	CDC-2	CRC-1	CRC-2	EGG-1	EGG-2	GDE-1	GDE-2	GEO-1	GEO-2	Totals
							Contractor/Run Number						
12101	TM62P	3	✓	✓	✓		✓	✓	✓	✓	✓	✓	9/10
12102	TM62M	Surface	✓	✓	✓	✓	✓	✓	✓	✓	✓	✓	10/10
12103	TM62M	4	✓	✓	✓	✓	✓	✓	✓	✓	✓	✓	10/10
12104	M19I	2	✓	✓	✓	✓	✓		✓		✓	✓	8/10
12107	M15I	Surface	✓	✓	✓	✓	✓	✓	✓	✓	✓	✓	10/10
12108	TMA4	Surface	✓	✓	✓	✓	✓	✓	✓	✓	✓	✓	10/10
12109	TM46	2	✓	✓	✓	✓	✓	✓	✓	✓	✓	✓	10/10
12110	TM62P	Surface	✓	✓			✓	✓	✓	✓	✓	✓	10/10
12111	M19	1.5	✓	✓			✓	✓	✓	✓	✓	✓	8/10
12114	TM62MI	2	✓	✓	✓	✓	✓	✓	✓	✓	✓	✓	8/10
12115	M19	Surface	✓	✓	✓	✓	✓	✓	✓	✓	✓	✓	10/10
12118	TMA4	2	✓	✓			✓	✓	✓	✓	✓	✓	8/10
12119	EM12	Surface	✓	✓	✓	✓	✓	✓	✓	✓	✓	✓	10/10
12120	M15	1.5	✓	✓	✓	✓	✓	✓	✓	✓	✓	✓	10/10
12121	M15I	Surface	✓	✓	✓	✓	✓	✓	✓	✓	✓	✓	10/10
12122	TM62MI	Surface	✓	✓	✓	✓	✓	✓	✓	✓	✓	✓	10/10
12123	M15	Surface	✓	✓	✓	✓	✓	✓	✓	✓	✓	✓	10/10
12124	TM62MI	4	✓	✓	✓	✓	✓	✓	✓	✓	✓	✓	10/10
12125	M15I	1.5	✓	✓	✓	✓	✓	✓	✓	✓	✓	✓	10/10
12126	M15I	1.5	✓	✓	✓	✓	✓	✓	✓	✓	✓	✓	10/10
12127	TMA4	2	✓	✓			✓	✓	✓	✓	✓	✓	7/10
12128	TM62P	3	✓	✓			✓	✓	✓		✓	✓	8/10
12129	M19	1.5	✓	✓			✓	✓	✓	✓	✓	✓	8/10
12132	TM62MI	2	✓	✓	✓	✓	✓	✓	✓	✓	✓	✓	10/10
12133	TM62MI	4	✓	✓	✓	✓	✓	✓	✓	✓	✓	✓	10/10
12134	TM62P	3		✓			✓	✓	✓	✓	✓	✓	7/10
12135	M19I	2	✓	✓	✓		✓	✓	✓	✓	✓	✓	7/10
12138	TM62P	Surface	✓	✓	✓		✓	✓	✓		✓	✓	8/10
12139	TMA4	Surface	✓	✓	✓	✓	✓	✓	✓	✓	✓	✓	10/10
12140	M19	1.5	✓	✓	✓		✓	✓	✓	✓	✓	✓	8/10
12143	M19	Surface	✓	✓	✓	✓	✓	✓	✓	✓	✓	✓	10/10
12146	M19I	Surface	✓	✓	✓		✓	✓	✓	✓	✓	✓	9/10
12149	TM46	2	✓	✓	✓	✓	✓	✓	✓	✓	✓	✓	10/10
12150	EM12	2	✓	✓			✓	✓	✓	✓	✓	✓	7/10
12151	M15	1.5	✓	✓	✓	✓	✓	✓	✓	✓	✓	✓	10/10
12152	TM62MI	Surface	✓	✓	✓	✓	✓	✓	✓	✓	✓	✓	10/10
12153	TMA4	2	✓	✓	✓	✓	✓	✓	✓	✓	✓	✓	9/10

	CDC-1	CDC-2	CRC-1	CRC-2	EGG-1	EGG-2	GDE-1	GDE-2	GEO-1	GEO-2
Totals	36/37	36/37	26/37	24/37	37/37	36/37	36/37	34/37	37/37	37/37
Alarms	157	108	119	127	220	261	210	75	171	195
Detections	36	36	26	24	37	36	36	34	37	37
False Alarms	111	63	44	51	148	202	150	37	101	119
Multiple Hits	10	9	49	52	35	23	24	4	33	39
P_d	0.973	0.973	0.703	0.649	1.0	0.973	0.973	0.919	1.0	1.0
FAR (m^{-2})	0.099	0.056	0.039	0.046	0.132	0.181	0.134	0.033	0.090	0.106

Table B-5. Lane 15 Results at Aberdeen

Mine ID	Mine Type	Depth (in.)	CDC-1	CDC-2	CRC-1	CRC-2	EGG-1	EGG-2	GDE-1	GDE-2	GEO-1	GEO-2	Totals
15101	TMA4	2		✓	✓	✓	✓	✓		✓		✓	7/10
15102	TM62MI	Surface	✓	✓	✓	✓	✓	✓	✓	✓	✓	✓	10/10
15103	M19I	Surface	✓	✓	✓		✓	✓		✓		✓	8/10
15106	TM62P	3	✓	✓	✓		✓	✓	✓	✓	✓	✓	9/10
15107	M15	Surface	✓	✓	✓	✓	✓	✓	✓	✓	✓	✓	10/10
15108	M15	1.5	✓	✓	✓	✓	✓	✓	✓	✓	✓	✓	10/10
15109	TM62MI	4	✓	✓	✓	✓	✓	✓	✓	✓	✓	✓	10/10
15110	TM46	2	✓	✓	✓	✓	✓	✓	✓	✓	✓	✓	10/10
15111	M19	1.5	✓	✓	✓	✓	✓	✓	✓	✓	✓	✓	10/10
15114	TM62P	Surface	✓	✓	✓	✓	✓	✓	✓	✓	✓	✓	10/10
15115	TM62MI	Surface	✓	✓	✓	✓	✓	✓	✓	✓	✓	✓	10/10
15116	M15	1.5	✓	✓	✓	✓	✓	✓	✓	✓	✓	✓	10/10
15117	TM62P	3	✓	✓	✓	✓	✓	✓	✓	✓		✓	9/10
15118	TMA4	Surface	✓		✓	✓	✓	✓		✓	✓	✓	8/10
15119	TMA4	2	✓	✓	✓	✓	✓	✓	✓	✓	✓	✓	10/10
15120	M15I	1.5		✓				✓	✓	✓	✓	✓	6/10
15121	M19I	2	✓		✓	✓	✓	✓	✓	✓	✓	✓	9/10
15124	M19I	Surface	✓	✓	✓	✓	✓	✓	✓	✓	✓	✓	10/10
15127	TM62MI	4	✓	✓	✓	✓	✓	✓	✓	✓	✓	✓	10/10
15128	M15	Surface	✓	✓	✓	✓	✓	✓	✓	✓	✓	✓	10/10
15129	TMA4	Surface	✓	✓	✓	✓	✓		✓		✓	✓	8/10
15130	M19	1.5	✓	✓	✓	✓	✓	✓	✓	✓	✓	✓	10/10
15133	TM62MI	2	✓	✓	✓	✓	✓	✓	✓	✓	✓	✓	10/10
15134	M19	Surface	✓	✓	✓	✓	✓	✓	✓	✓	✓	✓	10/10
15137	M19I	Surface	✓	✓	✓	✓	✓	✓	✓	✓	✓	✓	10/10
15140	M15I	Surface	✓	✓	✓	✓	✓	✓	✓	✓	✓	✓	10/10
15141	M19I	1.5	✓	✓	✓	✓	✓		✓	✓	✓	✓	9/10
15144	TMA4	2	✓	✓	✓	✓	✓	✓	✓	✓	✓	✓	10/10
15145	TM62P	3	✓	✓	✓	✓	✓	✓	✓	✓	✓	✓	10/10
15146	TM46	2	✓	✓	✓	✓	✓	✓	✓	✓	✓	✓	10/10
15147	TM62P	Surface	✓	✓	✓	✓	✓	✓	✓	✓	✓	✓	10/10
15148	M15	1.5	✓	✓	✓	✓	✓	✓	✓	✓	✓	✓	10/10
15149	EM12	2	✓	✓	✓	✓	✓	✓	✓		✓	✓	9/10
15150	EM12	Surface	✓	✓	✓	✓	✓	✓	✓	✓	✓	✓	10/10
15151	TM62MI	Surface	✓	✓	✓	✓	✓	✓	✓	✓	✓	✓	10/10
Totals			33/35	33/35	34/35	32/35	34/35	33/35	32/35	33/35	33/35	35/35	
Alarms			77	112	123	143	107	84	94	152	103	119	
Detections			33	33	34	32	34	33	32	33	33	35	
False Alarms			26	62	29	46	50	42	50	107	37	48	
Multiple Hits			18	17	60	65	23	9	12	12	33	36	
P_d			0.943	0.943	0.971	0.914	0.971	0.943	0.914	0.943	0.943	1.0	
FAR (m^{-2})			0.024	0.058	0.027	0.043	0.047	0.040	0.047	0.101	0.035	0.045	

Table B-6. Lane 11 Night, Tele-operated, and Physical-Marking Results at Aberdeen

Mine ID	Mine Type	Depth (in.)	Contractor/Run Number								Totals
			GEO-N1	GEO-N2	GDE-N1	GDE-N2	EGG-N2	GEO-T1	GEO-T2	CRC-PM1	
11101	TM62M	Surface	✓	✓	✓	✓	✓	✓	✓	✓	8/8
11102	TM62M	4	✓	✓	✓	✓	✓	✓	✓	✓	8/8
11103	TM62P	3	✓	✓	✓	✓		✓	✓		6/8
11104	M15	1.5	✓	✓	✓	✓	✓	✓	✓	✓	8/8
11105	M15	Surface	✓	✓	✓	✓	✓	✓	✓	✓	8/8
11106	M19	1.5	✓	✓	✓	✓		✓	✓		6/8
11109	TM62MI	2	✓	✓	✓	✓	✓	✓	✓	✓	8/8
11110	TM62P	Surface	✓	✓	✓	✓	✓	✓	✓	✓	8/8
11111	TM46	2	✓	✓	✓	✓	✓	✓	✓	✓	8/8
11112	M19	Surface	✓	✓	✓	✓	✓	✓	✓	✓	8/8
11115	M19I	2	✓	✓	✓	✓		✓	✓		6/8
11118	TMA4	2	✓	✓	✓	✓		✓	✓	✓	7/8
11119	M19	1.5	✓	✓	✓	✓	✓	✓	✓	✓	8/8
11122	M15I	Surface	✓	✓	✓	✓	✓	✓	✓	✓	8/8
11123	M15I	1.5	✓	✓	✓	✓	✓	✓	✓	✓	8/8
11124	TMA4	Surface	✓	✓	✓	✓	✓	✓	✓		7/8
11125	TM62P	3	✓	✓	✓	✓		✓	✓	✓	7/8
11126	TM62MI	Surface	✓	✓	✓	✓	✓	✓	✓	✓	8/8
11127	M15I	1.5	✓	✓	✓	✓	✓	✓	✓	✓	8/8
11128	TM62MI	4	✓	✓	✓	✓	✓	✓	✓	✓	8/8
11129	M15	1.5	✓	✓	✓	✓	✓	✓	✓	✓	8/8
11130	M15	Surface	✓	✓	✓	✓	✓	✓	✓	✓	8/8
11131	TM62MI	2	✓	✓	✓	✓	✓	✓	✓	✓	8/8
11132	M19	1.5	✓	✓	✓	✓		✓	✓	✓	7/8
11135	EM12	Surface	✓	✓	✓	✓	✓	✓	✓	✓	8/8
11136	TM62MI	Surface	✓	✓	✓	✓	✓	✓	✓	✓	8/8
11137	M19I	2	✓	✓	✓	✓	✓	✓	✓	✓	8/8
11140	TM46	2	✓	✓	✓	✓	✓	✓	✓	✓	8/8
11141	TM62P	Surface	✓	✓	✓	✓	✓	✓	✓	✓	8/8
11142	TMA4	2	✓	✓	✓	✓	✓	✓	✓		6/8
11143	M19I	Surface	✓	✓	✓	✓	✓	✓	✓	✓	8/8
11146	M19I	Surface	✓	✓	✓	✓	✓	✓	✓	✓	8/8
11149	TM62MI	4	✓	✓	✓	✓	✓	✓	✓	✓	8/8
11150	TMA4	Surface	✓	✓	✓	✓	✓	✓	✓	✓	8/8
11151	TM62P	3	✓	✓	✓	✓	✓	✓	✓	✓	8/8
11152	TMA4	2	✓	✓	✓	✓	✓	✓	✓		6/8
11153	EM12	2	✓	✓	✓	✓	✓	✓	✓	✓	8/8
		Totals	37/37	37/37	37/37	37/37	29/37	37/37	37/37	31/37	
		Alarms	92	98	51	63	113	71	68	109	
		Detections	37	37	37	37	29	37	37	31	
		False Alarms	27	35	9	21	47	15	13	21	
		Multiple Hits	28	26	5	5	37	19	18	57	
		P_d	1.0	1.0	1.0	1.0	0.784	1.0	1.0	0.838	
		FAR (m^{-2})	0.029	0.038	0.010	0.023	0.051	0.016	0.014	0.023	

Table B-7. Lane 12 Night and Physical-Marking Results at Aberdeen

Mine ID	Mine Type	Depth (in.)	Contractor/Run Number EGG-N1	GEO-EM1	GEO-PM1	Totals
12101	TM62P	3	✓			1/3
12102	TM62M	Surface	✓	✓	✓	3/3
12103	TM62M	4	✓	✓	✓	3/3
12104	M19I	2	✓	✓	✓	3/3
12107	M15I	Surface	✓	✓	✓	3/3
12108	TMA4	Surface	✓	✓	✓	3/3
12109	TM46	2	✓	✓	✓	3/3
12110	TM62P	Surface	✓	✓	✓	3/3
12111	M19	1.5	✓	✓	✓	3/3
12114	TM62MI	2	✓	✓	✓	3/3
12115	M19	Surface	✓	✓	✓	3/3
12118	TMA4	2	✓	✓	✓	3/3
12119	EM12	Surface	✓	✓	✓	3/3
12120	M15	1.5	✓	✓	✓	3/3
12121	M15I	Surface	✓	✓	✓	3/3
12122	TM62MI	Surface	✓	✓	✓	3/3
12123	M15	Surface	✓	✓	✓	3/3
12124	TM62MI	4	✓	✓	✓	3/3
12125	M15I	1.5	✓	✓	✓	3/3
12126	M15I	1.5	✓	✓	✓	3/3
12127	TMA4	2		✓	✓	2/3
12128	TM62P	3	✓	✓	✓	3/3
12129	M19	1.5		✓	✓	2/3
12132	TM62MI	2	✓	✓	✓	3/3
12133	TM62MI	4	✓	✓	✓	3/3
12134	TM62P	3				0/3
12135	M19I	2	✓	✓	✓	3/3
12138	TM62P	Surface	✓	✓	✓	3/3
12139	TMA4	Surface	✓	✓	✓	3/3
12140	M19	1.5	✓	✓	✓	3/3
12143	M19	Surface	✓	✓	✓	3/3
12146	M19I	Surface	✓	✓	✓	3/3
12149	TM46	2	✓	✓	✓	3/3
12150	EM12	2		✓	✓	2/3
12151	M15	1.5	✓	✓	✓	3/3
12152	TM62MI	Surface	✓	✓	✓	3/3
12153	TMA4	2	✓	✓	✓	3/3

	EGG-N1	GEO-EM1	GEO-PM1
Totals	33/37	35/37	35/37
Alarms	332	112	102
Detections	33	35	35
False Alarms	251	47	43
Multiple Hits	48	30	24
P_d	0.892	0.946	0.946
FAR (m^{-2})	0.224	0.042	0.038

B-11

Table B-8. Lane 15 Night and Physical-Marking Results at Aberdeen

Mine ID	Mine Type	Depth (in.)	CRC-N1	CRC-N2	CDC-N1	CDC-N2	EGG-EM1	EGG-PM1	GDE-PM1	Totals
					Contractor/Run Number					
15101	TMA4	2	✓	✓	✓	✓	✓		✓	6/7
15102	TM62MI	Surface	✓	✓	✓	✓	✓		✓	6/7
15103	M19I	Surface	✓	✓	✓	✓	✓		✓	6/7
15106	TM62P	3	✓	✓	✓	✓	✓	✓	✓	7/7
15107	M15	Surface	✓	✓	✓	✓	✓	✓	✓	7/7
15108	M15	1.5	✓	✓	✓	✓	✓	✓	✓	7/7
15109	TM62MI	4	✓	✓	✓	✓	✓	✓	✓	7/7
15110	TM46	2	✓	✓	✓	✓	✓	✓	✓	7/7
15111	M19	1.5	✓	✓	✓	✓			✓	5/7
15114	TM62P	Surface	✓	✓	✓	✓	✓	✓	✓	7/7
15115	TM62MI	Surface	✓	✓	✓	✓	✓	✓	✓	7/7
15116	M15	1.5	✓	✓	✓	✓	✓	✓	✓	7/7
15117	TM62P	3	✓	✓	✓	✓	✓		✓	6/7
15118	TMA4	Surface	✓	✓	✓	✓	✓	✓	✓	7/7
15119	TMA4	2	✓	✓	✓	✓	✓	✓	✓	7/7
15120	M15I	1.5	✓	✓	✓	✓	✓	✓	✓	7/7
15121	M19I	2	✓	✓	✓	✓	✓		✓	6/7
15124	M19I	Surface	✓		✓	✓	✓	✓	✓	6/7
15127	TM62MI	4	✓	✓	✓	✓	✓	✓	✓	7/7
15128	M15	Surface	✓	✓	✓	✓	✓	✓	✓	7/7
15129	TMA4	Surface	✓	✓	✓	✓	✓	✓	✓	7/7
15130	M19	1.5	✓	✓	✓	✓	✓	✓	✓	7/7
15133	TM62MI	2	✓	✓	✓	✓	✓	✓	✓	7/7
15134	M19	Surface	✓	✓	✓	✓	✓		✓	6/7
15137	M19I	Surface	✓	✓	✓	✓	✓	✓	✓	7/7
15140	M15I	Surface	✓	✓	✓	✓	✓	✓	✓	7/7
15141	M19I	1.5	✓		✓	✓			✓	4/7
15144	TMA4	2			✓	✓			✓	3/7
15145	TM62P	3	✓	✓	✓		✓		✓	5/7
15146	TM46	2	✓	✓	✓	✓	✓	✓	✓	7/7
15147	TM62P	Surface	✓	✓	✓	✓	✓	✓	✓	7/7
15148	M15	1.5	✓	✓	✓	✓	✓	✓	✓	7/7
15149	EM12	2	✓	✓	✓	✓			✓	5/7
15150	EM12	Surface	✓	✓	✓	✓	✓	✓	✓	7/7
15151	TM62MI	Surface	✓	✓	✓	✓		✓	✓	6/7
Totals			34/35	32/35	35/35	34/35	30/35	24/35	35/35	
Alarms			104	100	108	106	91	61	97	
Detections			34	32	35	34	30	24	35	
False Alarms			26	31	62	63	45	30	47	
Multiple Hits			44	37	11	9	16	7	15	
P_d			0.971	0.914	1.0	0.971	0.857	0.686	1.0	
FAR (m^{-2})			0.024	0.029	0.058	0.059	0.042	0.028	0.044	

Table B-9. Lane 1 Results at Socorro

Mine ID	Mine Type	Depth (in.)	CDC-1	CDC-2	CRC-1	CRC-2	EGG-1	EGG-2	GDE-1	GDE-2	GEO-1	GEO-2	Totals
			Contractor/Run Number									
1001	TM62M	4	✓	✓	✓	✓	✓	✓	✓	✓	✓	✓	10/10
1002	EM12	2	✓	✓	✓	✓	✓	✓	✓	✓		✓	9/10
1003	TM62P	3				✓	✓		✓		✓		4/10
1004	TM62M	Surface	✓	✓	✓	✓	✓	✓	✓	✓	✓	✓	10/10
1005	TM62MI	2	✓	✓	✓	✓	✓	✓	✓	✓	✓	✓	10/10
1006	TM62MI	Surface	✓	✓	✓	✓	✓	✓	✓	✓	✓	✓	10/10
1007	TM62P	Surface	✓	✓	✓	✓	✓	✓	✓	✓	✓	✓	10/10
1008	TM46	2	✓	✓	✓	✓	✓	✓	✓	✓	✓	✓	10/10
1009	TM62M	Surface	✓	✓	✓	✓	✓	✓	✓	✓	✓	✓	10/10
1010	TMA4	2	✓	✓	✓			✓	✓	✓			6/10
1011	M19	Surface	✓	✓	✓	✓	✓	✓	✓	✓	✓	✓	10/10
1014	M19	1.5		✓		✓	✓	✓	✓	✓	✓	✓	8/10
1017	M15	1.5	✓	✓	✓	✓	✓	✓	✓	✓	✓	✓	10/10
1018	M19I	1.5		✓		✓	✓	✓	✓	✓		✓	7/10

		Totals	11/14	13/14	11/14	12/14	13/14	13/14	14/14	13/14	11/14	12/14
		Alarms	17	26	55	52	35	27	34	24	34	35
		Detections	11	13	11	12	13	13	14	13	11	12
		False Alarms	6	10	11	11	12	6	16	7	6	8
		Multiple Hits	0	3	33	29	10	8	4	4	17	15
		P_d	0.786	0.929	0.786	0.857	0.929	0.929	1.0	0.929	0.786	0.857
		FAR (m^{-2})	0.025	0.042	0.046	0.046	0.050	0.025	0.067	0.029	0.025	0.033

Table B-10. Lane 4 Results at Socorro

Mine ID	Mine Type	Depth (in.)	Contractor/Run Number										Totals
			CDC-1	CDC-2	CRC-1	CRC-2	EGG-1	EGG-2	GDE-1	GDE-2	GEO-1	GEO-2	
4001	EM12	2	✓	✓	✓	✓	✓	✓	✓	✓	✓	✓	10/10
4002	TM46	2	✓	✓	✓	✓	✓	✓	✓	✓	✓	✓	10/10
4003	M19I	1.5	✓		✓	✓	✓	✓	✓	✓	✓	✓	9/10
4006	TMA4	2		✓	✓	✓	✓		✓	✓	✓	✓	8/10
4007	TM62M	Surface	✓	✓	✓	✓	✓	✓	✓	✓	✓	✓	10/10
4008	TM62M	4	✓	✓	✓	✓	✓	✓	✓	✓	✓	✓	10/10
4009	TM62P	Surface	✓	✓	✓	✓	✓	✓	✓	✓	✓	✓	10/10
4010	TM62M	Surface	✓	✓	✓	✓	✓	✓	✓	✓	✓	✓	10/10
4011	M15	1.5	✓	✓	✓	✓	✓	✓	✓	✓	✓	✓	10/10
4012	TMA4	Surface	✓	✓	✓	✓	✓	✓	✓	✓	✓	✓	10/10
4013	TM62P	3	✓		✓	✓	✓	✓	✓	✓	✓	✓	9/10
4014	M19	Surface	✓	✓	✓	✓	✓	✓	✓	✓	✓	✓	10/10
4017	TM62MI	2	✓	✓	✓	✓	✓	✓	✓	✓	✓	✓	10/10
4018	TM62MI	Surface	✓	✓	✓	✓	✓	✓	✓	✓	✓	✓	10/10
4019	M15	Surface	✓	✓	✓	✓	✓	✓	✓	✓	✓	✓	10/10
4020	M19	1.5	✓	✓	✓	✓	✓	✓	✓	✓	✓	✓	10/10
4023	M19	Surface	✓	✓	✓	✓	✓	✓	✓	✓	✓	✓	10/10
		Totals	16/17	15/17	17/17	17/17	17/17	16/17	17/17	17/17	17/17	17/17	
		Alarms	26	28	95	92	46	67	23	22	51	45	
		Detections	16	15	17	17	17	16	17	17	17	17	
		False Alarms	7	12	19	16	14	34	1	1	17	11	
		Multiple Hits	3	1	59	59	15	17	5	4	17	17	
		P_d	0.941	0.882	1.0	1.0	1.0	0.941	1.0	1.0	1.0	1.0	
		FAR (m^{-2})	0.014	0.024	0.037	0.031	0.027	0.067	0.002	0.002	0.033	0.022	

Table B-11. Lane 6 Results at Socorro

Mine ID	Mine Type	Depth (in.)	Contractor/Run Number										Totals
			CDC-1	CDC-2	CRC-1	CRC-2	EGG-1	EGG-2	GDE-1	GDE-2	GEO-1	GEO-2	
6001	TMA4	Surface	✓	✓	✓	✓	✓	✓	✓	✓	✓	✓	10/10
6002	M19I	1.5	✓	✓	✓	✓	✓	✓	✓	✓	✓	✓	10/10
6005	TM46	2	✓	✓	✓	✓	✓	✓	✓	✓	✓	✓	10/10
6006	M15I	1.5	✓	✓	✓	✓	✓	✓	✓	✓	✓	✓	10/10
6007	M19I	Surface	✓	✓	✓	✓	✓	✓	✓	✓	✓	✓	10/10
6010	TM62M	Surface	✓	✓	✓	✓	✓	✓	✓	✓	✓	✓	10/10
6011	TM62P	3	✓	✓	✓	✓	✓	✓	✓	✓	✓	✓	10/10
6012	TM62M	4	✓	✓	✓	✓	✓	✓	✓	✓	✓	✓	10/10
6013	M19	1.5	✓	✓	✓	✓	✓	✓	✓	✓	✓	✓	10/10
6016	TM62M	Surface	✓	✓	✓	✓	✓	✓	✓	✓	✓	✓	10/10
6017	TMA4	2	✓	✓	✓	✓	✓	✓	✓	✓	✓	✓	10/10
6018	TM62P	Surface	✓	✓	✓	✓	✓	✓	✓	✓	✓	✓	10/10
6019	M15	1.5	✓	✓	✓	✓	✓	✓	✓	✓	✓	✓	10/10
6020	EM12	2		✓	✓	✓	✓	✓	✓	✓			7/10
6021	TM62M	Surface	✓	✓	✓	✓	✓	✓	✓	✓	✓	✓	10/10
		Totals	14/15	15/15	15/15	15/15	15/15	15/15	15/15	15/15	14/15	14/15	
		Alarms	33	32	70	66	36	33	24	27	55	44	
		Detections	14	15	15	15	15	15	15	15	14	14	
		False Alarms	16	16	40	41	7	9	7	8	22	19	
		Multiple Hits	3	1	15	10	14	9	2	4	19	11	
		P_d	0.933	1.0	1.0	1.0	1.0	1.0	1.0	1.0	0.933	0.933	
		FAR (m^{-2})	0.033	0.033	0.031	0.021	0.029	0.019	0.015	0.017	0.046	0.040	

B-15

Table B-12. Lane 8 Results at Socorro

Mine ID	Mine Type	Depth (in.)	CDC-1	CDC-2	CRC-1	CRC-2	EGG-1	EGG-2	GDE-1	GDE-2	GEO-1	GEO-2	Totals
8001	TM62M	Surface	✓	✓	✓	✓	✓	✓	✓	✓	✓	✓	10/10
8002	TM62M	4	✓	✓	✓	✓	✓	✓	✓	✓	✓	✓	10/10
8003	TMA4	2				✓		✓	✓	✓	✓	✓	6/10
8004	M19I	2	✓	✓	✓	✓	✓	✓	✓	✓	✓	✓	10/10
8007	EM12	2	✓			✓		✓	✓	✓	✓	✓	7/10
8008	TM62P	Surface	✓	✓	✓	✓	✓	✓	✓	✓	✓	✓	10/10
8009	M15	1.5	✓	✓	✓	✓	✓	✓	✓	✓	✓	✓	10/10
8010	TM62P	3	✓	✓	✓	✓		✓		✓	✓	✓	8/10
8011	TMA4	Surface	✓	✓	✓	✓	✓	✓	✓	✓	✓	✓	10/10
8012	M19	1.5	✓	✓	✓	✓	✓	✓		✓	✓	✓	9/10
8015	TM62M	Surface	✓	✓	✓	✓	✓	✓	✓	✓	✓	✓	10/10
8016	M15	1.5	✓	✓	✓	✓	✓	✓	✓	✓	✓	✓	10/10
8017	TM62M	Surface	✓	✓	✓	✓	✓	✓	✓	✓	✓	✓	10/10
8018	TMA4	2		✓		✓	✓	✓			✓	✓	6/10
8019	TMA4	Surface	✓	✓	✓	✓	✓	✓	✓	✓	✓	✓	10/10
8020	M19I	1.5	✓	✓	✓	✓	✓	✓	✓	✓	✓	✓	10/10
8023	TM62M	4	✓	✓	✓	✓	✓	✓	✓	✓	✓	✓	10/10
8024	TM62P	3		✓	✓	✓	✓	✓				✓	6/10
8025	M15I	1.5	✓	✓	✓	✓	✓	✓	✓	✓	✓	✓	10/10
8026	M19I	Surface	✓	✓	✓	✓	✓	✓	✓	✓	✓	✓	10/10
8029	TM62MI	2	✓	✓	✓	✓	✓	✓	✓	✓	✓	✓	10/10
8030	TM46	2	✓	✓	✓	✓	✓	✓	✓	✓	✓	✓	10/10
8031	M19	1.5	✓	✓	✓			✓	✓		✓	✓	7/10
8034	M15	Surface	✓	✓	✓	✓	✓	✓	✓	✓	✓	✓	10/10
		Totals	21/24	22/24	21/24	23/24	20/24	24/24	20/24	21/24	23/24	24/24	
		Alarms	30	41	85	94	50	56	36	71	73	68	
		Detections	21	22	21	23	20	24	20	21	23	24	
		False Alarms	9	16	11	17	16	16	13	42	13	12	
		Multiple Hits	0	3	53	54	14	16	3	8	37	32	
		P_d	0.875	0.917	0.875	0.958	0.833	1.0	0.833	0.875	0.958	1.0	
		FAR (m^{-2})	0.016	0.028	0.019	0.030	0.028	0.028	0.023	0.074	0.023	0.021	

Contractor/Run Number

Table B-13. Lane 11 Results at Socorro

Mine ID	Mine Type	Depth (in.)	Contractor/Run Number CDC-1	CDC-2	CRC-1	CRC-2	EGG-1	EGG-2	GDE-1	GDE-2	GEO-1	GEO-2	Totals
11001	TM46	2	✓	✓	✓	✓	✓	✓	✓	✓	✓	✓	10/10
11002	M15I	1.5	✓	✓	✓	✓	✓	✓	✓	✓	✓	✓	10/10
11003	TM62P	Surface	✓	✓	✓	✓	✓	✓	✓	✓	✓	✓	10/10
11004	TM62P	3	✓		✓	✓	✓	✓	✓	✓		✓	8/10
11005	EM12	2	✓	✓	✓	✓	✓	✓	✓	✓	✓	✓	10/10
11006	M19	Surface	✓	✓	✓	✓	✓	✓	✓	✓	✓	✓	10/10
11009	M19	1.5	✓	✓	✓	✓	✓	✓	✓	✓	✓	✓	10/10
11012	TM62MI	2	✓	✓	✓	✓	✓	✓	✓	✓	✓	✓	10/10
11013	TM62MI	Surface	✓	✓	✓	✓	✓	✓	✓	✓	✓	✓	10/10
11014	TMA4	Surface	✓	✓	✓	✓	✓	✓	✓	✓	✓	✓	10/10
11015	TM62MI	4	✓	✓	✓	✓	✓	✓	✓	✓	✓	✓	10/10
11016	M15	Surface	✓	✓	✓	✓	✓	✓	✓	✓	✓	✓	10/10
11017	M15	1.5	✓	✓	✓	✓	✓	✓	✓	✓	✓	✓	10/10
11018	TM62MI	Surface	✓	✓	✓	✓	✓	✓	✓	✓	✓	✓	10/10
11019	TMA4	2	✓	✓	✓	✓	✓		✓		✓	✓	8/10
11020	M19I	1.5	✓	✓	✓	✓	✓	✓	✓		✓	✓	9/10
11023	M15I	1.5	✓	✓	✓	✓	✓	✓	✓	✓	✓	✓	10/10
11024	M19I	Surface	✓	✓	✓	✓	✓	✓	✓	✓	✓	✓	10/10
11027	TM62MI	Surface	✓	✓	✓	✓	✓	✓	✓	✓	✓	✓	10/10
Totals			19/19	18/19	19/19	19/19	19/19	18/19	19/19	17/19	18/19	19/19	
Alarms			34	33	96	112	59	71	66	37	48	58	
Detections			19	18	19	19	19	18	19	17	18	19	
False Alarms			14	14	16	26	20	28	41	10	13	18	
Multiple Hits			1	1	61	67	20	25	6	10	17	21	
P_d			1.0	0.947	1.0	1.0	1.0	0.947	1.0	0.895	0.947	1.0	
FAR (m^{-2})			0.029	0.029	0.033	0.054	0.042	0.058	0.085	0.021	0.027	0.037	

Table B-14. Lane 12 Results at Socorro

Mine ID	Mine Type	Depth (in.)	Contractor/Run Number										Totals
			CDC-1	CDC-2	CRC-1	CRC-2	EGG-1	EGG-2	GDE-1	GDE-2	GEO-1	GEO-2	
12001	TM62M	Surface	✓	✓	✓	✓	✓	✓	✓	✓	✓	✓	10/10
12002	M15I	1.5	✓	✓	✓	✓	✓	✓	✓	✓	✓	✓	10/10
12003	TM62M	4	✓	✓	✓	✓	✓	✓	✓	✓	✓	✓	10/10
12004	TM46	2	✓	✓	✓	✓	✓	✓	✓	✓	✓	✓	10/10
12005	TM62M	Surface	✓	✓	✓	✓	✓	✓	✓	✓	✓	✓	10/10
12006	TM62MI	2	✓	✓	✓	✓	✓	✓	✓	✓	✓	✓	10/10
12007	M15	1.5	✓	✓	✓	✓	✓	✓	✓	✓	✓	✓	10/10
12008	EM12	2	✓	✓	✓	✓		✓	✓	✓	✓	✓	9/10
12009	TM62P	Surface	✓	✓	✓	✓	✓	✓	✓	✓	✓	✓	10/10
12010	TM62P	3		✓	✓		✓	✓					4/10
12011	TMA4	2		✓	✓		✓	✓			✓	✓	6/10
12012	TMA4	Surface	✓	✓	✓	✓	✓	✓	✓	✓	✓	✓	10/10
12013	M19	1.5	✓	✓	✓	✓	✓	✓	✓	✓	✓	✓	10/10
12016	M19I	1.5	✓	✓	✓	✓	✓	✓	✓	✓		✓	9/10
12019	M19I	Surface	✓	✓	✓	✓	✓	✓	✓	✓	✓	✓	10/10
Totals			13/15	15/15	15/15	13/15	14/15	15/15	13/15	13/15	13/15	14/15	
Alarms			42	39	51	53	41	47	45	43	39	45	
Detections			13	15	15	13	14	15	13	13	13	14	
False Alarms			27	22	27	31	19	21	23	19	10	13	
Multiple Hits			2	2	2	9	8	11	9	11	16	18	
P_d			0.867	1.0	1.0	0.867	0.933	1.0	0.867	0.867	0.867	0.933	
FAR (m^{-2})			0.082	0.067	0.027	0.027	0.058	0.064	0.070	0.058	0.030	0.039	

Table B-15. Lane 13 Results at Socorro

Mine ID	Mine Type	Depth (in.)	Contractor/Run Number										Totals
			CDC-1	CDC-2	CRC-1	CRC-2	EGG-1	EGG-2	GDE-1	GDE-2	GEO-1	GEO-2	
13001	M15	1.5	✓	✓	✓	✓	✓	✓	✓	✓	✓	✓	10/10
13002	TM62MI	2	✓	✓	✓	✓	✓	✓	✓	✓	✓	✓	10/10
13003	TM62MI	Surface	✓	✓	✓	✓	✓		✓	✓	✓	✓	9/10
13004	TMA4	Surface	✓	✓	✓	✓	✓		✓	✓	✓	✓	9/10
13005	M15	Surface	✓	✓	✓	✓	✓		✓	✓	✓	✓	9/10
13006	TMA4	2	✓	✓	✓	✓			✓	✓	✓		7/10
13007	M15I	1.5	✓	✓	✓	✓	✓	✓	✓	✓	✓	✓	10/10
13008	TM46	2	✓	✓	✓	✓	✓	✓	✓	✓	✓	✓	10/10
13009	EM12	2	✓	✓	✓	✓	✓	✓	✓	✓	✓	✓	10/10
13010	M19	Surface	✓	✓	✓	✓	✓	✓	✓	✓	✓	✓	10/10
13013	M19I	1.5	✓	✓	✓	✓	✓	✓	✓	✓	✓	✓	10/10
13016	M19I	Surface	✓	✓	✓	✓	✓	✓	✓	✓	✓	✓	10/10
13019	M19I	1.5	✓	✓	✓		✓		✓	✓	✓	✓	8/10
13022	TM62MI	Surface	✓	✓	✓	✓	✓	✓	✓	✓	✓	✓	10/10
13023	TM62P	Surface	✓	✓	✓	✓	✓	✓	✓	✓	✓	✓	10/10
13024	TM62M	4	✓	✓	✓	✓	✓	✓	✓	✓	✓	✓	10/10
13025	TM62P	3	✓	✓			✓	✓		✓	✓	✓	7/10
13026	TM62M	Surface	✓	✓	✓	✓	✓	✓	✓	✓	✓	✓	10/10
		Totals	18/18	18/18	17/18	16/18	17/18	13/18	17/18	18/18	18/18	17/18	
		Alarms	44	29	82	88	65	55	31	58	51	58	
		Detections	18	18	17	16	17	13	17	18	18	17	
		False Alarms	21	8	34	22	29	28	10	32	18	19	
		Multiple Hits	5	3	31	50	19	14	4	8	15	22	
		P_d	1.0	1.0	0.944	0.889	0.944	0.722	0.944	1.0	1.0	0.944	
		FAR (m^{-2})	0.044	0.017	0.071	0.046	0.060	0.058	0.021	0.067	0.038	0.040	

Table B-16. Lane 16 Results at Socorro

Mine ID	Mine Type	Depth (in.)	Contractor/Run Number										Totals
			CDC-1	CDC-2	CRC-1	CRC-2	EGG-1	EGG-2	GDE-1	GDE-2	GEO-1	GEO-2	
16001	TMA4	Surface	✓	✓	✓	✓	✓	✓	✓	✓	✓	✓	10/10
16002	TMA4	2							✓				1/10
16003	M15	1.5	✓	✓	✓	✓	✓	✓	✓	✓	✓	✓	10/10
16004	TM62M	Surface	✓	✓	✓	✓	✓	✓	✓	✓	✓	✓	10/10
16005	TM62M	4	✓	✓	✓	✓	✓	✓	✓	✓	✓	✓	10/10
16006	M19	Surface	✓	✓	✓	✓	✓	✓	✓	✓	✓	✓	10/10
16009	M15	1.5	✓	✓	✓	✓	✓	✓	✓	✓	✓	✓	10/10
16010	TM62M	Surface	✓	✓	✓	✓	✓	✓	✓	✓	✓	✓	10/10
16011	TMA4	2				✓			✓	✓			3/10
16012	TM62M	Surface	✓	✓	✓	✓	✓	✓	✓	✓	✓	✓	10/10
16013	M15	Surface	✓	✓	✓	✓	✓	✓	✓	✓	✓	✓	10/10
16014	TM62M	4	✓	✓	✓	✓	✓	✓	✓	✓	✓	✓	10/10
16015	TM62P	3				✓			✓				2/10
16016	TM62M	4	✓	✓	✓	✓	✓	✓	✓	✓	✓	✓	10/10
16017	M19	1.5		✓		✓	✓		✓		✓		4/10
16020	TM46	2	✓	✓	✓	✓	✓	✓	✓	✓	✓	✓	10/10
16021	TM62P	3		✓			✓					✓	3/10
16022	M19	1.5		✓		✓		✓		✓		✓	5/10
16025	M15	1.5	✓	✓	✓	✓	✓	✓	✓	✓	✓	✓	10/10
16026	TM62M	Surface	✓	✓	✓	✓	✓	✓	✓	✓	✓	✓	10/10
16027	TM62M	4	✓	✓	✓	✓	✓	✓	✓	✓	✓	✓	10/10
16028	TM62M	Surface	✓	✓	✓	✓	✓	✓	✓	✓	✓	✓	10/10
16029	TM62P	Surface	✓	✓	✓	✓	✓	✓	✓	✓	✓	✓	10/10
16030	M19	1.5		✓	✓	✓	✓	✓	✓	✓	✓	✓	9/10
Totals			17/24	20/24	18/24	22/24	20/24	19/24	22/24	20/24	19/24	20/24	
Alarms			30	42	81	93	44	60	70	53	51	52	
Detections			17	20	18	22	20	19	22	20	19	20	
False Alarms			8	18	6	16	11	20	21	14	6	13	
Multiple Hits			5	4	57	55	13	21	27	19	26	19	
P_d			0.708	0.833	0.750	0.917	0.833	0.792	0.917	0.833	0.792	0.833	
FAR (m^{-2})			0.030	0.067	0.022	0.060	0.041	0.074	0.078	0.052	0.022	0.048	

Table B-17. Lane 4 Physical-Marking Results at Socorro

Mine ID	Mine Type	Depth (in.)	Contractor/Run Number						Totals
			EGG-EM1	EGG-PM1	EGG-EM2	EGG-PM2	EGG-EM3	EGG-PM3	
4001	EM12	2	✓	✓	✓	✓	✓	✓	6/6
4002	TM46	2	✓	✓	✓	✓	✓	✓	6/6
4003	M19I	1.5	✓	✓	✓	✓	✓	✓	6/6
4006	TMA4	2	✓	✓	✓	✓	✓	✓	6/6
4007	TM62M	Surface	✓	✓	✓	✓	✓	✓	6/6
4008	TM62M	4	✓	✓	✓	✓	✓	✓	6/6
4009	TM62P	Surface	✓	✓	✓	✓	✓	✓	6/6
4010	TM62M	Surface	✓	✓	✓	✓	✓	✓	6/6
4011	M15	1.5	✓	✓	✓	✓	✓	✓	6/6
4012	TMA4	Surface	✓	✓	✓	✓	✓	✓	6/6
4013	TM62P	3	✓	✓	✓	✓	✓	✓	6/6
4014	M19	Surface	✓	✓	✓	✓	✓	✓	6/6
4017	TM62MI	2	✓	✓	✓	✓	✓	✓	6/6
4018	TM62MI	Surface	✓	✓	✓	✓	✓	✓	6/6
4019	M15	Surface	✓	✓	✓	✓	✓	✓	6/6
4020	M19	1.5	✓	✓	✓	✓	✓	✓	6/6
4023	M19	Surface	✓	✓	✓	✓	✓	✓	6/6
		Totals	17/17	17/17	17/17	17/17	17/17	17/17	
		Alarms	85	79	91	80	131	131	
		Detections	17	17	17	17	17	17	
		False Alarms	47	43	54	48	95	95	
		Multiple Hits	21	19	20	15	19	19	
		P_d	1.0	1.0	1.0	1.0	1.0	1.0	
		FAR (m^{-2})	0.092	0.084	0.106	0.094	0.186	0.186	

Table B-18. Lane 4 Night and Morning Results at Socorro

Mine ID	Mine Type	Depth (in.)	Contractor/Run Number								Totals
			EGG-N2	EGG-N3	CRC-N1	CRC-N2	CRC-M1	CRC-M2	GDE-M1	GDE-M2	
4001	EM12	2	✓	✓	✓	✓	✓	✓	✓	✓	8/8
4002	TM46	2	✓	✓	✓	✓	✓	✓	✓	✓	8/8
4003	M19I	1.5	✓	✓	✓	✓	✓	✓	✓	✓	8/8
4006	TMA4	2		✓	✓	✓	✓	✓	✓	✓	7/8
4007	TM62M	Surface	✓	✓	✓	✓	✓	✓	✓	✓	8/8
4008	TM62M	4	✓	✓	✓	✓	✓	✓	✓	✓	8/8
4009	TM62P	Surface	✓	✓	✓	✓	✓	✓	✓	✓	8/8
4010	TM62M	Surface	✓	✓	✓	✓	✓	✓	✓	✓	8/8
4011	M15	1.5	✓	✓	✓	✓	✓	✓	✓	✓	8/8
4012	TMA4	Surface	✓	✓	✓	✓	✓	✓	✓	✓	8/8
4013	TM62P	3	✓	✓	✓	✓	✓	✓	✓	✓	8/8
4014	M19	Surface	✓	✓	✓	✓	✓	✓	✓	✓	8/8
4017	TM62MI	2	✓	✓	✓	✓	✓	✓	✓	✓	8/8
4018	TM62MI	Surface	✓	✓	✓	✓	✓	✓	✓	✓	8/8
4019	M15	Surface	✓	✓	✓	✓	✓	✓	✓	✓	8/8
4020	M19	1.5	✓	✓	✓	✓	✓		✓	✓	7/8
4023	M19	Surface	✓	✓	✓	✓	✓	✓	✓	✓	8/8
		Totals	16/17	17/17	17/17	17/17	17/17	16/17	17/17	17/17	
		Alarms	50	40	70	90	51	56	27	32	
		Detections	16	17	17	17	17	16	17	17	
		False Alarms	23	9	10	16	16	21	3	5	
		Multiple Hits	11	14	43	57	18	19	7	10	
		P_d	0.941	1.0	1.0	1.0	1.0	0.941	1.0	1.0	
		FAR (m^{-2})	0.045	0.018	0.020	0.031	0.031	0.041	0.006	0.010	

Table B-19. Lane 6 Night, Morning and Tele-operated Results at Socorro

Mine ID	Mine Type	Depth (in.)	Contractor/Run Number						Totals
			EGG-N1	CRC-N3	CRC-M3	EGG-T1	EGG-T2	EGG-T3	
6001	TMA4	Surface	✓	✓	✓	✓	✓	✓	6/6
6002	M19I	1.5	✓	✓	✓	✓	✓		5/6
6005	TM46	2	✓	✓	✓	✓	✓	✓	6/6
6006	M15I	1.5	✓	✓	✓	✓	✓	✓	6/6
6007	M19I	Surface	✓	✓	✓	✓	✓	✓	6/6
6010	TM62M	Surface	✓	✓	✓	✓	✓	✓	6/6
6011	TM62P	3		✓	✓	✓	✓	✓	5/6
6012	TM62M	4	✓	✓	✓	✓	✓	✓	6/6
6013	M19	1.5	✓	✓	✓	✓	✓	✓	6/6
6016	TM62M	Surface	✓	✓	✓	✓	✓	✓	6/6
6017	TMA4	2	✓	✓	✓	✓	✓	✓	6/6
6018	TM62P	Surface	✓	✓	✓	✓	✓	✓	6/6
6019	M15	1.5	✓	✓	✓	✓	✓	✓	6/6
6020	EM12	2			✓	✓	✓	✓	4/6
6021	TM62M	Surface	✓	✓	✓	✓	✓	✓	6/6
Totals			13/15	14/15	15/15	15/15	15/15	14/15	
Alarms			30	67	50	61	57	58	
Detections			13	14	15	15	15	14	
False Alarms			10	12	15	32	25	33	
Multiple Hits			7	41	20	14	17	11	
P_d			0.867	0.933	1.0	1.0	1.0	0.933	
FAR (m^{-2})			0.021	0.025	0.031	0.067	0.052	0.069	

Table B-20. Lane 8 Physical-Marking Results at Socorro

Contractor/Run Number

Mine ID	Mine Type	Depth (in.)	GEO-EM1	GEO-PM1	GEO-EM2	GEO-PM2	CRC-EM1	CRC-PM1	CRC-EM2	CRC-PM2	GDE-EM1	GDE-PM1	GDE-EM2	GDE-PM2	Totals
8001	TM62M	Surface	✓	✓	✓	✓	✓	✓	✓	✓	✓	✓	✓	✓	12/12
8002	TM62M	4	✓	✓	✓	✓	✓	✓	✓	✓	✓	✓	✓	✓	12/12
8003	TMA4	2			✓		✓	✓	✓	✓	✓	✓	✓	✓	9/12
8004	M19I	2	✓	✓	✓	✓	✓	✓	✓	✓	✓	✓	✓	✓	12/12
8007	EM12	2			✓	✓	✓	✓	✓	✓	✓	✓	✓	✓	10/12
8008	TM62P	Surface	✓	✓	✓	✓	✓	✓	✓	✓	✓	✓	✓	✓	12/12
8009	M15	1.5	✓	✓	✓	✓	✓	✓	✓	✓	✓	✓	✓	✓	12/12
8010	TM62P	3			✓	✓	✓	✓	✓	✓	✓	✓	✓	✓	10/12
8011	TMA4	Surface	✓	✓	✓	✓	✓	✓	✓	✓	✓	✓	✓	✓	12/12
8012	M19	1.5	✓	✓	✓	✓	✓	✓	✓	✓	✓	✓	✓	✓	12/12
8015	TM62M	Surface	✓	✓	✓	✓	✓	✓	✓	✓	✓	✓	✓	✓	12/12
8016	M15	1.5	✓	✓	✓	✓	✓	✓	✓	✓	✓	✓	✓	✓	12/12
8017	TM62M	Surface	✓	✓	✓	✓	✓	✓	✓	✓	✓	✓	✓	✓	12/12
8018	TMA4	2	✓		✓	✓	✓	✓	✓	✓	✓	✓	✓	✓	11/12
8019	TMA4	Surface	✓	✓	✓	✓	✓	✓	✓	✓	✓	✓	✓	✓	12/12
8020	M19I	1.5	✓	✓	✓	✓	✓	✓	✓	✓	✓	✓	✓	✓	12/12
8023	TM62M	4	✓	✓	✓	✓	✓	✓	✓	✓	✓	✓	✓	✓	12/12
8024	TM62P	3	✓	✓	✓	✓	✓	✓	✓	✓					8/12
8025	M15I	1.5	✓	✓	✓	✓	✓	✓	✓	✓	✓	✓	✓	✓	12/12
8026	M19I	Surface	✓	✓	✓	✓	✓	✓	✓	✓	✓	✓	✓	✓	12/12
8029	TM62MI	2	✓	✓	✓	✓	✓	✓	✓	✓	✓	✓	✓	✓	12/12
8030	TM46	2	✓	✓	✓	✓	✓	✓	✓	✓	✓	✓	✓	✓	12/12
8031	M19	1.5	✓	✓	✓	✓	✓	✓	✓	✓	✓	✓	✓	✓	12/12
8034	M15	Surface	✓	✓	✓	✓	✓	✓	✓	✓	✓	✓	✓	✓	12/12
		Totals	21/24	20/24	24/24	23/24	24/24	24/24	24/24	24/24	23/24	23/24	23/24	23/24	
		Alarms	64	50	79	68	85	77	176	79	50	51	70	69	
		Detections	21	20	24	23	24	24	24	24	23	23	23	23	
		False Alarms	12	9	19	16	10	10	32	16	9	10	22	22	
		Multiple Hits	31	21	36	29	51	43	120	39	18	18	25	24	
		P_d	0.875	0.833	1.0	0.958	1.0	1.0	1.0	1.0	0.958	0.958	0.958	0.958	
		FAR (m^{-2})	0.021	0.016	0.033	0.028	0.018	0.018	0.056	0.028	0.016	0.018	0.039	0.039	

Table B-21. Lane 8 Night and Tele-operated Results at Socorro

Mine ID	Mine Type	Depth (in.)	Contractor/Run Number					Totals
			GDE-N1	GDE-N2	GEO-T1	GEO-T2		
8001	TM62M	Surface	✓	✓	✓	✓		4/4
8002	TM62M	4	✓	✓	✓	✓		4/4
8003	TMA4	2	✓		✓	✓		3/4
8004	M19I	2	✓	✓	✓	✓		4/4
8007	EM12	2		✓	✓	✓		3/4
8008	TM62P	Surface	✓	✓	✓	✓		4/4
8009	M15	1.5	✓	✓	✓	✓		4/4
8010	TM62P	3		✓	✓	✓		3/4
8011	TMA4	Surface	✓	✓	✓	✓		4/4
8012	M19	1.5	✓	✓	✓	✓		4/4
8015	TM62M	Surface	✓	✓	✓	✓		4/4
8016	M15	1.5	✓	✓	✓	✓		4/4
8017	TM62M	Surface	✓	✓	✓	✓		4/4
8018	TMA4	2	✓	✓				2/4
8019	TMA4	Surface	✓	✓	✓	✓		4/4
8020	M19I	1.5	✓	✓	✓	✓		4/4
8023	TM62M	4	✓	✓	✓	✓		4/4
8024	TM62P	3	✓	✓	✓			3/4
8025	M15I	1.5	✓	✓	✓	✓		4/4
8026	M19I	Surface	✓	✓	✓	✓		4/4
8029	TM62MI	2	✓	✓	✓	✓		4/4
8030	TM46	2	✓	✓	✓	✓		4/4
8031	M19	1.5	✓	✓	✓	✓		4/4
8034	M15	Surface	✓	✓	✓	✓		4/4
		Totals	22/24	23/24	23/24	22/24		
		Alarms	39	47	56	53		
		Detections	22	23	23	22		
		False Alarms	8	10	10	12		
		Multiple Hits	9	14	23	19		
		P_d	0.917	0.958	0.958	0.917		
		FAR (m^{-2})	0.014	0.018	0.018	0.021		

Table B-22. Lane 11 Night Results at Socorro

Mine ID	Mine Type	Depth (in.)	Contractor/Run Number		Totals
			GEO-N1	CDC-N1	
11001	TM46	2	✓	✓	2/2
11002	M15I	1.5	✓	✓	2/2
11003	TM62P	Surface	✓	✓	2/2
11004	TM62P	3			0/2
11005	EM12	2	✓	✓	2/2
11006	M19	Surface	✓	✓	2/2
11009	M19	1.5	✓	✓	2/2
11012	TM62MI	2	✓	✓	2/2
11013	TM62MI	Surface	✓	✓	2/2
11014	TMA4	Surface	✓	✓	2/2
11015	TM62MI	4	✓	✓	2/2
11016	M15	Surface	✓	✓	2/2
11017	M15	1.5	✓	✓	2/2
11018	TM62MI	Surface	✓	✓	2/2
11019	TMA4	2			0/2
11020	M19I	1.5	✓	✓	2/2
11023	M15I	1.5	✓	✓	2/2
11024	M19I	Surface	✓	✓	2/2
11027	TM62MI	Surface	✓	✓	2/2

	GEO-N1	CDC-N1
Totals	17/19	17/19
Alarms	59	45
Detections	17	17
False Alarms	19	27
Multiple Hits	23	1
P_d	0.895	0.895
FAR (m^{-2})	0.040	0.056

Table B-23. Lane 12 Night Results at Socorro

Mine ID	Mine Type	Depth (in.)	Contractor/Run Number GEO-N2	Totals
12001	TM62M	Surface	✓	1/1
12002	M15I	1.5	✓	1/1
12003	TM62M	4	✓	1/1
12004	TM46	2	✓	1/1
12005	TM62M	Surface	✓	1/1
12006	TM62MI	2	✓	1/1
12007	M15	1.5	✓	1/1
12008	EM12	2		0/1
12009	TM62P	Surface	✓	1/1
12010	TM62P	3		0/1
12011	TMA4	2	✓	1/1
12012	TMA4	Surface	✓	1/1
12013	M19	1.5	✓	1/1
12016	M19I	1.5	✓	1/1
12019	M19I	Surface	✓	1/1
		Totals	13/15	
		Alarms	37	
		Detections	13	
		False Alarms	5	
		Multiple Hits	19	
		P_d	0.867	
		FAR (m^{-2})	0.015	

B-27

Table B-24. Lane 13 Night Results at Socorro

Mine ID	Mine Type	Depth (in.)	CDC-N1	CDC-N2	GEO-N3	Totals
13001	M15	1.5	✓	✓	✓	3/3
13002	TM62MI	2	✓	✓	✓	3/3
13003	TM62MI	Surface	✓	✓	✓	3/3
13004	TMA4	Surface	✓	✓	✓	3/3
13005	M15	Surface	✓	✓	✓	3/3
13006	TMA4	2	✓	✓		2/3
13007	M15I	1.5	✓	✓	✓	3/3
13008	TM46	2	✓	✓	✓	3/3
13009	EM12	2	✓	✓	✓	3/3
13010	M19	Surface	✓	✓	✓	3/3
13013	M19I	1.5	✓	✓	✓	3/3
13016	M19I	Surface	✓	✓	✓	3/3
13019	M19I	1.5	✓	✓	✓	3/3
13022	TM62MI	Surface	✓	✓	✓	3/3
13023	TM62P	Surface	✓	✓	✓	3/3
13024	TM62M	4	✓	✓	✓	3/3
13025	TM62P	3	✓		✓	2/3
13026	TM62M	Surface	✓	✓	✓	3/3
		Totals	18/18	17/18	17/18	

	CDC-N1	CDC-N2	GEO-N3
Alarms	42	50	56
Detections	18	17	17
False Alarms	23	33	13
Multiple Hits	1	0	26
P_d	1.0	0.944	0.944
FAR (m^{-2})	0.048	0.069	0.027

B-28

APPENDIX C

TABLES OF PROBABILITIES OF DETECTION AND FALSE-ALARM RATES CATEGORIZED BY SENSOR TYPE AND METAL CONTENT OF MINES

APPENDIX C
TABLES OF PROBABILITIES OF DETECTION AND FALSE-ALARM RATES CATEGORIZED BY SENSOR TYPE AND METAL CONTENT OF MINES

Tables C-1 through C-102 summarize the probabilities of detections (P_d) and false alarm rates (FAR) for subsurface and surface mines for a variety of conditions: on-road, off-road, night, physical-marking, teleoperated, and morning. The statistics are compiled for each sensor (GPR, EMI, and IR), sensor pairs (GPR-EMI, EMI-IR, GPR-IR), and all sensors. The sensor pairs are for either sensor alone or both sensors together. "All Sensors" refers to one or more sensors either individually or together. The P_ds are subcategorized according to metal content of the mines: Total (all mines), M (metal), LM (low metal), and NM (nonmetal).

The tables are organized by contractor (CDC, CRC, EG&G, GDE, and GeoCenters) and test location [Aberdeen, Socorro, and Combined (Aberdeen and Socorro]. For the "Combined" cases, only the statistics for the on-road and off-road tests were given. For each contractor, the tables are presented in the following order, as applicable:

- On-road, subsurface
- On-road, surface
- Off-road, subsurface
- Off-road, surface
- Night, subsurface
- Night, surface
- Physical-marking, EM, subsurface
- Physical-marking, EM, surface
- Morning, subsurface
- Morning, surface
- Tele-operated, subsurface
- Tele-operated, surface

For the physical-marking tests, only the EM statistics are given here, since no information was available on which sensor detected the mines for the PM cases. See Appendix B for a description of physical-marking (EM and PM) runs.

"N/A" (not applicable) means that particular type of mine was not used for the test under the conditions specified by the table header.

A. CDC

1. Aberdeen

Table C-1. CDC, Aberdeen On-Road, Subsurface, P_ds and FARs

	GPR	EMI	IR	GPR-EMI	EMI-IR	GPR-IR	All Sensors
P_d, Total	0.909	0.606	0.720	0.932	0.871	0.924	0.932
P_d, M	0.984	0.984	0.726	1.000	1.000	0.984	1.000
P_d, LM	0.828	0.281	0.688	0.859	0.734	0.859	0.859
P_d, NM	1.000	0.167	1.000	1.000	1.000	1.000	1.000
FAR	0.039	0.029	0.012	0.053	0.036	0.045	0.054

Table C-2. CDC, Aberdeen, On-Road, Surface, P_ds and FARs

	GPR	EMI	IR	GPR-EMI	EMI-IR	GPR-IR	All Sensors
P_d, Total	0.942	0.628	1.000	0.965	1.000	1.000	1.000
P_d, M	0.944	1.000	1.000	1.000	1.000	1.000	1.000
P_d, LM	0.932	0.386	1.000	0.932	1.000	1.000	1.000
P_d, NM	1.000	0.167	1.000	1.000	1.000	1.000	1.000
FAR	0.039	0.029	0.012	0.053	0.036	0.045	0.054

Table C-3. CDC, Aberdeen, Off-Road, Subsurface, P_ds and FARs

	GPR	EMI	IR	GPR-EMI	EMI-IR	GPR-IR	All Sensors
P_d, Total	0.927	0.647	0.838	0.941	0.882	0.985	0.985
P_d, M	0.974	1.000	0.947	1.000	1.000	1.000	1.000
P_d, LM	0.867	0.200	0.700	0.867	0.733	0.967	0.967
P_d, NM	N/A	N/A	N/A	N/A	N/A	N/A	N/A
FAR	0.040	0.021	0.008	0.049	0.027	0.041	0.050

Table C-4. CDC, Aberdeen, Off-Road, Surface, P_ds and *FAR*s

	GPR	EMI	IR	GPR-EMI	EMI-IR	GPR-IR	All Sensors
P_d, Total	1.000	0.604	1.000	1.000	1.000	1.000	1.000
P_d, M	1.000	1.000	1.000	1.000	1.000	1.000	1.000
P_d, LM	1.000	0.208	1.000	1.000	1.000	1.000	1.000
P_d, NM	N/A	N/A	N/A	N/A	N/A	N/A	N/A
FAR	0.040	0.021	0.008	0.049	0.027	0.041	0.050

Table C-5. CDC, Aberdeen, Night, Subsurface, P_ds and *FAR*s

	GPR	EMI	IR	GPR-EMI	EMI-IR	GPR-IR	All Sensors
P_d, Total	0.950	0.725	0.600	0.975	0.900	0.975	0.975
P_d, M	1.000	1.000	0.667	1.000	1.000	1.000	1.000
P_d, LM	0.900	0.550	0.550	0.950	0.850	0.950	0.950
P_d, NM	1.000	0.000	0.500	1.000	0.500	1.000	1.000
FAR	0.038	0.030	0.012	0.055	0.035	0.044	0.055

Table C-6. CDC, Aberdeen, Night, Surface, P_ds and *FAR*s

	GPR	EMI	IR	GPR-EMI	EMI-IR	GPR-IR	All Sensors
P_d, Total	1.000	0.400	1.000	1.000	1.000	1.000	1.000
P_d, M	1.000	1.000	1.000	1.000	1.000	1.000	1.000
P_d, LM	1.000	0.000	1.000	1.000	1.000	1.000	1.000
P_d, NM	1.000	0.000	1.000	1.000	1.000	1.000	1.000
FAR	0.038	0.030	0.012	0.055	0.035	0.044	0.055

2.   Socorro

Table C-7. CDC, Socorro, On-Road, Subsurface, P_ds and *FAR*s

	GPR	EMI	IR	GPR-EMI	EMI-IR	GPR-IR	All Sensors
P_d, Total	0.811	0.588	0.696	0.885	0.858	0.865	0.892
P_d, M	0.900	1.000	0.743	1.000	1.000	0.971	1.000
P_d, LM	0.719	0.219	0.625	0.781	0.703	0.750	0.781
P_d, NM	0.786	0.214	0.786	0.786	0.857	0.857	0.857
FAR	0.024	0.013	0.012	0.032	0.022	0.027	0.032

Table C-8. CDC, Socorro, On-Road, Surface, P_ds and FARs

	GPR	EMI	IR	GPR-EMI	EMI-IR	GPR-IR	All Sensors
P_d, Total	0.979	0.500	0.990	0.979	1.000	1.000	1.000
P_d, M	1.000	1.000	0.979	1.000	1.000	1.000	1.000
P_d, LM	0.958	0.000	1.000	0.958	1.000	1.000	1.000
P_d, NM	N/A	N/A	N/A	N/A	N/A	N/A	N/A
FAR	0.024	0.013	0.012	0.032	0.022	0.027	0.032

Table C-9. CDC, Socorro, Off-Road, Subsurface, P_ds and FARs

	GPR	EMI	IR	GPR-EMI	EMI-IR	GPR-IR	All Sensors
P_d, Total	0.467	0.567	0.267	0.633	0.567	0.500	0.633
P_d, M	0.688	1.000	0.438	1.000	1.000	0.750	1.000
P_d, LM	0.214	0.071	0.071	0.214	0.071	0.214	0.214
P_d, NM	N/A	N/A	N/A	N/A	N/A	N/A	N/A
FAR	0.022	0.007	0.035	0.028	0.037	0.048	0.048

Table C-10. CDC, Socorro, Off-Road, Surface, P_ds and FARs

	GPR	EMI	IR	GPR-EMI	EMI-IR	GPR-IR	All Sensors
P_d, Total	0.889	0.667	1.000	0.889	1.000	1.000	1.000
P_d, M	1.000	1.000	1.000	1.000	1.000	1.000	1.000
P_d, LM	0.667	0.000	1.000	0.667	1.000	1.000	1.000
P_d, NM	N/A	N/A	N/A	N/A	N/A	N/A	N/A
FAR	0.022	0.007	0.035	0.028	0.037	0.048	0.048

Table C-11. CDC, Socorro, Night, Subsurface, P_ds and FARs

	GPR	EMI	IR	GPR-EMI	EMI-IR	GPR-IR	All Sensors
P_d, Total	0.807	0.516	0.903	0.839	0.903	0.903	0.903
P_d, M	0.938	1.000	1.000	1.000	1.000	1.000	1.000
P_d, LM	0.583	0.000	0.750	0.583	0.750	0.750	0.750
P_d, NM	1.000	0.000	1.000	1.000	1.000	1.000	1.000
FAR	0.042	0.019	0.026	0.056	0.040	0.049	0.058

Table C-12. CDC, Socorro, Night, Surface, P_ds and FARs

	GPR	EMI	IR	GPR-EMI	EMI-IR	GPR-IR	All Sensors
P_d, Total	0.917	0.500	1.000	1.000	1.000	1.000	1.000
P_d, M	0.833	1.000	1.000	1.000	1.000	1.000	1.000
P_d, LM	1.000	0.000	1.000	1.000	1.000	1.000	1.000
P_d, NM	N/A	N/A	N/A	N/A	N/A	N/A	N/A
FAR	0.042	0.019	0.026	0.056	0.040	0.049	0.058

3. Combined (Aberdeen and Socorro)

Table C-13. CDC, Combined (Aberdeen and Socorro), On-Road, Subsurface, P_ds and FARs

	GPR	EMI	IR	GPR-EMI	EMI-IR	GPR-IR	All Sensors
P_d, Total	0.857	0.596	0.707	0.907	0.864	0.893	0.911
P_d, M	0.939	0.992	0.735	1.000	1.000	0.977	1.000
P_d, LM	0.773	0.250	0.656	0.820	0.719	0.805	0.820
P_d, NM	0.850	0.200	0.850	0.850	0.900	0.900	0.900
FAR	0.032	0.021	0.012	0.042	0.029	0.036	0.043

Table C-14. CDC, Combined (Aberdeen and Socorro), On-Road, Surface, P_ds and FARs

	GPR	EMI	IR	GPR-EMI	EMI-IR	GPR-IR	All Sensors
P_d, Total	0.962	0.560	0.995	0.973	1.000	1.000	1.000
P_d, M	0.976	1.000	0.988	1.000	1.000	1.000	1.000
P_d, LM	0.946	0.185	1.000	0.946	1.000	1.000	1.000
P_d, NM	1.000	0.167	1.000	1.000	1.000	1.000	1.000
FAR	0.032	0.021	0.012	0.042	0.029	0.036	0.043

Table C-15. CDC, Combined (Aberdeen and Socorro), Off-Road, Subsurface, P_ds and FARs

	GPR	EMI	IR	GPR-EMI	EMI-IR	GPR-IR	All Sensors
P_d, Total	0.786	0.622	0.663	0.847	0.786	0.837	0.878
P_d, M	0.889	1.000	0.796	1.000	1.000	0.926	1.000
P_d, LM	0.659	0.159	0.500	0.659	0.523	0.727	0.727
P_d, NM	N/A	N/A	N/A	N/A	N/A	N/A	N/A
FAR	0.037	0.019	0.014	0.045	0.029	0.043	0.049

Table C-16. CDC, Combined (Aberdeen and Socorro), Off-Road, Surface, P_ds and FARs

	GPR	EMI	IR	GPR-EMI	EMI-IR	GPR-IR	All Sensors
$P_{d'}$ Total	0.970	0.621	1.000	0.970	1.000	1.000	1.000
$P_{d'}$ M	1.000	1.000	1.000	1.000	1.000	1.000	1.000
$P_{d'}$ LM	0.933	0.167	1.000	0.933	1.000	1.000	1.000
$P_{d'}$ NM	N/A	N/A	N/A	N/A	N/A	N/A	N/A
FAR	0.037	0.019	0.014	0.045	0.029	0.043	0.049

B. CRC

1. Aberdeen

Table C-17. CRC, Aberdeen, On-Road, Subsurface, P_ds and FARs

	GPR	EMI	IR	GPR-EMI	EMI-IR	GPR-IR	All Sensors
$P_{d'}$ Total	0.553	0.477	0.000	0.773	0.477	0.553	0.773
$P_{d'}$ M	0.532	1.000	0.000	1.000	1.000	0.532	1.000
$P_{d'}$ LM	0.563	0.016	0.000	0.563	0.016	0.563	0.563
$P_{d'}$ NM	0.667	0.000	0.000	0.667	0.000	0.667	0.667
FAR	0.031	0.003	0.000	0.034	0.003	0.031	0.034

Table C-18. CRC, Aberdeen, On-Road, Surface, P_ds and FARs

	GPR	EMI	IR	GPR-EMI	EMI-IR	GPR-IR	All Sensors
$P_{d'}$ Total	0.907	0.407	0.000	0.919	0.407	0.907	0.919
$P_{d'}$ M	0.972	0.972	0.000	1.000	0.972	0.972	1.000
$P_{d'}$ LM	0.864	0.000	0.000	0.864	0.000	0.864	0.864
$P_{d'}$ NM	0.833	0.000	0.000	0.833	0.000	0.833	0.833
FAR	0.031	0.003	0.000	0.034	0.003	0.031	0.034

Table C-19. CRC, Aberdeen, Off-Road, Subsurface, P_ds and FARs

	GPR	EMI	IR	GPR-EMI	EMI-IR	GPR-IR	All Sensors
P_d, Total	0.779	0.588	0.000	0.912	0.588	0.779	0.912
P_d, M	0.790	1.000	0.000	1.000	1.000	0.790	1.000
P_d, LM	0.767	0.067	0.000	0.800	0.067	0.767	0.800
P_d, NM	N/A	N/A	N/A	N/A	N/A	N/A	N/A
FAR	0.183	0.018	0.000	0.201	0.018	0.183	0.201

Table C-20. CRC, Aberdeen, Off-Road, Surface, P_ds and FARs

	GPR	EMI	IR	GPR-EMI	EMI-IR	GPR-IR	All Sensors
P_d, Total	0.896	0.563	0.000	0.958	0.563	0.896	0.958
P_d, M	0.917	1.000	0.000	1.000	1.000	0.917	1.000
P_d, LM	0.875	0.125	0.000	0.917	0.125	0.875	0.917
P_d, NM	N/A	N/A	N/A	N/A	N/A	N/A	N/A
FAR	0.183	0.018	0.000	0.201	0.018	0.183	0.201

Table C-21. CRC, Aberdeen, Night, Subsurface, P_ds and FARs

	GPR	EMI	IR	GPR-EMI	EMI-IR	GPR-IR	All Sensors
P_d, Total	0.775	0.450	0.000	0.900	0.450	0.775	0.900
P_d, M	0.722	1.000	0.000	1.000	1.000	0.722	1.000
P_d, LM	0.800	0.000	0.000	0.800	0.000	0.800	0.800
P_d, NM	1.000	0.000	0.000	1.000	0.000	1.000	1.000
FAR	0.020	0.002	0.000	0.022	0.002	0.020	0.022

Table C-22. CRC, Aberdeen, Night, Surface, P_ds and FARs

	GPR	EMI	IR	GPR-EMI	EMI-IR	GPR-IR	All Sensors
P_d, Total	1.000	0.400	0.000	1.000	0.400	1.000	1.000
P_d, M	1.000	1.000	0.000	1.000	1.000	1.000	1.000
P_d, LM	1.000	0.000	0.000	1.000	0.000	1.000	1.000
P_d, NM	1.000	0.000	0.000	1.000	0.000	1.000	1.000
FAR	0.020	0.002	0.000	0.022	0.002	0.020	0.022

2. Socorro

Table C-23. CRC, Socorro, On-Road, Subsurface, P_ds and FARs

	GPR	EMI	IR	GPR-EMI	EMI-IR	GPR-IR	All Sensors
P_d, Total	0.818	0.473	0.000	0.905	0.473	0.818	0.905
P_d, M	0.814	1.000	0.000	1.000	1.000	0.814	1.000
P_d, LM	0.797	0.000	0.000	0.797	0.000	0.797	0.797
P_d, NM	0.929	0.000	0.000	0.929	0.000	0.929	0.929
FAR	0.037	0.000	0.000	0.037	0.000	0.037	0.037

Table C-24. CRC, Socorro, On-Road, Surface, P_ds and FARs

	GPR	EMI	IR	GPR-EMI	EMI-IR	GPR-IR	All Sensors
P_d, Total	1.000	0.500	0.000	1.000	0.500	1.000	1.000
P_d, M	1.000	1.000	0.000	1.000	1.000	1.000	1.000
P_d, LM	1.000	0.000	0.000	1.000	0.000	1.000	1.000
P_d, NM	N/A	N/A	N/A	N/A	N/A	N/A	N/A
FAR	0.037	0.000	0.000	0.037	0.000	0.037	0.037

Table C-25. CRC, Socorro, Off-Road, Subsurface, P_ds and FARs

	GPR	EMI	IR	GPR-EMI	EMI-IR	GPR-IR	All Sensors
P_d, Total	0.300	0.533	0.000	0.733	0.533	0.300	0.733
P_d, M	0.188	1.000	0.000	1.000	1.000	0.188	1.000
P_d, LM	0.429	0.000	0.000	0.429	0.000	0.429	0.429
P_d, NM	N/A	N/A	N/A	N/A	N/A	N/A	N/A
FAR	0.041	0.000	0.000	0.041	0.000	0.041	0.041

Table C-26. CRC, Socorro, Off-Road, Surface, P_ds and FARs

	GPR	EMI	IR	GPR-EMI	EMI-IR	GPR-IR	All Sensors
P_d, Total	1.000	0.667	0.000	1.000	0.667	1.000	1.000
P_d, M	1.000	1.000	0.000	1.000	1.000	1.000	1.000
P_d, LM	1.000	0.000	0.000	1.000	0.000	1.000	1.000
P_d, NM	N/A	N/A	N/A	N/A	N/A	N/A	N/A
FAR	0.041	0.000	0.000	0.041	0.000	0.041	0.041

Table C-27. CRC, Socorro, Night, Subsurface, P_ds and FARs

	GPR	EMI	IR	GPR-EMI	EMI-IR	GPR-IR	All Sensors
P_d, Total	0.815	0.444	0.000	0.963	0.444	0.815	0.963
P_d, M	0.667	1.000	0.000	1.000	1.000	0.667	1.000
P_d, LM	1.000	0.000	0.000	1.000	0.000	1.000	1.000
P_d, NM	0.667	0.000	0.000	0.667	0.000	0.667	0.667
FAR	0.025	0.000	0.000	0.025	0.000	0.025	0.025

Table C-28. CRC, Socorro, Night, Surface, P_ds and FARs

	GPR	EMI	IR	GPR-EMI	EMI-IR	GPR-IR	All Sensors
P_d, Total	1.000	0.500	0.000	1.000	0.500	1.000	1.000
P_d, M	1.000	1.000	0.000	1.000	1.000	1.000	1.000
P_d, LM	1.000	0.000	0.000	1.000	0.000	1.000	1.000
P_d, NM	N/A	N/A	N/A	N/A	N/A	N/A	N/A
FAR	0.025	0.000	0.000	0.025	0.000	0.025	0.025

Table C-29. CRC, Socorro, Physical-Marking, EM, Subsurface, P_ds and FARs

	GPR	EMI	IR	GPR-EMI	EMI-IR	GPR-IR	All Sensors
P_d, Total	0.781	0.438	0.000	1.000	0.438	0.781	1.000
P_d, M	0.500	1.000	0.000	1.000	1.000	0.500	1.000
P_d, LM	1.000	0.000	0.000	1.000	0.000	1.000	1.000
P_d, NM	1.000	0.000	0.000	1.000	0.000	1.000	1.000
FAR	0.037	0.000	0.000	0.037	0.000	0.037	0.037

Table C-30. CRC, Socorro, Physical-Marking, EM, Surface, P_ds and FARs

	GPR	EMI	IR	GPR-EMI	EMI-IR	GPR-IR	All Sensors
P_d, Total	1.000	0.500	0.000	1.000	0.500	1.000	1.000
P_d, M	1.000	1.000	0.000	1.000	1.000	1.000	1.000
P_d, LM	1.000	0.000	0.000	1.000	0.000	1.000	1.000
P_d, NM	N/A	N/A	N/A	N/A	N/A	N/A	N/A
FAR	0.037	0.000	0.000	0.037	0.000	0.037	0.037

Table C-31. CRC, Socorro, Morning, Subsurface, P_ds and FARs

	GPR	EMI	IR	GPR-EMI	EMI-IR	GPR-IR	All Sensors
P_d, Total	0.667	0.444	0.000	0.963	0.444	0.667	0.963
P_d, M	0.333	1.000	0.000	1.000	1.000	0.333	1.000
P_d, LM	0.917	0.000	0.000	0.917	0.000	0.917	0.917
P_d, NM	1.000	0.000	0.000	1.000	0.000	1.000	1.000
FAR	0.034	0.001	0.000	0.035	0.001	0.034	0.035

Table C-32. CRC, Socorro, Morning, Surface, P_ds and FARs

	GPR	EMI	IR	GPR-EMI	EMI-IR	GPR-IR	All Sensors
P_d, Total	1.000	0.500	0.000	1.000	0.500	1.000	1.000
P_d, M	1.000	1.000	0.000	1.000	1.000	1.000	1.000
P_d, LM	1.000	0.000	0.000	1.000	0.000	1.000	1.000
P_d, NM	N/A	N/A	N/A	N/A	N/A	N/A	N/A
FAR	0.034	0.001	0.000	0.035	0.001	0.034	0.035

3. Combined (Aberdeen & Socorro)

Table C-33. CRC, Combined (Aberdeen and Socorro), On-Road, Subsurface, P_ds and FARs

	GPR	EMI	IR	GPR-EMI	EMI-IR	GPR-IR	All Sensors
P_d, Total	0.693	0.475	0.000	0.843	0.475	0.693	0.843
P_d, M	0.682	1.000	0.000	1.000	1.000	0.682	1.000
P_d, LM	0.680	0.008	0.000	0.680	0.008	0.680	0.680
P_d, NM	0.850	0.000	0.000	0.850	0.000	0.850	0.850
FAR	0.034	0.002	0.000	0.035	0.002	0.034	0.035

Table C-34. CRC, Combined (Aberdeen and Socorro), On-Road, Surface, P_ds and FARs

	GPR	EMI	IR	GPR-EMI	EMI-IR	GPR-IR	All Sensors
P_d, Total	0.956	0.456	0.000	0.962	0.456	0.956	0.962
P_d, M	0.988	0.988	0.000	1.000	0.988	0.988	1.000
P_d, LM	0.935	0.000	0.000	0.935	0.000	0.935	0.935
P_d, NM	0.833	0.000	0.000	0.833	0.000	0.833	0.833
FAR	0.034	0.002	0.000	0.035	0.002	0.034	0.035

Table C-35. CRC, Combined (Aberdeen and Socorro), Off-Road, Subsurface, P_ds and FARs

	GPR	EMI	IR	GPR-EMI	EMI-IR	GPR-IR	All Sensors
P_d, Total	0.633	0.571	0.000	0.857	0.571	0.633	0.857
P_d, M	0.611	1.000	0.000	1.000	1.000	0.611	1.000
P_d, LM	0.659	0.046	0.000	0.682	0.046	0.659	0.682
P_d, NM	N/A	N/A	N/A	N/A	N/A	N/A	N/A
FAR	0.156	0.015	0.000	0.171	0.015	0.156	0.171

Table C-36. CRC, Combined (Aberdeen and Socorro), Off-Road, Surface, P_ds and FARs

	GPR	EMI	IR	GPR-EMI	EMI-IR	GPR-IR	All Sensors
P_d, Total	0.924	0.591	0.000	0.970	0.591	0.924	0.970
P_d, M	0.944	1.000	0.000	1.000	1.000	0.944	1.000
P_d, LM	0.900	0.100	0.000	0.933	0.100	0.900	0.933
P_d, NM	N/A	N/A	N/A	N/A	N/A	N/A	N/A
FAR	0.156	0.015	0.000	0.171	0.015	0.156	0.171

C. EG&G

1. Aberdeen

Table C-37. EG&G, Aberdeen, On-Road, Subsurface, P_ds and FARs

	GPR	EMI	IR	GPR-EMI	EMI-IR	GPR-IR	All Sensors
P_d, Total	0.697	0.470	0.621	0.727	0.856	0.924	0.932
P_d, M	0.936	1.000	0.500	1.000	1.000	0.984	1.000
P_d, LM	0.484	0.000	0.703	0.484	0.703	0.859	0.859
P_d, NM	0.500	0.000	1.000	0.500	1.000	1.000	1.000
FAR	0.036	0.000	0.047	0.036	0.047	0.081	0.081

Table C-38. EG&G, Aberdeen, On-Road, Surface, P_ds and FARs

	GPR	EMI	IR	GPR-EMI	EMI-IR	GPR-IR	All Sensors
P_d, Total	0.977	0.419	0.779	0.977	0.884	1.000	1.000
P_d, M	1.000	1.000	0.750	1.000	1.000	1.000	1.000
P_d, LM	0.977	0.000	0.773	0.977	0.773	1.000	1.000
P_d, NM	0.833	0.000	1.000	0.833	1.000	1.000	1.000
FAR	0.036	0.000	0.047	0.036	0.047	0.081	0.081

Table C-39. EG&G, Aberdeen, Off-Road, Subsurface, P_ds and FARs

	GPR	EMI	IR	GPR-EMI	EMI-IR	GPR-IR	All Sensors
P_d, Total	0.794	0.559	0.456	0.897	0.779	0.868	0.956
P_d, M	0.816	1.000	0.421	1.000	1.000	0.842	1.000
P_d, LM	0.767	0.000	0.500	0.767	0.500	0.900	0.900
P_d, NM	N/A	N/A	N/A	N/A	N/A	N/A	N/A
FAR	0.078	0.004	0.020	0.081	0.023	0.095	0.099

Table C-40. EG&G, Aberdeen, Off-Road, Surface, P_ds and FARs

	GPR	EMI	IR	GPR-EMI	EMI-IR	GPR-IR	All Sensors
P_d, Total	0.938	0.500	0.896	0.938	0.917	0.958	0.958
P_d, M	1.000	1.000	0.958	1.000	1.000	1.000	1.000
P_d, LM	0.875	0.000	0.833	0.875	0.833	0.917	0.917
P_d, NM	N/A	N/A	N/A	N/A	N/A	N/A	N/A
FAR	0.078	0.004	0.020	0.081	0.023	0.095	0.099

Table C-41. EG&G, Aberdeen, Night, Subsurface, P_ds and FARs

	GPR	EMI	IR	GPR-EMI	EMI-IR	GPR-IR	All Sensors
P_d, Total	0.717	0.478	0.022	0.739	0.478	0.717	0.739
P_d, M	0.955	1.000	0.046	1.000	1.000	0.955	1.000
P_d, LM	0.500	0.000	0.000	0.500	0.000	0.500	0.500
P_d, NM	0.500	0.000	0.000	0.500	0.000	0.500	0.500
FAR	0.129	0.000	0.014	0.129	0.014	0.143	0.143

Table C-42. EG&G, Aberdeen, Night, Surface, P_ds and FARs

	GPR	EMI	IR	GPR-EMI	EMI-IR	GPR-IR	All Sensors
P_d, Total	1.000	0.429	0.393	1.000	0.607	1.000	1.000
P_d, M	1.000	1.000	0.500	1.000	1.000	1.000	1.000
P_d, LM	1.000	0.000	0.286	1.000	0.286	1.000	1.000
P_d, NM	1.000	0.000	0.500	1.000	0.500	1.000	1.000
FAR	0.129	0.000	0.014	0.129	0.014	0.143	0.143

Table C-43. EG&G, Aberdeen, Physical-Marking, EM, Subsurface, P_ds and FARs

	GPR	EMI	IR	GPR-EMI	EMI-IR	GPR-IR	All Sensors
P_d, Total	0.550	0.450	0.350	0.600	0.650	0.700	0.750
P_d, M	0.889	1.000	0.333	1.000	1.000	0.889	1.000
P_d, LM	0.300	0.000	0.400	0.300	0.400	0.600	0.600
P_d, NM	0.000	0.000	0.000	0.000	0.000	0.000	0.000
FAR	0.005	0.000	0.035	0.005	0.035	0.039	0.039

Table C-44. EG&G, Aberdeen, Physical-Marking, EM, Surface, P_ds and FARs

	GPR	EMI	IR	GPR-EMI	EMI-IR	GPR-IR	All Sensors
P_d, Total	0.933	0.400	1.000	0.933	1.000	1.000	1.000
P_d, M	1.000	1.000	1.000	1.000	1.000	1.000	1.000
P_d, LM	1.000	0.000	1.000	1.000	1.000	1.000	1.000
P_d, NM	0.000	0.000	1.000	0.000	1.000	1.000	1.000
FAR	0.005	0.000	0.035	0.005	0.035	0.039	0.039

2. Socorro

Table C-45. EG&G, Socorro, On-Road, Subsurface, P_ds and FARs

	GPR	EMI	IR	GPR-EMI	EMI-IR	GPR-IR	All Sensors
P_d, Total	0.905	0.466	0.243	0.905	0.601	0.919	0.919
P_d, M	1.000	0.971	0.229	1.000	0.971	1.000	1.000
P_d, LM	0.797	0.016	0.234	0.797	0.250	0.828	0.828
P_d, NM	0.929	0.000	0.357	0.929	0.357	0.929	0.929
FAR	0.036	0.001	0.007	0.037	0.008	0.042	0.043

Table C-46. EG&G, Socorro, On-Road, Surface, P_ds and FARs

	GPR	EMI	IR	GPR-EMI	EMI-IR	GPR-IR	All Sensors
P_d, Total	0.969	0.479	0.802	0.969	0.865	0.969	0.969
P_d, M	0.958	0.958	0.833	0.958	0.958	0.958	0.958
P_d, LM	0.979	0.000	0.771	0.979	0.771	0.979	0.979
P_d, NM	N/A	N/A	N/A	N/A	N/A	N/A	N/A
FAR	0.036	0.001	0.007	0.037	0.008	0.042	0.043

Table C-47. EG&G, Socorro, Off-Road, Subsurface, P_ds and FARs

	GPR	EMI	IR	GPR-EMI	EMI-IR	GPR-IR	All Sensors
P_d, Total	0.600	0.533	0.100	0.700	0.533	0.633	0.700
P_d, M	0.813	1.000	0.188	1.000	1.000	0.875	1.000
P_d, LM	0.357	0.000	0.000	0.357	0.000	0.357	0.357
P_d, NM	N/A	N/A	N/A	N/A	N/A	N/A	N/A
FAR	0.041	0.000	0.019	0.041	0.019	0.058	0.058

Table C-48. EG&G, Socorro, Off-Road, Surface, P_ds and FARs

	GPR	EMI	IR	GPR-EMI	EMI-IR	GPR-IR	All Sensors
P_d, Total	1.000	0.667	0.889	1.000	1.000	1.000	1.000
P_d, M	1.000	1.000	0.833	1.000	1.000	1.000	1.000
P_d, LM	1.000	0.000	1.000	1.000	1.000	1.000	1.000
P_d, NM	N/A	N/A	N/A	N/A	N/A	N/A	N/A
FAR	0.041	0.000	0.019	0.041	0.019	0.058	0.058

Table C-49. EG&G, Socorro, Night, Subsurface, P_ds and FARs

	GPR	EMI	IR	GPR-EMI	EMI-IR	GPR-IR	All Sensors
P_d, Total	0.889	0.444	0.185	0.889	0.556	0.889	0.889
P_d, M	1.000	1.000	0.167	1.000	1.000	1.000	1.000
P_d, LM	0.833	0.000	0.250	0.833	0.250	0.833	0.833
P_d, NM	0.667	0.000	0.000	0.667	0.000	0.667	0.667
FAR	0.019	0.000	0.009	0.019	0.009	0.028	0.028

Table C-50. EG&G, Socorro, Night, Surface, P_ds and FARs

	GPR	EMI	IR	GPR-EMI	EMI-IR	GPR-IR	All Sensors
P_d, Total	1.000	0.500	1.000	1.000	1.000	1.000	1.000
P_d, M	1.000	1.000	1.000	1.000	1.000	1.000	1.000
P_d, LM	1.000	0.000	1.000	1.000	1.000	1.000	1.000
P_d, NM	N/A	N/A	N/A	N/A	N/A	N/A	N/A
FAR	0.019	0.000	0.009	0.019	0.009	0.028	0.028

Table C-51. EG&G, Socorro, Physical-Marking, EM, Subsurface, P_ds and FARs

	GPR	EMI	IR	GPR-EMI	EMI-IR	GPR-IR	All Sensors
P_d, Total	0.963	0.444	0.704	0.963	0.852	1.000	1.000
P_d, M	1.000	1.000	0.667	1.000	1.000	1.000	1.000
P_d, LM	0.917	0.000	0.750	0.917	0.750	1.000	1.000
P_d, NM	1.000	0.000	0.667	1.000	0.667	1.000	1.000
FAR	0.031	0.000	0.103	0.031	0.103	0.128	0.128

Table C-52. EG&G, Socorro, Physical-Marking, EM, Surface, P_ds and FARs

	GPR	EMI	IR	GPR-EMI	EMI-IR	GPR-IR	All Sensors
P_d, Total	1.000	0.500	1.000	1.000	1.000	1.000	1.000
P_d, M	1.000	1.000	1.000	1.000	1.000	1.000	1.000
P_d, LM	1.000	0.000	1.000	1.000	1.000	1.000	1.000
P_d, NM	N/A	N/A	N/A	N/A	N/A	N/A	N/A
FAR	0.031	0.000	0.103	0.031	0.103	0.128	0.128

Table C-53. EG&G, Socorro, Tele-operated, Subsurface, P_ds and FARs

	GPR	EMI	IR	GPR-EMI	EMI-IR	GPR-IR	All Sensors
P_d, Total	0.963	0.444	0.333	0.963	0.667	0.963	0.963
P_d, M	1.000	1.000	0.250	1.000	1.000	1.000	1.000
P_d, LM	0.917	0.000	0.333	0.917	0.333	0.917	0.917
P_d, NM	1.000	0.000	0.667	1.000	0.667	1.000	1.000
FAR	0.038	0.000	0.025	0.038	0.025	0.063	0.063

Table C-54. EG&G, Socorro, Tele-operated, Surface, P_ds and FARs

	GPR	EMI	IR	GPR-EMI	EMI-IR	GPR-IR	All Sensors
$P_{d'}$ Total	1.000	0.500	0.889	1.000	0.889	1.000	1.000
$P_{d'}$ M	1.000	1.000	1.000	1.000	1.000	1.000	1.000
$P_{d'}$ LM	1.000	0.000	0.778	1.000	0.778	1.000	1.000
$P_{d'}$ NM	N/A	N/A	N/A	N/A	N/A	N/A	N/A
FAR	0.038	0.000	0.025	0.038	0.025	0.063	0.063

3. Combined (Aberdeen & Socorro)

Table C-55. EG&G, Combined (Aberdeen and Socorro), On-Road, Subsurface, P_ds and FARs

	GPR	EMI	IR	GPR-EMI	EMI-IR	GPR-IR	All Sensors
$P_{d'}$ Total	0.807	0.468	0.421	0.821	0.721	0.921	0.925
$P_{d'}$ M	0.970	0.985	0.356	1.000	0.985	0.992	1.000
$P_{d'}$ LM	0.641	0.008	0.469	0.641	0.477	0.844	0.844
$P_{d'}$ NM	0.800	0.000	0.550	0.800	0.550	0.950	0.950
FAR	0.036	0.001	0.027	0.036	0.028	0.062	0.062

Table C-56. EG&G, Combined (Aberdeen and Socorro), On-Road, Surface, P_ds and FARs

	GPR	EMI	IR	GPR-EMI	EMI-IR	GPR-IR	All Sensors
$P_{d'}$ Total	0.973	0.451	0.791	0.973	0.874	0.984	0.984
$P_{d'}$ M	0.976	0.976	0.798	0.976	0.976	0.976	0.976
$P_{d'}$ LM	0.978	0.000	0.772	0.978	0.772	0.989	0.989
$P_{d'}$ NM	0.833	0.000	1.000	0.833	1.000	1.000	1.000
FAR	0.036	0.001	0.027	0.036	0.028	0.062	0.062

Table C-57. EG&G, Combined (Aberdeen and Socorro), Off-Road, Subsurface, P_ds and FARs

	GPR	EMI	IR	GPR-EMI	EMI-IR	GPR-IR	All Sensors
$P_{d'}$ Total	0.735	0.551	0.347	0.837	0.704	0.796	0.878
$P_{d'}$ M	0.815	1.000	0.352	1.000	1.000	0.852	1.000
$P_{d'}$ LM	0.636	0.000	0.341	0.636	0.341	0.727	0.727
$P_{d'}$ NM	N/A	N/A	N/A	N/A	N/A	N/A	N/A
FAR	0.071	0.003	0.020	0.073	0.022	0.088	0.091

Table C-58. EG&G, Combined (Aberdeen and Socorro) Off-Road, Surface, P_ds and FARs

	GPR	EMI	IR	GPR-EMI	EMI-IR	GPR-IR	All Sensors
P_d, Total	0.955	0.546	0.894	0.955	0.939	0.970	0.970
P_d, M	1.000	1.000	0.917	1.000	1.000	1.000	1.000
P_d, LM	0.900	0.000	0.867	0.900	0.867	0.933	0.933
P_d, NM	N/A	N/A	N/A	N/A	N/A	N/A	N/A
FAR	0.071	0.003	0.020	0.073	0.022	0.088	0.091

D. GDE

1. Aberdeen

Table C-59. GDE, Aberdeen, On-Road, Subsurface, P_ds and FARs

	GPR	EMI	IR	GPR-EMI	EMI-IR	GPR-IR	All Sensors
P_d, Total	0.871	0.439	0.000	0.909	0.439	0.871	0.909
P_d, M	0.871	0.936	0.000	0.952	0.936	0.871	0.952
P_d, LM	0.906	0.000	0.000	0.906	0.000	0.906	0.906
P_d, NM	0.500	0.000	0.000	0.500	0.000	0.500	0.500
FAR	0.067	0.002	0.000	0.068	0.002	0.067	0.068

Table C-60. GDE, Aberdeen, On-Road, Surface, P_ds and FARs

	GPR	EMI	IR	GPR-EMI	EMI-IR	GPR-IR	All Sensors
P_d, Total	0.919	0.407	0.000	0.965	0.407	0.919	0.965
P_d, M	0.861	0.972	0.000	0.972	0.972	0.861	0.972
P_d, LM	0.955	0.000	0.000	0.955	0.000	0.955	0.955
P_d, NM	1.000	0.000	0.000	1.000	0.000	1.000	1.000
FAR	0.067	0.002	0.000	0.068	0.002	0.067	0.068

Table C-61. GDE, Aberdeen, Off-Road, Subsurface, P_ds and FARs

	GPR	EMI	IR	GPR-EMI	EMI-IR	GPR-IR	All Sensors
P_d, Total	0.618	0.632	0.412	0.824	0.765	0.838	0.912
P_d, M	0.658	1.000	0.447	1.000	1.000	0.895	1.000
P_d, LM	0.567	0.167	0.367	0.600	0.467	0.767	0.800
P_d, NM	N/A	N/A	N/A	N/A	N/A	N/A	N/A
FAR	0.063	0.018	0.012	0.079	0.029	0.070	0.085

Table C-62. GDE, Aberdeen, Off-Road, Surface, P_ds and FARs

	GPR	EMI	IR	GPR-EMI	EMI-IR	GPR-IR	All Sensors
P_d, Total	0.771	0.563	0.625	0.917	0.833	0.854	0.938
P_d, M	0.708	1.000	0.667	1.000	1.000	0.833	1.000
P_d, LM	0.833	0.125	0.583	0.833	0.667	0.875	0.875
P_d, NM	N/A	N/A	N/A	N/A	N/A	N/A	N/A
FAR	0.063	0.018	0.012	0.079	0.029	0.070	0.085

Table C-63. GDE, Aberdeen, Night, Subsurface, P_ds and FARs

	GPR	EMI	IR	GPR-EMI	EMI-IR	GPR-IR	All Sensors
P_d, Total	1.000	0.478	0.000	1.000	0.478	1.000	1.000
P_d, M	1.000	1.000	0.000	1.000	1.000	1.000	1.000
P_d, LM	1.000	0.000	0.000	1.000	0.000	1.000	1.000
P_d, NM	1.000	0.000	0.000	1.000	0.000	1.000	1.000
FAR	0.012	0.002	0.000	0.015	0.002	0.012	0.015

Table C-64. GDE, Aberdeen, Night, Surface, P_ds and FARs

	GPR	EMI	IR	GPR-EMI	EMI-IR	GPR-IR	All Sensors
P_d, Total	1.000	0.429	0.250	1.000	0.571	1.000	1.000
P_d, M	1.000	1.000	0.250	1.000	1.000	1.000	1.000
P_d, LM	1.000	0.000	0.214	1.000	0.214	1.000	1.000
P_d, NM	1.000	0.000	0.500	1.000	0.500	1.000	1.000
FAR	0.012	0.002	0.000	0.015	0.002	0.012	0.015

2. Socorro

Table C-65. GDE, Socorro, On-Road, Subsurface, P_ds and *FAR*s

	GPR	EMI	IR	GPR-EMI	EMI-IR	GPR-IR	All Sensors
P_d, Total	0.885	0.480	0.000	0.899	0.480	0.885	0.899
P_d, M	0.971	1.000	0.000	1.000	1.000	0.971	1.000
P_d, LM	0.766	0.016	0.000	0.766	0.016	0.766	0.766
P_d, NM	1.000	0.000	0.000	1.000	0.000	1.000	1.000
FAR	0.033	0.002	0.003	0.035	0.004	0.036	0.037

Table C-66. GDE, Socorro, On-Road, Surface, P_ds and *FAR*s

	GPR	EMI	IR	GPR-EMI	EMI-IR	GPR-IR	All Sensors
P_d, Total	1.000	0.490	0.208	1.000	0.594	1.000	1.000
P_d, M	1.000	0.979	0.208	1.000	0.979	1.000	1.000
P_d, LM	1.000	0.000	0.208	1.000	0.208	1.000	1.000
P_d, NM	N/A	N/A	N/A	N/A	N/A	N/A	N/A
FAR	0.033	0.002	0.003	0.035	0.004	0.036	0.037

Table C-67. GDE, Socorro, Off-Road, Subsurface, P_ds and *FAR*s

	GPR	EMI	IR	GPR-EMI	EMI-IR	GPR-IR	All Sensors
P_d, Total	0.800	0.533	0.000	0.800	0.533	0.800	0.800
P_d, M	1.000	1.000	0.000	1.000	1.000	1.000	1.000
P_d, LM	0.571	0.000	0.000	0.571	0.000	0.571	0.571
P_d, NM	N/A	N/A	N/A	N/A	N/A	N/A	N/A
FAR	0.063	0.002	0.000	0.065	0.002	0.063	0.065

Table C-68. GDE, Socorro, Off-Road, Surface, P_ds and *FAR*s

	GPR	EMI	IR	GPR-EMI	EMI-IR	GPR-IR	All Sensors
P_d, Total	1.000	0.667	0.222	1.000	0.722	1.000	1.000
P_d, M	1.000	1.000	0.250	1.000	1.000	1.000	1.000
P_d, LM	1.000	0.000	0.167	1.000	0.167	1.000	1.000
P_d, NM	N/A	N/A	N/A	N/A	N/A	N/A	N/A
FAR	0.063	0.002	0.000	0.065	0.002	0.063	0.065

Table C-69. GDE, Socorro, Night, Subsurface, P_ds and *FAR*s

	GPR	EMI	IR	GPR-EMI	EMI-IR	GPR-IR	All Sensors
P_d, Total	0.875	0.438	0.000	0.906	0.438	0.875	0.906
P_d, M	0.929	1.000	0.000	1.000	1.000	0.929	1.000
P_d, LM	0.875	0.000	0.000	0.875	0.000	0.875	0.875
P_d, NM	0.500	0.000	0.000	0.500	0.000	0.500	0.500
FAR	0.014	0.002	0.000	0.016	0.002	0.014	0.016

Table C-70. GDE, Socorro Night, Surface, P_ds and *FAR*s

	GPR	EMI	IR	GPR-EMI	EMI-IR	GPR-IR	All Sensors
P_d, Total	1.000	0.500	0.500	1.000	0.563	1.000	1.000
P_d, M	1.000	1.000	0.875	1.000	1.000	1.000	1.000
P_d, LM	1.000	0.000	0.125	1.000	0.125	1.000	1.000
P_d, NM	N/A	N/A	N/A	N/A	N/A	N/A	N/A
FAR	0.014	0.002	0.000	0.016	0.002	0.014	0.016

Table C-71. GDE, Socorro, Physical-Marking, EM, Subsurface, P_ds and *FAR*s

	GPR	EMI	IR	GPR-EMI	EMI-IR	GPR-IR	All Sensors
P_d, Total	0.938	0.438	0.000	0.938	0.438	0.938	0.938
P_d, M	1.000	1.000	0.000	1.000	1.000	1.000	1.000
P_d, LM	0.875	0.000	0.000	0.875	0.000	0.875	0.875
P_d, NM	1.000	0.000	0.000	1.000	0.000	1.000	1.000
FAR	0.027	0.000	0.000	0.027	0.000	0.027	0.027

Table C-72. GDE, Socorro, Physical-Marking, EM, Surface, P_ds and *FAR*s

	GPR	EMI	IR	GPR-EMI	EMI-IR	GPR-IR	All Sensors
P_d, Total	1.000	0.500	0.000	1.000	0.500	1.000	1.000
P_d, M	1.000	1.000	0.000	1.000	1.000	1.000	1.000
P_d, LM	1.000	0.000	0.000	1.000	0.000	1.000	1.000
P_d, NM	N/A	N/A	N/A	N/A	N/A	N/A	N/A
FAR	0.027	0.000	0.000	0.027	0.000	0.027	0.027

Table C-73. GDE, Socorro, Morning, Subsurface, P_ds and FARs

	GPR	EMI	IR	GPR-EMI	EMI-IR	GPR-IR	All Sensors
P_d, Total	0.944	0.444	0.000	1.000	0.444	0.944	1.000
P_d, M	0.875	1.000	0.000	1.000	1.000	0.875	1.000
P_d, LM	1.000	0.000	0.000	1.000	0.000	1.000	1.000
P_d, NM	1.000	0.000	0.000	1.000	0.000	1.000	1.000
FAR	0.008	0.000	0.000	0.008	0.000	0.008	0.008

Table C-74. GDE, Socorro, Morning, Surface, P_ds and FARs

	GPR	EMI	IR	GPR-EMI	EMI-IR	GPR-IR	All Sensors
P_d, Total	1.000	0.500	0.000	1.000	0.500	1.000	1.000
P_d, M	1.000	1.000	0.000	1.000	1.000	1.000	1.000
P_d, LM	1.000	0.000	0.000	1.000	0.000	1.000	1.000
P_d, NM	N/A	N/A	N/A	N/A	N/A	N/A	N/A
FAR	0.008	0.000	0.000	0.008	0.000	0.008	0.008

3. Combined (Aberdeen and Socorro)

Table C-75. GDE, Combined (Aberdeen and Socorro), On-Road, Subsurface, P_ds and FARs

	GPR	EMI	IR	GPR-EMI	EMI-IR	GPR-IR	All Sensors
P_d, Total	0.879	0.461	0.000	0.904	0.461	0.879	0.904
P_d, M	0.924	0.970	0.000	0.977	0.970	0.924	0.977
P_d, LM	0.836	0.008	0.000	0.836	0.008	0.836	0.836
P_d, NM	0.850	0.000	0.000	0.850	0.000	0.850	0.850
FAR	0.050	0.002	0.001	0.051	0.003	0.051	0.053

Table C-76. GDE, Combined (Aberdeen and Socorro), On-Road, Surface, P_ds and FARs

	GPR	EMI	IR	GPR-EMI	EMI-IR	GPR-IR	All Sensors
P_d, Total	0.962	0.451	0.110	0.984	0.506	0.962	0.984
P_d, M	0.941	0.976	0.119	0.988	0.976	0.941	0.988
P_d, LM	0.978	0.000	0.109	0.978	0.109	0.978	0.978
P_d, NM	1.000	0.000	0.000	1.000	0.000	1.000	1.000
FAR	0.050	0.002	0.001	0.051	0.003	0.051	0.053

Table C-77. GDE, Combined (Aberdeen and Socorro), Off-Road, Subsurface, P_ds and FARs

	GPR	EMI	IR	GPR-EMI	EMI-IR	GPR-IR	All Sensors
P_d, Total	0.674	0.602	0.286	0.816	0.694	0.827	0.878
P_d, M	0.759	1.000	0.315	1.000	1.000	0.926	1.000
P_d, LM	0.568	0.114	0.250	0.591	0.318	0.705	0.727
P_d, NM	N/A	N/A	N/A	N/A	N/A	N/A	N/A
FAR	0.063	0.015	0.010	0.076	0.024	0.069	0.081

Table C-78. GDE, Combined (Aberdeen and Socorro), Off-Road, Surface, P_ds and FARs

	GPR	EMI	IR	GPR-EMI	EMI-IR	GPR-IR	All Sensors
P_d, Total	0.833	0.591	0.515	0.939	0.803	0.894	0.955
P_d, M	0.806	1.000	0.528	1.000	1.000	0.889	1.000
P_d, LM	0.867	0.100	0.500	0.867	0.567	0.900	0.900
P_d, NM	N/A	N/A	N/A	N/A	N/A	N/A	N/A
FAR	0.063	0.015	0.010	0.076	0.024	0.069	0.081

E. GEOCENTERS

1. Aberdeen

Table C-79. GeoC, Aberdeen, On-Road, Subsurface, P_ds and FARs

	GPR	EMI	IR	GPR-EMI	EMI-IR	GPR-IR	All Sensors
P_d, Total	0.977	0.447	0.000	0.985	0.447	0.977	0.985
P_d, M	1.000	0.936	0.000	1.000	0.936	1.000	1.000
P_d, LM	0.953	0.016	0.000	0.969	0.016	0.953	0.969
P_d, NM	1.000	0.000	0.000	1.000	0.000	1.000	1.000
FAR	0.048	0.008	0.000	0.056	0.008	0.048	0.056

Table C-80. GeoC, Aberdeen, On-Road, Surface, P_ds and FARs

	GPR	EMI	IR	GPR-EMI	EMI-IR	GPR-IR	All Sensors
P_d, Total	0.965	0.430	0.988	1.000	0.988	1.000	1.000
P_d, M	0.917	0.972	1.000	1.000	1.000	1.000	1.000
P_d, LM	1.000	0.046	0.977	1.000	0.977	1.000	1.000
P_d, NM	1.000	0.000	1.000	1.000	1.000	1.000	1.000
FAR	0.048	0.008	0.000	0.056	0.008	0.048	0.056

Table C-81. GeoC, Aberdeen, Off-Road, Subsurface, P_ds and FARs

	GPR	EMI	IR	GPR-EMI	EMI-IR	GPR-IR	All Sensors
P_d, Total	0.897	0.441	0.000	0.897	0.441	0.897	0.897
P_d, M	1.000	0.790	0.000	1.000	0.790	1.000	1.000
P_d, LM	0.767	0.000	0.000	0.767	0.000	0.767	0.767
P_d, NM	N/A	N/A	N/A	N/A	N/A	N/A	N/A
FAR	0.065	0.001	0.000	0.066	0.001	0.065	0.066

Table C-82. GeoC, Aberdeen, Off-Road, Surface, P_ds and FARs

	GPR	EMI	IR	GPR-EMI	EMI-IR	GPR-IR	All Sensors
P_d, Total	0.979	0.479	1.000	0.979	1.000	1.000	1.000
P_d, M	1.000	0.958	1.000	1.000	1.000	1.000	1.000
P_d, LM	0.958	0.000	1.000	0.958	1.000	1.000	1.000
P_d, NM	N/A	N/A	N/A	N/A	N/A	N/A	N/A
FAR	0.065	0.001	0.000	0.066	0.001	0.065	0.066

Table C-83. GeoC, Aberdeen, Night, Subsurface, P_ds and FARs

	GPR	EMI	IR	GPR-EMI	EMI-IR	GPR-IR	All Sensors
P_d, Total	1.000	0.478	0.000	1.000	0.478	1.000	1.000
P_d, M	1.000	1.000	0.000	1.000	1.000	1.000	1.000
P_d, LM	1.000	0.000	0.000	1.000	0.000	1.000	1.000
P_d, NM	1.000	0.000	0.000	1.000	0.000	1.000	1.000
FAR	0.033	0.000	0.000	0.033	0.000	0.033	0.033

Table C-84. GeoC, Aberdeen, Night, Surface, P_ds and FARs

	GPR	EMI	IR	GPR-EMI	EMI-IR	GPR-IR	All Sensors
P_{d} Total	1.000	0.393	1.000	1.000	1.000	1.000	1.000
	1.000	0.917	1.000	1.000	1.000	1.000	1.000
P_{d} LM	1.000	0.000	1.000	1.000	1.000	1.000	1.000
P_{d} NM	1.000	0.000	1.000	1.000	1.000	1.000	1.000
FAR	0.033	0.000	0.000	0.033	0.000	0.033	0.033

Table C-85. GeoC, Aberdeen, Physical-Marking, EM, Subsurface, P_ds and FARs

	GPR	EMI	IR	GPR-EMI	EMI-IR	GPR-IR	All Sensors
P_{d} Total	0.913	0.478	0.000	0.913	0.478	0.913	0.913
P_{d} M	1.000	1.000	0.000	1.000	1.000	1.000	1.000
P_{d} LM	0.818	0.000	0.000	0.818	0.000	0.818	0.818
P_{d} NM	1.000	0.000	0.000	1.000	0.000	1.000	1.000
FAR	0.037	0.002	0.004	0.038	0.005	0.040	0.042

Table C-86. GeoC, Aberdeen, Physical-Marking, EM, Surface, P_ds and FARs

	GPR	EMI	IR	GPR-EMI	EMI-IR	GPR-IR	All Sensors
P_{d} Total	1.000	0.286	0.714	1.000	0.857	1.000	1.000
P_{d} M	1.000	0.667	0.667	1.000	1.000	1.000	1.000
P_{d} LM	1.000	0.000	0.714	1.000	0.714	1.000	1.000
P_{d} NM	1.000	0.000	1.000	1.000	1.000	1.000	1.000
FAR	0.037	0.002	0.004	0.038	0.005	0.040	0.042

Table C-87. GeoC, Aberdeen, Tele-operated, Subsurface, P_ds and FARs

	GPR	EMI	IR	GPR-EMI	EMI-IR	GPR-IR	All Sensors
P_{d} Total	1.000	0.478	0.000	1.000	0.478	1.000	1.000
P_{d} M	1.000	1.000	0.000	1.000	1.000	1.000	1.000
P_{d} LM	1.000	0.000	0.000	1.000	0.000	1.000	1.000
P_{d} NM	1.000	0.000	0.000	1.000	0.000	1.000	1.000
FAR	0.013	0.002	0.000	0.015	0.002	0.013	0.015

Table C-88. GeoC, Aberdeen, Tele-operated, Surface, P_ds and FARs

	GPR	EMI	IR	GPR-EMI	EMI-IR	GPR-IR	All Sensors
P_d, Total	1.000	0.357	0.000	1.000	0.357	1.000	1.000
P_d, M	1.000	0.833	0.000	1.000	0.833	1.000	1.000
P_d, LM	1.000	0.000	0.000	1.000	0.000	1.000	1.000
P_d, NM	1.000	0.000	0.000	1.000	0.000	1.000	1.000
FAR	0.013	0.002	0.000	0.015	0.002	0.013	0.015

2. Socorro

Table C-89. GeoC, Socorro, On-Road, Subsurface, P_ds and FARs

	GPR	EMI	IR	GPR-EMI	EMI-IR	GPR-IR	All Sensors
P_d, Total	0.912	0.473	0.176	0.912	0.595	0.912	0.912
P_d, M	1.000	1.000	0.114	1.000	1.000	1.000	1.000
P_d, LM	0.859	0.000	0.266	0.859	0.266	0.859	0.859
P_d, NM	0.714	0.000	0.071	0.714	0.071	0.714	0.714
FAR	0.032	0.000	0.000	0.032	0.001	0.032	0.032

Table C-90. GeoC, Socorro, On-Road, Surface, P_ds and FARs

	GPR	EMI	IR	GPR-EMI	EMI-IR	GPR-IR	All Sensors
P_d, Total	1.000	0.500	0.833	1.000	0.917	1.000	1.000
P_d, M	1.000	1.000	0.833	1.000	1.000	1.000	1.000
P_d, LM	1.000	0.000	0.833	1.000	0.833	1.000	1.000
P_d, NM	N/A	N/A	N/A	N/A	N/A	N/A	N/A
FAR	0.032	0.000	0.000	0.032	0.001	0.032	0.032

Table C-91. GeoC, Socorro, Off-Road, Subsurface, P_ds and FARs

	GPR	EMI	IR	GPR-EMI	EMI-IR	GPR-IR	All Sensors
P_d, Total	0.700	0.533	0.000	0.700	0.533	0.700	0.700
P_d, M	1.000	1.000	0.000	1.000	1.000	1.000	1.000
P_d, LM	0.357	0.000	0.000	0.357	0.000	0.357	0.357
P_d, NM	N/A	N/A	N/A	N/A	N/A	N/A	N/A
FAR	0.035	0.000	0.000	0.035	0.000	0.035	0.035

Table C-92. GeoC, Socorro Off-Road, Surface, P_ds and FARs

	GPR	EMI	IR	GPR-EMI	EMI-IR	GPR-IR	All Sensors
$P_{d'}$ Total	1.000	0.667	0.944	1.000	0.944	1.000	1.000
$P_{d'}$ M	1.000	1.000	1.000	1.000	1.000	1.000	1.000
$P_{d'}$ LM	1.000	0.000	0.833	1.000	0.833	1.000	1.000
$P_{d'}$ NM	N/A	N/A	N/A	N/A	N/A	N/A	N/A
FAR	0.035	0.000	0.000	0.035	0.000	0.035	0.035

Table C-93. GeoC, Socorro, Night, Subsurface, P_ds and FARs

	GPR	EMI	IR	GPR-EMI	EMI-IR	GPR-IR	All Sensors
$P_{d'}$ Total	0.807	0.516	0.000	0.839	0.516	0.807	0.839
$P_{d'}$ M	0.938	1.000	0.000	1.000	1.000	0.938	1.000
$P_{d'}$ LM	0.667	0.000	0.000	0.667	0.000	0.667	0.667
$P_{d'}$ NM	0.667	0.000	0.000	0.667	0.000	0.667	0.667
FAR	0.029	0.000	0.000	0.029	0.000	0.029	0.029

Table C-94. GeoC, Socorro, Night, Surface, P_ds and FARs

	GPR	EMI	IR	GPR-EMI	EMI-IR	GPR-IR	All Sensors
$P_{d'}$ Total	1.000	0.476	1.000	1.000	1.000	1.000	1.000
$P_{d'}$ M	1.000	1.000	1.000	1.000	1.000	1.000	1.000
$P_{d'}$ LM	1.000	0.000	1.000	1.000	1.000	1.000	1.000
$P_{d'}$ NM	N/A	N/A	N/A	N/A	N/A	N/A	N/A
FAR	0.029	0.000	0.000	0.029	0.000	0.029	0.029

Table C-95. GeoC, Socorro, Physical-Marking, EM, Subsurface, P_ds and FARs

	GPR	EMI	IR	GPR-EMI	EMI-IR	GPR-IR	All Sensors
$P_{d'}$ Total	0.875	0.438	0.125	0.906	0.531	0.875	0.906
$P_{d'}$ M	0.929	1.000	0.071	1.000	1.000	0.929	1.000
$P_{d'}$ LM	0.875	0.000	0.188	0.875	0.188	0.875	0.875
$P_{d'}$ NM	0.500	0.000	0.000	0.500	0.000	0.500	0.500
FAR	0.027	0.000	0.000	0.027	0.000	0.027	0.027

Table C-96. GeoC, Socorro, Physical-Marking, EM, Surface, P_ds and FARs

	GPR	EMI	IR	GPR-EMI	EMI-IR	GPR-IR	All Sensors
$P_{d'}$ Tota	1.000	0.500	1.000	1.000	1.000	1.000	1.000
$P_{d'}$ M	1.000	1.000	1.000	1.000	1.000	1.000	1.000
$P_{d'}$ LM	1.000	0.000	1.000	1.000	1.000	1.000	1.000
$P_{d'}$ NM	N/A	N/A	N/A	N/A	N/A	N/A	N/A
FAR	0.027	0.000	0.000	0.027	0.000	0.027	0.027

Table C-97. GeoC, Socorro, Tele-operated, Subsurface, P_ds and FARs

	GPR	EMI	IR	GPR-EMI	EMI-IR	GPR-IR	All Sensors
$P_{d'}$ Total	0.844	0.438	0.000	0.906	0.438	0.844	0.906
$P_{d'}$ M	0.857	1.000	0.000	1.000	1.000	0.857	1.000
$P_{d'}$ LM	0.813	0.000	0.000	0.813	0.000	0.813	0.813
$P_{d'}$ NM	1.000	0.000	0.000	1.000	0.000	1.000	1.000
FAR	0.019	0.000	0.000	0.019	0.000	0.019	0.019

Table C-98. GeoC, Socorro, Tele-operated, Surface, P_ds and FARs

	GPR	EMI	IR	GPR-EMI	EMI-IR	GPR-IR	All Sensors
$P_{d'}$ Total	1.000	0.500	0.000	1.000	0.500	1.000	1.000
$P_{d'}$ M	1.000	1.000	0.000	1.000	1.000	1.000	1.000
$P_{d'}$ LM	1.000	0.000	0.000	1.000	0.000	1.000	1.000
$P_{d'}$ NM	N/A	N/A	N/A	N/A	N/A	N/A	N/A
FAR	0.019	0.000	0.000	0.019	0.000	0.019	0.019

3. Combined (Aberdeen & Socorro)

Table C-99. GeoC, Combined (Aberdeen and Socorro), On-Road, Subsurface, P_ds and FARs

	GPR	EMI	IR	GPR-EMI	EMI-IR	GPR-IR	All Sensors
$P_{d'}$ Total	0.943	0.461	0.093	0.946	0.525	0.943	0.946
$P_{d'}$ M	1.000	0.970	0.061	1.000	0.970	1.000	1.000
$P_{d'}$ LM	0.906	0.008	0.133	0.914	0.141	0.906	0.914
$P_{d'}$ NM	0.800	0.000	0.050	0.800	0.050	0.800	0.800
FAR	0.040	0.004	0.000	0.044	0.004	0.040	0.044

Table C-100. GeoC, Combined (Aberdeen and Socorro),
On-Road, Surface, P_ds and FARs

	GPR	EMI	IR	GPR-EMI	EMI-IR	GPR-IR	All Sensors
$P_{d'}$ Total	0.984	0.467	0.907	1.000	0.951	1.000	1.000
$P_{d'}$ M	0.964	0.988	0.905	1.000	1.000	1.000	1.000
$P_{d'}$ LM	1.000	0.022	0.902	1.000	0.902	1.000	1.000
$P_{d'}$ NM	1.000	0.000	1.000	1.000	1.000	1.000	1.000
FAR	0.040	0.004	0.000	0.044	0.004	0.040	0.044

Table C-101. GeoC, Combined (Aberdeen and Socorro),
Off-Road, Subsurface, P_ds and FARs , CRC

	GPR	EMI	IR	GPR-EMI	EMI-IR	GPR-IR	All Sensors
$P_{d'}$ Total	0.837	0.469	0.000	0.837	0.469	0.837	0.837
$P_{d'}$ M	1.000	0.852	0.000	1.000	0.852	1.000	1.000
$P_{d'}$ LM	0.636	0.000	0.000	0.636	0.000	0.636	0.636
$P_{d'}$ NM	N/A	N/A	N/A	N/A	N/A	N/A	N/A
FAR	0.059	0.001	0.000	0.060	0.001	0.059	0.060

Table C-102. GeoC, Combined (Aberdeen and Socorro)
Off-Road, Surface, P_ds and FARs

	GPR	EMI	IR	GPR-EMI	EMI-IR	GPR-IR	All Sensors
$P_{d'}$ Total	0.985	0.530	0.985	0.985	0.985	1.000	1.000
$P_{d'}$ M	1.000	0.972	1.000	1.000	1.000	1.000	1.000
$P_{d'}$ LM	0.967	0.000	0.967	0.967	0.967	1.000	1.000
$P_{d'}$ NM	N/A	N/A	N/A	N/A	N/A	N/A	N/A
FAR	0.059	0.001	0.000	0.060	0.001	0.059	0.060

REPORT DOCUMENTATION PAGE

Public Reporting burden for this collection of information is estimated to average 1 hour per response, including the time for reviewing instructions, searching existing data sources, gathering and maintaining the data neec completing and reviewing the collection of information. Send comments regarding this burden estimate or any other aspect of this collection of information, including suggestions for reducing this burden, to Was Headquarters Services, Directorate for Information Operations and Reports, 1215 Jefferson Davis Highway, Suite 1204, Arlington, VA 22202-4302, and to the Office of Management and Budget, Paperwork Reduction I (0704-0188), Washington, DC 20503.

1. AGENCY USE ONLY *(Leave blank)*	2. REPORT DATE October 1998	3. REPORT TYPE AND DATES COVERED Final—April 1998–November 1998

4. TITLE AND SUBTITLE Report on the Advanced Technology Demonstration (ATD) of the Vehicular-Mounted Mine Detection (VMMD) Systems at Aberdeen, Maryland, and Socorro, New Mexico	5. FUNDING NUMBERS DASW01 94 C 0054 T-AI2-1473

6. AUTHOR(S)
Frank Rotondo, Tom Altshuler, Erik Rosen, Cynthia Dion-Schwarz, Elizabeth Ayers

7. PERFORMING ORGANIZATION NAME(S) AND ADDRESS(ES) Institute for Defense Analyses 1801 N. Beauregard St. Alexandria, VA 22311-1772	8. PERFORMING ORGANIZATION REPORT NUMBER IDA Document D-2203

9. SPONSORING/MONITORING AGENCY NAME(S) AND ADDRESS(ES) Department of the Army Night Vision and Electronic Sensors Directorate 10221 Burbeck Rd., Bldg. 392 Ft. Belvoir, VA 22060	10. SPONSORING/MONITORING AGENCY REPORT NUMBER

11. SUPPLEMENTARY NOTES

12a. DISTRIBUTION/AVAILABILITY STATEMENT Approved for public release; distribution unlimited.	12b. DISTRIBUTION CODE

13. ABSTRACT *(Maximum 180 words)*

This document presents an analysis of the results of an advanced technology demonstration of five vehicular-mounted mine detection systems developed for the detection of antitank land mines. The five contractors were Coleman Research Corporation; Computing Devices Canada; EG&G, Inc.; GDE Systems, Inc.; and GeoCenters, Inc. The systems were developed for the U.S. Army Night Vision and Electronic Sensors Directorate. The advanced technology demonstration took place at the Aberdeen Test Center, Aberdeen, Maryland, on June 8–19, 1998, and the Energetic Materials Research and Testing Center, Socorro, New Mexico, on July 13–24, 1998. The purpose of the program is to develop the technology for a remotely operated vehicle that will detect mines and mark their locations during military mine-clearance operations. The system will ultimately consist of a mine overpass vehicle upon which is mounted a sensor system that detects mines and a communication system that provides data transfer between the detection vehicle and the remote operator. The mine threats include both metal-cased mines and mines with low-metal content. These mines may be laid on ground surface or buried underground. The report outlines the systems' performance, in particular their detection probability and false-alarm rates, compared to the program's requirements.

14. SUBJECT TERMS Mine detection, ground-penetrating radar, metal detector, infrared detector, vehicular mounted mine detection, ground standoff mine detection, countermine	15. NUMBER OF PAGES 208
	16. PRICE CODE

17. SECURITY CLASSIFICATION OF REPORT UNCLASSIFIED	18. SECURITY CLASSIFICATION OF THIS PAGE UNCLASSIFIED	19. SECURITY CLASSIFICATION OF ABSTRACT UNCLASSIFIED	20. LIMITATION OF ABSTRACT SAR

NSN 7540-01-280-5500

Standard Form 298 (Rev. 2-89)
Prescribed by ANSI Std. Z39-18
298-102